Prepared for:

Rijkswaterstaat Dienst Getijdewateren

ISOS*2 Project, Phase 2

Impact of sea level rise on the morphology of the Wadden Sea in the scope of its ecological function

Investigations on empirical morphological relations

September 1992

delft hydraulics

Impact of sea level rise on the morphology of the Wadden Sea in the scope of its ecological function

Investigations on empirical morphological relations

W.D. Eysink and E.J. Biegel

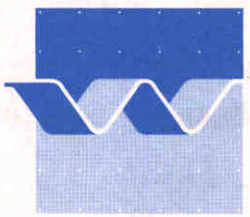

delft hydraulics

CONTENTS

CONTENTS (continued)

LIST OF TABLES

LIST OF FIGURES

LIST OF FIGURES (continued)

LIST OF FIGURES (continued)

LIST OF FIGURES (continued)

1. Introduction

1.1 Purpose of the study

The Dutch Wadden Sea consists of a number of tidal basins and barrier islands separated by inlets. The morphology of the Wadden Sea area is determined by numerous factors and mechanisms, such as:

- tidal range and flow,
- seasonal wind and waves,
- geometry of the basins,
- pre-existing morphological and sedimentary structures due to geological processes,
- sediment transport mechanisms with related erosion, sedimentation and hydraulic sorting of sediment types,
- inland discharge and related salinity variation in time and space resulting in density currents and flocculation of particles, and
- biogenic input on coagulation of particles and on critical shear stress with respect to initial motion.

Also the Wadden Sea is an area with ecological functions which are of great national and international importance. In this respect the following functions can be recognized:

- spawning grounds and nursery area for fish, shell fish and shrimps,
- feeding grounds and resting place for many kinds of birds, among others large quantities of migratory birds,
- habitat of seals, and
- natural salt marsh and dune vegetation.

The above functions are mutually related through the food chain and dependant on the characteristics of the habitat such as the water quality, availability of nutrients, disturbance by man and the morphology of the area.

An accelerated increase of relative sea-level rise may create severe problems for coastal protection and will induce changes in the morphological development and in the related multivarious but vulnerable ecosystem of the Wadden Sea area. These alterations will also effect the functional uses of the area like fishery and natural potentials.

The acceleration of relative sea-level rise due to global climatic changes is a realistic expectation and will become an enormous challenge for coastal defence management. Its effects will not only require the redesign and strengthening of existing coastal structures, but will probably also demand whole new concepts. Therefore the future morphological development will be of crucial importance for coastal defence management as well for barrier islands as for Wadden Sea coasts.

Due to these facts the main objective of the ISOS*2 project will be the development of methods which allow a reliable forecast of the future morphological response of the Wadden Sea area under both natural and human influences. Special emphasis is given to the effects of an acceleration in relative sea-level rise.

A reproduction of the morphological development of the Wadden Sea area by use of high resolution numerical modelling techniques with consideration of the above mentioned boundary conditions, is with presently available knowledge and tools not possible in a reliable way. Nevertheless, a distinct need exists to predict the impact of changing hydrodynamical conditions in the Wadden Sea due to both impacts of nature and human interventions with a fair degree of accuracy, as there are for example:

- relative sea-level rise,
- change of tidal amplitude,
- closure works,
- systematic sand borrowing and dumping of dredged sediments, and
- bottom subsidence due to extraction of natural resources.

Therefore, a more simple model is looked for which can be used to predict this impact with a sufficient degree of confidence. A promising option is the development of a conceptual model which is based on a number of empirical morphological relationships. Such relationships are valid on a high integration level and are not sensitive for instabilities and extrapolation errors like numerical models. A disadvantage is that the conceptual model will present less detailed results.

Main objective of the project is therefore the development and improvement of a conceptual morphodynamic model as a tool for predictions of the resulting morphological response on an accelerating sea-level rise in a long-term time scale (100 years).

This model should be able to present predictions on morphological changes as a result of increased sea level rise which are sufficiently detailed and reliable for predictions on the related ecological impact.

The developed knowledge and models will allow policy-makers, engineers and scientists to predict and control natural and human interferences on the Wadden Sea and adjacent coast. Furthermore, also other disciplines planning and working in the Wadden Sea area will benefit from their results.

1.2 Terms of reference

At the request of the Public Works Department of the Dutch Government DELFT HYDRAULICS made a proposal (Ref. HK8335/H1300/FH/Im dd 13th February, 1991) for:

- The development of conceptual models of the tidal basins of the Dutch Wadden Sea with the assistance of the Public Works Department and a study on the impact of sea level rise on the morphology of that sea. The study was done in close cooperation with the Public Works Department of the Dutch Government.
- Guidance of the inventorization and brainstorming for the sedimentological study.
- Participation in the project group ISOS*2.

The investigations have been performed in the years 1991-1992 and are divided into three phases.

The first phase was the initiation of the study which comprised:

- Making an inventory of all relevant existing field data such as sounding maps, tide data, flow data, sediment data, wave data, activities of man, etc.
  A comprehensive data inventory for the evaluated research areas and suitable data processing provided both phenomenological analysis and verification of the initial version of the quasi-equilibrium model. Phenomenological analysis not only yielded a deeper insight into morphodynamical processes of the Wadden Sea area but was preliminarily used to deliver results for improvements of the conceptual model.
- Set-up of a central data base.
- Literature survey on existing morphological relationships.
- Selection of empirical morphological relationships to be studied in more detail to arrive at a consistent set of generally valid relationships.
- Reporting of the findings of phase 1.

The second phase of the study consisted of the processing of the most suitable existing data. The selection of those data sets was done in close cooperation with the client. After the data processing, various correlations were made aiming at the assessment of suitable morphological relationships which will be generally valid for (dynamic) equilibrium conditions. Based on a selection of suitable relationships a conceptual equilibrium model will be made which will be verified based on, for example, data of the tidal basin of the Zoutkamperlaag.
Wishes from an ecological point of view will be incorporated if possible.
The findings of this part of the study should be reported in a separate phase 2 report. Depending on the results of phase 2, the client will make a decision wether or not to start with phase 3 of the ISOS*2 project.

In phase 3 of the study an attempt will be made to make a transition model which can be used to describe the way of adaptation with time from the original equilibrium situation to another after the original equilibrium is disturbed in one way or another. Also this phase will be reported separately.

The above reflects the broad lines of the proposal. The Public Works Department commissioned the phases 1 and 2 of the study to DELFT HYDRAULICS in their letter BXFO/914230 of 18th February, 1991 (Order no. DG-255).

The results of phase 1 of the study are reported in Kleef (1991a, b), Eysink (1991a), Biegel (1991) and Lambeek (1991).

This report deals with phase 2 of the study which has been executed by W.D. Eysink of DELFT HYDRAULICS and E.J. Biegel of the University of Utrecht. The study has been guided by Dr. J.P.M. Mulder and T. Louters representing the client and F.M.J. Hoozemans of DELFT HYDRAULICS. The report has been drawn up by W.D. Eysink. The Annexes to this report, i.e. Data report ISOS*2, Part 1: Results, Calculations and Methods phase 2 and Part 2: Selected data of the Dutch Wadden Sea, have been drawn up by E.J. Biegel.

1.3 Results, conclusions and recommendations

The present study yielded a great number of empirical relations which are shown on various figures of this report. In a number of cases those relations have been checked with physical relations and with relations and data from literature. In

some cases also mutual checks have been made by comparing the results of a combination of relations with a directly obtained relation, such as the product of the width and the mean depth compared with the cross-sectional area. Thus, it was tried to arrive at a consistent set of empirical relations for the Dutch Wadden Sea, which may have a more universal applicability. The most relevant results are briefly presented below.

Hydraulic parameters

In a number of cases it appears possible to derive a relationship between a morphological quantity and a hydraulic parameter. The latter actually represents the hydraulic energy that shapes the morphologic unit that is considered and, somehow, must be related to sediment transport. In tidal areas such a parameter can be a characteristic tidal volume, discharge rate, velocity, shear stress velocity or shear stress. Also a combination of two or more of such paramters is possible.

Various options as used in literature have been discussed extensively in Chapter 3. It was concluded, at least for the Dutch Wadden Sea data, that the following holds:

- The best correlations are obtained for the dominant tidal volume DV (i.e. the largest of the flood volume FV or ebb volume EV) and the maximum tidal discharge (ebb or flood) Q_{max}. The application of the tidal volume TV or tidal prism P (=TV/2) yields practically the same results.
- For practical reasons the use of DV, TV or P is preferred above that of Q_{max}. Only in some occasions, where maximum flow does not occur at a water level around MSL, the application of Q_{max} may be favoured.
- The average tidal velocity $\overline{u}$ and the maximum sinusoidal velocity $\hat{u}$ and discharge rate $\hat{Q}$ are directly related to TV or P and, hence, are similar.
- The maximum tidal velocity u_{max} is directly related to Q_{max} and, hence, is similar.
- The above mentioned hydraulic parameters may be based on a mean tide, a mean springtide or a diurnal tide. The data related to a diurnal tide are directly comparable with those of a mean springtide and fit in the same relation. Relations based on a mean tide easily can be converted to mean spring tide conditions by introducing a conversion factor equal to the ratio mean springtide range over mean tidal range. This ratio generally will be within the range of 1.1 to 1.2.

- The application of a characteristic shear stress velocity ($\overline{u}_*$ or u_{*max}) or stability shear stress (τ_s) does not reduce the scatter of the data around the relation obtained. However, it is believed to improve the general validity of the relation. This parameter explicitely allows for taking into account the effects of bed roughness (through the Chezy coëfficient) and of waves (through the Bijker factor) on the morphological quantity (see Eqs. 3.2, 3.6-3.10).
- The introduction of a dimensionless shear stress parameter τ_s^* as proposed by Gerritsen (1990) is not considered useful. It introduces too many drawbacks and is not feasible to be used in a predictive way.
- It is suggested to use Eq. 3.16a to calculate the bed roughness k_s if no reliable field data are available.

Cross section of tidal channels

During this century a lot of investigations have been performed on the size of a tidal inlet in a sandy environment in relation with the size of the tidal basin and/or tidal parameters. Generally this resulted in a relationship like:

$$A_{c,MSL} = c_A P^n + a \qquad (3.1)$$

In the last decades it is shown that such a relation also holds for inlets of estuaries and also locally inside estuaries and in areas like the Wadden Sea. At first glance the various relations seem rather different with the empirical coefficients c_A, n and a fitted to different data sets. Some of them are related to small tidal inlets only, others to large inlets only and a few cover a large range of inlet size. Some American authors also presented relations for tidal inlets which are protected by two jetties. Comparison of all the different relations (see Fig. 3.53) shows that all relations fit within a certain range if the validity range of the individual relations is taken into account. Differences mainly may be caused by differences in the local wave climate.

Small inlets and channels can be described by relation (3.1) with the constant a = 0 or close to it and an exponent n of approximately 0.7 (see Fig. 3.50). For large inlets and channels the exponent varies closely around unity. Consequently, the value of n ranges between 0.8 and 0.95 if relation (3.1) is derived for a large range of inlet or channel sizes. If the data set comprises a lot of small channels n will be lower than in the opposite case. The difference is largely caused by the effects of bed roughness and small waves which play a significant role in small channels.

The effect of jetties on the inlet size is believed to be the result of the absence of relevant action of sea waves which results in relatively small inlets. Channels in the outer delta of a tidal inlet are more exposed to sea waves and, consequently, have relatively large cross sections.

The effects of bed roughness and small waves on the size of small tidal channels and of sea waves on channel profiles in the outer delta and tidal inlets suggest that the application of the shear stress velocity in the hydraulic parameters would improve the validity of the empirical relation. This better satisfies the condition that equilibrium along a tidal channel only can exist if there are no longitudinal gradients in the sediment transport capacity per metre width. This is strongly determined by the longitudinal gradient in a characteristic shear stress velocity which should be zero. Therefore, parameters as shown in equations (3.8) through (3.10) are preferred.

By using e.g. equation (3.8) in a relative sense a practical reference parameter is obtained, which represents a kind of virtual tidal volume i.e.:

$$TV_{rv} = TV_r \left\{1 + \frac{1}{2} (\xi \hat{U}_o/\overline{u})^2\right\}^{1/2} C_r/C \qquad (3.28)$$

The reference conditions are relatively large tidal channels and inlets with modest or negligible wave influence (term $\{...\}_r^{1/2} \approx 1$) which is already included in the constant c_A.
A reasonable reference value for the Chezy coefficient for those channels will be $C_r = 55\ m^{1/2}/s$.
Thus, in most cases the term $\{...\}^{1/2}\ C_r/C$ will be close to unity. Only in small channels or in large channels in the outer delta it will exceed unity yielding a virtually larger tidal volume which takes into account the extra effects of waves and increased bed roughness on sediment transport.
This yields the more universily valid relation (Fig. 3.45):

$$A_{c,MSL} = -157 + 448\ 10^{-6} \left[P_m \left\{1 + \frac{1}{2} (\xi \hat{U}_o/\overline{u})^2\right\}^{1/2} 55/C\right]^{0.90} \qquad (3.51)$$

This equation rather well compares with those derived for a wide range of larger inlets or tidal channel cross sections as presented by Jarret (Eq. 3.32), Hume and Herdendorf (Eq. 3.33), Dieckmann (Eq. 3.44) or derived based on data of O'Brien (Eq. 3.29) and Walton and Adams (Eq. 3.52).

It is proposed to use relation (3.51) for $A_{c,MSL}$ as a basis for engineering. The related sizes for the cross-sectional area $A_{c,MHW}$, A_c' and $A_{c,MLW}$ best can be obtained through firm direct relations between those and $A_{c,MSL}$ (Eqs. 4.18-4.20) as presented on Figs. 3.30-3.32 or, even better, relations (3.17) and (3.18) which take into account the physics of the cross-sectional profile. This prevents the risk of inconsistent results such as $A_{c,MLW}$ becoming larger than $A_{c,MHW}$ which can happen if independent relations with P are used.

Channel depth and width

The channel profile has a degree of freedom in its shape to compensate for the effect of different factors which limit the extension in width or depth. This implies that empirical relations for the channel depth or width will show a much weaker correlation with actual data than those for the channel profile and, so, are less reliable.

For the Dutch Wadden Sea the following best fits have been derived for the channel depths:

$$d_{NAP,max} = 0.0098\ P_m^{0.39} \qquad (4.2)$$

$$\overline{d}_{NAP} = 0.00094\ P_m^{0.47} \qquad (4.4)$$

$$\overline{d}_{MLW} = 0.00090\ P_m^{0.47} \qquad (4.7)$$

For the channel widths the following best fits have been derived:

$$W_{NAP} = 0.155\ P^{0.5} + 200 \qquad (4.9)$$

$$W_{MLW} = 0.049\ P^{0.55} \qquad (4.11)$$

The great variety in relations in literature and the considerable scatter in the different data sets confirm that reliable relations on channel width, mean and maximum channel depth do not really exist. These quantities strongly depend on local flow and bed conditions. They never should be used in combination to derive the cross sectional area, but only as a secondary relationship to get an idea of the shape of a cross section of a certain size.

side slopes

Channel width is not always determined by waterlines on two banks. Generally this does happen at MLW. At higher waterlevels, however, two adjacent channels often are separated by a watershed. At NAP this occurs rather frequently and at MHW it even is common. Considering the definition of the average side slopes 1/S1 between MHW and NAP and 1/S2 between NAP and MLW (Section 4.3), this implies that S2 and particularly S1 are not representing the actual average bed slopes. They merely represent fictive slopes which can be used in relations like (3.17), (3.18) and (4.16).

Best fits for the fictive side slopes do not really exist (see Figs. 4.14 and 4.15). The relations between the parameters S1 and S2 and both P and $A_{c,NAP}$ show a huge scatter. In general the average value of S1 ranges between 100 and 200 and that of S2 between 200 and 300. In S2 a weak positive correlation with P and $A_{c,NAP}$ seems to exist.

Channel volumes

In literature also quite strong correlations are shown between the volume of a channel system behind a particular cross section and the size of the related basin or the tidal prism at that cross section. This holds for the volumes below MHW, MSL and MLW. The best fit relations generally are of the form:

$$V_{rl} = \alpha_{rl} P^n$$

were α_{rl} and n are empirical constants related to the reference level rl below which the volume is determined. In those relations n increases with decreasing reference level. This means that the relations intersect at some high value of P which is unrealistic. Therefore it is proposed to bring more physics in the relationships as shown in equations (5.8), (5.9) and (5.10). Thus a consistent set of relations is derived of which only one must be determined fully empirically, e.g. the one for V_{MSL} or V_{MLW} (see Eqs. 5.13 and 5.14). Of these V_{MSL} is preferred. The others can be derived from that by means of the relations for β_p (Eq. 5.15) and γ_p (Eq. 5.16). Thus quite reliable results can be obtained.

Based on theoretical considerations the volume V_{NAP} below NAP ($\approx V_{MSL}$) also has been correlated with the parameters PL and $\{(L/B)/\overline{\Delta h}\}^{0.5}.P^{1.5}$. In this L and B are the maximum length and width of the basin respectively and $\overline{\Delta h}$ the average mean tidal range. The derived relations (Eqs. (5.17) and (5.18)) thus partly include the effect of the shape of the basin and of the tidal range.
It is proposed to use one of these relations to determine V_{MSL} and the equations (5.9), (5.10), (5.15) and (5.16) to calculate the related volumes V_{MLW} and V_{MHW}.

Sand volumes in outer deltas

In front of each tidal inlet an outer delta or ebb delta has formed as a result of a balance between sediments thrown into the sea by the ebb currents and sediments which are removed by the action of waves and flood currents. Walton and Adams (1976) derived empirical relations for the amount of sand that is stored in such a delta compared with a situation with a normal shore profile. They found for a large data set of American inlets that distinct relations exists between the sand storage in the outer deltas and the tidal prism of the inlets and the local wave climate (Fig. 6.1). In spite of the scatter around the relations for three different classes of wave climate, these relations give a good approximation of morphological tendenses.

In the present study the sand storage of the outer deltas of the inlets Marsdiep, Eierlandsche Gat, Vlie and Borndiep have been determined and plotted in the diagram of Walton and Adams. These data quite well fit the relation for the highly exposed coasts in which class they belong. So, this confirms that the relation of Walton and Adams for highly exposed deltas is also valid for the Dutch outer deltas.

Relative tidal flat areas

The tidal flat area or the intertidal zone of the Wadden Sea, that is the area that normally inundates and dries twice a day, is of great importance as feeding ground for many birds. In this study the tidal flat area A_f is defined between MLW and MHW.

From a morphological point of view the tidal flats reduce the tidal prism of the basin and, hence, effect the size of the channels. The larger and the higher the

intertidal zone, the smaller the tidal prism is. This directly follows from the following equation:

$$P = (1-\alpha_f A_f/A_b) A_b \overline{\Delta h} \qquad (7.1)$$

This equation gives the calculated tidal prism, i.e. V_{MHW} - V_{MLW}. For large basins this should be reduced with the factor γ_p presented in Eq. (5.16) to approximate the actual mean tidal prisms for the Dutch Wadden Sea basins.

The relation for α_f is presented in Fig. 7.16 and the relation for A_f/A_b can be derived from Fig. 7.5 through $A_f/A_b = 1 - A_{ch}/A_b$. Finally, the average mean tidal range $\overline{\Delta h}$ can be determined from Fig. 7.6.

According to general classifications the presence of tidal flats depends on the tidal range. This parameter is not the only one though. For the Dutch Wadden Sea with a meso-tidal range, the relative tidal flat area A_f/A_b can not be directly correlated with the tidal range as suggested by Dieckmann (1985). His relation is believed to be accidental as argued in Section 7.2. It is believed that the main quantities that determine A_f/A_b are the size A_b and the shape of the basin which might be classified by a length over average width ratio L^2/A_b. Other relevant quantities might be the orientation of the basin relative to the dominating wind, the width over depth ratio of the main tidal channels and the local wind climate. At first glance there seems to be no systematic influence of the tidal range. Further investigations on this aspect are recommended by including data of the Dutch Delta area or other areas in the study. Attention should be focussed on characteristic fetch lengths, wind energy and tidal range.

Height of tidal flats

The heights and profiles of individual tidal flats show a great variety. In the Dutch Wadden Sea the crest levels of most of the flats range between MSL and MHW - 0.3 m (Fig. 7.7). Only in the Dollard the crest levels in some places reach up to almost MHW. On the watersheds between the basins the bed levels roughly varies around MHW -1 m.

The crest of a tidal flat is located at the watershed between two channels and generally the level seems more or less related to the width of the tidal flat. A

second factor governing the crest level seems to be the stability of the watershed. If it is rather stable and the same for ebb and flood, the crest level will be relatively high. If not, the tidal flat may remain relatively low. This might be the case in the area of the Pollen.
The height limitation of crest levels to MHW -0.3 m may be caused by local wave action and/or regular storm surges with combined wave action and drift currents passing over the flats at HW.

It is believed that the height of a tidal flat somehow is related to MHW and the local flow and wave conditions. Evidence to support this hypothesis is scarce and indicative only. The most firm support is found in the rapid adaptation of the tidal flat levels in the Dollard after the increase of the MHW level due to deepening of the navigation channel to Emden (Fig. 7.13).

A general relationship for the height of tidal flats only is possible at a high integration level. Therefore, Dieckmann (1985) used the median heights of all tidal flats in a basin or sub-basin ($H_{0,5A}$ i.e. 50% in area is lower and 50% is higher) and in this study the average height of the flats above MSL was used (i.e. $\alpha_f\overline{\Delta h}$). Dieckmann related $H_{0,5A}$ to MLW though a relation with MHW seems more realistic (Fig. 7.15). In this study the average tidal flat level was related with MHW and basin size A_b (Fig. 7.16). The results show α_f to be related with A_b (Fig. 7.16). The distance of the average flat level below MHW, i.e. $\overline{\Delta h} - \alpha_f\overline{\Delta h}$, appears to be rather constant and generally fluctuates between 1.1 m and 1.5 m below MHW with an average of 1.3 m. In small basins the latter may increase to 1.4 m to 1.5 m below local MHW.

2. Selected data of the Dutch Wadden Sea

2.1 General

An important activity of the present study was to create an extensive file with reliable basic data of all tidal basins of the Dutch Wadden Sea consisting of:

- sounding maps of the entire basin and its outer delta of a period of a few years not preceeded by important changes by man,
- discharge measurements in the tidal inlet and in other cross sections (if available) of the same period,
- characteristic tide levels of a number of stations in the basin of that period,
- wave climate data of the adjacent North Sea and in the tidal basin (if available).

To that end Van Kleef made an inventory of available field data with Rijkswaterstaat and of relevant reports and literature of that area (Kleef, 1991b). The inventory was focussed on the period since 1945 but also includes data back to 1932 (closure of the Zuiderzee) or even 1910. Based on the results of this inventory a period was selected for each tidal basin in which a complete set of bathymetric maps was available as well as discharge measurements. The periods were selected bearing in mind that no relevant human interference had occurred in the preceeding period or that the time elapsed since such an event was as long as possible to be sure that the data are representative for an equilibrium situation. In general this will be true except for, may be, the tidal basin of the inlet Marsdiep.

During the collection of the selected data Biegel extended the inventory to some extent (Biegel, 1991), whereas Lambeek among others made an inventory of sedimentological data (Lambeek, 1991).

From the above data set a great number of relevant parameters can be derived such as:

- size of the basin, channel area and tidal flat area,
- characteristics tidal levels and ranges,
- storage curves of the basins and parts of it, i.e. the horizontal (wet) area as a function of the level relative to NAP,
- flow areas (below MHW, NAP (≈ MSL), MLW and level at maximum flow) and profiles of selected channel cross sections in the basin, the inlet and at the outer

delta where a tidal prism has been measured or can be reliably derived from a measured one,

- mean and maximum channel depths below NAP and channel width at NAP and MSL,
- channel volumes (below MHW, NAP and MLW) of the entire tidal basin and parts of it behind selected cross sections,
- sand volumes stored in the outer deltas according to the definition of Walton and Adams (1976),
- tidal volumes passing the selected cross section,
- maximum discharge rates and related water levels,
- maximum and mean tidal flow velocities,
- maximum and mean tidal shear stress velocities,
- weighted wave heights and periods at selected, cross sections to determine the relevant wave effect on the shear stress velocity (Bijker factor),
- hydraulic radius of selected cross sections,
- stability shear stress as defined by Bruun (1960) and Gerritsen (1990).

This list can be extended with other parameters if considered useful.

2.2 Bathymetric data and ripple data

Of all areas the sounding maps at a scale of 1:10,000 where available with depth information at a 25 m interval along the sounding tracks and 200 m, 100 m or 50 m spacing between the tracks depending on the complexity of the seabed. In general the tracks are as much as possible oriented perpendicular to the channels. This results in reliable bathymetric maps with accurate depth-contour lines, except for the bathymetry of small gullies and creeks smaller than 25 m especially if those run parallel to the sounding tracks. Often those gullies are indicated on the maps based on information from aerial photographs.

All soundings are digitized and fed into a computer data base. For the basins of Marsdiep, Eierlandse Gat, Vlie and Borndiep in the western Wadden Sea the average depths is determined for grid cells of 250 x 250 m based on a minimum of 20 observations per cell. Due to this coarse grid this information is not suitable anymore to be used for the study on parts of the basins with smaller channels.

The bathymetric data of the basins of the eastern Wadden Sea, i.e. Pinkegat, Zoutkamperlaag, Eilanderbalg, Lauwers, Schild and Eems, are digitized in a different and more detailed way. There the depth contour lines are digitized at a 25 m interval. Through linear interpolation between the depth contour lines the average depth is determined in grid cells of 25 x 25 m, 50 x 50 m or 100 x 100 m depending on the complexity of the sea bed. In this way hardly any accuracy is lost in cross-sectional profiles, areas within contour lines and depth. This data base also can be used to study subsystems in a tidal basin. The selected sounding maps of the various basins are shown in Table 2.1.

In 1976 ripple measurements have been performed in a great number of locations in the channels of the basins of Marsdiep and Vlie. The results of these measurements can be used in the derivation of hydraulic parameters like the roughness coefficient of Chézy, the shear stress velocity or the stability shear stress.

2.3 Tide data

Water levels have been and are recorded in a great number of stations along the bank of the Wadden Sea and in front of the tidal inlets (see Fig. 2.1). Most of those stations have a permanently recording gauge. On top of that records are available of a great number of temporary tide gauges at different places scattered all over the Dutch Wadden Sea. Based on this maps have been drawn up with lines of equal MHW and MLW as well as lines of simultaneous MHW and MLW (Fig. 2.2). These maps originate from the early seventies and are presented in Mazure et al (1974). They distinctly show that the levels of MHW and MLW in the Wadden Sea are not horizontal levels.

Data of the standard tide stations are available at Rijkswaterstaat in the DTBEST data base and in annual and ten-yearly reports. These reports also present monthly and annual mean values of HW and LW and for a number of stations also MSL. From these data long-term trends and effects of human interference in the Wadden Sea can be recognized.

2.4 Tidal flow data

Over the years Rijkswaterstaat has conducted a lot of tidal flow and discharge measurements in all tidal basins of the Dutch Wadden Sea, sometimes combined with sediment transport measurements.
Generally the tidal flow measurements in channels have been done from an anchored survey vessel and flow velocities have been regularly measured at different positions in depth. This provides the vertical velocity profile over a full tidal cycle. In case of discharge measurements simultaneous flow measurements have been carried out in a number of points in a cross-section to cover the horizontal flow profile over that section. If necessary, autonomous recording current meters were installed at relevant (parts of the) sections in the intertidal zone to cover that part too. During the discharge measurement a local tide gauge was installed to record the local water level and the actual bed profile along the cross-section was sounded shortly before or after the flow measurements. Based on these measuring data reliable discharge data could be derived and subsequently actual tidal volumes passing that cross-section.

Through the tidal range at a suitable reference station the measured flow data can be converted to mean tidal conditions or mean spring tide conditions. These data of various measuring locations can be reliably transformed to a consistent set of "simultaneous" flow data for each tidal basin.

In Table 2.2 the years are presented in which discharge measurements have been performed at least in the throat of the tidal inlet. Also is indicated if more discharge measurements have been performed in that basin at other locations. From these data the most appropriate ones are selected with the selected bathymetrical data (see Table 2.1).

2.5 Wave data

According to the inventory of available data (Kleef, 1991b) wave data are collected over a period of at least one year in 14 stations along the North Sea coast of the Wadden Islands, in some of the tidal inlets or inside the basins of the Zoutkamperlaag and the Eems-Dollard. The rough data are stored in the database DTBEST of Rijkswaterstaat. Unfortunately, most of these wave records have not been processed into wave roses or wave-height exceedance curves and, hence, are unsuitable for this study.

Roskam (1988) presents wave climate data for 8 North Sea stations along the Dutch coast. Processed wind and wave data of the lightvessels Goeree, Texel and Terschellingerbank are presented by Bakker and Bangert (1971). Wind, sea and swell data of the lightvessel Texel are also presented by Hoozemans (1988). For the more northern station at the North Sea "Schiermonnikoog-Noord" wind and wave climate data are presented by Van Urk (1985). Ribberink and De Vroeg (1991) present wave climate data of the North Sea station Eierland in front of the inlet Eierlandse Gat. Moreover they present the transferred wave climates at water depths of NAP -10 m and -6 m. Besides wave propagation computations have been performed for the Eierlandse Gat basin and its outer delta, which provides information on wave height reduction in the area of interest. The latter also has been done for the inlet of Texel by Den Adel to verify and compare the wave propagation models CREDIZ and HISWA (Adel, 1988).
Wave height reduction studies also have been performed by Niemeyer for the tidal basin of the inlet of Norderney (Niemeyer, 1986) and the Ley Bay (Niemeyer, 1991). Koning and Kreuk (1976) present the results of wave measurements in two stations due south of the island of Terschelling and, finally, Van Urk (1982) describes the wave climate in the throat of the inlet Schild based on some 4 years of wave data.

Based on the wave information in the above mentioned literature it is possible to get a fair estimate on the occurrence of waves at various characteristic locations in the Wadden system. This will be sufficient to determine representative morphological wave parameters for the present study.

2.6 Sediment data

A general relation between hydraulic conditions and sediment characteristics of the top of the bottom of the Dutch Wadden Sea is presented in (Eysink, 1979). This is based on results of extensive investigations of the former Rijksdienst IJsselmeerpolders (RIJP) and Land Reclamation Department of Rijkswaterstaat in Baflo in the period after World War 2, when empoldering of the Wadden Sea still was an option, and of scientific researchers of the former geological department of the University of Groningen and of NIOZ in Texel. The general patterns showed great similarity with those in the Western Scheldt estuary (Salomons et al, 1981).

More recently investigators tried to establish relations between abiotic and biotic parameters in the Dutch Wadden Sea as described in Lambeek (1991).

3. Morphological relations of tidal channel profiles

3.1 General

It appears from literature that people are aware of some relation between size and tidal volume of a tidal inlet since at least the beginning of this century (Le Conte, 1905; Brown, 1928 and O'Brien, 1931). This resulted in a general relationship like:

$$A_{c,MSL} = c_A P^n + a \qquad (3.1)$$

where:

$A_{c,MSL}$ = flow area below MSL in the throat of the inlet,

P = representative tidal prism of the basin,

n = empirical coefficient,

c_A, a = empirical coefficients depending on the definition of P, the value of n and the selected reference level (in this case MSL).

This relation has been confirmed many times ever since, where the empirical coefficients n, a and/or c_A seem to be dependent on local conditions such as:

- type of tide (semi-diurnal, diurnal or mixed),
- wave climate (calm, moderate, rough),
- size of inlet (small, general range, large),
- presence of jetties, and possibly,
- type of bed material, upland sediment transport rate, littoral drift and/or salinity effects on flow profiles.

To some extent the data in literature will be effected by inaccuracies in particularly the tidal prism. In several cases the tidal prism has been calculated based on the tidal range and the size of the basin behind the inlet. Especially for large basins this may introduce significant inaccuracies.

The tidal prism in equation (3.1) must be considered as a characteristic hydraulic parameter representing the integrated hydraulic energy which is present in the everlasting tidal flow passing the inlet. Other authors used related parameters such as:

- Flood volume FV,
- Ebb volume EV,
- Tidal volume TV = FV + EV,
- Maximum discharge rate Q_{max} related to P, FV or EV,
- Maximum discharge rate $\hat{Q}$ related to a sinusoidal tide,
- Maximum flow velocity u_{max} or $\hat{u}$ related to Q_{max} and $\hat{Q}$ respectively,
- Average tidal velocity $\overline{u}$ related to P, FV, EV or TV,
- Stability shear stress velocity u_{*_s} or shear stress τ_s related to Q_{max}.

This was done to arrive at a better fit and a trial to find the best physical parameter related as closely as possible with sediment transport. The need for distinction between ebb and flood arose from studies on inlets of estuaries with upland discharge and of tidal channels with ebb or flood dominance.

The use of the stability shear stress τ_s is introduced by Bruun and Gerritsen (1960) and used by the latter et al in studies on the stability of Dutch inlets and tidal channels in the western Wadden Sea (Gerritsen, 1990; Gerritsen and De Jong, 1983, 1985; Jong and Gerritsen, 1984; Gerritsen et al, 1990). Through τ_s the effect of waves can be taken into account by applying the concept of Bijker (1967). A promising option might be the application of the parameter with τ_s:

$$A_c = c_\tau \{Q_{max} / (C\sqrt{\tau_s / \rho g})\}^n + a \qquad (3.2)$$

where:

A_c = flow area of tidal channel below MSL or, even better, below the water level at which Q_{max} occurs,

c_τ, a = empirical coefficients,

n = empirical exponent,

C = roughness coefficient of Chézy,

ρ = density of water,

g = gravitational acceleration.

In this way also the effect of the bed roughness and the hydraulic radius of the channel profile is taken into account through the Chézy coefficient which could be a relevant parameter.

3.2 Correlation of channel profiles with hydraulic parameters

3.2.1 Basic considerations on hydraulic parameters

To derive a practical and reliable empirical relationship on channel profiles for the Dutch Wadden Sea a great number of cross-sections has been selected in the different basins of that sea for correlation with different hydraulic parameters. Basically, each hydraulic parameter is correlated with the cross-sectional area below a number of releference levels, that is: MHW, NAP (≈ MSL), MLW and the water level at which maximum flow occurred.

For a proper understanding it is noted that the different hydraulic parameters in fact are interrelated and generally incorporate minor differences. For example: A relation between A_c and a reference tidal volume TV_r is directly related to the mean velocity $\overline{u}_r$ through:

$$TV_r = \int_0^{T_r} u\, A_c\, dt = \overline{u}_r\, A_c\, T_r \qquad (3.3)$$

If we assume $A_c = c_A.TV_r$ than the interrelation reads:

$$\overline{u}_r = TV_r/(A_c\, T_r) = 1/(c_A.T_r) \qquad (3.4)$$

Or in general (see Eq. (3.1)):

$$\overline{u}_r = \{(1-a/A_c)/(c_A\, T_r)\}^{1/n} * (1/A_c\, T_r)^{(n-1)/n} \qquad (3.4a)$$

Hence, both parameters TV_r and $\overline{u}_r$ are fully comparable and ignore the effect of the flow velocity history, bed roughness and waves.

A relation between A_c and the maximum discharge rate Q_{max} in fact means a relation with the maximum flow velocity u_{max} through:

$$Q_{max} = u_{max}\, A_c \qquad (3.5)$$

This actually assumes a relation between A_c and extreme flow conditions when most of the sediment is transported. This ignores the effect of the flow velocity history, flow duration, bed roughness and waves. In case the flow velocity

histories and shapes of the tidal wave for different situations are comparable, this parameter will not yield better fits than obtained with $\overline{u}_r$ or TV_r.

In most cases u_{max} and $\overline{u}_r$ are fairly well related to the tidal range. At least locally the ratio of the springtide range over the meantide range is constant. Consequently, the fits for A_c with springtide parameters will be similar to those for meantide parameters; only the empirical constants will differ.

Significant differences in this respect may occur in areas with tides with a significant daily component and where the shape of the tide changes over the neaptide-springtide cycle. This is not the case in the Wadden Sea.

A principal difference is introduced if not the ordinary flow velocity is taken as the major hydraulic parameter but the shear stress velocity u_*. In that case also the effects of bed roughness and waves on the morphological parameters can be taken into account through:

$$u_* = \frac{\sqrt{g}}{C}\, u \{1 + \tfrac{1}{2} (\xi \frac{\hat{u}_o}{u})^2\}^{\frac{1}{2}} \qquad (3.6)$$

where:

( ) : wave effect parameter of Bijker (1967)

ξ : empirical parameter

$\hat{u}_o$: maximum orbital velocity at the channel bed

The application of u_* or the bed shear τ is similar as they are directly related through:

$$u_* = \sqrt{\tau/\rho} \qquad (3.7)$$

Replacing u by u_* in the equations (3.3) and (3.5) actually means:

TV_r becomes $TV_{*r} = TV_r \{1 + \tfrac{1}{2} (\xi\, \hat{u}_o/\overline{u}_r)^2\}^{\frac{1}{2}} \sqrt{g}/C$ (3.8)

$\overline{u}_r$ becomes $\overline{u}_{*r} = \overline{u}_r \{1 + \tfrac{1}{2} (\xi\, \hat{u}_o/\overline{u}_r)^2\}^{\frac{1}{2}} \sqrt{g}/C$ (3.9)

Q_{max} becomes $Q_{*max} = Q_{max} \{1 + \tfrac{1}{2} (\xi\, \hat{u}_o/u_{max,r})^2\}^{\frac{1}{2}} \sqrt{g}/C$ (3.10)

The corrected parameters include now that sediment is transported more easily under conditions with waves (term $(\ )^{\frac{1}{4}} > 1$) or if bed roughness increases (C decreases). If we look into the longitudinal direction of a tidal channel, equilibrium only can exist if the sediment transport capacity does not change in that direction (no transport gradients). This only holds in case u_* does not show a gradient in that direction. Consequently, the flow velocity u must be lower in areas with waves or with a high bed roughness and, so, the cross-sectional area there must be larger than under "normal" conditions. This tendency is clearly demonstrated in channels in the outer delta (waves) and in small tidal channels (small hydraulic radius and small C-values) (Gerritsen, 1990).

Hydraulic parameter (3.10) basically is the same as the parameter proposed by Gerritsen which is shown in equation 3.2. He divided this parameter by $\sqrt{\tau_s/\rho}$ to achieve a dimensionless coefficient c_τ. τ_s represents a constant reference shear stress which should be valid in all situations, except for wave effects. In the latter case the discharge rate Q_{max} should be increased by multiplying with the square root of the Bijker parameter to include the wave effect in the shear stress velocity represented by $Q_{max}.\sqrt{g}/C$ in equation (3.2).

3.2.2 Basic considerations on sediment related parameters

Gerritsen (1990) tried to further improve relation (3.2) by replacing the stability shear stress τ_s by the dimensionless shear stress parameter τ_s^* defined as:

$$\tau_s^* = \mu\ \tau_s/\{(\rho_s-\rho)\ g\ D_{50}\} \qquad (3.11)$$

where:

μ : ripple factor

ρ_s : density of sediment

D_{50} : median grain size of sediment

Thus also the properties of the sediment are included in the empirical relationship as well as the effect of bed forms on the bed shear through:

$$\tau_s' = \mu\ \tau_s \qquad (3.12)$$

where τ_s' : effective stability shear stress

and:

$$\mu = (C/C')^{3/2} \qquad (3.13)$$

with

$$C = 18 \log(12R/k_s) \qquad (3.14)$$

and

$$C' = 18 \log \{12R/(D_{90})\} \qquad (3.15)$$

where:

D_{90} : sieve diameter through which 90% of the sediment (by weight) passes

C' : grain related Chézy coefficient.

Though the above idea seems logic it includes some serious drawbacks. In the first place the relation becomes very complicated without achieving a significant improvement at least not in a practical sense. Even if this approach might result in the best fit after a thorough study on the additionally required data on sediment properties, it very likely introduces inaccuracies if the relationship is used for predictions and the then unknown data have to be estimated. So, from a practical point of view this approach is not favoured. Besides, the ripple factor μ and the grain related Chézy coefficient are not always defined in the same way in literature, which may cause confusion. Moreover, they are specifically related to bedload transport which in general only plays a modest role in tidal channels. Finally, it is known that tidal motion in the Wadden Sea and in estuaries acts as a hydraulic sorting machine and sorts sediments according to their fall velocity. The coarse and heavy minerals with a relatively high fall velocity are found in areas with strong currents and/or wave action (high energy level) whereas fine and generally lighter minerals with a low rollability and low fall velocity are found in areas with weak currents and modest wave action (Eysink, 1979). Consequently, it may be expected that a rather close relation will exist between channel dimension and the composition of the bed. This relation will show a trend correlating large channels with relatively coarse sand and small

channels with relatively fine sand. So, applying equations (3.11)-(3.13) will not reduce the scatter but only may result in systematic changes in the empirical constants.

For above reasons the parameters τ_s^* and τ_s' have not been taken into consideration. The effect of the sediment properties indirectly are taken into account through the definition for the bed roughness k_s. This parameter largely depends on the bedforms which on their turn are determined by the sediment properties and the flow regime.
A lot of studies have been performed on this parameter which nearly all are related to rivers and flume studies, though, with steady state flow conditions or wave conditions. Only a few studies are known in which k_s has been considered for tidal channels. These studies did not result in generally accepted relationships which can be used in this study.
Gerritsen (1990) referred in his report to the work of Boender (1977) and Van der Berg (1987). Boender used a lot of flow measurements from the Wadden Sea and the Western Scheldt to find a relation between the instantaneous depth-averaged flow velocity and the Chézy bed-roughness coefficient. The latter is determined in two different ways from flow velocity profiles at different tidal stages throughout the tide and on different locations. This is done through fitting the flow profiles to a logarithmic velocity profile. Thus values are obtained for k_s and C. Then C is plotted versus the depth average flow velocity $\bar{u}$. This results in a relation between the two parameters with a rather low correlation coefficient. In these relations the effect of the differences in the hydraulic radii in time and place is ignored. To avoid this a relation should have been studied between $\bar{u}$ and k_s instead of C. A check on this, however, showed no relation at all.

Boender and De Reus (1978) did a check on the relation of Boender in a flume study using a fixed sinusoidal bed and a fixed water depth. This study resulted in a similar relation indicating that a fixed physical bedform in fact should not be represented by a constant bed roughness k_s. Obviously, this value virtually changes somewhat with the flow velocity due to local changes in the flow pattern near the bed in the wake of the bedform. For this study this is not of any interest as only tide-averaged characteristic parameters are relevant. In this respect we are looking for a relation between k_s and for example the tide-averaged flow velocity $\bar{u}$ or a representative maximum flow velocity u_{max} (mean or springtide) which would represent k_s as a function of the local flow regime.

Van den Berg (1987) concludes on the basis of fitting measured and computed sand transports in the Eastern and Western Scheldt that with a velocity dependent k_s better results are obtained than with a constant k_s. Based on this he suggests a relation for k_s which is valid for flow velocities of 1 m/s and higher. He states that this is realistic for those velocities (at least for u > 1.5 m/s) as then the sediment transports are sufficiently high to change the bedforms with changing velocity. However, the one example of bedform behaviour around maximum flow (u varied from 1.0 m/s through 1.5 m/s to low velocities) he presents did not show a significant change in the bedforms at all.

Voogt et al (1991) describe field measurements in the closure gab of a sand closure in the tidal channel Krammer. This included ripple measurements on the top of the 300 m wide sand sill in the gab. Measurements were made during a tide under four different conditions. The results showed bedforms that hardly changed over a tidal period, but did change with the tidal conditions. The bed roughness k_s was determined from the bedforms and related to the maximum flow velocity over the tide (see Fig. 3.1). This is the kind of relation we are looking for. Unfortunately, the results only are valid for a range of u_{max} from about 1.3 m/s to 2.7 m/s because of the high flow velocities in the closure gab. The waterdepths generally were within the range of 6 to 8 m.

Ripple measurements of Rijkswaterstaat in the Wadden Sea (Borndiep) supplemented with data of Van den Berg (1987), Voogt et al (1991) and some data presented by Van Rijn (1989) are presented in Table 3.1. These data suggest the average bedform (mega-ripples) height is roughly related to the waterdepth and generally is within the range of 4 to 8 per cent of the waterdepth. According to Van Rijn (1989) the roughness parameter k_s is related to the bedform height, length and shape with a minimum that is related to D_{90} of the bed material:

$$k_s = 3\,D_{90} + 20\,\gamma_r\,\Delta_r\,(\Delta_r/L_r) + 1.1\,\gamma_d\,\Delta_d\,\{1 - \exp.\,(-25\,\Delta_d/L_d)\} \qquad (3.16)$$

where:

Δ = height of bedform (r = ripple, d = dune or mega-ripple)

L = length of bedform (r = ripple, d = dune)

γ_d = shape effect parameter for dunes

γ_t = ripple presence parameter (0.6 - 0.8)

Van Rijn (1989) suggests $\gamma_d = 1$ for asymmetrical sand dunes with a leeside slope of 1:3 and $\gamma_d = 0.2$ for nearly symmetrical sand dunes with leeside slopes of 1:10.

In the latter case the flow remains attached to the bed and hardly experiences head losses due to deceleration behind a sand dune crest.
A transition between $\gamma_d = 1$ and $\gamma_d = 0.2$ for other leeside slopes could be derived from head loss data for a gradually widening channel presented by Thijsse (1951). The results are:

$\gamma_d = 1.0$ for leeside slopes steeper than 1:5 (flow separation)

$\gamma_d = 0.4$ for a leeside slope of 1:7

$\gamma_d = 0.2$ for leeside slopes flatter than 1:10

γ_d can be obtained by linear interpolation for leeside slopes between 1:5, 1:7 and 1:10 respectively.

In tidal areas equation (3.16) generally will result in a bed roughness k_s in the order of 1 cm to 15 cm. More investigation on this aspect is recommended which should focus on relating the occurrence of bedforms e.g. to waterdepth, mean tidal peak velocities, tidal range and location (channel, flats and outer delta).
In this study equation (3.16) has been simplified to:

$$k_s = 0.001 + 0.03 + 0.007\ R\ (m) \qquad (3.16a)$$

This has been used to derive the shear stress and shear stress velocity related parameters. As an alternative use could be made of a constant bed roughness:

$$k_s = 0.1\ m \qquad (3.16b)$$

3.2.3 Results of correlations

Correlation with normal flow parameters

Correlation with normal flow parameters, that is FV, EV, TV, $Q_{max,flood}$, $Q_{max,ebb}$ or the maximum of FV and EV (DV = dominant volume) or of $Q_{max,flood}$ and $Q_{max,ebb}$ (Q_{max}), generally shows similar and distinct correlations with $A_{c,MHW}$, $A_{c,NAP}$, $A_{c,MLW}$ and A_c'. In general scatter of the data around the average value is relatively larger for small channels, but of the same order of magnitude for the different hydraulic parameters (see Figs. 3.2-3.29). The best correlations are obtained for DV and Q_{max}. The application of TV (or the average of FV and EV) yields practically comparable results. The application of FV or EV yields only slightly worse results.

Taking into account practical aspects, the use of DV or TV is recommended above Q_{max}.

The relations for the considered cross-sectional profiles with the different hydraulic parameters all show a slightly non-linear character, though in a practical sense a linear fit shows a good approximation (see e.g. Figs. 3.2-3.29). The relation for $A_{c,MLW}$ shows the most linear character over (almost) the entire range of the selected tidal volume or Q_{max}. Besides, it shows the least scatter for all Wadden Sea data (same constants for all basins).

Part of the scatter in the data around the empirical relationships is determined by systematic deviations and part of it is caused by inaccuracies and incidental deviations in the individual data themself. The latter (partly) masks the systematic deviations in which we are interested in to improve the empirical relationships. To get a better impression in this respect the different cross-sectional profiles have also been mutually correlated. This resulted in very strong correlations which are shown in Figs. 3.30-3.32. The results show, at least for the Wadden Sea, that A_c' is almost equal to $A_{c,NAP}$. For the profiles $A_{c,MHW}$ and $A_{c,MLW}$ some systematic deviations of the linear relations can be noticed. A somewhat better fit is achieved by non-linear relations. Taking into account the physics of the cross-sectional profile the following relations can be derived (see Fig. 3.33):

$$A_{c,MHW} = A_{c,NAP} + W_{NAP} \cdot p\,\Delta h + S1\,(p\Delta h)^2 \qquad (3.17)$$

and

$$A_{c,MLW} = A_{c,NAP} - W_{NAP}(1-p)\Delta h + S2\,(1-p)^2\,\Delta h^2 \qquad (3.18)$$

where

W_{NAP} : channel width at NAP
p : part of the tidal range above NAP
Δh : local mean tidal range
S1,2 : mean side slopes of the channel between MHW and NAP and NAP and MLW respectively

This introduces the parameters channel width, side slopes and tidal range in the relation on top of the tidal volume or Q_{max} which may represent $A_{c,NAP}$. If W_{NAP} and S can be related to the same hydraulic parameter and Δh this will yield firm relationships between the cross-sectional profiles and the selected hydraulic parameter and the tidal range. This will be further elaborated in the next chapter.

The above suggests that the best results will be obtained if the best of the relationships between channel profile and hydraulic parameter is selected (either $A_{c,NAP}$ or $A_{c,MLW}$) and the others are derived from direct relations with that profile like equations (3.17) and (3.18).

Correlation with flow velocities

The mean tidal flow velocities related to the tidal volume TV or DV show a distinct relation with the hydraulic radius of the cross-section, though a considerable scatter in the data can be observed (Figs. 3.34 and 3.35). The relation is non-linear and can be expressed as:

$$\overline{u} = \alpha R^{\beta} \qquad (3.19)$$

where α, β = empirical constants

Considering Chézy's Law

$$u = C \sqrt{RI} \qquad (3.20)$$

the velocity u is proportional to $C \sqrt{R}$ for river flow where the slope of the energy level I is more or less dictated by the bed slope. In tidal areas the energy slope is not fixed and may partly compensate for a higher resistance. Thus, in tidal areas a relation may be expected with β in the range of 1/6 to 2/3 if C is taken proportional to $R^{1/6}$ (Manning). A proper value for β seems to be 0.3 to 0.4 which is valid for channels with a hydraulic radius exceeding say 2 m. For smaller channels the flow velocities drop below this relationship, presumably due to the effect of (small) waves.

The maximum flow velocity u_{max} related to Q_{max} also shows a relation with R but with much more scatter in the data (Fig. 3.36). This makes this quantity less meaningful for this study than $\overline{u}$.

Also the direct relation between $\overline{u}$ and u_{max} shows a lot of scatter and generally varies between (Fig. 3.37):

$$u_{max} = 1.2\ \overline{u} \quad \text{(lower limit)} \tag{3.21a}$$

and

$$u_{max} = 1.6\ \overline{u}^{0.5} \quad \text{(practical upper limit)} \tag{3.21b}$$

For a sinusoïdal tide the constant is equal to $\pi/2 = 1.57$. In general this gives a fair fit for the range of $\overline{u}$ above 0.5 m/s or rather for channels with R above 6 m. In part of the shallow channels relatively high maximum flow velocities occur.
Ignoring some extreme data a generally fair fit is obtained by (see Fig. 3.37):

$$u_{max} = 1.5\ \overline{u}^{0.8} \tag{3.22}$$

As stated before $\overline{u}$ seems to be a better parameter for morphological relations than u_{max}. The tide average flow velocity is related to the tidal volume and the cross section through:

$$\overline{u} = TV/(T.A_{NAP}) \tag{3.23}$$

Substitution of equation (3.23) and TV = 2P in equation (3.19) yields:

$$A_{NAP} = 2P/(\alpha T R^{\beta}) \tag{3.24}$$

Correlation of R with P shows a distinct relation which can be approximated by (Fig. 3.38):

$$R = \gamma\ P^{\delta} \quad \text{that is:} \quad R_{NAP} = 12\ 10^{-4}\ P^{0.46} \quad \text{or} \quad R_{NAP} = 5.3\ 10^{-4}\ P^{0.5} \tag{3.25}$$

where γ, δ = empirical constants

Substitution of this relation in equation (3.24) yields:

$$A_{NAP} = \{2/(\alpha T \gamma^{\beta})\}\ P^{(1-\beta.\delta)} \tag{3.26}$$

This very well explains the slight non-linearity in the relation between A_{NAP} and the tidal volumes (and Q_{max}) as mentioned before. With β = 0.3 to 0.4 and δ = 0.46 to 0.5 this yields an exponent n of 0.80 to 0.86 which very well matches the results of the direct correlations (see Figs. 3.3, 3.7, 3.11 and 3.23).

Correlation with shear stress parameters

The correlation with the shear stress parameters is restricted to the shear stress velocity defined in equation (3.6) and the related shear stress according to equation (3.7). Basically this results in the parameters defined in equations (3.8), (3.9) and (3.10). The Chézy-roughness coefficient is described by equation (3.14) with k_s defined by equation (3.16a).
The empirical parameter ξ from Bijker (1967) is described by:

$$\xi = 0.0575\ C \qquad (3.27)$$

Characteristic wave heights and periods are required for the computation of the different maximum orbital velocities. These waves should be representative for the effect of the local wave climate, that is they should give an increase in the local sediment transport by currents which is the same as the weighted average increase due to the local wave climate. Due to the non-linear effects this morphological wave has a height which is higher than the median wave height, but lower than waves which occur at a rather low frequency. To determine the exact morphological waves is rather difficult and time consuming. Therefore, these waves have been estimated by sound engineering judgement and are taken as those wave heights which are exceeded approximately during 25 percent of time. Taking into account the available data on wave statistics from literature and breaking of waves in shallow water this resulted in characteristic wave data as presented in Table 3.2. In general this means:

North Sea (deep water):	H_s = 1.5 m	T_s = 5.7 s
Channels in outer delta and inlet:	H_s = 0.6 - 1 m	T_s = 4 - 5.5 s
Wadden area inside the basins:	H_s = 0.3 m	T_s = 2.5 s

The results of the correlations with shear stress parameters based on the above mentioned starting points are discussed below.

For practical reasons correlations only have been made between $A_{c,NAP}$ and the hydraulic parameters FV_*, EV_*, TV_*, $Q_{*,max,f}$, $Q_{*,max,e}$ and $Q_{*,max}$. The results are shown in Figures 3.39 through 3.44 respectively. Mutual comparison of these figures shows that the correlation of $A_{c,NAP}$ with TV_* and $Q_{*,max}$ are the best. Next, comparison of these relations with those between $A_{c,NAP}$ and TV and Q_{max} (see Figs. 3.11 and 3.27) shows some more scatter for TV_* and $Q_{*,max}$ and a somewhat lower correlation coefficient. However, the relations become closer to a linear one with $n = 0.90$ instead of 0.80 as in case of correlation with TV or Q_{max}. As the data set of this study contains a lot of data of small channels, this has a distinct effect on the relations derived. For that reason the power n of the relations for the channel cross sections is lower than generally presented in literature (see Section 3.3.1). By applying the shear stress parameters including the wave effect this difference disappears. Therefore, it is believed that the principle of correlation with a hydraulic shear stress parameter is physically correct and should yield the best relation. A problem obviously is to find the proper characteristic roughness and wave data for each channel cross section, especially for the individual small channels. The application of $k_s = 0.1$ m (Eq. 3.16b) has not been considered anymore, as it is believed this would only further increase the scatter.

By using e.g. equation (3.8) in a relative sense a practical reference parameter is obtained, which represents a kind of virtual tidal volume, i.e.:

$$TV_{rv} = TV_r \cdot \{1 + \tfrac{1}{2}(\xi\, \hat{u}_o/\overline{u})^2\}^{\frac{1}{2}}\, C_r/C \qquad (3.28)$$

where:

TV_{rv} : virtual tidal volume

C_r : reference Chézy roughness, e.g. 55 $m^{\frac{1}{2}}/s$

The reference conditions are relatively large tidal channels and inlets with modest or negligible wave influence (term $\{...\}_r^{\frac{1}{2}} \approx 1$) which is already included in the constant C_A.

A reasonable reference value for the Chézy coefficient for those channels will be $C_r = 55$ $m^{\frac{1}{2}}/s$.

Thus, in most cases the term $\{...\}^{\frac{1}{2}}\, C_r/C$ will be close to unity. Only in small channels or in large channels in the outer delta it will exceed unity yielding a virtually larger tidal volume which takes into account the extra effects of waves and increased bed roughness on sediment transport.

Results of such a correlation with $TV_r = P_m$ are shown in Fig. 3.45.

3.3 Comparison of results with other data

3.3.1 Relations with tidal volumes

In 1931 **O'Brien** published his relation for the cross-sectional areas for inlets protected by two jetties along sandy coasts of the USA on the Pacific Ocean. The related tidal prisms for diurnal tide were computed from the bay dimension at mean sea level (MSL) and the tidal range.
In 1969 O'Brien published the same data and a lot of additional data on inlets with only one jetty or no jetties at all situated along the Pacific, Gulf and Atlantic coasts of the USA. The tidal prisms were based on springtide or diurnal tidal range. The cross-sectional areas are believed to be accurate within 10% and the tidal prisms within 15%. It appears that the whole set of data fits within one and the same relation (see Fig. 3.46). This relation also can be approximated by the relation:

$$A_{c,MSL} = 181\ 10^{-6}\ P_s^{0.94} \qquad (3.29)$$

It covers a large range of cross-sectional areas of 43 m² (Pendleton Boat Basin) to 232,260 m² (Delaware Bay).

Johnson (1972, 1973) studied virtually all of the inlets on the coasts of Washington, Oregon and California (Pacific Ocean) and used a mean tidal prism. He found similar results as O'Brien:

$$A_c = 678\ 10^{-6}\ P_m^{0.88} \qquad \text{(two jetties)} \qquad (3.30)$$

and

$$A_c = 60\ 10^{-6}\ P_m \qquad \text{(one or no jetty)} \qquad (3.31)$$

Comparison of the equations of O'Brien and Johnson for one or no jetty suggests a ratio $P_{spring}/P_{mean} = 1.1$. Johnson suggests that differences between protected and unprotected inlets are largely caused by wave influence.
In general the effect of jetties on the cross-sectional area seems to be small, that is in the range of inaccuracies as also suggested by O'Brien.
The major effect of the jetties is the positive effect on the depth to width ratio which is important for navigation.

Jarret (1976) studied a data set of 162 inlets of the Pacific, Gulf and Atlantic coasts. The tidal prisms (springtide or diurnal) were based on measurements, cubature from maps and/or data of other investigators. The data set contained inlets without, with one and two jetties. The relations obtained for the different coasts and types of inlets are shown in Table 3.3 and Figs. 3.47-3.49.
The relation valid for all inlets reads:

$$A_{c,MSL} = 158\ 10^{-6}\ P_s^{0.95} \qquad (3.32)$$

This shows a remarkable agreement with equation (3.29) based on O'Briens data.

It is noted that with the introduction of more data the scatter around the derived relationships distinctly increased relative to the data of O'Brien.

The data of Jarret have been extended with data of **small tidal inlets** by **Riedel and Gourlay** (4 small and sheltered Australian creek inlets, 1980), **Shaw and Elsawy** (7 small and exposed Arabian Gulf inlets, 198?), **Byrne et al** (14 inlets without jetties in the lower Chesapeake Bay, 1980) and **Mayor-Mora** (19 tidal inlets, sinusoidal tide with and without waves in a physical model, 1977). The results shown in Fig.3.50 distinctly deviate from the general trend found for the larger inlets.

Hume and Herdendorf (1990) presented data of 14 inlets in New Zealand ranging in size below MSL from about 80 m^2 to about 20,000 m^2 for mean tidal ranges of 1.2 to 2.2 m. The mean tidal prisms were based on discharge measurements and converted to mean springtide prisms. The relation they found for springtide reads:

$$A_{c,MSL} = 159\ 10^{-6}\ P_s^{0.953} \qquad (3.33)$$

Shigemura (1976, 1980) presented data of a great number of Japanese inlets on coasts with rocky headlands. He determined the cross-sectional areas below MLLW and related those to the computed tidal prisms for the mean tidal ranges in the bays. He found a very poor correlation which he improved by sorting the inlets into classes related to the parameter $r_A = A_{c,MLLW}/A_{basin,MSL}$. The physical meaning of this parameter seems doubtful.

Haring (1967) found for the inlets of the Dutch Delta area (5 inlets) the following relation:

$$A_{c,NAP} = 82.6\ 10^{-6}\ P_m \qquad \text{(with NAP} \approx \text{MSL)} \qquad (3.34)$$

For cross-sections of sub-channels or sections which were situated slightly more inland of the inlet he found relationships which can be transformed to:

$$A_{c,NAP} = 72 \text{ to } 75\ 10^{-6}\ P_m \qquad (3.35)$$

The size of the cross-sections ranged from about 4000 to 90,000 m².
The two above mentioned relations typically correspond with tide averaged flow velocities of 0.55 m/s and 0.60 to 0.62 m/s respectively.

For cross-sections of the Western Scheldt at the inlet at Flushing and landward **Gerritsen and De Jong** found good relationships for mean tidal prisms (1983, 1984):

$$\begin{aligned} A_c &= 78.3\ 10^{-6}\ EV - 988 \\ A_c &= 77.3\ 10^{-6}\ FV - 124 \\ A_c &= 76.9\ 10^{-6}\ DV - 1704 \qquad \text{(DV = max. of EV and FV)} \qquad (3.36) \\ A_c &= 38.9\ 10^{-6}\ TV - 557 \\ A_c &= 77.8\ 10^{-6}\ P_m - 557 \end{aligned}$$

This very well agreed with relations for the Western Scheldt found by **Eysink** (1991b) and **Allersma** (1991). They found respectively (mean tide):

$$A_c = 80\ 10^{-6}\ P_m \qquad (A_c = 5000 - 95{,}000\ m^2) \qquad (3.37)$$

$$A_c = 40\ 10^{-6}\ TV \qquad (A_c = 2500 - 90{,}000\ m^2) \qquad (3.38)$$

Allersma studied only the eastern part of the Western Scheldt. For the individual ebb and flood channels in that part he found a relation:

$$A_c = (1 \text{ to } 1.1)\ 10^{-3}\ TV^{5/6} \qquad (3.39)$$

He suggests that this relation is followed until the mean tidal volume reaches a value of about 750 million m³. Then the channel seems to become unstable and tends to split into two channels with a larger total area as the original channel. This

phenomenon seems to repeat itself at each next step of about 750 million m^3 in the tidal volume. Thus he found a general relationship which follows equation (3.38) around which the total cross-sectional area of 1, 2 or 3 channels respectively fluctuates (Fig. 3.51).

For the inlets and channels of the Eastern Scheldt and Grevelingen basins in the Dutch Delta area **Van den Berg** derived (1986) (mean tide):

$$A_c = 82\ 10^{-6}\ DV - 164 \qquad (3.40)$$

Considering that no noticeable upland discharge is present in those basins (DV ≈ P), this relation and the relations of Haring, Gerritsen and De Jong, Eysink and Allersma are very similar.

Gerritsen and De Jong (1985) also determined empirical relationships for a number of data of 4 tidal inlets of the western part of the Dutch Wadden Sea and for 12 cross sections of tidal channels in one of the basins (Vlie). These relationships read:

Tidal inlets western Wadden Sea

$$A_c = 58.5\ 10^{-6}\ EV + 4630$$
$$A_c = 62.1\ 10^{-6}\ FV + 3008 \qquad (3.41)$$
$$A_c = 30.1\ 10^{-6}\ TV + 3844$$

Tidal channels Vlie basin

$$A_c = 73.9\ 10^{-6}\ EV - 107$$
$$A_c = 69.4\ 10^{-6}\ FV + 362 \qquad (3.42)$$
$$A_c = 35.8\ 10^{-6}\ TV + 135$$

Also **Misdorp et al** (1990) determined a relation for 3 inlets of the western Wadden Sea based on data of different years. They found (mean tide):

$$A_c = 27.8\ 10^{-6}\ TV + 4227 \qquad (3.43)$$

This is rather similar to the relationship (3.41) of Gerritsen and De Jong. Both relationships are valid for cross sections of 10,000 to 70,000 m^2.

Haring as also Gerritsen and De Jong found the cross sections of the channels in the outer delta seaward of the throat of the inlet to be wider than according to the presented relations. This is expected to be caused by the increasing wave action going towards the fringe of the outer delta.

Dieckmann et al. (1988) presented a relation which is based on 26 of a total of 28 tidal inlets of the entire Wadden area along the Dutch, German and Danish coasts of the German Bight. The cross sections ranged from 2000 to 70,000 m^2. The tide in this region varies from low mesotidal to low macrotidal. They also included data of 11 inlet-type structures along this coast. The cross sections were derived from sounding charts and the tidal prisms from hypsometric curves of the different basins. The following relation for mean tide was obtained:

$$A_c = 372\ 10^{-6}\ P_m^{0.915} \tag{3.44}$$

Applying a ratio $P_s/P_m = 1.16$ for the German Bight data, those relations can be easily converted to mean spring tide and compared with the relations for the USA and New Zealand.

Eysink (1983) determined a similar relation for a study on the Nakdong Estuary in the South of South-Korea, applying a characteristic ebb volume which included the effect of the upland discharge of the river (see Fig. 3.52):

$$A_{c,MWL} = 80\ 10^{-6}\ EV_c \tag{3.45}$$

where

$$EV_c = P_m + Q_{bsr}T/2 \tag{3.46}$$

with $A_{c,MWL}$: area below MWL for a river discharge Q_{bsr}
EV_c : characteristic ebb volume
P_m : mean tidal prism in the dry season
Q_{bsr} : bed shaping river discharge, i.e. the discharge that yields the same annual sediment transport on the river as the regime does.

It is noted that by far most of the river flow occurred in a period of only about 2 months per year. During the rest of the year the river flow was very low. It was

encouraging that a relation was found which was valid for the entire estuary from the inlet to the actual river above the tidal region and that also would be valid in tidal channels without upland discharge.

Barua and Koch (1976), finally, determined a relationship for tidal channels in the Lower Meghna estuary in Bangladesh. They found:

$$A_c = 58\ 10^{-6}\ P_m \qquad (A_c = 10{,}000 - 75{,}000\ m^2) \qquad (3.47)$$

with the coefficient ranging between 51 and 90 10^{-6} with a best fit at 58 10^{-6}. The tidal prism was derived from flow measurements with often only 1 or 2 locations in very wide profiles. The hydraulic conditions in the area are rather complex with normal tidal channels with maximum flow around MSL and shortcut channels with maximum flow at distinctly different water levels. Further, there is a distinct seasonal effect with high river flow and a raised MSL. Insufficient information is presented to judge to what extent those effects have been taken into account. Nevertheless, this relation very well resembles the one of Johnson for inlets with one or no jetty (Eq. 3.31).
Both result in cross sectional areas which are about 25 percent below the relation for inlets with no or one jetty of O'Brien.

In general it can be stated that most relations for inlets with one or no jetty are quite comparable for inlet cross sections exceeding 100 to 500 m^2 below MSL (Fig. 3.53). They generally show a relation between the cross section and the tidal prism (mean or springtide) as presented by equation (3.1) with the constant a = 0 and the power n ranging between 0.915 (Dieckmann et al.) and 1.03 (Jarrett, all USA coasts; unjettied or single jettied inlets).
Some authors use a linear relation with the tidal prism and a certain value for the constant a (Gerritsen and De Jong, Van den Berg, Misdorp et al). In general this limits the validity of the relation to relatively large inlet sizes.

For **small inlets** of less than 500 to 100 m^2 the relation changes and seems to follow a relation with a power n = 0.7, i.e. (see Fig. 3.50):

$$A_c = 5.5\ 10^{-3}\ P^{0.7} \qquad (3.48)$$

Inlets protected by two jetties among others have been considered by O'Brien, Johnson and Jarrett partly based on the same data. This resulted in the following relations respectively:

$$A_c = 902\ 10^{-6}\ P_s^{0.85} \qquad \text{(all USA coasts)} \qquad (3.49)$$

$$A_c = 678\ 10^{-6}\ P_m^{0.88} \qquad \text{(Pacific coast of USA)} \qquad (3.30)$$

$$A_c = 749\ 10^{-6}\ P_s^{0.86} \qquad \text{(all USA coasts)} \qquad (3.50)$$

These relations have a slightly lower value of the power n than the partly or unprotected inlets, which results in somewhat smaller inlet areas.
On the one hand this may be explained by the reduced wave action in the sheltered inlets. This should result in smaller cross sections with higher flow velocities to compensate for the missing wave effect on the sediment transport in the inlet. On the other hand the data of the protected inlets remain within the scatter zone of all data and, as O'Brien (1969) already suggested, establishing a greater precision for these inlets may be unjustified.

The present study resulted in a tidal prism relation for a wide range of tidal inlets that reads:

$$A_c = -157 + 448\ 10^{-6} \left[P_m\{1 + 1/2\ (\xi\Omega_o/\overline{u})^2\}^{1/2}\ 55/C\right]^{0.90} \qquad (3.51)$$

This very well agrees with the other relations, especially those of Jarret (Eq. 3.32), Hune and Herdendorf (Eq. 3.33), Dieckmann (Eq. 3.44) or derived based on data of O'Brien (Eq. 3.29).

It is noteworthy to mention that Walton and Adams (1976) made a correlation between the sand volume stored in other deltas and both the tidal prism and the cross-sectional area of the tidal inlets. From these relations also a relation between P and $A_{c,MSL}$ can be derived which reads:

$$A_{c,MSL} = 124 \text{ to } 136\ 10^{-6}\ P_s^{0.96} \qquad (3.52)$$

This relation based on 44 tidal inlets very well corresponds with the relation for all inlets of Jarret (1976).

3.3.2 Relations with characteristic velocities

A linear relation between A_c and P without a constant "a" as found by some investigators implies:

$$P/A_c = 1/c_A$$

or

$$2P/(A_cT) = 2/(c_AT) = \overline{u} = \text{constant} \qquad (3.53)$$

It has been show by various investigators that this is not true over a large range of the size of the cross section. Also the results of this study demonstrate that the mean tidal velocity $\overline{u}$ is related to A_c or better the hydraulic resistance, which can be related to R, and the wave action which can be accounted for through the Bijker factor.
The first factor becomes increasingly noticeable in smaller channels and inlets, whereas the wave effect becomes particularly noticeable in channels in exposed areas, e.g. in the outer deltas.

To some extent the above mentioned effects counter balance each other. This can be explained as follows. A channel only can be in a state of equilibrium (migration not considered) if the sediment transport along the channel does not show gradients. So, in areas where waves contribute noticeably in the sediment transport, the same transport is achieved at lower flow velocities. This means that the cross-sectional profiles there will be relatively wider than those in areas without significant wave influence.
Solely arguing from the shear stress, the cross-sectional average velocity must increase with the size or rather hydraulic radius of the cross section to yield the same shear stress velocity and, hence, the same sediment transport. So, from that point of view the velocity level must increase (logarithmically) with the size of the channel. As the size of the channels generally grows from the inside of the basin towards the sea, the mean tidal velocity $\overline{u}$ increases in that direction. Near the inlet and on the outer delta, however, the influence of sea waves and swell increases, which tends to reduce the mean tidal velocity as explained before.

Considering different sizes of inlets a similar tendency can be recognized. With the size of the inlets also the size of the channels in the outer delta grow and the general bed level there drops. Therefore, larger waves can penetrate the outer delta and inlet area of larger inlets which counter balances the normal tendency of increasing $\overline{u}$ with increasing size of inlet.
In very small channels, however, even small local wind waves also may effect the sediment transport. There wave action and the reduction in water depth both result in lower flow velocities.

The above mentioned effects and the scatter in the data explain why linear relationships for large channels (i.e. 1,000 - 100,000 m²) yield good results; the smaller the range the better the fit of the linear relation.
The linear relationships without a constant presented in literature yield the following characteristic mean tidal velocities:

O'Brien	: $\overline{u}_s$ = 0.68 m/s	or	$\overline{u}_m$ = 0.60 m/s
Johnson	:		$\overline{u}_m$ = 0.75 m/s
Haring	:		$\overline{u}_m$ = 0.55 - 0.62 m/s
Eysink, Allersma:			$\overline{u}_m$ = 0.56 m/s
Barua and Koch	:		$\overline{u}_m$ = 0.77 m/s

The velocities obtained from Johnson and Barua and Koch are rather high, whereas the others are well comparable. Data on $\overline{u}_m$ presented by Gerritsen and De Jong read:

Western Scheldt estuary (excl. outer delta):	$\overline{u}_m$ = 0.55 - 0.65 m/s
Tidal inlets of western Wadden Sea :	$\overline{u}_m$ = 0.50 - 0.75 m/s
Vlie basin (more scatter) :	$\overline{u}_m$ = 0.40 - 0.80 m/s

In case of a non-linear relation between A_c and P the mean tidal velocity $\overline{u}_c$ is not longer a constant, but becomes dependent on the tidal prism:

$$\overline{u} = \frac{2}{c_A T} P^{(1-n)} \qquad (3.54)$$

This shows $\overline{u}$ will increase with increasing tidal prism and, hence, increasing channel cross-section, if n is smaller than 1. The opposite occurs if n is larger than 1.

Basically only Jarrett's results for the unprotected and partly protected inlets (no or one jetty) on the Atlantic and Pacific coasts suggest such a situation ($n = 1.07$ and 1.10 respectively). The actual maximum flow data (Fig. 3.54) to some extent may support this, though they also can be represented by a constant value (i.e. $n = 1$).

The flow data of the present study, valid for the throat of tidal inlets and channels in the Wadden basins, distinctly show an increasing trend in $\overline{u}_m$ with increasing channel size or hydraulic radius. This fits with the best fit relation for A_c with TV or P which shows n below unity. The data also fit with the mean tidal velocities mentioned before and similar data presented by Gerritsen en De Jong.

Some authors considered the cross-sectional averaged maximum flow velocity (u_{max}) as a hydraulic parameter, e.g. Byrne et al. They also found a decreasing flow velocity with decreasing channel area. The flow velocity tends to go to a minimum of about 0.35 m/s which might be related to the critical velocity for incepient motion. The data show a lot of scatter as also those presented by Hume and Herdendorf.

All data have been plotted in one figure to obtain a better view on the general tendency (Fig. 3.55).
The data have been compared with the maximum flow velocities computed based on as well the regression lines of Byrne et al. as on a smooth curve through the A_c-P data points and a sinusoidal tide (solid line). In general it can be stated that the actual maximum velocities for very small inlets (less than 10 m^2) and for the large inlets (more then 10,000 m^2) exceed the computed maximum velocities. Especially in small inlets this may be the effect of small waves and the distortion of the tide resulting in short periods with relatively high flow velocities which are needed to exceed the critical flow velocity for incepient motion. For the large inlets it may indicate an inaccurate regression.
The results confirm that u_{max} is not the most suitable parameter for a reliable morphological relationship valid over a large range.

3.3.3 Relation with maximum discharge rate

Van der Kreeke en Haring (1979) found a good relationship between A_c and the sinusoidal maximum discharge rate $\hat{Q}$ for mean tidal conditions that reads:

$$A_c = 1.17\ \hat{Q} \tag{3.55}$$

In fact this is the same as:

$$\hat{u}_m = 1/1.17 = 0.85 \text{ m/s}$$

or for spring tide ($P_s/P_m \approx 1.16$):

$$\hat{u}_m = 1.0 \text{ m/s}$$

As $\hat{u}$ has a fixed relation with $\bar{u}$, relation (3.55) is implicitely the same as a relation with P. Therefore, it is further disregarded in this study.

In literature successful linear correlations between A_c and the measured maximum discharge rate Q_{max} have been made by Gerritsen and De Jong in their studies of the Western Scheldt and the western part of the Dutch Wadden Sea (1983, 1984, 1985). These relations hold for areas exceeding 2000 m². Deviations of the relationships were found for cross sections seaward of the actual inlet. They also made correlations with other parameters such as $\bar{u}$, u_{max}, EV, FV and TV. Also in those studies the results of the correlations between A_c and EV, FV and TV as also those between A_c' and Q_{max} were quite comparable with respect to accuracy (see e.g. Figs. 3.56 and 3.57). They also are in good agreement with the results of the present study.

3.3.4 Relation with stability shear stress

Based on the concept of Bretting's Stable Channel Theory (1958) Bruun and Gerritsen (1960) introduced the stability parameter (see Eq. 3.2):

$$Q_{max}/(C\sqrt{\tau_s/\rho g})$$

To include wave effects Q_{max} should be multiplied with the Bijker factor as shown in equation (3.10).

Substitution in equation (3.2) yields:

$$A_{c,comp} = c_\tau \frac{u_{*,max}}{u_{*s}} A_c'$$

The coefficient c_τ should be unity if $A'_{c,comp}$ is considered and generally very close to unity for $A_{c,comp}$. In fact this coefficient only represents the ratio between the target area A_c or A_c' and A_c' which is related to Q_{max}.

This equation only is correct if holds:

$$u_{*,actual} = u_{*s} = \sqrt{\tau_s/\rho} = \text{constant}$$

To compare if this method yields more accurate results than the use of the tidal volume or the tidal prism, the scatter in $u_{*,max}$ around a constant u_{*s} should be compared with the relative scatter around the A_c - P relation. The latter also can be compared with the $A_{c,comp}$ - A_c relation where $A_{c,comp}$ is computed with a selected constant value of τ_s. In principle this is taken as the average of τ_{max} of all the selected channel profiles.

Bruun and Gerritsen (1960) presented results on τ_s for different tidal inlets, that is:

Small inlets : τ_s = 3.9 N/m² (spring tide)
Small and big inlets : τ_s = 3.9 N/m² (spring tide)
Absecon inlet : τ_s = 6.3 N/m² (spring tide)
Thyborøn inlet : τ_s = 5.0 N/m² (spring tide)
Eems estuary : τ_s = 2.64 N/m² (mean tide)

Based on their study they ultimately proposed characteristic values of τ_s presented in two tables; that is (spring tide conditions):

Condition	τ_s (N/m²)
heavier littoral drift and sediment load	5.0
medium conditions of littoral drift and sediment load	4.5
lighter littoral drift and sediment load	3.5

and (M = annual littoral drift in m³):

P/M	≥ 600	150 to 600	≤ 150
Q_{max}/M	≥ 0.03	0.01 to 0.03	0.01
τ_s (N/m²)	4.6	5.0	5.1

The relation between the two tables is not clear. The stability shear stress for the Eems estuary for spring tide condition is about 1.3 times that for mean tide, i.e. 3.5 N/m².

All results still showed a noticeable scatter around the proposed relationships.

Gerritsen and De Jong (1983, 1984, 1985) found the following representative stability shear stresses in their studies (mean tidal conditions):

Western Scheldt: τ_s = 3.3 N/m² (flood)
Wadden inlets : τ_s = 4.0 N/m² (ebb and flood)
Vlie basin : τ_s = 4.0 N/m² (ebb and flood)

For springtide conditions these values should be increased by a factor 1.3 and become 4.3 N/m² and 5.2 N/m² respectively. It is noted that these values have been determined based on formulas for the Chezy roughness (Beyl, Boender) which are not representative for this type of investigations. Nevertheless, the results fit within those of Bruun and Gerritsen. This also holds for the results of the present study (see Fig. 3.58).

A problem remains that obviously τ_s may change with the area considered and, hence, has to be checked first. Also it presents no additional accuracy, which means there is no actual reason to use this parameter instead of for example P or Q_{max}

4. Morphological relations of channel depth and width

4.1 General

In the previous chapter it has been shown that a fairly strong correlation exists between the cross-section of a tidal channel and local hydraulic parameters. For practical reasons it is of interest to know the shape of the cross section, that are the relations between maximum or mean depth and width and the tidal prism.

In general it must be expected that such relationships will not be strong. On top of the hydraulic parameters other parameters will play a role in the shaping of the cross section. As in rivers spiral flow in bends will play a role resulting in different shapes in bends and straight parts of a channel. This process is even more complicated in tidal areas with flood and ebb flow. This may cause composite cross sections with two deep parts and a shoal in between. Natural or artificial hard layers or banks may obstruct the channel growth in one direction which will be compensated by growth in the other direction. River and estuary training works are based on this principle.
Coastal protection works in tidal inlets usually suffer from this effect and have to be regularly fortified and extended in depth as the approaching channel is pushed against the defense works. The channel creates its required flow area by deepening to compensate for the loss of area on the other side of the channel which continues its migration until a more or less stable situation develops.

The above known phenomena make it obvious that the channel profile has a degree of freedom in its shape to compensate for the effects of different factors. Nevertheless, it may be expected that a natural channel which is free to mould itself will tend to a certain shape.
In this chapter it is tried to determine this tendency.

4.2 Relations on channel depth

The channel depth is a relevant quantity for navigation. In this study three depths have been considered, that is the maximum depth below NAP, the average depth below NAP and the average below MLW. The latter two are defined as $A_{c,NAP}/W_{NAP}$ and $A_{c,MLW}/W_{MLW}$ respectively.

The maximum depth below NAP (≈ MSL) has been correlated with DV and TV (= 2P) respectively which resulted in a best fit of (Figs. 4.1 and 4.2):

$$d_{NAP,max} = 0.0096\ DV^{0.39} \tag{4.1}$$

and

$$d_{NAP,max} = 0.0075\ TV^{0.39} = 0.0098\ P^{0.39} \tag{4.2}$$

Considering that DV in general is close to P in the Dutch Wadden Sea, these relations match very well in spite of the considerable scatter of the actual data around these relations.

The data of the average depth below NAP show less scatter than those of the maximum depth and fit rather well to the following relations (Figs. 4.3 and 4.4):

$$\overline{d}_{NAP} = 0.00094\ DV^{0.47} \tag{4.3}$$

and

$$\overline{d}_{NAP} = 0.00068\ TV^{0.47} = 0.00094\ P^{0.47} \tag{4.4}$$

Based on the above relations the following relation between $d_{NAP,max}$ and $\overline{d}_{NAP}$ can be derived:

$$d_{NAP,max} = 3.12\ \overline{d}_{NAP}^{0.83} \tag{4.5}$$

This relation fits well to the data if directly correlated which provides a check of all above mentioned formulae (Fig. 4.5).

The data of the average depth below MLW show a modest scatter and a good fit to the following relations (Figs. 4.6 and 4.7):

$$\overline{d}_{MLW} = 0.00088\ DV^{0.47} \tag{4.6}$$

and

$$\bar{d}_{MLW} = 0.00065\ TV^{0.47} = 0.00090\ P^{0.47} \qquad (4.7)$$

4.3 Relations on channel width and side slopes

Also the data on the width of the channel show a considerable scatter. This holds for both the channel width at NAP and at MLW (see Figs. 4.8 through 4.11). Based on the available data the following best fits were derived:

$$W_{NAP} = 0.15\ DV^{0.5} + 200 \qquad (4.8)$$

$$W_{NAP} = 0.11\ TV^{0.5} + 200 = 0.155\ P^{0.5} + 200 \qquad (4.9)$$

$$W_{MLW} = 0.050\ DV^{0.55} \qquad (4.10)$$

$$W_{MLW} = 0.034\ TV^{0.55} = 0.049\ P^{0.55} \qquad (4.11)$$

In general the correlation coëfficients of these relations are relatively low. A general check can be obtained by comparing the product of channel width and depth with the channel cross section, that is the product of equations (4.9) and (4.4) and that of (4.11) and (4.7) should yield the same relations for A_{NAP} and A_{MLW} respectively as obtained by a direct correlation of the latter quantities with DV and TV. This check yields:

$$A_{c,NAP} = 0.00094\ P^{0.47} * (0.155\ P^{0.5} + 200) = 146\ 10^{-6}\ P^{0.97} + 0.19\ P^{0.47} \qquad (4.12)$$

and

$$A_{c,MLW} = 0.00090\ P^{0.47} * 0.049\ P^{0.55} = 44\ 10^{-6}\ P^{1.02} \qquad (4.13)$$

The results show rather comparable relations as directly obtained.

A second check is to compare the average depth over width ratios with the directly obtained relation between average depth and width. For the NAP level equations (4.3) and (4.9) yield:

$$\bar{d}_{NAP} = 0.0054\ (W_{NAP} - 200)^{0.94} \qquad (4.14)$$

This doesnot fully comply with the trend of the actual data in spite of the large scatter which does not allow any reliable correlation (Fig. 4.12). This suggests that the power of the average depth relation is slightly too high and that of the width relation possibly slightly too low.

A direct correlation between W_{NAP} and W_{MLW} yields (Fig. 4.13):

$$W_{NAP} = (1.25 \text{ to } 1.5)\ W_{MLW} + 250 \qquad (4.15)$$

This fits fairly well with the equations (4.8) and (4.10) which would result in:

$$W_{NAP} = 2.3\ W_{MLW}^{0.91} + 200$$

The scatter around relation (4.15) is considerable. The physics of the channel width yields (Fig. 3.33):

$$W_{NAP} = W_{MLW} + 2.S2\ .\ \Delta h(p-1) \qquad (4.16)$$

From the equations (4.15) and (4.16) it follows that the slope S2 would be dependent on the size of the channel:

$$S2 = \{(0.25 \text{ to } 0.5)\ W_{MLW} + 250\}/\{2\ \Delta h(p-1)\} \qquad (4.17)$$

With $\Delta h(p-1)$ = GLW generally ranging from 0.85 to 1.35 m this yields a typical average slope 1/S2 between MLW and NAP of less than 1 in 110. This value fits in the results on $S2 = (W_{NAP} - W_{MLW})/\{2\ \Delta h(p-1)\}$ which are directly determined and plotted against W_{MLW} in Figure 4.14. It should be mentioned, though, that those show a considerable scatter and actually do not allow for a reliable fit. In general the value of S2 ranges between 25 and 600 and a weak positive correlation with $A_{c,NAP}$ or P seems to exist.
A similar plot has been made for the average slope 1/S1 between NAP and MHW. For the Wadden Sea this slope generally is fictive as in most occasions W_{MHW} is determined by the width between watersheds instead of the bed level at MHW. The results are plotted in Figure 4.15. This results in a representative average slope 1/S1 of about 1 in 100 to 200. Also here the larger scatter does not allow for a reasonable correlation.

Substitution of these slopes, equations (4.9) and (3.24) and the representative values of P and $p\Delta h$ (=MHW) or $(1-p)\Delta h$ (=MLW) in equations (3.17) and (3.18) will yield fair estimates of the cross sections $A_{c,MHW}$ and $A_{c,MLW}$.
Instead, also the following relations resulting from direct correlations can be used (Figs. 3.30, 3.31 and 3.32):

$$A_{c,MHW} = 1.07\ A_{c,NAP} + 560 \qquad (4.18)$$

$$A_c' = 1.00\ A_{c,NAP} + 80 \qquad (4.19)$$

$$A_{c,MLW} = 0.90\ A_{c,NAP} + 640 \qquad (4.20)$$

4.4 Comparison of results with other data

Byrne et al (1980) present a relation of the mean depth below MSL versus the width of tidal inlets at MSL of model data (Mayor-Mora, 1977) and data of North American inlets collected by Mehta (1976), Winton (1979) and by the authors themselves. The results are shown in Figure 4.16. The data cover a wide range of inlet widths (0.5 m to 20 km) and depths (0.15 to 20 m). In spite of the large scatter (up to a factor 4 to both sides of the best fit line) the data show a distinct relation which can be approximated by:

$$\bar{d}_{MSL} = 0.13\ W_{MSL}^{0.5} \qquad (W_{MSL} > 2 \text{ to } 5 \text{ m}) \qquad (4.21)$$

and

$$\bar{d}_{MSL} = 0.032\ W_{MSL}^{1.4} \qquad (W_{MSL} < 4 \text{ m}) \qquad (4.21a)$$

The data of the present study covering channel widths of about 100 m to 4300 m completely fall within the cloud of data presented by Mehta and Winton. The trend of equation (4.14), however, is different from the general trend of Fig. 4.16.

Boon and Byrne (1981) present a relation between the mean depth and the width at MSL which is closer to the one of the present study:

$$\bar{d}_{MSL} = 0.042\ W_{MSL}^{0.92} \qquad (4.22)$$

Fitzgerald et al. (1976) established a relationship between the inlet width and the basin area:

$$W_{MSL} = 43.10^{-6}\ A_b - 547 \qquad (4.23)$$

This can be rewritten to:

$$W_{MSL} = 43.10^{-6}\ P/\overline{\Delta h} - 547 \qquad (4.23a)$$

This relation is not valid for small basins.

Dieckmann et al (1988) presented a graph of the maximum depth of inlets in the German Bight versus the tidal prism and the shape of the inlets (Fig. 4.17). The data set of the present study very well fits within those data and extends it towards smaller inlets. The relation derived for $d_{NAP,max}$ (Eq. 4.2) does also fairly fit to the combined data set. Dieckman et al. also presented a plot of the mean water depth and the maximum water depth below MSL. This plot consists of their findings for the German Bight and data of American inlets of Vincent and Carson (1980). The results show a wide scatter generally within the range (Fig. 4.18):

$$d_{MSL,max} = 1.5 \text{ to } 6\ \overline{d}_{MSL} \tag{4.24}$$

The Duits-Nederlandse Eemscommissie (1989) showed a rather good correlation between a tide average velocity and the maximum water depth of Dutch tidal channels and inlets (Fig. 4.19). This relation can be represented by:

$$d_{NAP,max} = 237\ (P_m/(A_c T))^2 = 59\overline{u}^2 \tag{4.25}$$

Sha (1990) presents a different relation for the maximum depths in the Dutch Wadden Sea inlets (Fig. 4.20):

$$d_{NAP,max} = 35.10^{-9}\ P_m + 13 \tag{4.26}$$

The latter holds for inlets with a tidal prism in the range of 60 to 1000 million m^3.

Hume and Herdendorf (1990), finally, present plots of the mean and maximum depths of some New Zealand inlets versus the inlet width. Also these data show a considerable scatter (Fig. 4.21) but the following relations might be derived from it:

$$\overline{d}_{MSL} = 0.022\ W_{MSL} \tag{4.27}$$

$$d_{MSL,max} = 0.038\ W_{MSL} \tag{4.28}$$

From the above equations the ratio $d_{MSL,max}/\overline{d}_{MSL}$ would be 1.73. Based on the direct relation this ratio varies between 1.35 and 3.5 with an average value of 1.97.

The great variety in relations and the considerable scatter in the different data sets confirm that reliable relations on channel width, mean and maximum channel depth do not really exist. These quantities strongly depend on local flow and bed conditions. They never should be used in combination to derive the cross sectional area, but only as a secondary relationship to get an idea of the shape of a cross section of a certain size.

5. Morphological relations of volume of channel system

5.1 General

The rather firm relation between the size of a tidal channel and the tidal prism makes it likely that also the volume of the channel system behind a certain cross section is related to the tidal prism at that cross section. This, of course, does not hold without saying for lagoons in which the inner tidal delta covers only a part of the lagoon. For basins of the Wadden Sea and of the Dutch Delta area, however, such relations have been proven to exist (Renger and Partenscky (1974, 1980), Renger (1976), Eysink (1979, 1990, 1991), Dieckmann (1985), Dieckmann and Partenscky (1986)).

From these relations it can be concluded that the channel volume will change if the tidal prism is changed by man or by natural causes. This is clearly confirmed by observations in nature, e.g. in the basin of the Zoutkamperlaag after closure of the Lauwers Sea in 1969. This makes this type of relation interesting for engineering application to predict what amount of sand will be ultimately withdrawn from or becomes available in the system of the sea coast adjacent to the inlet (Eysink, 1990).

5.2 Theoretical considerations

In literature the channel volume appeared to be proportional to the tidal prism to the power 1.5 or close to that. In an attempt to explain the power to the tidal volume in these relationships the channel volume was derived in a theoretical way through integration of:

$$V_{MSL} = \int_{0}^{L} A(x)\, dx \qquad (5.1)$$

In general the relations for A_c show a proportionality to the tidal prism to a power close to unity. For simplicity the following relation for A_c has been adopted for these theoretical considerations:

$$A_c = c_A\, P \qquad (5.2)$$

This relation is valid over a wide range of channel sizes down to rather small channel profiles.

Substitution of (5.2) in (5.1) yields:

$$V_{MSL} = \int_0^L c_A \, P(x) \, dx \qquad (5.3)$$

Integration of (5.3) for a few schematized situations (Fig. 5.1) typically yields:

$$V_{MSL} = c_A \cdot c_s \, PL \qquad (5.4)$$

where:

c_s = constant depending on the shape of the basin

L = characteristic length of the basin

L can be expressed in the tidal prism, the length-width ratio of the basin and the tidal range. Substitution in equation (5.4) then yields:

$$V_{MSL} = c_A \cdot c_s^1 \, (\frac{L/B}{\Delta h})^{1/2} \, P^{1.5} \qquad (5.5)$$

where:

c_s^1 = constant depending on the shape of the basin

B = characteristic maximum width of the basin

Δh = average tidal range in the basin

The shape coefficients for the different situations are presented below.

Situation	c_s	c_s^1
1	0.333	0.497
2	0.407	0.536
3	0.452	0.541
4	0.555	0.907

It is obvious that the channel volume increases with a relative increase of the storage in the back of the basin (situation 1 → 4).

A more general expression for the shape coefficients can be obtained by defining the width of the entrance of schematic situation 4 as aB. This results in the following expressions for c_s and c_s^1:

$$c_s = \frac{1}{3}\left(\frac{3}{2} + (a-\frac{1}{2})\ x/L\right)/\left(1 + (a-\frac{1}{2})x/L\right) \qquad (5.6)$$

and

$$c_s' = c_s\left(2/(L/x + a - \frac{1}{2})\right)^{1/2} \quad \text{with } a \leq 1 \qquad (5.7)$$

$$c_s' = c_s\left(2a/(L/x + a - \frac{1}{2})\right)^{1/2} \quad \text{with } a > 1 \text{ and } B = aB \qquad (5.7a)$$

For the total basin (x=L) this results in diagrams as presented in Figure 5.2. If only a part of the basin is considered the coefficients also depend on the parameter x/L. Diagrams for those situations are presented in Figs. 5.3 and 5.4.

The above results obviously give a firm support of the empirical relations presented in literature and also present the influence of the shape of the basin and the tidal range on the channel volume. This may explain the differences in the empirical constants of those relations.

If a tidal basin is composed of two or more sub-basins with a combined inlet, equation (5.5) can be applied to either the total basin or to the individual sub-basins. If the ratio factor "a" is the same for all sub-basins, the sum of the volumes of the sub-basins is the same as the volume derived for the total basin (see Fig. 5.5). This is true since the non-linear effect in $P^{1.5}$ is compensated for in the parameter $(L/B)^{0.5}$. This indicates that type of relation presented in equation (5.5) is sensitive to the shape of the basin. This is once more demonstrated in the relation for c_s' which also is rather sensitive to errors in the other shape parameter "a". The constant c_s in equation (5.4) generally is less sensitive to errors in the parameter "a".

The above theory, although based on a schematized approach, provides a good basis for the study of relations on channel volumes.

5.3 Correlation of channel volume with relevant parameters

From the foregoing part of the study it was learned that the tidal prism is a suitable and practical hydraulic parameter to determine the cross sectional channel profile. Inside a tidal basin waves generally are too low to play a significant role in the shaping of a channel (Bijker factor close to unity) or at least the differences in the wave effects are small (Bijker factor more or less the same everywhere). Therefore, a correlation of the channel volumes with the tidal prism ignoring the wave effect (Bijker factor = 1) is realistic.

It is assumed that the tidal channels basically are shaped during maximum tidal flow which generally occurs around MSL. Therefore, the channel volume below MSL (or NAP) is considered as a basic quantity to which the channel volumes below MLW and MHW are related. This can be demonstrated by the following set of equations:

$$V_{MSL} = \alpha_M P^n \tag{5.8}$$

$$V_{MLW} = V_{MSL} - \beta_p P/\gamma_p \tag{5.9}$$

$$V_{MHW} = V_{MSL} + (1-\beta_p) P/\gamma_p \tag{5.10}$$

where:

α_M = empirical coefficient related to V_{MSL}

β_p = empirical coefficient = $(V_{MSL} - V_{MLW})/(V_{MHW} - V_{MLW})$

γ_p = empirical coefficient = $P/(V_{MHW} - V_{MLW})$

Based on these equations the following relations can be derived:

$$V_{MLW} = (1-\beta_p P^{1-n}/(\gamma_p . \alpha_M))V_{MSL} \tag{5.11}$$

$$V_{MHW} = (1+(1-\beta_p) P^{1-n}/(\gamma_p . \alpha_M))V_{MSL} \tag{5.12}$$

With n being greater than unity the above equations indicate that those relations asymptotically approach the relation for V_{MSL} with increasing P. Indirectly this is demonstrated by data presented by Dieckmann (1985) (see Figure 5.6) and confirmed by the data of the present study (see Fig. 5.7). If the volumes V_{MLW} and V_{MHW} would be determined directly this yields equations like equation (5.8) but

with different constants α and n. This implies a restricted validity as this means that the relations will intersect somewhere which is unrealistic. This will be avoided by using the consistent set of equations as derived above. Only for comparison with data from literature both for V_{NAP} and V_{MLW} relations like equation 5.8 have been derived. The results are (see Figs. 5.8 and 5.9):

$$V_{NAP} = 0.11\ P^{1.11} \quad \text{if} \quad 10^6 < P < 160\ 10^6\ m^3 \tag{5.13}$$

$$V_{NAP} = 259\ 10^{-6}\ P^{1.43} \quad \text{if}\ 160\ 10^6 < P < 1000\ 10^6\ m^3$$

$$V_{MLW} = 16\ 10^{-6}\ P^{1.55} \tag{5.14}$$

For basis with a mean tidal prism of more than 1000 million m^3 the effect of the small channels along the basin boundaries will become negligible and the best relation for the channel volume then probably is:

$$V_{NAP} = 61\ 10^{-6}\ P^{1.5} \quad \text{if} \quad P > 1000\ 10^6\ m^3 \tag{5.13a}$$

The coefficients β_p and γ_p are important parameters for the relations defined in equations (5.9) through (5.12). Therefore, both parameters have been determined and correlated with P. The results for β_p are (see Fig. 5.10):

$$\beta_p = 0.16\ P^{0.055} \quad \text{if } P < 160\ 10^6\ m^3 \tag{5.15}$$

$$\beta_p = 0.44 + 7.74\ 10^{-11}\ P \quad \text{if } P > 160\ 10^6\ m^3$$

It is noted that the results of γ_p show a lot of scatter in the range for small basins with P less than 15 million m^3. A best fit there would result in unrealistic values of γ_p probably due to effects of inaccuracies in the measured values of P or erratic residual volumes due to drift currents which are included. Therefore, a relation is selected for γ_p which is equal to unity for P = 0 and passes through the data for large values of P, i.e.:

$$\gamma_p = 1 - 1.0\ 10^{-10}\ P \tag{5.16}$$

Substitution of the above relations in equations (5.11) and (5.12) and plotting the ratios V_{MLW}/V_{NAP} and V_{MHW}/V_{NAP} versus P shows that this approach generally yields consistent and good results (See Fig. 5.11).

As a result of the theory presented in the previous section V_{NAP} also has been correlated with the parameters PL and $((L/B)/\overline{\Delta h})^{0.5} \cdot P^{1.5}$ which yielded (see Figs. 5.12 and 5.13):

$$V_{NAP} = 25.5\ 10^{-3}\ (PL)^{0.79} \qquad \text{if } PL < 2.5\ 10^{12}\ m^4 \qquad (5.17)$$
$$V_{NAP} = 84.2\ 10^{-6}\ (PL)^{0.99} \qquad \text{if } 2.5\ 10^{12} < PL < 50\ 10^{12}\ m^4$$

$$V_{NAP} = 0.10\ [((L/B)/\overline{\Delta h})^{0.5} \cdot P^{1.5}]^{0.75} \qquad \text{if } [\ldots] < 1.15\ 10^{12}\ m^4 \qquad (5.18)$$
$$V_{NAP} = 679\ 10^{-6}\ [((L/B)/\overline{\Delta h})^{0.5} \cdot P^{1.5}]^{0.93} \qquad \text{if } 1.15\ 10^{12} < [\ldots] < 40\ 10^{12}\ m^4$$

These relations already partly include the effect of the shape of the basin and of the tidal range. As a result the data around these relations show less scatter than in case of relation (5.13).

In addition to the above it was also intended to compute the coefficients $c_A \cdot c_s$ and $c_A \cdot c_s'$ and to correlate them with the ratio $a = W_{NAP}/B$ of the basin entrance. If the results would show a rather similar tendency as theoretically obtained for c_s and c_s' (see Fig. 5.2) then the scatter might further reduce in case $c_s PL$ or $c_s'\ ((L/B)/\overline{\Delta h})^{0.5}\ P^{1.5}$ are used for correlation. Unfortunately, time constraints did not allow for this investigation.

5.4 Comparison of results with other data

A relation on channel volume was firstly presented by Renger and Partenscky (1974). Based on the data they had collected by then they derived the following expression for the channel volume below MLW:

$$V_{MLW} = 8 * 10^{-9}\ A_b^2 \qquad (5.19)$$

For the channel volume below a level z in the range from MLW to MHW they presented the relation (converted for A_b in m^2):

$$V_z = V_{MLW} * \overline{a}^{\,z} \qquad (5.20)$$

with

$$\overline{a} = 214 * A_b^{-0.272} \qquad (5.21)$$

Equations (5.20) with (5.21) yield odd results for large values of A_b. This could be avoided if $\overline{a}$ would be defined in the form:

$$\overline{a} = 1 + \alpha A_b^{-n} \qquad (5.22)$$

Based on data presented in 1974 this would yield $\alpha = 4.5$ and $n = 0.5$. In principle this corresponds rather well with Equation (5.12) of Section 5.3.

Later Renger and Partenscky (1980) presented different relations (also shown in Dieckmann, 1985):

$$V_{MLW} = 6.1 * 10^{-6} A_b^{1.643} \qquad (5.23)$$

$$P = 1.00 * A_b^{1.036} \qquad (5.24)$$

$$\overline{a} = 28.7 * A_b^{-0.161} \qquad (5.25)$$

From these equations also the following relation can be derived:

$$V_{MLW} = 6.1 * 10^{-6} P^{1.586} \qquad (5.23a)$$

Equation (5.23a) very much resembles the directly derived relation of Renger and Partenscky:

$$V_{MLW} = 8.7 * 10^{-6} P^{1.566} \qquad (5.26)$$

The most recent relations of Renger and Partenscky correspond quite well with the findings of Eysink (1979, 1990, 1991b) who found:

$$V_{MAP} = 1.0 * 10^{-4} A_b^{1.5} \text{ (Wadden Sea)} \qquad (5.27)$$

$$V_{MAP} = 65 * 10^{-6} P^{1.5} \text{ (Wadden Sea)} \qquad (5.28)$$

$$V_{MAP} = (73 \text{ to } 80) * 10^{-6} P^{1.5} \text{ (Dutch Delta area)} \qquad (5.29)$$

Dieckmann (1985) and Dieckmann and Partenscky (1986) presented a great number of data on V_{MLW} and V_{MHW} (Fig. 5.6). They followed a different approach to describe the channel volume and used:

$$V_{MLW} = \alpha_1 \, (d_{MLW} \cdot A_{MLW})^{\beta_1} \tag{5.30}$$

$$V_z = V_{MLW} + \alpha_2 \{z \, (A_z - A_{MLW})\}^{\beta_2} \tag{5.31}$$

with d_{MLW} = maximum depth below MLW, z = distance above MLW and:

$$\alpha_1 = 0.383 - 0.0133 \, \overline{\Delta h}$$

$$\beta_1 = 0.883 - 0.004 \, \overline{\Delta h} \tag{5.32}$$

$$\alpha_2 = 1.115 - 0.161 \, \overline{\Delta h}$$

$$\beta_2 = 0.989 - 0.026 \, \overline{\Delta h} \tag{5.33}$$

The relations for α_2 and β_2 are believed to be derived for a level of MHW only ($z = \overline{\Delta h}$ and $A_z = A_{MHW}$).

The relations of Dieckmann and Partenscky are hard to compare with those of this study and of Renger and Partenscky and Eysink. Also a direct comparison with field data can not be made easily as this requires the knowledge of the quantities d_{MLW}, A_{MLW}, A_{MHW} and $\overline{\Delta h}$ going with the channel volumes V_{MLW} and V_{MHW}. The only judgement on accuracy can be done through the scatter of the values of the coefficients α_1, α_2, β_1 and β_2. This scatter is relatively modest for β_1 and β_2 but rather large for the coefficients α_1 and α_2 (see Fig. 5.14).

6. Morphological relations of sand volume in outer deltas

6.1 General

Outer deltas in front of tidal inlets pertinently should be considered as part of the morphological unit tidal basin-inlet-outer delta. It has been shown that the size of the tidal channels and the total channel volume below MSL in a basin is related to its tidal prism as also the size of the outer delta and the volume of sand stored in it. If the tidal prism of a basin is changed by natural causes or human interference, this affects both the channel volume of the basin and the sand volume stored in the outer delta as discussed by Eysink (1990). The balance of the two will have consequences for the adjacent sea coast and its foreshore.

Because of its relevance for coastal managing, the sand storage in the outer deltas of the Dutch Wadden Sea has been included in the present study and is dealt with in this chapter.

6.2 Approach

To determine the sand volume which is stored in an outer delta it is necessary to follow a procedure which will yield a unique result.
Besides, the procedure should result in data which are comparable with data of American inlets presented before by Walton and Adams (1976). Therefore, basically the same procedure was followed as used by them. Firstly, coastal profiles were selected on both sides of the inlet where the depth-contourlines where not effected by the outer delta anymore and ran more or less parallel. Those coastal profiles were considered to represent a stable profile of an uninterrupted coast. Based on this the bathymetry of such a coast was constructed which represents the situation without an outer delta. In this case, where the basins are filled from the south or south-west, this basic coastline is not a straight line as the coasts of the chain of islands are not in line. In reality such a coast can not exist and will straighten out. To comply with the data of Walton and Adams and to keep the procedures simple and clear this aspect has been disregarded.

The sand volume stored in the outer delta now can be determined relative to the constructed bathymetry of the reference coast. The volume of sand in the parts of the outer delta exceeding the reference plane has been determined as well as the

volume of the channels in the outer delta which reach below the reference plane. The difference of these volumes is the actual amount of sand which is stored in the outer delta and is relevant for the sand balance of the adjacent sea coasts and the tidal basin.

The advantage of this approach is that the results are not very sensitive to errors in the selection of the area boundaries as changes in that vicinity are minor and extra area does not yield extra sand storage in the outer delta. Besides, the method basically complies with the one of Walton and Adams which makes the results comparable. The volumes in this case have been based on mean depths in rather small grid cells of 90 x 90 m^2 to 250 x 250 m^2 of digitized sounding maps.

For this study only well defined outer deltas of the Dutch Wadden Sea have been used. This implies that in some cases the outer deltas of two inlets which are close together, e.g. Pinkegat and Zoutkamperlaag between the islands of Ameland and Schiermonnikoog, should be considered as one outer delta of the combined inlets of Het Friesche Zeegat. In other cases, such as for the inlets Lauwers, Schild and Eems-Dollard estuary, the situation is so complex that a reliable reference coast could not be constructed. In that case no sand volume has been determined.

6.3 Correlation of sand volume outer delta with relevant parameters

Based on the described procedures data have been derived for the inlets of Texel till the Friesche Zeegat between the islands of Ameland and Schiermonnikoog for available soundings within the period of 1925 to 1987. The results are shown in Table 6.1.
In general the different volumes only show a modest fluctuation over the years part of which can be ascribed to changes in the hydraulic conditions. This gives confidence in the applied method and the results.

The data of the Texel inlet show an increase in the period from 1925 to 1933 which might be caused by the closure of the Zuiderzee in 1932. This resulted in an increase of the tidal prism of about 10 to 20 per cent and at the same time an annual deposition rate of about 10 million m^3 of sand in the basin near the closure dike (Rietveld, 1962).

Since 1933 the channel volume in the outer delta increased gradually and the sand volumes decreased gradually. This might be the result of the sand influx into the basin which lasted at least until the sixties and of considerable sand borrowing just inside the basin and at the outer delta in the seventies and eighties. A representative sand storage volume in the outer delta may be taken at 600 to 650 million m^3 which is related to a mean tidal prism of 1000 million m^3.

The data of the Eierlandsche Gat delta show a smaller delta in 1926 and a more or less constant one in the period 1971 to 1987.
The tidal prism of this inlet also was affected by the closure of the Zuiderzee in 1932 and increased. Also in this basin some sand borrowing occurred in the eighties. A representative sand storage volume in the outer delta is taken at 130 to 135 million m^3 in the present situation with a mean tidal prism of about 200 million m^3.

The data of the Terschelling inlet show a somewhat larger sand storage in the outer delta in 1933 relative to that in the period of 1972 to 1982. This very likely is the result of inaccuracies as the tidal prism of this inlet also increased due to the closure of the Zuiderzee in 1932. Sand borrowing occurred also in this basin in the seventies and eighties. A representative sand storage volume in the outer delta of this tidal inlet is taken at 340 to 370 million m^3 with a tidal prism of about 1000 million m^3.

The data of the Ameland inlet show a remarkable development. The sand volume above the reference plane shows an increase in the period from 1926 to 1958 and remained more or less constant since then. The channel volume below the reference plane, though, remained constant in that first period and increased in the period from 1958 to 1974 and then remained constant again. It is believed that this is related to the morphological developments of Ameland since the construction of the Kooioerder Stuifdijk in 1880-1893. This very likely trickered a strong extension of the eastern tip of Ameland which also must have resulted in a shift of the watershed of Ameland (DELFT HYDRAULICS, 1987). This shift was the largest around 1950 and may have stabilized or decreased somewhat in the period from 1950 to 1980. This will have increased the tidal prism in the period of around 1900 to 1950 and a retarded morphological effect in the tidal basin and its outer delta. At present a sand storage volume of 125 to 145 million m^3 with a tidal prism of 400 million m^3 is taken representative for this inlet.

6.4 Comparison of results with other data and conclusion

The adopted results for the selected outer deltas of the Dutch Wadden Sea have been plotted in the diagram presented by Walton and Adams taking into account a factor 1.15 to convert the mean tidal prism to springtide prisms (see Fig. 6.1). The data very well fit in this diagram for American outer deltas and generally match the best with the relation for a highly exposed outer delta. Only the outer delta of the Eierlandsche Gat shows a relatively high sand storage volume which tends to fit in the relation for moderately exposed outer deltas. However, in view of the general scatter of the data, it also may be considered as a normal deviation from the relation of a highly exposed outer delta. The criteria adopted for this by Walton and Adams are:

mildly exposed : $H^2T^2 < 2.8 \quad m^2.s^2$
moderately exposed: H^2T^2 2.8 to 28 $m^2.s^2$
highly exposed : $H^2T^2 > 28 \quad m^2.s^2$

The wave parameters H and T represent the average wave height and period respectively on a water depth of 4.5 to 6 m below MLW. For the North Sea coast along the Dutch Wadden Islands these quantities amount to about 1.0 m and 5.5 s respectively (Ribberink and De Vroeg, 1991), yielding a wave energy parameter of 30 $m^2.s^2$. This confirms the high wave energy level for the Dutch outer deltas and that the relation of Walton and Adams for the highly exposed deltas is also valid for the Dutch outer deltas.

7. Morphological relations of tidal flats

7.1 General

The tidal flat area or the intertidal zone of the Wadden Sea, that is the area that normally inundates and dries twice a day, is of great importance as feeding ground for many birds. In this study the tidal flat area A_f is defined between MLW and MHW.

From a morphological point of view the tidal flats reduce the tidal prism of the basin and, hence, effect the size of the channels. The larger and the higher the intertidal zone, the smaller the tidal prism is. This directly follows from the following equation:

$$P = (1-\alpha_f A_f/A_b) A_b \overline{\Delta h} \qquad (7.1)$$

where:

A_f = intertidal area in the basin

A_b = basin area at MHW

α_f = average bed level in the intertidal zone above MLW and relative to $\overline{\Delta h}$ (see Fig. 7.1).

In this respect it is relevant to look for possible relations for the quantities A_f and α_f.

An other interesting quantity is the height and the shape of the crest of individual tidal flats located between two tidal channels. The higher the crest the longer birds can fourage. In general it is believed that crest levels of tidal flats are related among others to MHW. However, this will not be the only hydraulic parameter. Local wave intensity and tidal range may also play an important role in this respect. To get a better understanding attention is also paid to this item.

7.2 Relative tidal flat area

According to general classifications of coastal features the presence of tidal flats depends on the tidal range (Davis, 1964; Hayes, 1979). This parameter is not

the only one though. For the Dutch Wadden Sea with a meso-tidal range, the relative tidal flat area A_f/A_b can not be directly correlated with the tidal range as suggested by Dieckmann (1985) (see Fig. 7.2). His relation is believed to be accidental as it does not include the small basin of the Eierlandse Gat (β = 25%) in the low mesotidal reach, but does include the sub-basin of the Inschot which includes part of the Pollen. The latter may still be an effect of the closure of the Zuiderzee. Further, there is a general tendency of increasing tidal range and decreasing basin size going from the Marsdiep at Den Helder to the Jade. This may result in an accidental correlation. It is believed that the actual main cause of the changing relative channel area should be found in the size of the basin. For the Dutch Wadden Sea the relative tidal flat area shows a distinct relation with the size of the basin (Fig. 7.3). Indirectly the same was found by Renger and Partenscky (1974) for the German Bight. They found a distinct relationship between the channel area and the size of the basin which can be converted to (basin size: 5 - 200 km^2):

$$A_f/A_b = 1 - 2.5 * 10^{-5} A_b^{0.5} \qquad (7.2)$$

Later Renger et al (1976) came to a similar but different relation which would yield (basin size 8-200 km^2):

$$A_f/A_b = 1 - 2.53 * 10^{-3} A_b^{0.25} \qquad (7.3)$$

If all the data on the relative channel areas of the Wadden Sea presented in Walther (1972), Renger and Partenscky (1974), Renger (1976) and Eysink (1990, 1991b) are plotted in one figure a best fit is obtained by (see Fig. 7.4):

$$A_{ch}/A_b = 1.57 * 10^{-4} A_b^{0.40} \pm 0.1 \qquad (7.4)$$

or

$$A_f/A_b = 1 - 1.57 * 10^{-4} A_b^{0.40} \pm 0.1 \qquad (7.5)$$

The results of the present study quite well fit in this relationship (see Fig. 7.5). On average they are slightly higher than according to equation (7.4).

The reason for the scatter is not clear. It may be caused by:

- differences in tidal range,
- differences in the shape of the basin,

- differences in orientation of the basin relative to the dominating wind direction (fetch) and wave directions at sea (open or sheltered),
- natural scatter due to natural variations in the width-depth ratio of the tidal channels,
- differences in local wind climate.

At first glance there seems to be no systematic influence of the tidal range.

The dependence of the relative channel area and, hence, of the relative tidal flat area of the basin in the first place is caused by the relative growth of the channels. For example, the channel systems in a tidal basin have been compared with a tree. In the wide basins of the Wadden Sea the channel systems look like heavily branched apple trees, whereas in the Dutch Delta area they look more like tall poplars with small branches. If the basin area is extended on the seaward side with an extra area, all the water in the upper area has to pass this extra area as well. Hence, a large part of this extra area will consist of the main channel which has to convey the tidal prism of the upper area and of the extra area. So, the existing tree is extended with a thick stem and relatively with only a few or no extra branches. In this way it is likely that the relative channel area will increase with increasing basin size.

This, however, does not explain the difference between the relative channel areas in the Wadden Sea and the Delta area. It is believed this difference is caused by the shape of the basin. If relatively most of the storage is in the back of the basin then the stem of the tree becomes thick over a greater length yielding a larger channel volume and a larger relative channel area. Besides, in case of a long basin the amplification of the tide in the basin becomes more important (see Fig. 7.6) which also results in a relatively high storage of tidal water in the back of a large basin. In basins which are long relative to the length of the tidal wave (e.g. the former Zuiderzee) this effect reduces again due to damping of the tide.

The size and shape of the different basins in general have been affected by land reclamation activities. In the Wadden Sea land generally was reclamed from the top of the tree making it shorter. In the Dutch Delta area, however, most of the land was reclaimed along the main channels and side branches were closed off (e.g. Sloe, Braakman). This accentuated the narrow poplar shape of the channel systems there. In general the basins might be classified by a length over average width

ratio (i.e. L^2/A_b) where L is the length of the longest main channel. The impression exists that a subdivision of three classess may practically make sense, that is for example:

$$\begin{aligned} &L^2/A_b < 5 \\ &L^2/A_b = 5 \text{ to } 10 \\ &L^2/A_b > 10 \end{aligned} \qquad (7.6)$$

In general the relative channel area seems to increase with increasing class of L^2/A_b. The Wadden Sea basins generally are in class 1 for which equation (7.4) is valid. Exceptions might be the basins of Marsdiep and Eems. Unfortunately insufficient time and information going with the data from literature are available to check this idea in more detail.

Finally, the size of the basin represents a fetch length. Large basins, especially long basins orientated in the direction of the dominant wind, allow for more wave action around HW. This very likely prevents the growth of extensive areas of tidal flats to a height above MLW, particularly between channels where the sediment is not so easily trapped.

7.3 Height and profiles of tidal flats

In general the heights and profiles of individual tidal flats show a great variety. This is not surprisingly as flats grow out of emerging shoals and, hence, may vary in height between MLW and MHW. Thus the flats range from small or relatively narrow low flats in or along large tidal channels to wide and high tidal flats. For the situation around 1985 the crest levels of all relevant tidal flats in the Dutch Wadden Sea have been determined and related to MHW and the tidal range (Fig. 7.7). The results show that the crest levels of most of the flats range between MSL and MHW -0.3 m. Only in the Dollard the crest levels in some places reach up to almost MHW. This may be caused either by the sheltered location of the Dollard or because the Dollard is a pocked from which sediment can hardly escape. On the watersheds between the basins the bed level roughly varies around MHW -1 m.

The profiles of the different tidal flats show a great variety in shape. It is strongly depending on the size of the tidal flat complex and the local flow

conditions and related secondary or tertiary tidal channels which feed and drain the area of the flats. The crest is located at the local watershed between two channels and generally the level seems more or less related to the width of the flat. A second factor governing the height of the crest of the flat seems to be the stability of the watershed. If it is rather stable and the same for ebb and flood the crest level will be relatively high. If, however, the local watershed is different for ebb and flood as for example in the area of the Pollen, then the crest of the tidal flat may remain relatively low.

In general it seems that the height of a tidal flat in the Dutch Wadden Sea doesnot exceed a level of local MHW -0.3 m except in the sheltered Dollard. This may be caused by local wave action and/or regular storm surges with combined wave action and drift currents passing over the flats at HW. It is believed that the height of a tidal flat somehow is related to MHW and the local flow and wave conditions. Obviously, a level exists where the sediment supply towards the flat during flood on average balances the sediment losses during ebb considering all conditions over the year. Ongoing growth is possible along banks where the (fine) sediments are trapped and cannot be washed over the flat during storm but are only stirred up during storm and largely redeposit thereafter. This allows for a gradual accretion of the basin but doesnot effect the flat levels at some distance of the banks. Evidence to support this hypothesis is scarce and indicative only.

The German authorities reconstructed historical maps of the East Frisian Wadden Sea for the years 1650, 1750, 1860 and 1960 (Forschungsstelle Norderney, 1963-1976) which covers a period of 310 years. In this period the sea level must have risen between 0.5 and 1 m (based on sea level rise data presented in Eysink (1979), Lassen and Sieffert (1991) and Schönfeld and Jensen (1991). In spite of this the general features of the area did not noticeable change; the relative tidal flat area remained virtually the same in spite of many changes in detail. An example of this for the period 1860 to 1975 is presented in Figure 7.8. Assuming that the level of the tidal flats and their size are related this indicates that the level of the flats must have followed this sea level rise. Unfortunately, no firm data on the flat levels and the actual sea levels are available over the long period since 1650 to actually prove this. Firm data only exist (presently not available though) over the past 100 years and the changes over that period are generally within the sounding inaccuracy.

High flats such as Noorderhaak, Richel, Engelsmanplaat, Simonszand, Lütje Hoogehörn and Memmert generally only exist in the vicinity of a tidal inlet where breaking sea waves can build such high levels. If those flats are sufficiently large and high, sediment transport by wind can build small dunes on it thus creating a small islet (e.g. Memmert). Often these high flats tend to migrate with the inlet channels or into the basin (e.g. Engelsmanplaat). In the latter case it moves out of the influence zone of the sea waves which built it. Then the short local wind waves attack it during storms and reduce it in size. Once the high part is eroded and the size is sufficiently reduced, the wind induced sediment transport reduces. Consequently, the downdrift side of the flat doesnot grow above MHW anymore and the flat will gradually vanish and become the high crest of the tidal flat on which it is situated. This has occurred with the islet of Buise (Luck, 1975) and would also occur with the islet of Griend if no measures were taken to extend its lifetime (Eysink et al, 1986). Also this phenomenon indicates that the crests of the tidal flats in the Wadden Sea are related to MHW and the local wave conditions.

Niemeyer (1986) presents wave data of simultaneous measurements at sea, in the outer delta and just inside of the inlet Norderneyer Seegat. He finds a strong correlation between the maximum and significant wave heights and the water depths in the two latter locations. In general the wave height reduces by energy loss when going inward. This is also demonstrated by the strong correlations between local wave height and the wave height in the station at sea (Fig. 7.9). The loss of wave energy from the sea into the basin is very large and just inside the inlet only a minor part is left (Fig. 7.10) which suggests that the effect of sea waves inside the basin is very modest. In a recent publication Niemeyer presented a maximum wave height versus water depth relation for stable tidal flats and salt marshes in the Ley Bay (Niemeyer, 1991). He also shows wave data on a location which remain below the relation for a stable tidal flat and argues that therefore the level of that flat is likely to rise (Fig. 7.11). If the reduced wave activity is the result of manmade shelter or due to shifting of tidal channels and flats in front of that location, this seems to be a realistic assumption. If not, also the difference in flow conditions may cause the difference in bed level. In that respect it can be noted that the relations for the Ley Bay and station III in the Norderneyer Seegat are not the same. Actually it resembles more the relation of station II in the outer delta. It is also believed that for that reason the tidal flat Lange Zand does not expand towards the South-East into the Pollen (Vlie

basin) though it is likely that the wave activity there is less than on the North side of that tidal flat.
Nevertheless, the idea of Niemeyer looks promising and also suggests that waves play an important role in the height of the tidal flats.

Some confirmation on the relation between MHW and the crest level of a tidal flat was found in the behaviour of the Grienderwaard after the closure of the Zuiderzee. The latter caused a rise of the local MHW of about 0.25 m. The history of the crest levels West and East of the islet of Griend suggests that they followed the change in MHW (Fig. 7.12).
Another and probably more firm example is the behaviour of the Dollard after a rise of the local MHW due to human interference in the Eems (deepening and relocation of the fairway to Emden in the periode 1971-1976) (Eysink, 1991c). This raised the MHW level in the Dollard with about 0.25 to 0.3 m. The hypsometric curve of the Dollard shows that this change in level caused a quick and similar response of the bed levels above MLW (Fig. 7.13).

Especially the latter example provides support to the idea that a morphological system responds the fastest on a disturbance in locations where the disturbance of the equilibrium is the greatest. In case of sea level rise this is on the tidal flats where the water depths (relative to MHW) are the least. The data of the Dollard suggest a very quick response to water level changes, that is the tidal flat levels follow within a few years. In more open areas this might take some more time, say five years.

In literature Dieckmann (1985) has also looked into the height of the tidal flats in the entire Wadden Sea from Holland to Denmark. He as well recognized the difficulties in finding a reliable relation for individual tidal flats. To circumvent that he introduced an approximation of the average height of the tidal flat area. This height is defined as the level which is exceeded on 50 per cent of the total tidal flat area in the basin considered and can be directly derived from the hypsometric curve of that basin. In fact he defines the median height of the tidal flats.

He also refers to literature, i.e. Bendegom (1950), Göhren (1968) and in fact Straaten (1975) (see Fig. 7.14), in which it was stated that the bed level of the tidal flats

must be related to tide levels. Based on this he related the median heights of the tidal flats to MLW and the tidal range (Fig. 7.15). Based on that he concludes:

$$H_{0,5A} = MLW + y \tag{7.7}$$

with

$h_{0,5A}$ = median tidal flat height

and

$$\begin{aligned} y &= (0.5 \text{ to } 0.6)\ \Delta h \quad && \text{low macro tide} \\ y &= (0.4 \text{ to } 0.5)\ \Delta h \quad && \text{high meso tide} \\ y &= (0.3 \text{ to } 0.4)\ \Delta h \quad && \text{low meso tide} \end{aligned} \tag{7.8}$$

A problem in this respect is that it is not fully clear where he defined the tidal range. It seems he took the values at the nearest tidal station which sometimes is located near the entrance of the basin and sometimes in the back of it. Considering his first figure (Fig. 7.15A) it seems to indicate the effect of the tidal amplification in elongated systems with high levels in the back of the system where the tidal range and MHW are higher than at the entrance. This again seems to support the idea that the levels are related to MHW rather than MLW. Also Fig. 7.15B gives support to this idea as in general the median tidal flat height tends to follow MHW. In general the data suggest the following relation for both meso and low macro tidal range:

$$h_{0,5A} = MHW_{inlet} - 1.25 \text{ to } 1.5 \text{ m} \tag{7.9}$$

This picture is only slightly disturbed by the data of the Jade, Till, Süder Au and Norder Au where the tidal flat levels are some 0.25 m lower. The location of the tide gauges for these basins may have effected these points. If these tide gauges are in the back of the basins instead of in the entrance, this difference can be easily explained by the amplification of the tide in the basins.
A better and more general relation might be obtained by using the average MHW of the considered basins as a reference level which is higher than the one in the inlet.

In the present study the average level of the tidal flat relative to MLW was determined in a dimensionless way through the parameter α_f of equation (7.1). This parameter is related with the size of the basin (see Fig. 7.16a) and can be described by:

$$\alpha_f = 0.41 - 0.24\ 10^{-9}\ A_b \qquad (7.10)$$

Further, the distance between MHW and the average flat level is considered by relating $(1 - \alpha_f)\ \overline{\Delta h}$ with A_b (see Fig. 7.16b). This shows a generally fixed level below MHW which fluctuates between 1.1 m and 1.5 m with an average of about 1.3 m. In small basins the latter may increase to 1.4 m to 1.5. m.

REFERENCES

Adel, J.D. den, 1988
Verificatie van de numerieke golfvoortplantingsmodellen CREDIZ en HISWA bij het Zeegat van Texel,
Rijkswaterstaat, Dienst Getijdewateren, Notitie GWAO-89.282, aug. 1988.

Allersma, E., 1991
Personal communications of a morphological study of the Western Scheldt estuary,
Delft Hydraulics, Draft report Z368, 1991

Bakker, W.T. en Bangert, P.W., 1971
Analyse van wind- en golfgegevens van de Nederlandse Lichtschepen,
Rijkswaterstaat, Dir. Waterh. en Waterbew., Afd. Kustonderzoek, Studierapport W.W.K. 71-3.

Barua, D.K. and F.G. Koch, 1976
Characteristic morphological relationship for tide dominated channels of the Meghna estuary.
Proc. Regional workshop on erosion and sediment transport processes,
UNESCO, BUET and BWBD, Bangladesh, 1976, pp. 68-82

Bendegom, L. van, 1950
Enkele beschouwingen over de vorming en vervorming van Wadden,
Kon. Ned. Aardrijksk. Gen., 2e reeks, 67, 1950, pp. 326-333

Berg, J.H. van den, 1986
Aspects of sediment- and morphodynamics of subtidal deposits of the Oosterschelde (The Netherlands)
Rijkswaterstaat, Communications no. 43/1986

Berg, J.H. van der, 1987
Konfrontratie sedimenttransportformules met metingen van het suspensief zandtransport in de Westerschelde en de Eendracht,
Rijkswaterstaat, Dir. Zeeland, Proj. Buro Zierikzee, Nota ZL-87.0002, April 1987.

REFERENCES (continued)

Biegel, E.J., 1991
Fase-Rapport ISOS*2,
Fase 1: Inventarisatie, bewerking en analyse,
Rijksuniv. Utrecht, Vakgr. Fys. Geogr., Den Haag, 16-12-1991.

Boender, J., 1977
Toetsing van gemeten snelheids- en zandconcentratievertikalen aan de aannamen van Bijker en de bepaling van de parameters b en μ uit de bodemtransportformule van Bijker,
T.U. Delft, Vakgr. Kustw. Bouwk., Civiele Techn., Afstudeerversl. 1977, 91. p.

Boender, J. en Reus, J. de, 1978
Beschouwingen over de bodemruwheid in stationaire en niet-stationaire stroming,
TU-Delft, Vakgr. Kustw. Bouwk., Civiele Techn., Afstudeerverslag 1977 of 1978,
27 p.

Boon, J.D. and R.J. Byrne, 1981
On basin hyposometry and morphodynamic response of coastal inlet systems.
In: Nichols and Allen (eds.), 1981, Marine Geology 40 (1-2), 1981, pp. 27-48

Bretting, A.E., 1958
Stable Channels,
Acta Polytechnica Skandinavia 245, Copenhagen, Denmark, 1958

O'Brien, M.P., 1931
Estuary tidal prisms related to entrance areas,
Civil Eng., ASCE, Vol. 1, No. 8, 1931, pp. 738-739.

O'Brien, M.P., 1969
Equilibrium flow areas of inlets on sandy coasts.
J. of the Waterways and Harbors Div., Proc. Am. Soc. Civ. Eng., 1969

Brown, 1928
Inlets on sandy coasts,
Proc. ASCE, Vol. 54, Part II, Febr. 1928.

REFERENCES (continued)

Bruun, P. and F. Gerritsen, 1960
Stability of coastal inlets,
North Holland Publishing Company, Amsterdam, 1960, 123 p.

Bijker, E.W., 1967
'Some considerations about scales for coastal models with movable bed'.
DELFT HYDRAULICS, Publication No. 50, 1967.

Byrne, R.J., R.A. Gammisch and G.R. Thomas, 1980
Tidal prism-inlet area relations for small tidal inlets.
Proc. 17th Coast. Eng. Conf., ASCE, Vol. 3, ch. 151, 1980, pp. 2517-2533

Davis, J.J., 1964
A morphogenic approach to world shorelines
Zeitschrift für Geomorph., Bd. 8, 1964

Delft Hydraulics, 1987
Gaswinning op Ameland-oost, effekten van bodemdaling
Delft Hydraulics, Report H114, April 1987

Dieckmann, R., 1985
Geomorphologie, Stabilitäts- und Langzeitverhalten von Watteinzugsgebieten der Deutschen Bucht,
Mitt. Franzius-Institut, Univ. Hannover, Heft 60, 1985, pp. 133-361

Dieckmann, R. and H.W. Partenscky, 1986
A new equilibrium analysis for nearshore tidal basins
Proc. 20th CEC, Taiwan, ROC (1986), pp. 1077-1091

Dieckmann, R., M. Osterthun and H.W. Partenscky, 1988
A comparison between German and North American tidal inlets.
Proc. 21st Coast. Eng. Conf., ASCE, Vol. 3, ch. 199, 1988, pp. 2681-2691

Duits-Nederlandse Eemscommissie, 1989
Rapport Hydrologisch onderzoek, Huibergat-Westereems, Zeegat van de Eems, Meting 1989,
Wasser- und Schiffahrtsamt Emden, Rijkswaterstaat, - Dir. Groningen

REFERENCES (continued)

Eysink, W.D., 1979
Morfologie van de Waddenzee, gevolgen van zand- en schelpenwinning,
Waterloopkundig Laboratorium, verslag Literatuuronderzoek, Rap. R1336, 1979
(in Dutch).

Eysink, W.D., 1983
Nakdong estuary barrage and land reclamation, Morphological aspects.
Symp. Integr. of Ecol. Aspects in Coast. Eng., Rotterdam, The Netherlands, June
1983. Also DELFT HYDRAULICS, Publ. 297, March 1983

Eysink, W.D., 1990
Morphologic response of tidal basins to changes.
Proc. 22nd Coast. Eng. Conf., A.S.C.E., Delft, July 2-6, Vol. 2,
The Dutch Coast, Paper no. 8, 1990, pp. 1948-1961

Eysink, W.D. et al, 1986
Vogeleiland Griend in de Waddenzee, Voorstel voor maatregelen ter behoud van
het eiland
Delft Hydraulics, Report H262, Oct. 1986

Eysink, W.D., 1991a
Impact of sea level rise on the morphology of the Wadden Sea in the scope of
its ecological function, ISOS*2 Project, Phase 1,
Inventory of available data and literature and recommendations on aspects to be
studied,
DELFT HYDRAULICS, Report H1300, August 1991.

Eysink, W.D., 1991b
Simple morphologic relationships for estuaries and tidal channels; handy tools
for engineerings
COPEDEC III, Mombassa, Kenya, 16-20 Sept. 1991, Vol. II, pp. 1003-1014

Eysink, W.D., 1991c
Mogelijke oorzaken van de verdieping voor de hoofden van de Eemshaven
Delft Hydraulics, Report H1433, Nov. 1991

REFERENCES (continued)

Fitzgerald, D.M., D. Nummedal and T.W. Kana, 1976
Sand circulation pattern at Price Inlet, South Carolina
Proc. 15th Coast. Eng. Conf., ASCE, Vol. 2, ch. 109, 1976, pp. 1868-1880

Gerritsen, F. en H. de Jong, 1983
Stabiliteit van doorstroomprofielen in de Westerschelde.
Nota WWKZ-83.V008, Rijkswaterstaat Adviesdienst Vlissingen, 1983.

Gerritsen, F. en H. de Jong, 1985
Stabiliteit van doorstroomprofielen in het Waddengebied.
Nota WWKZ-84.V016, Rijkswaterstaat Adviesdienst Vlissingen, 1985.

Gerritsen, F., 1990
Morphological stability of inlets and channels of the western Wadden Sea,
Rijkswaterstaat, Report GWAO-90.019, Oct. 1990.

Gerritsen, F., H. de Jong and A. Langerak, 1990
Cross-sectional stability of estuary channels in the Netherlands.
Proc. 22nd Coast. Eng., ASCE, abstract, 1990.

Göhren, H., 1968
Triftströmungen im Wattenmeer, Mitteilungen des Franzius-Instituts für Grund- und Wasserbau der TU Hannover, Heft 30

Haring, J. (in Dutch), 1967
De verhouding van getijvolume en doorstroomprofiel in de zeegaten Haringvliet, Brouwershavense Gat, Oosterschelde en in de mond van de Rotterdamse Waterweg uit alle beschikbare waarnemingen tot heden.
Rijkswaterstaat, Deltadienst WA, Nota K-271, aug. 1967

Hayes, M.O., 1979
Barrier island morphology as a function of tidal and wave regime in:
Leatherman, S.P. (ed.), Barrier Islands from the Gulf of St. Lawrence to the Gulf of Mexico;
Acad. Press, New York; 1979, pp. 1-27

REFERENCES (continued)

Hoozemans, F., 1988
Golfklimaat ter hoogte van het eiland Texel,
Rijkswaterstaat, Dienst Getijdewateren, Notitie GWAO-88.243, 29 februari 1988.

Hume, T.M. and Herdendorf, C.E, 1990
Morphologic and Hydraulic Characteristics of Tidal Inlets on a Headland
Dominated, Low Littoral Drift Coast, Northeastern New Zealand.
J. of Coast. Research, Proc. Skagen Symposium, 1990, pp. 527-563
(special issue)

Jarret, J.T., 1976
Tidal prism-inlet area relationship, Rep. no. 3,
Coastal Engineering Research Center, Ft. Belvoir, Virginia, 1976, 32 pp.

Johnson, J.W., 1972
Tidal inlets on the California, Oregon and Washington coasts,
Hydr. Eng. Lab., Univ. of California, Berkeley, Techn. Report HEL 24-12, 1972

Johnson, J.W., 1973
Characteristics and behaviour of Pacific Coast Tidal Inlets,
Proc. ASCE, Journal of Waterways, Harbors and Coastal Eng. Div., Vol. 99,
p. 325, August, 1973

Jong, H. de and F. Gerritsen, 1984
Stability parameters of Western Scheldt Estuary.
Proc. 19th Coast. Eng. Conf., ASCE, Vol. 3, ch. 205, 1984, pp. 3078-3093.
Ook: nota WWKZ-84.V029, Rijkswaterstaat Adviesdienst Vlissingen.

Kleef, A.W. van, 1991a
Empirical relationships for tidal inlets, basins and deltas,
Inst. of Geogr. Res., Univ. of Utrecht, Report GEOPRO 1991. 19, July 1991.

Kleef, A.W. van, 1991b
Inventarisatie meetgegevens Waddenzee,
Inst. of Geogr. Res., Univ. of Utrecht, Report GEOPRO 1991.04 (IRO),
Notitie AOFM-91.10.010 (Rijkswaterstaat, DGW).

REFERENCES (continued)

Koning, J.C.F.M. en Kreuk, J.J.N., 1976
De golfbeweging in het waddengebied van Terschelling,
Rijkswaterstaat, Studiedienst Hoorn, Nota 76.5, mei 1976.

Kreeke, J. van de, and Haring, J., 1979
Equilibrium flow areas in the Rhine/Meuse Delta,
Coastal Eng., 3: 97-111, 1979

Lambeek, J.J.P., 1991
Biotic-abiotic relations in the Dutch Wadden Sea,
Rijkswaterstaat, DGW, Draft report, 09-01-1991.

Lassen, H. and Siefert, W., 1991
Mittlere Tidewasserstände in der südöstlichen Nordsee-Säkularer Trend und
Verhältnisse um 1880 (Schlussbericht eines KFK1-Projektes)
Die Küste, Heft 52, 1991, pp. 85-137

Le Conte, 1905
Discussion of "Notes on the improvement of river and harbour outlets in the
USA", Paper no. 1009 by D.A. Watts, Transactions,
ASCE, Vol. LV, Dec. 1905, pp. 306-308.

Luck, G., 1975
Der Einflus der Schutzwerke der Ostfriesischen Inseln auf die morphologischen
Vorgänge im Bereich der Seegaten und ihrer Einzugsgebiete,
Proefschrift, Mitt. des Leichtweiss. Inst. für Wasserbau der Techn. Universität
Braunsweig, Heft 47, 1975, pp. 1-122

Mayor-Mora, R.E., 1977
Laboratory investigations of tidal inlets on sandy coasts,
GITI Rep. 11, US Army Corps of Eng., Coastal Eng. Res. Centre, Fort Belvoir,
Va., and US Army Eng. WES, Vicksburg, Miss., 1977

Mazure, J.P., et al., 1974
Report of the Wadden Sea Comittee (in Dutch); Advice on the fundamental options
and the benefits and disadvantages of empoldering in the Wadden Sea,
RWS, Alg. Zaken, The Hague, May 1974, 325 p.

REFERENCES (continued)

Mehta, A.J., 1976
Stability of some New Zealand Coastal Inlets
New Zealand J. of Marine and Freshwater Research, Wellington, New Zealand,
Letter to the editor, Vol. 10, no. 4, 1976, p. 737-742

Misdorp, R., Steyaert, F., Hallie, F. and Ronde, J. de, 1990
Climate change, sea level rise and morphological developments in the Dutch Wadden Sea, a marine wetland,
In: J.J. Beukema et.al. (eds), Expected effects of climatic change on marine coastal ecosystems,
Kluwer Ac. Publ., The Netherlands, 1990, pp. 123-131

Niemeyer, H.D., 1986
Ausbreitung und Dämpfung des Seegangs im See- und Wattengebiet von Norderney,
Niedersächsisches Landesambt für Wasserwirtschaft,
Forschungsstelle Küste, Norderney, Jahresber. 1985, band XXXVII,
Okt. 1986, p. 49-95.

Niemeyer, H.D., 1991
Case study, Ley Bay: An alternative to traditional enclosure,
Proc. COPEDEC, Mombasa, Kenya, Sept. 1991.

Renger, E., 1976
Quantitative Analyse der Morphologie von Watteinzugsgebieten und Tidebecken,
Mitt. Franzius-Inst., Hannover, heft 43, 1976, pp. 1-161

Renger, E. and Partenscky, H.W., 1974
Stability criteria for tidal basins
Proc. 14th Coast. Eng. Conf., Vol. 2, ch. 93, 1974, pp. 1605-1618

Renger, E. and Partenscky, H.W., 1980
Sedimentation processes in tidal channels and tidal basins caused by artificial constructions
Proc. 17th Coast. Eng. Conf., ASCE, Vol. 3, ch. 148, 1980, pp. 2481-2494

REFERENCES (continued)

Ribberink, J.S. en Vroeg, J.H. de, 1991
Kustverdediging Eierland (Texel), hydraulisch morfologische effectstudie, fase I,
WL, Rapport H1241, deel I, Morf. Analyses, juni 1991.

Riedel, H.P. and M.R. Gourlay, 1980
Inlets/estuaries discharging into sheltered waters.
Proc. 17th Coast. Eng., ASCE, Vol. 3, ch. 153, 1980, pp. 2550-2564

Rietveld, C.F.W., 1963
Natural development of the Wadden Sea after the enclosure of the Zuidersea,
Proc. 8th Conf. Coastal Eng., Mexico City, Nov. 1962, PUbl. 1963, pp. 765-781

Roskam, A.P., 1988
Golfklimaten voor de Nederlandse kust,
Rijkswaterstaat, Dienst Getijdewateren, nota GWAO-88.046, nov. 1988.

RWS, 1974
Bodemribbels Borndiep
Rijkswaterstaat, Studiedienst Hoorn, 14-3-1974, Drawings 74.2.918-921

Rijn, L.C. van, 1989
Handbook Sediment Transport by Currents and Waves,
DELFT HYDRAULICS, Rep. H461, June 1989.

Salomons, W., Eysink, W.D. and Kerdijk, H.N., 1981
Inventarisatie en geochemisch gedrag van zware metalen in de Schelde en Westerschelde,
DELFT HYDRAULICS, Report M1640/M1736, Dec. 1981 (in Dutch).

Schönfeld, W. von, and Jensen, J., 1991
Anwendung der Hauptkomponentenanalyse auf Wasserstandszeitreihen von Deutschen Nordseepegeln
Die Küste, Heft 52, 1991, pp. 191-224

REFERENCES (continued)

Sha Li ping, 1990
Sedimentological studies of the ebb-tidal deltas along the West Frisian Islands, The Netherlands
Thesis, Instituut voor Aardwetenschappen, Rijksuniversiteit Utrecht, 1990, 160 p.

Shaw, M.R. and Elsawy, E.M., 198?
Field study of the hydraulic characteristics of tidal inlets on the Arabian Gulf Coast,
?? pp. 350-360, 198?

Shigemura, T., 1976
Characteristics of tidal inlets on the Pacific coast of Japan
Proc. 15th Coast. Eng. Conf., ASCE, Vol. 2, 1976, pp. 1666-1680

Shigemura, T., 1980
Tidal prism - throat area relationships of the bays of Japan
Shore and Beach, Vol. 28, 1980, pp. 30-35

Straaten, L.M.J.U. van, 1975
De Sedimenthuishouding in de Waddenzee
Amsterdam, Symp. Waddenonderz., april 1973, Werkgroep Waddengebied,
Meded. nr. 1, 1975, pp. 5-20

Thijsse, J.Th., 1951
Hydraulica,
Technische Vraagbaak, deel W, Hoofdst. 3, NV. Kluwer, Deventer-Djakarta, 1951.

Urk, T.W. van, 1982
Golfklimaat Schild,
Rijkswaterstaat, Meet- en Adviesdienst Delfzijl, Nota 82-28, nov. 1982.

Urk, T.W. van, 1985
Golfklimatologie Schiermonnikoog-Noord,
Rijkswaterstaat, Meet- en Adviesdienst Delfzijl, Project: GOLFDOOR,
Nota 85-23, oktober 1985.

REFERENCES (continued)

Vincent, C.L. and Carson, W.D., 1981
Geometry of tidal inlets: empirical equations, Journ. of Waterway, Port, Coastal and Ocean Div., Proc. ASCE, Vol. 107, No. WW1, Febr. 1981, pp. 1-9

Voogt, L., Rijn, L.C. van, and Berg, J.H. van den, 1991
Sediment transport of fine sands at high velocities,
ASCE, J. Hydr. Eng., Vol. 117, No. 7, July 1991, p. 869-890.

Walter, F., 1972
Zusammenhänge zwischen der Grösse der Ostfriesischen Seegaten mit ihren Wattgebieten sowie den Gezeiten und Strömungen, Forschungsstelle für Insel- under Küstenschutz,
Jahresbericht 1971, Band XXIII, 1972, pp. 7-33

Walton, R.L. and W.D. Adams, 1976
Capacity of inlet outer bars to store sand.
Proc. 15th Coast. Eng. Conf., ASCE, Vol. 2, ch. 112, 1976, pp. 1919-1937.

Winton, T.C., 1979
Long and short term stability of small tidal inlets
Coastal and Oceanographic Eng. Lab., Univ. of Florida, Guinesville, Florida, UFL/COEL Report 79/004, 1979

Basin		Periods of selected soundings		Year of discharge measurement
No.	Inlet	Outer delta	Basin	
1	Marsdiep	1925		
		1933	1933	
		1950	1951	
			1965	1965!
		1972	1972	
			1977	
		1981		
2	Eijerlandse Gat	1926		
			1933	
			1949	1949!
			1962	
		1971	1971	1971!
		1976	1976	1977
		1982	1982	1979
		1987		
3	Vlie	1933	1933	
			1951	
			1965	
		1972	1972	1972!
		1974		
		1976		1976
		1978	1977	
		1980		
		1982	1982	
4	Borndiep	1926	1926	
		1934		
			1950	
		1958		
		1966	1967	1968
		1974	1973	
		1976	1978	
		1982	1984	
5	Pinkegat	-	1957/1959	1959
6	Zoutkamperlaag	-	1957/1959	1957*
7	Eilander Balg	-	-	1965
8	Lauwers	-	1962	1962
9	Schild	-	1958	1958
		-	1962	1962
10	Westereems	-	-	1975*

Note: ! Discharge modified based on data of Gerritsen and Jong (1985)
* No discharge measurements in inlet itself

Table 2.1 Selected data sets of Wadden Sea basins

Tidal inlet	M	EG	V	BD	PG	ZL	EB	L	S	WE
year	1948!	1948	(1948)	1968!	1959	1955!	1951	1953	1954	1971!
	1950	1953	1971	1969	1969	1961	1953!	1954	1958!	1973
	1951	1971	1976!	1970	1973	1968	1954	1962!	1960!	1979!
	1959!	1979		1971		1971	(1956)!	1972	1962!	1980!
	1962	1980		1989		1975	1965!	1977	1965!	1981!
	1966					1981!	1971	1984	1969!	1985!
	1971					1987			1973!	
	1973								1974!	
	1974!								1976!	
	1975!								1980!	
	1978!								1982!	
	1981!									

Notes: ! Discharge measurements in tidal inlet as well as in a number of other channel sections inside the basin
( ) Not sure of measuring row covered the entire inlet

Table 2.2 Years with discharge measurements in tidal inlets

Source	Location	Peak velocity (m/s)	Water depth h (m)	Bedform				Δ/h (%)
				average height Δ (m)	average length L (m)	L/Δ (-)	symmetric (-)	
RWS, 1974	Borndiep	approx. 1	3-4	0.2-1.0 (0.3)	25	25-125 (80)	yes	5-30
			6-7	0.2-0.4	10	25- 50		3- 7
			8-9	0.2-0.6	35	60-175		2- 7
			8-9	0.6	18	30		7
			9-10	0.4-0.5	14	40		4- 5
			9-11	0.8-1.0	18	20		7-11
			10-11	0.4-1.2	35	30- 90		4-12
			11	0.2-0.6	18	30- 90		2- 6
			11-12	0.6-1.4	35	25- 60		5-12
			12-13	0.2-0.7	35	50-175		2- 6
			13-15	0.6-1.7	35	20- 60		5-10
Berg, 1987	Schaar v. Valkenisse	approx. 1	3 -4	0.1-0.2				2- 7
			3 -5	0.5-0.6				10-20
								8-14
	Zimmermangeul		3.5-4	0.3-0.5				1- 3
	Zuidergat		7	0.05-0.2				
Voogt et al, 1991	Sluitgat	1.4-1.5	10	0.4-0.5	10	20-25		4- 5
	Krammer	1.6-1.8	10	0.6-0.8	10-15	15-20	no	6- 8
		2.4-2.6	10	0.4	30	75	yes	4
Rijn, 1989	Eastern part of Western Scheldt	1-1.5	7-25	0.2-1 (0.6)	10	10-50 (17)	yes	1-14
			25	2	100	50	no	8

Table 3.1 Bedform data of RWS and from Literature

Area	H_s (m)	T_s (s)
North Sea (deep water)	1.5	5.7
Tidal inlets and channels in outer deltas of:		
Marsdiep	1.0	5.5
Eierlandse Gat	0.7	4.3
Vlie	1.0	5.5
Borndiep	0.85	5.0
Pinkegat/Holwerderbalg	0.65	4.1
Zoutkamperlaag	0.75	4.5
Eilander Balg	0.6	4.0
Lauwers	0.7	4.3
Schild	0.6	4.0
Westereems	1.0	5.5
Channel areas inside basins	0.3	2.5

Table 3.2 Selected morphological wave data

Equation	95% Confidence Limits of n		Number of Data Points
	Lower	Upper	
1. All Inlets			
a. Atlantic, Gulf, and Pacific coasts			
$A = 158 \times 10^{-6}P^{0.95}$	0.91	1.00	162
b. Atlantic coasts			
$A = 30.4 \times 10^{-6}P^{1.05}$	0.99	1.12	79
c. Gulf coast			
$A = 931 \times 10^{-6}P^{0.84}$	0.73	0.95	36
d. Pacific coast			
$A = 283 \times 10^{-6}P^{0.91}$	0.86	0.97	47
2. Unjettied or Single-Jettied Inlets			
a. Atlantic, Gulf, and Pacific coasts			
$A = 38.0 \times 10^{-6}P^{1.03}$	0.97	1.10	96
b. Atlantic coasts			
$A = 22.6 \times 10^{-6}P^{1.07}$	0.99	1.16	50
c. Gulf coast			
$A = 699 \times 10^{-6}P^{0.86}$	0.73	0.99	30
d. Pacific coast			
$A = 8.95 \times 10^{-6}P^{1.10}$	0.99	1.21	16
3. Inlets with Two Jetties			
a. Atlantic, Gulf, and Pacific coasts			
$A = 749 \times 10^{-6}P^{0.86}$	0.81	0.92	66
b. Atlantic coasts			
$A = 158 \times 10^{-6}P^{0.95}$	0.81	1.09	29
c. Gulf coast			
Insufficient data for regression analysis			
d. Pacific coast			
$A = 1015 \times 10^{-6}P^{0.85}$	0.81	0.88	31

Regression Equations of P Versus A; Form of Equations $A = CP^n$

Table 3.3 Relations derived by Jarret (1976)

Tidal inlet		Year	Tidal prism	Sand volume above ref. plane	Channel volume below ref. plane	Net sand volume outer delta
Name	Main channel(s)		(10^6 m^3)	(10^6 m^3)	(10^6 m^3)	(10^6 m^3)
Zeegat van Texel	Marsdiep	1925		708.3	111.9	596.4
		33		754.2	104.2	650.0
		50		742.9	141.1	601.8
		72	996 (1965)	686.9	177.7	509.2
		81		674.2	185.2	489.0
Eierlandse Gat	Engelsmangat	1926		117.8	6.8	111.0
	Robbengat	71	162	138.8	11.0	127.8
		76		143.7	11.1	132.6
		82	205	147.2	12.2	135.0
		87		141.2	13.6	127.6
Zeegat van Terscheling	Vlie	1933		503.4	87.0	416.4
	Vliesloot	72	954	468.7	99.0	369.7
		74		452.4	104.9	347.5
		76		466.3	102.0	364.3
		78	1003 (1977)	461.5	98.1	363.4
		80		442.8	103.3	339.5
		82		454.6	99.9	354.7
Zeegat van Ameland	Borndiep	1926		173.9	59.6	114.3
	Boschgat	34		202.7	57.2	145.5
		58		223.3	59.9	163.4
		66	389 (1967)	220.8	75.2	145.6
		74		216.9	88.4	128.5
		76		228.6	87.3	141.3
		82		209.4	88.5	120.9

Table 6.1 Sand volumes stored in outer deltas of Dutch Wadden Sea inlets

STATIONS ALONG THE DUTCH WADDEN SEA
WITH WATER LEVEL GAUGES

DELFT HYDRAULICS | H 1300 | FIG. 2.1

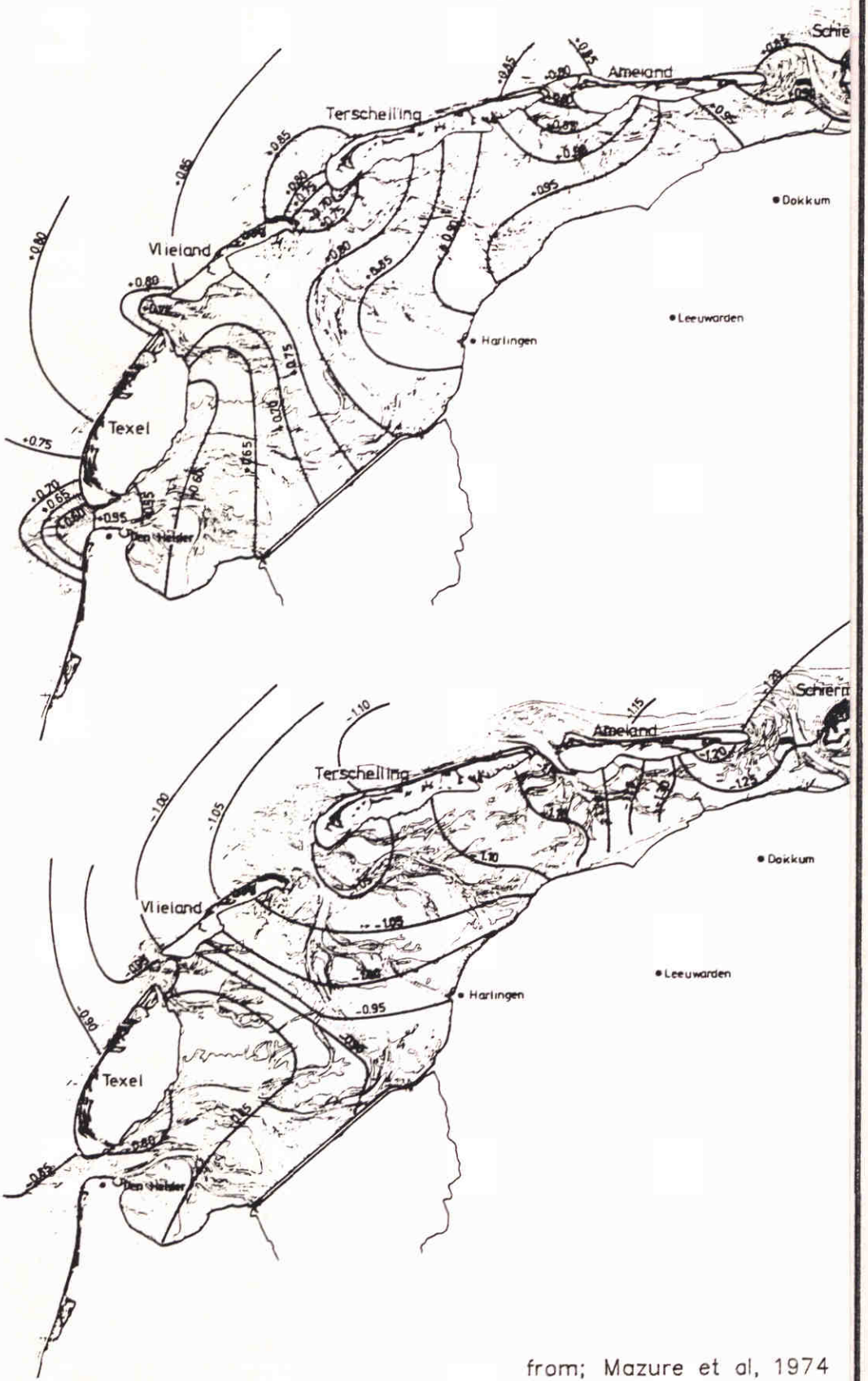

from; Mazure et al, 1974

MHW AND MLW ISO–LINES IN THE DUTCH WADDEN SEA		
DELFT HYDRAULICS	H 1300	FIG. 2.2

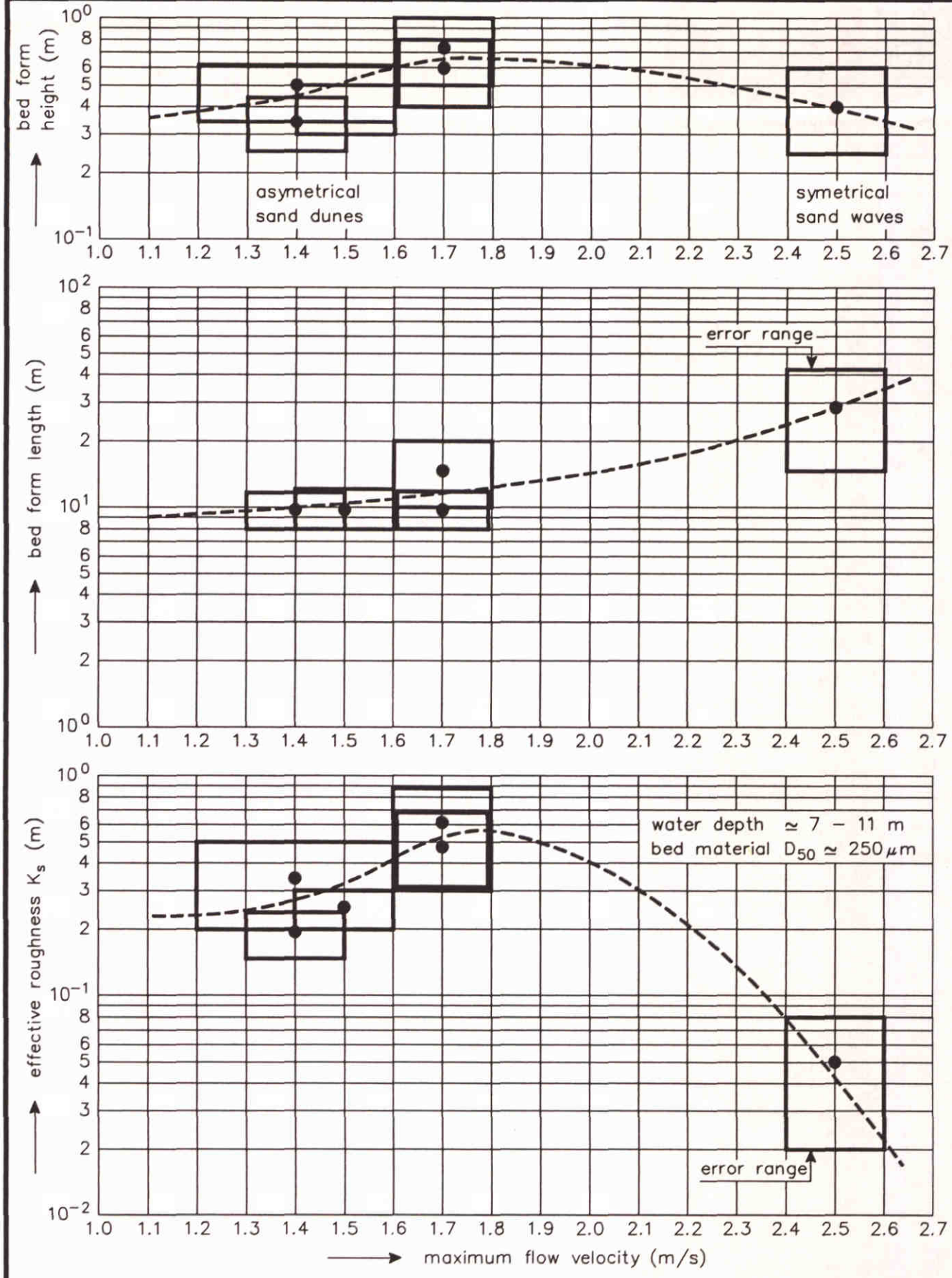

MEASURED BED FORM DIMENSIONS AND COMPUTED ROUGHNESS IN TIDAL FLOW (VOOGT ET AL, 1991)

DELFT HYDRAULICS | H 1300 | FIG. 3.1

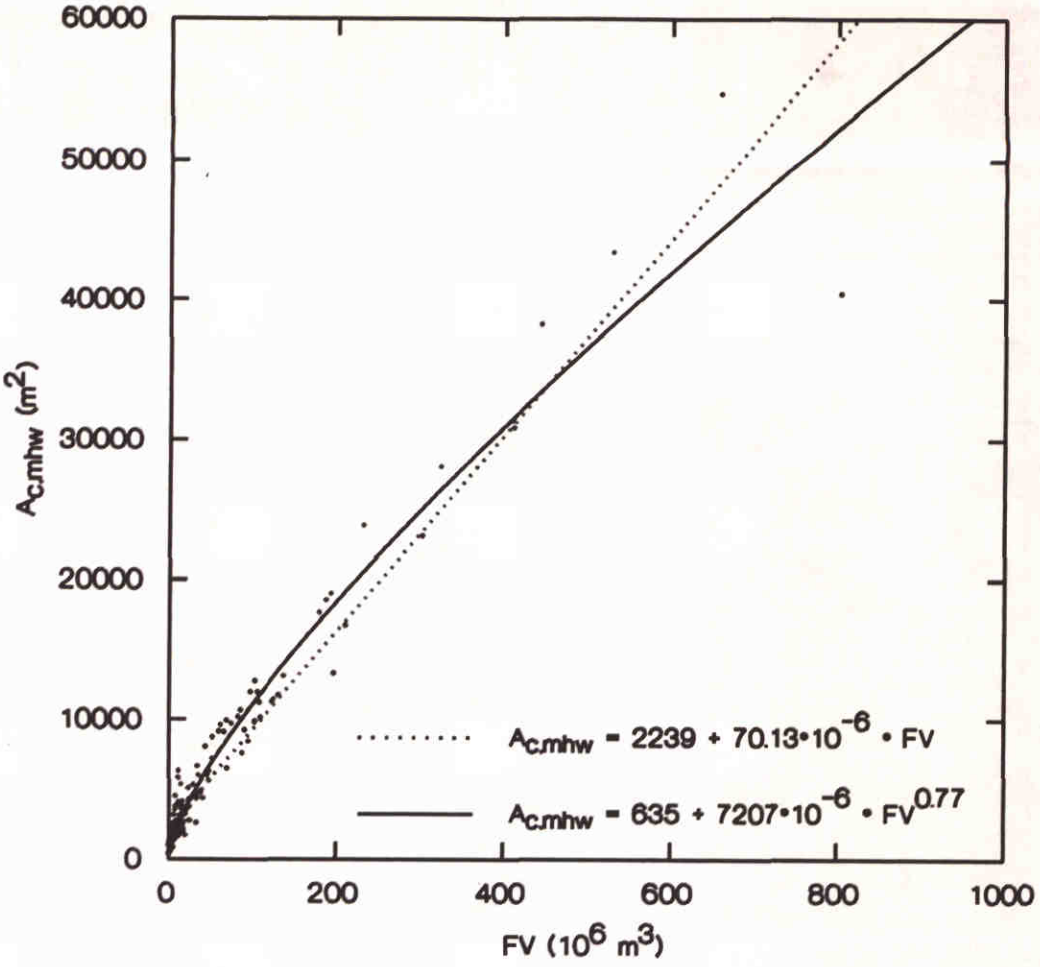

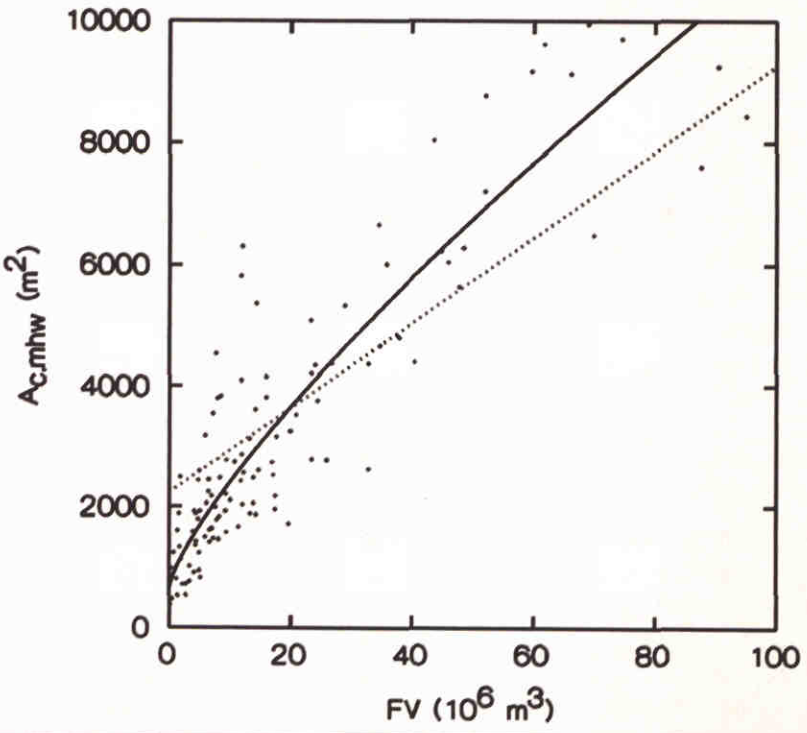

CORRELATION OF FV WITH $A_{c,mhw}$

DELFT HYDRAULICS | H 1300 | FIG. 3.2

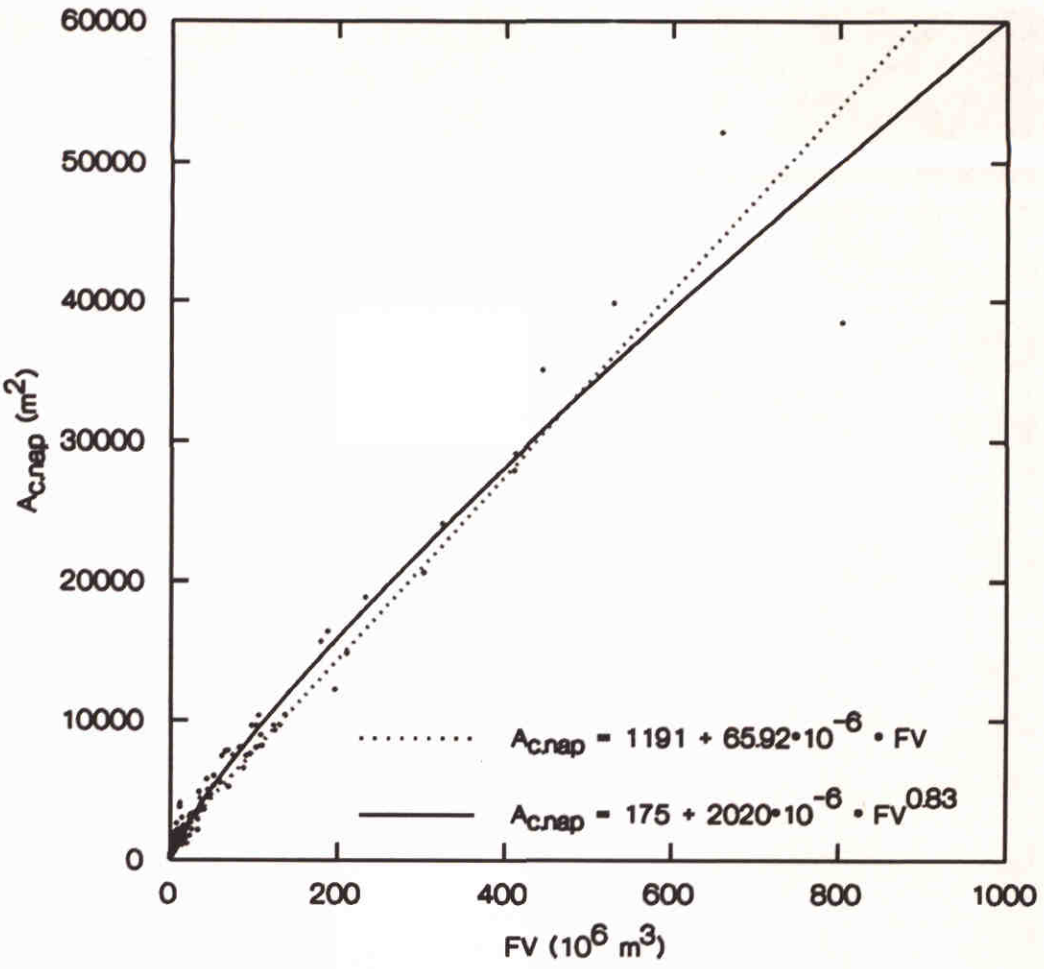

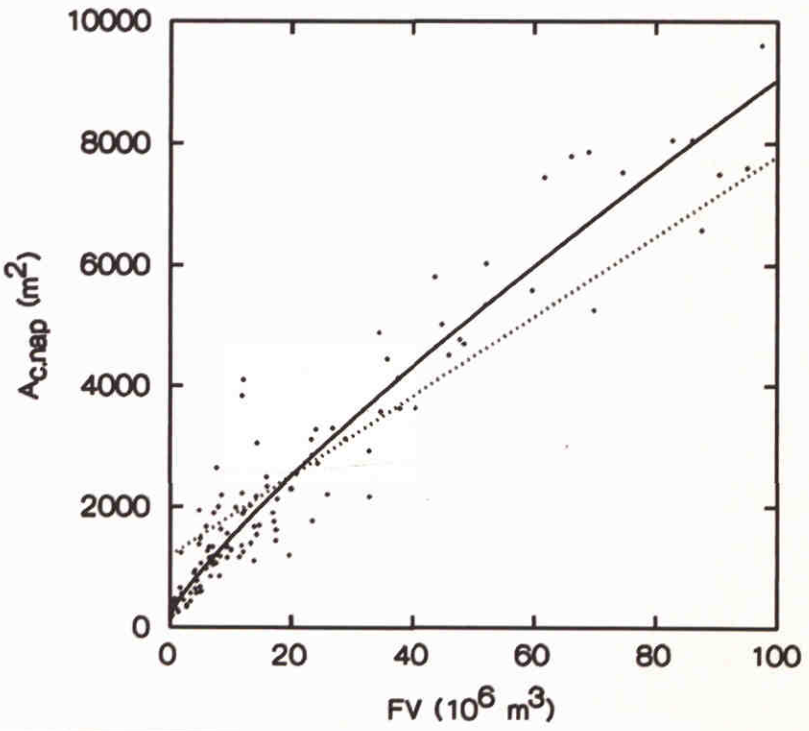

CORRELATION OF FV WITH $A_{c.nap}$

DELFT HYDRAULICS | H 1300 | FIG. 3.3

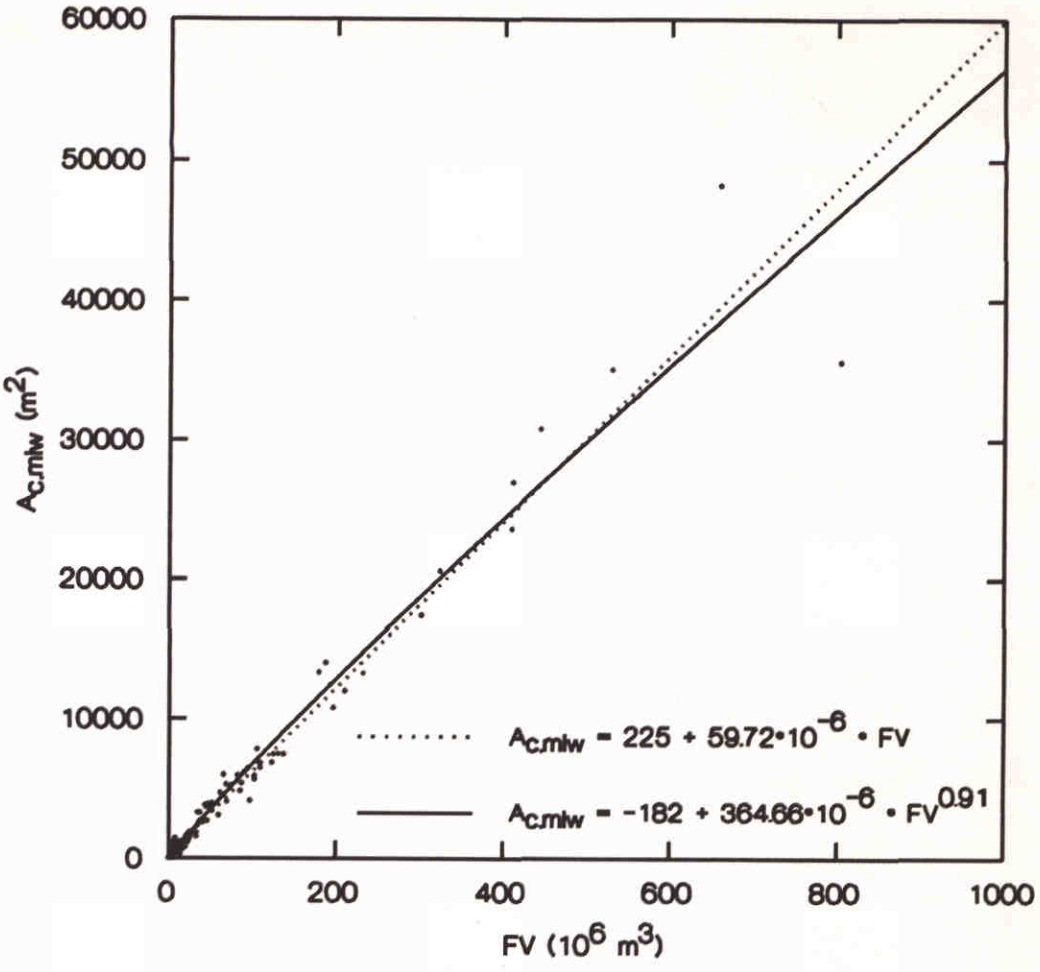

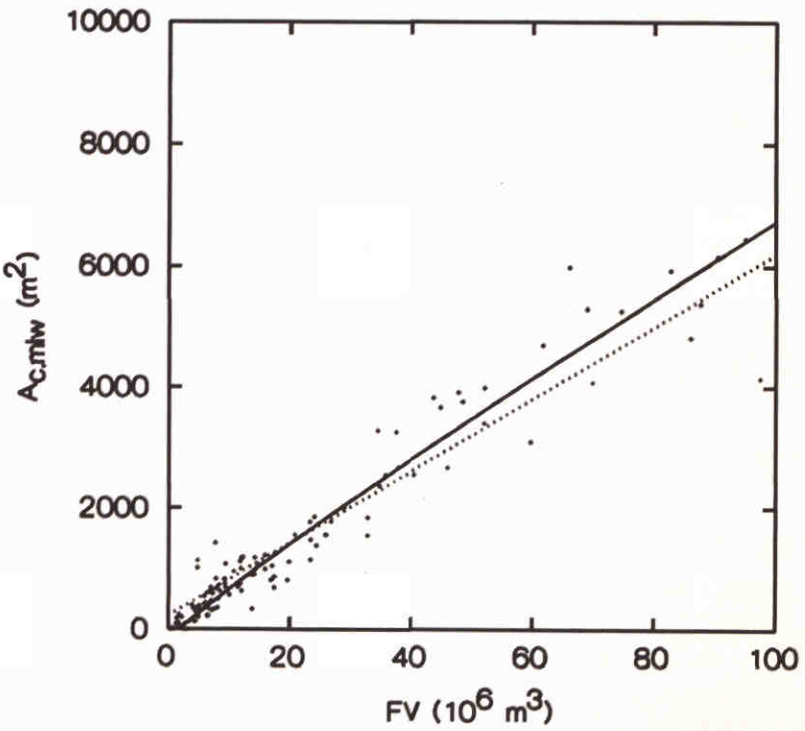

CORRELATION OF FV WITH $A_{c,mlw}$

DELFT HYDRAULICS | H 1300 | FIG. 3.4

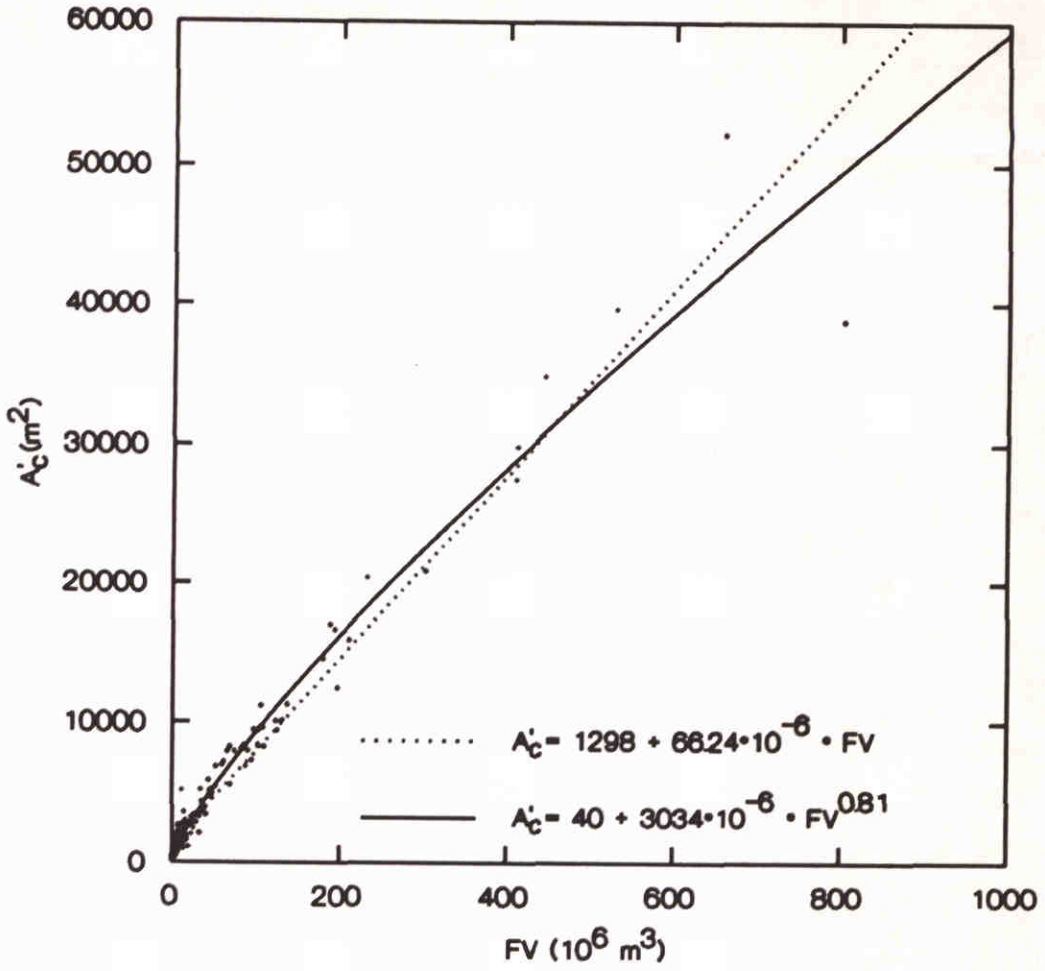

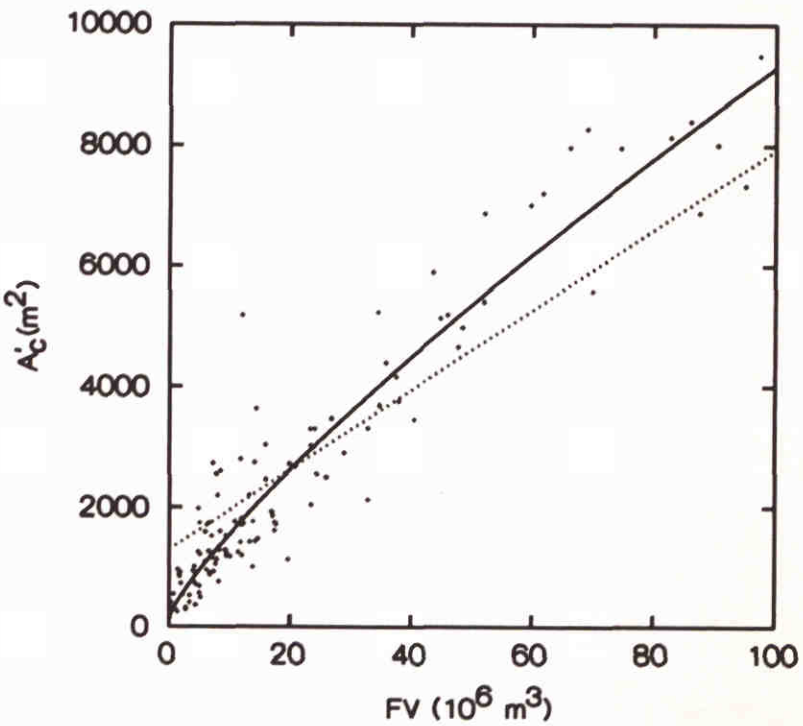

CORRELATION OF FV WITH A'_c

DELFT HYDRAULICS | H 1300 | FIG. 3.5

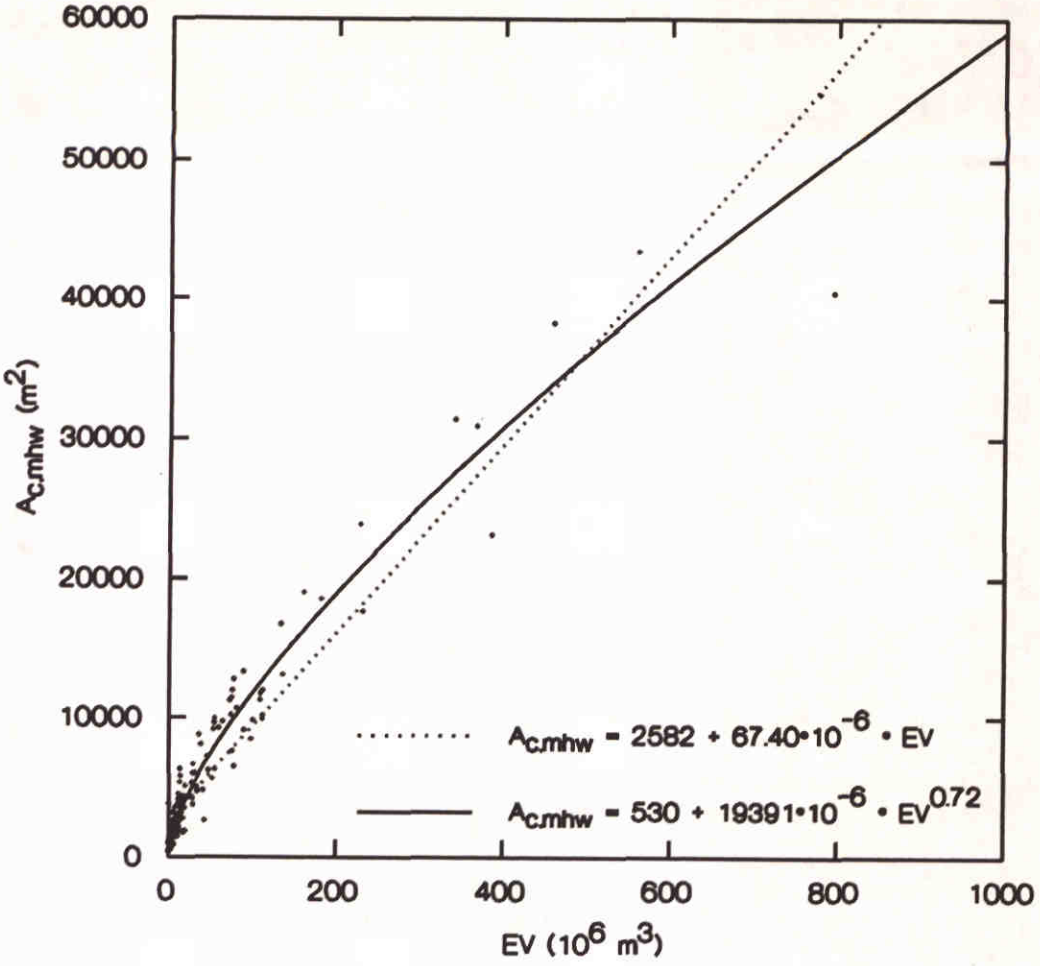

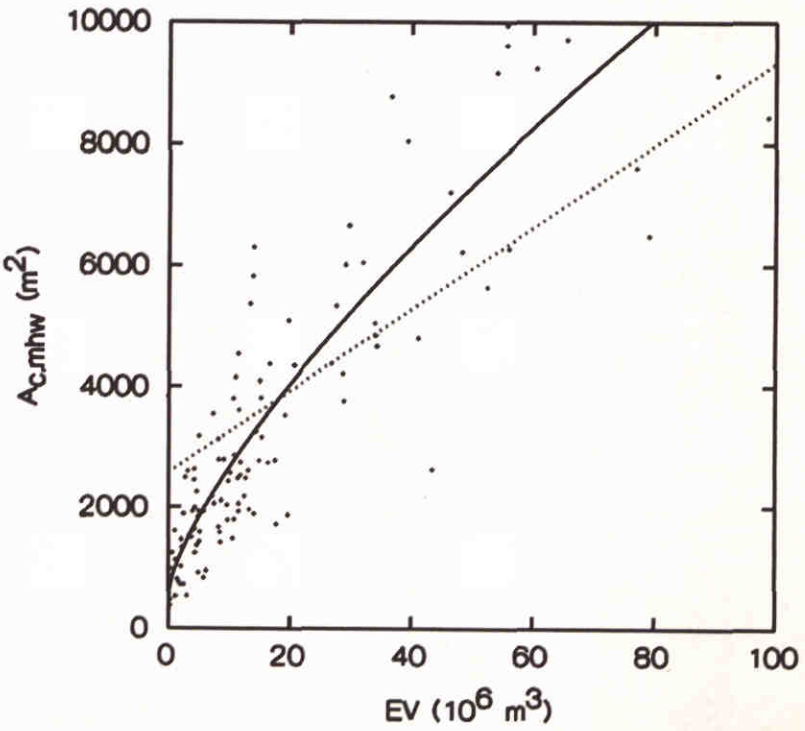

CORRELATION OF EV WITH $A_{c.mhw}$

DELFT HYDRAULICS | H 1300 | FIG. 3.6

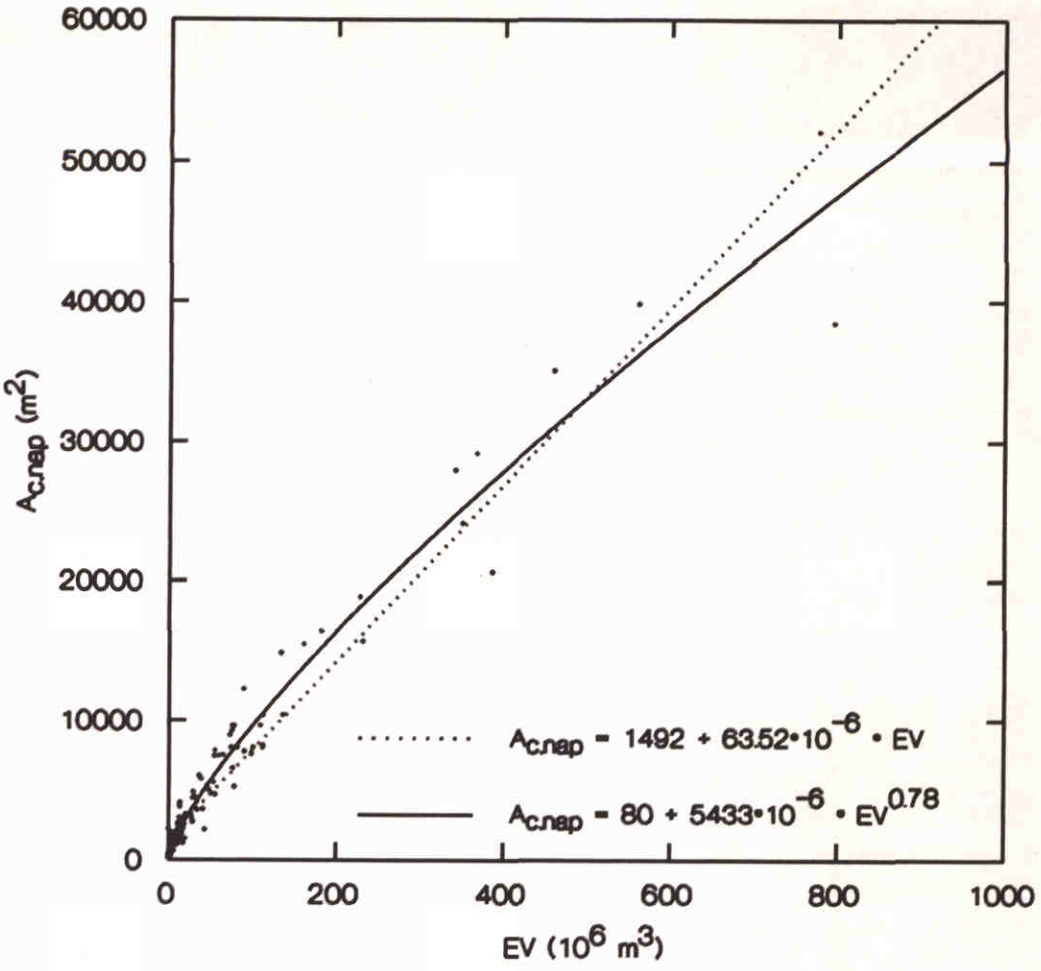

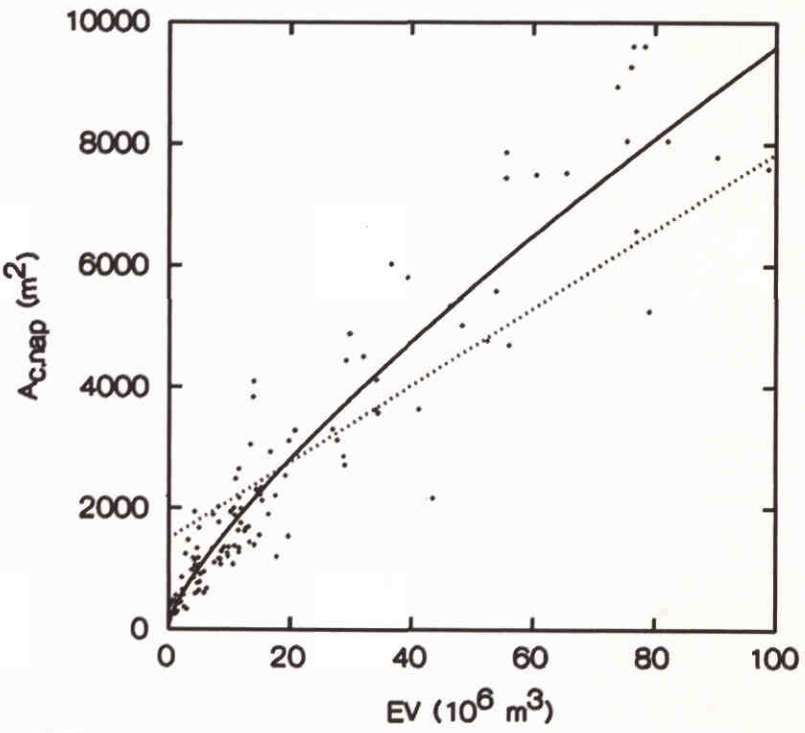

CORRELATION OF EV WITH $A_{c.nap}$

DELFT HYDRAULICS | H 1300 | FIG. 3.7

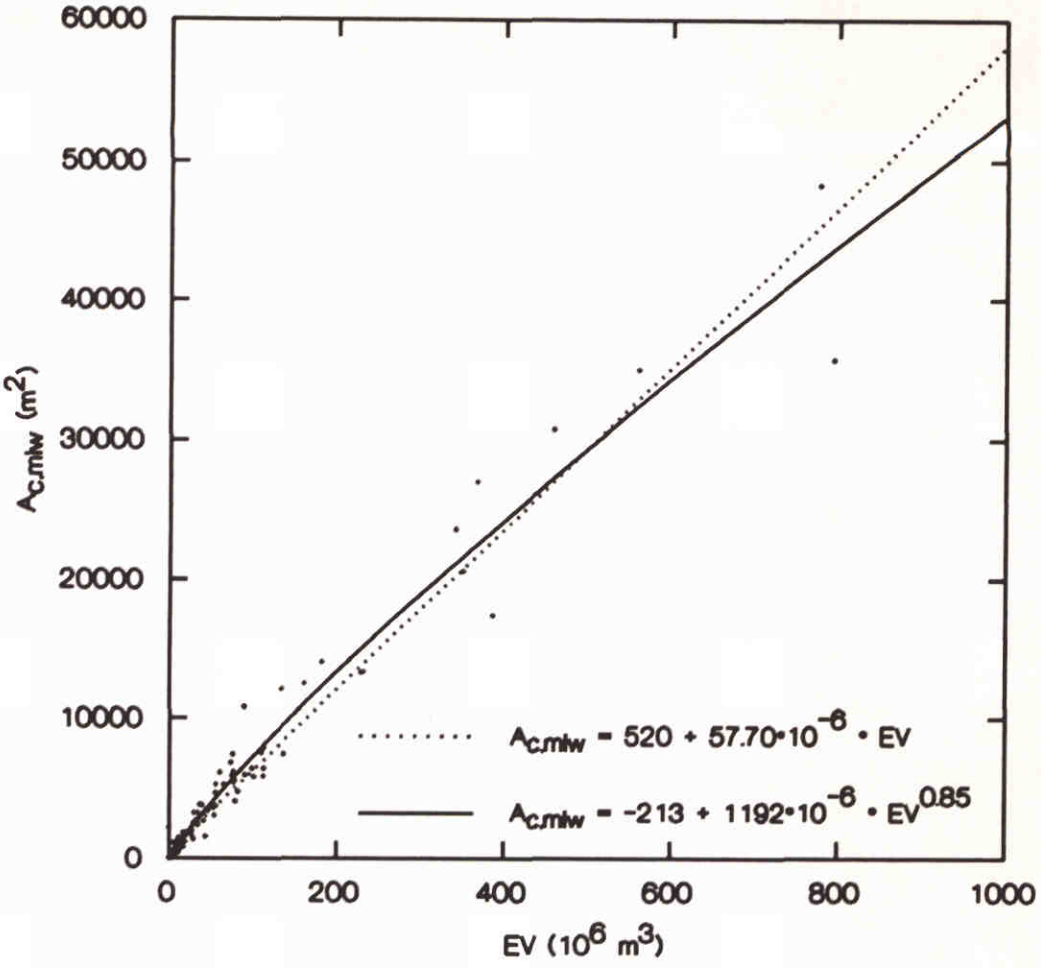

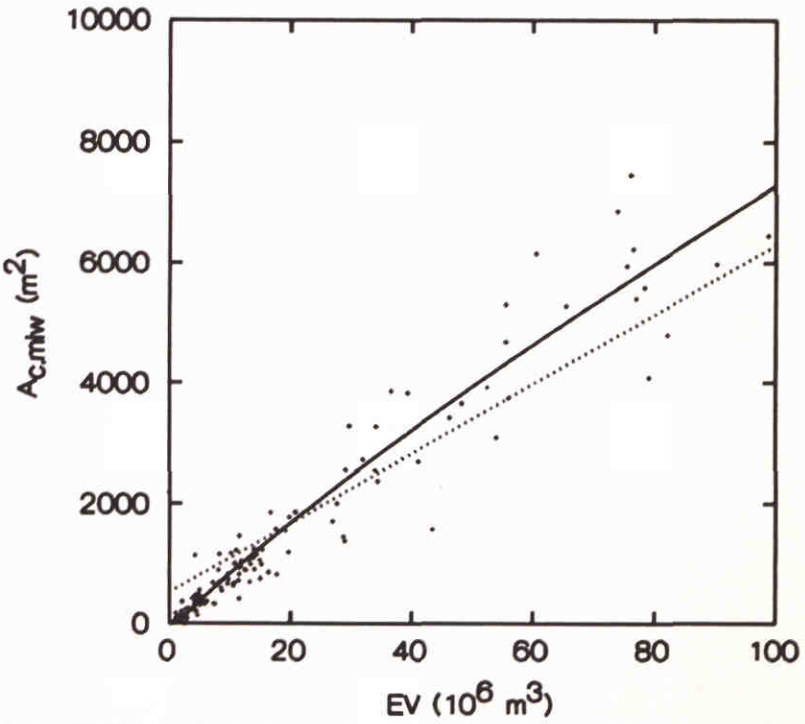

CORRELATION OF EV WITH $A_{c.mlw}$

DELFT HYDRAULICS | H 1300 | FIG. 3.8

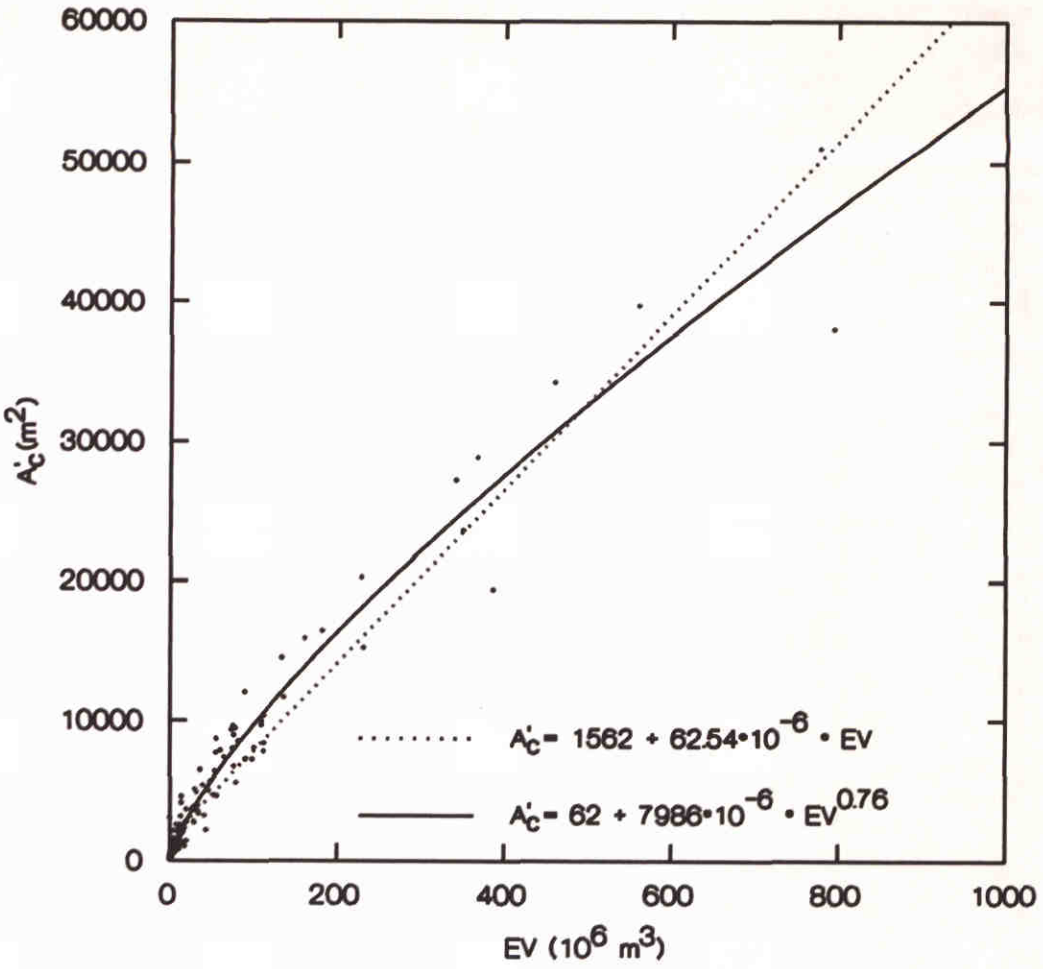

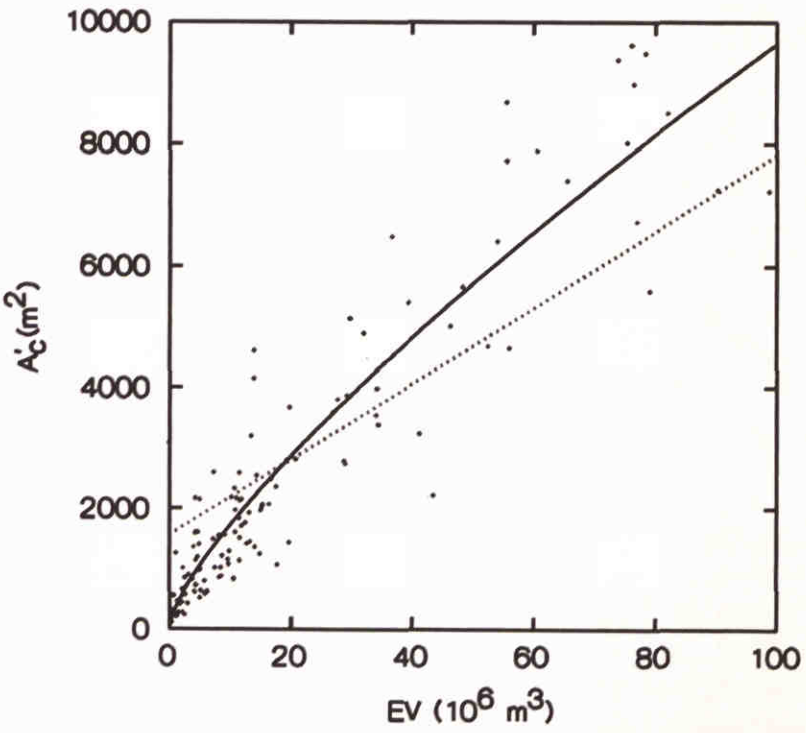

CORRELATION OF EV WITH A'_c

DELFT HYDRAULICS | H 1300 | FIG. 3.9

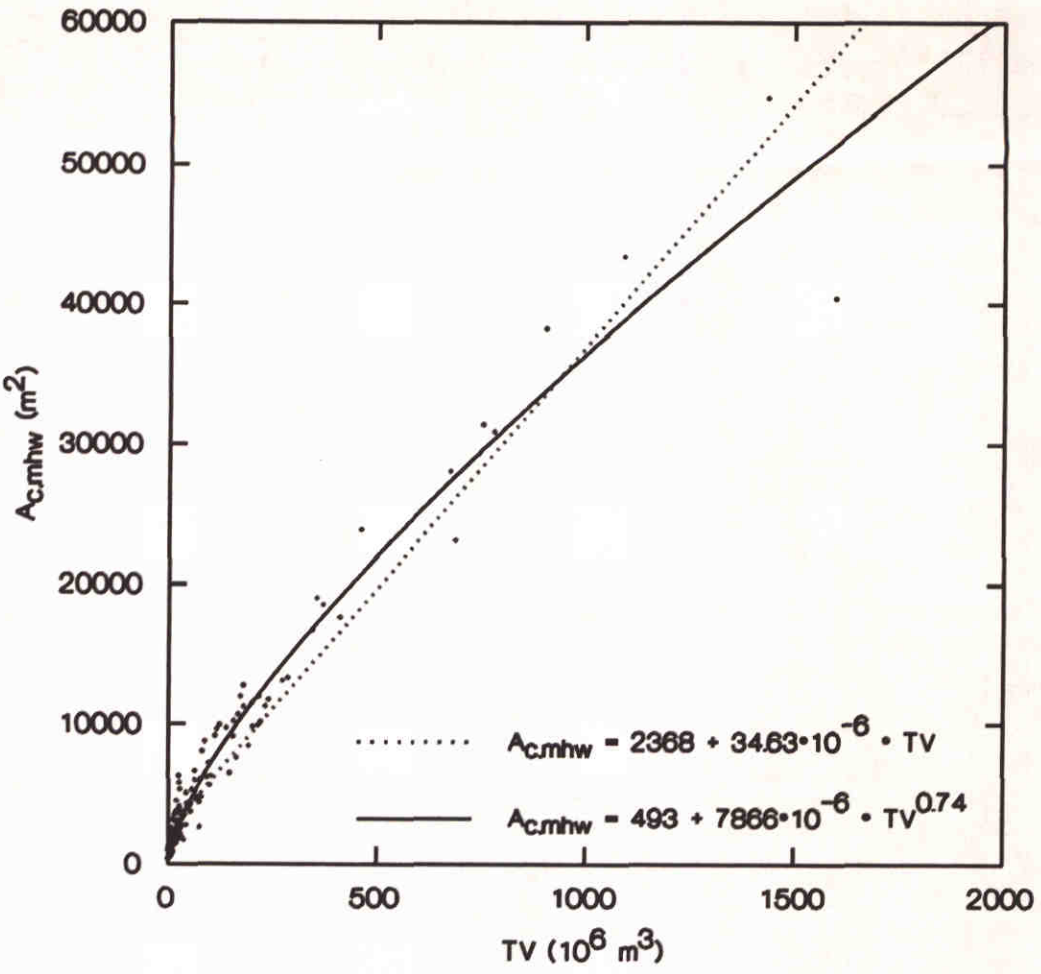

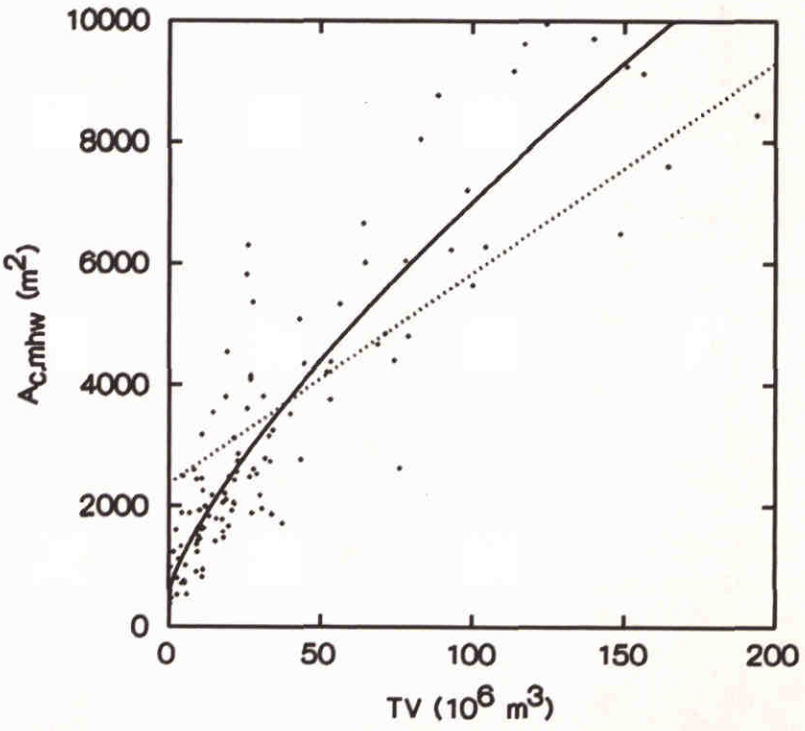

CORRELATION OF TV WITH $A_{c,mhw}$

DELFT HYDRAULICS | H 1300 | FIG. 3.10

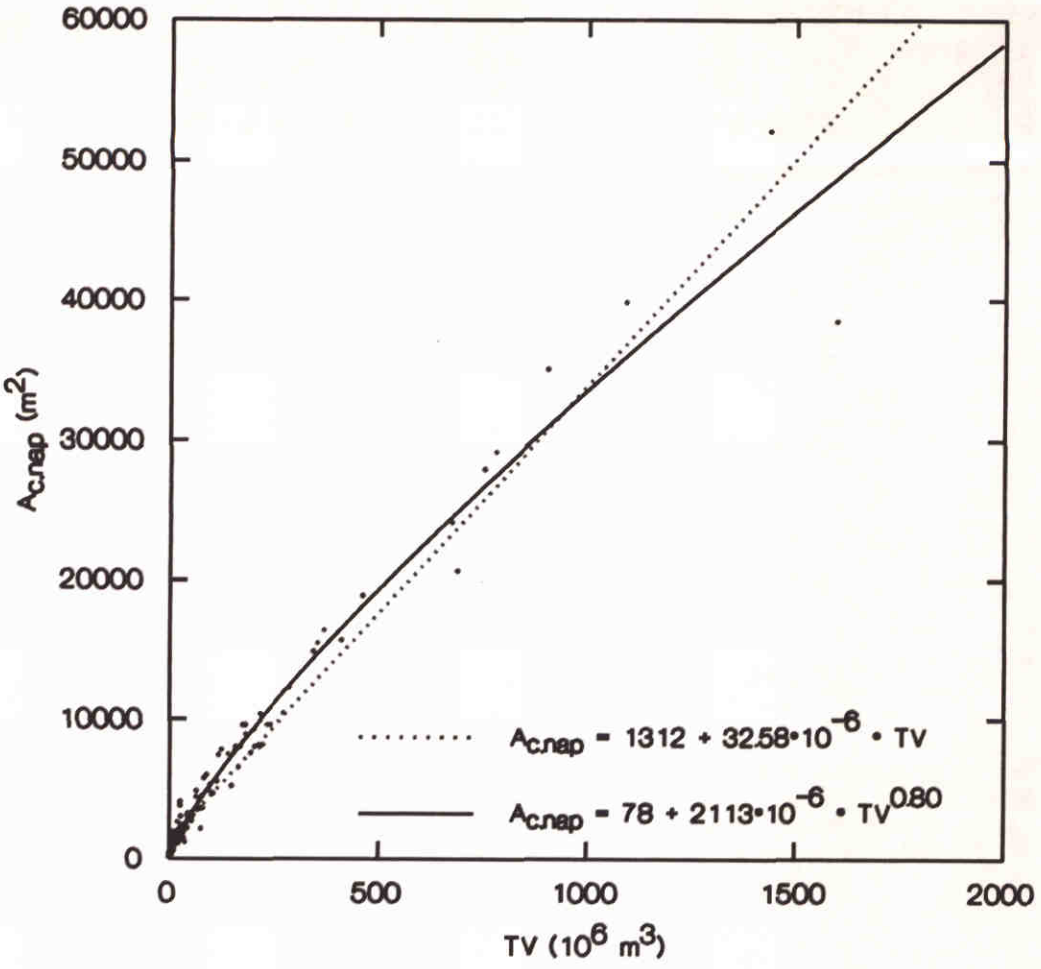

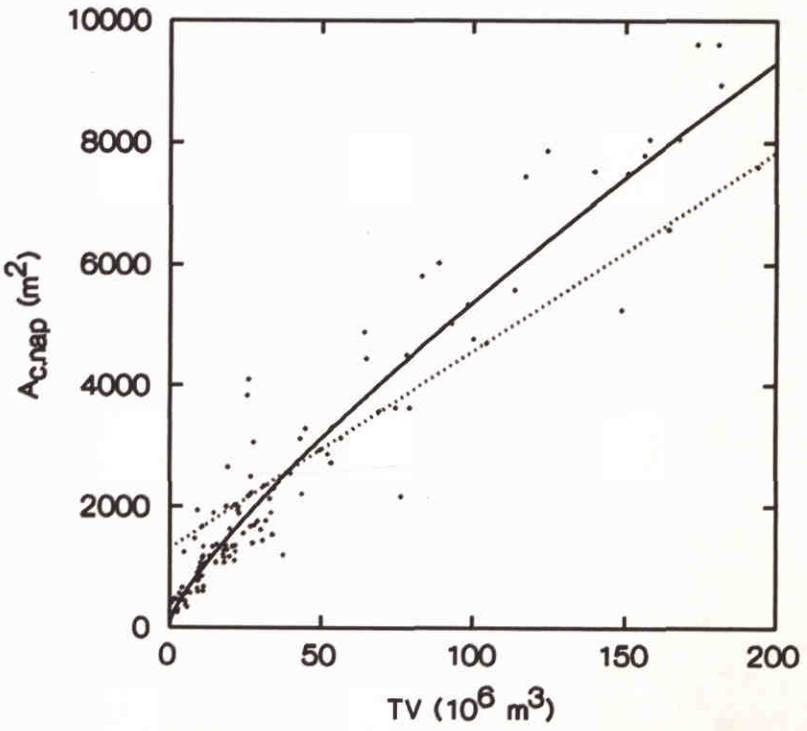

CORRELATION OF TV WITH $A_{c.nap}$

DELFT HYDRAULICS | H 1300 | FIG. 3.11

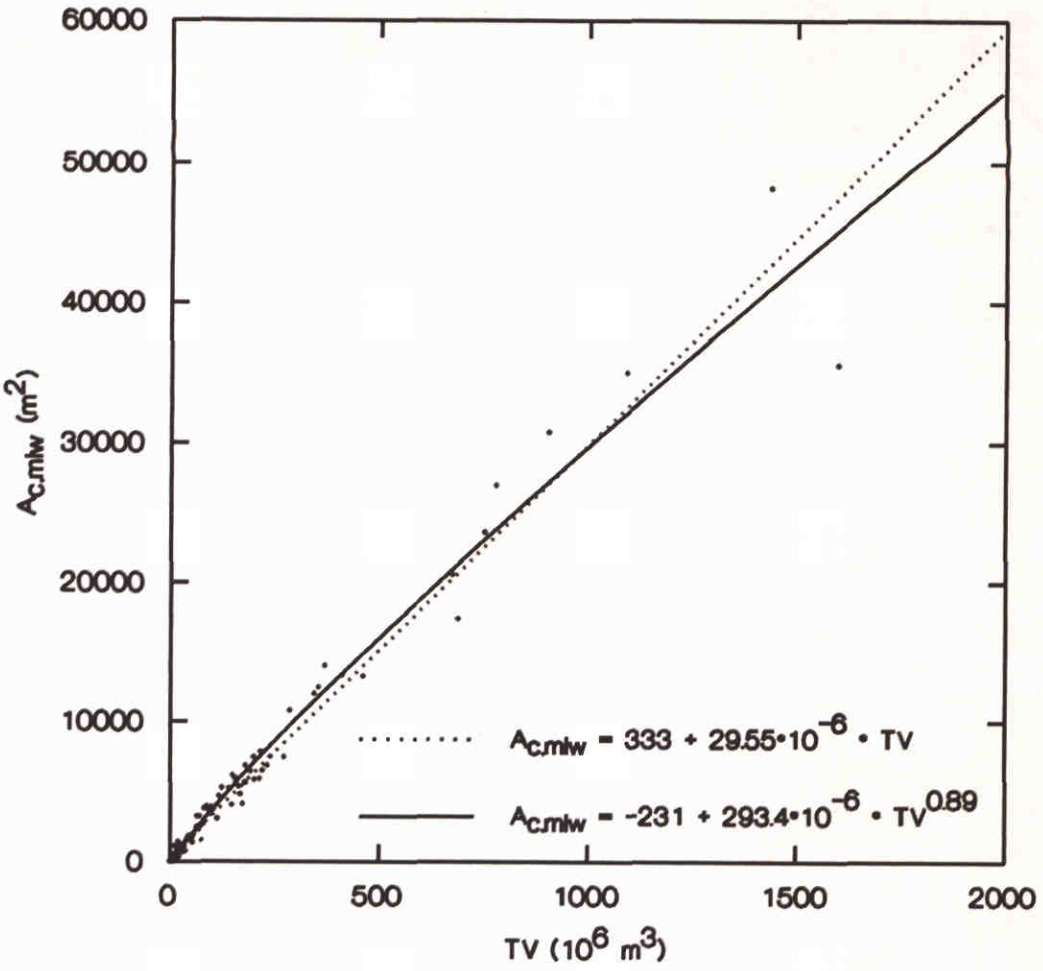

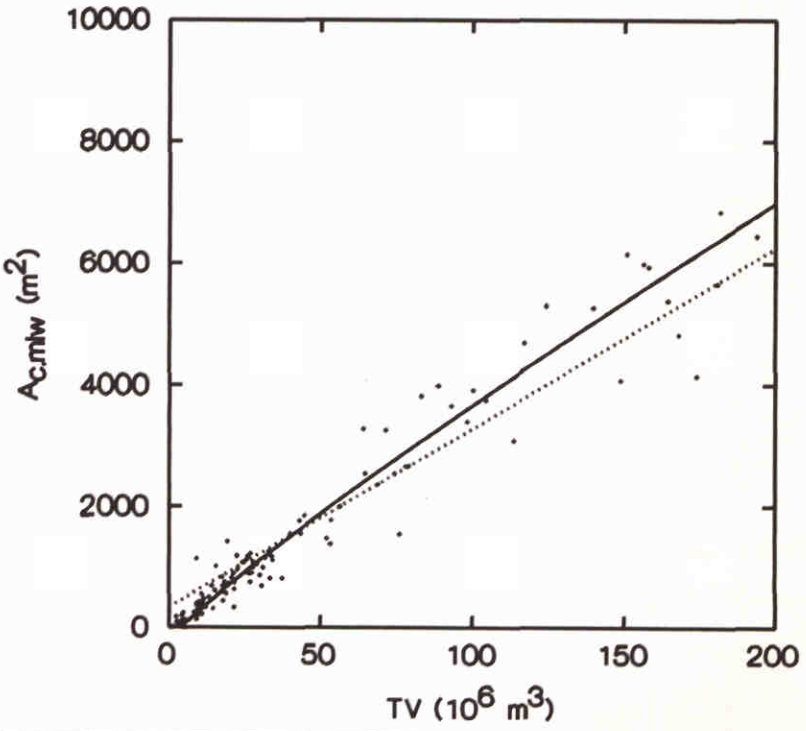

CORRELATION OF TV WITH $A_{c.mlw}$

DELFT HYDRAULICS | H 1300 | FIG. 3.12

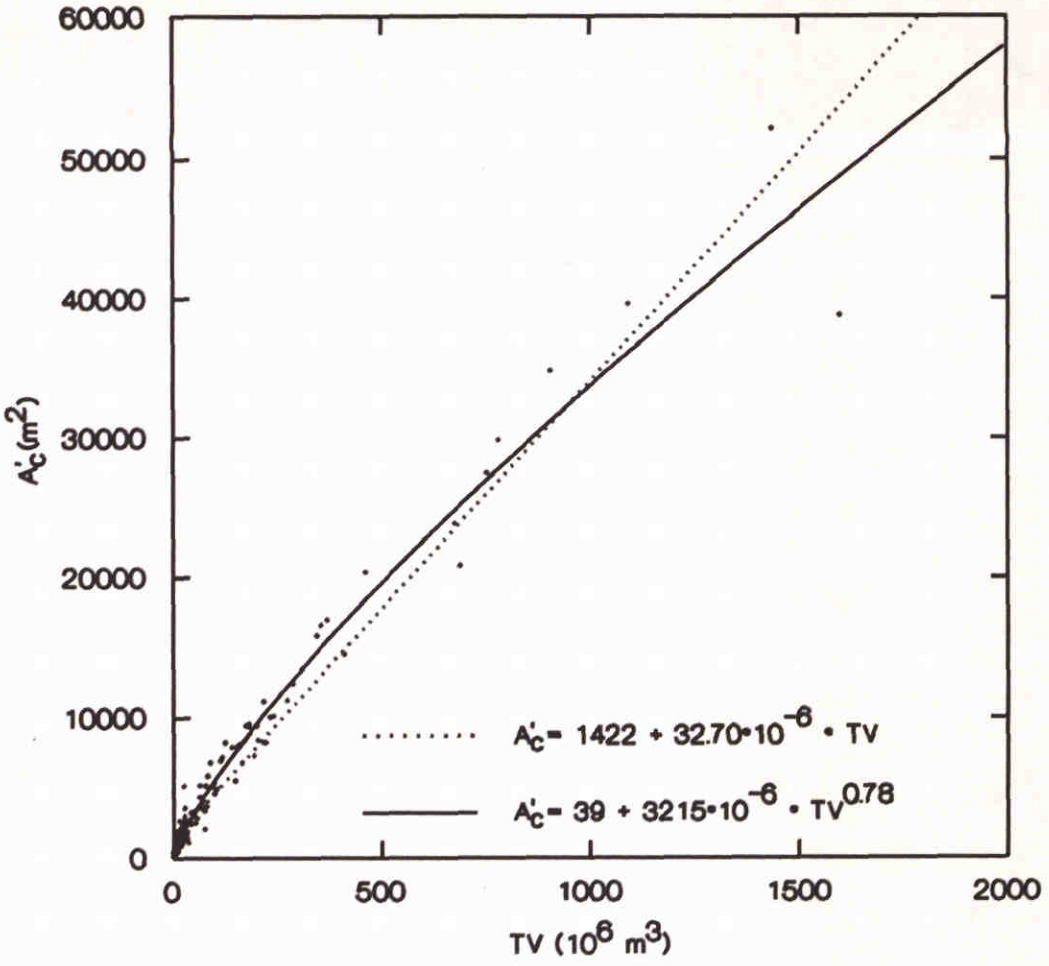

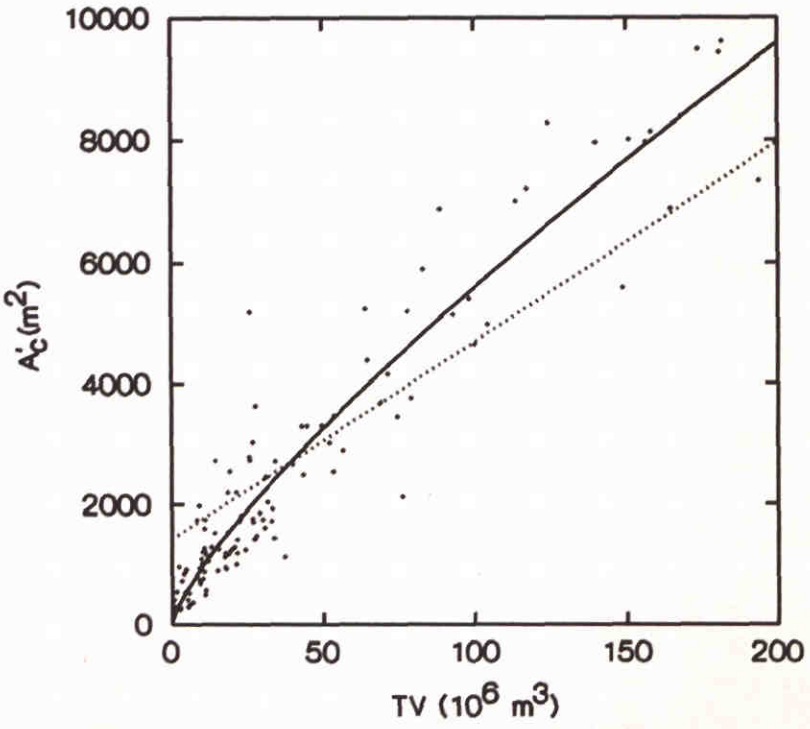

CORRELATION OF TV WITH A'_c

DELFT HYDRAULICS | H 1300 | FIG. 3.13

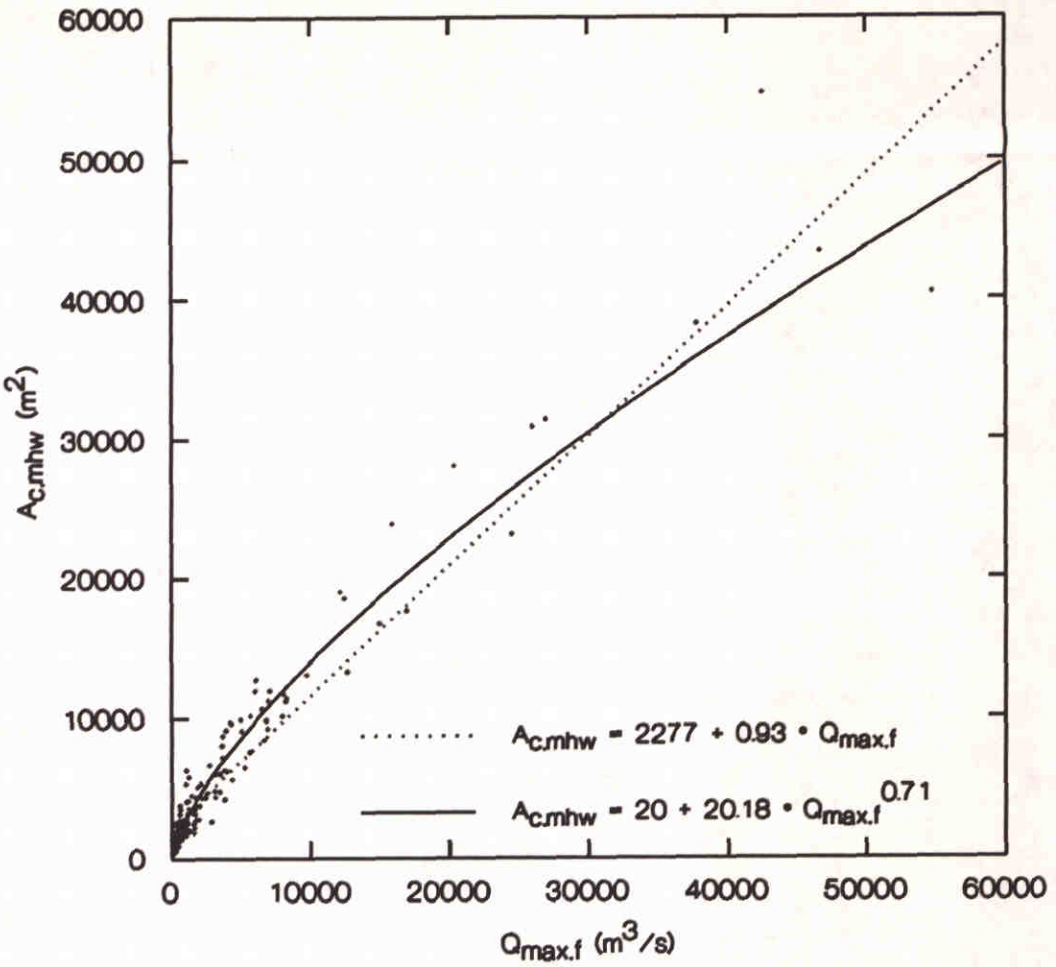

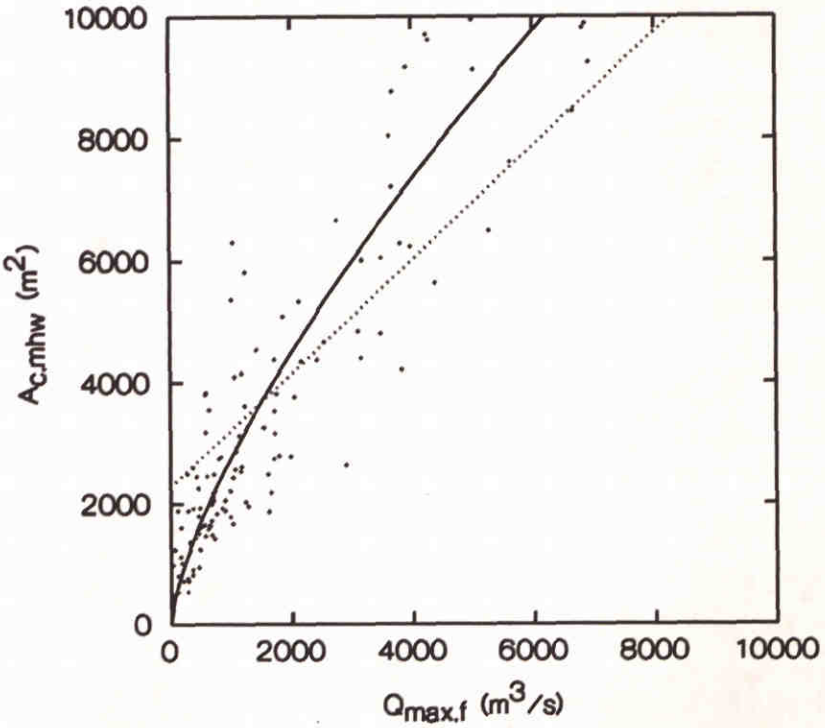

CORRELATION OF $Q_{max.f}$ WITH $A_{c.mhw}$

DELFT HYDRAULICS | H 1300 | FIG. 3.14

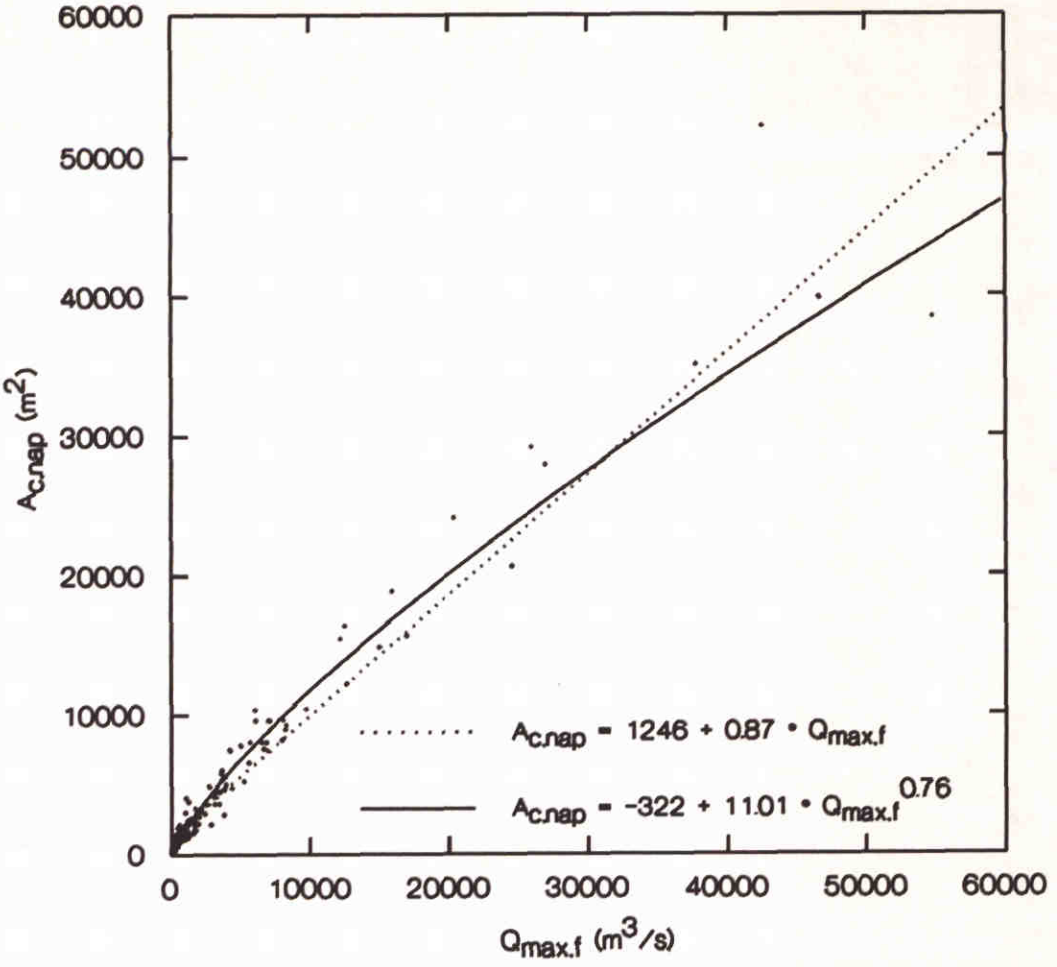

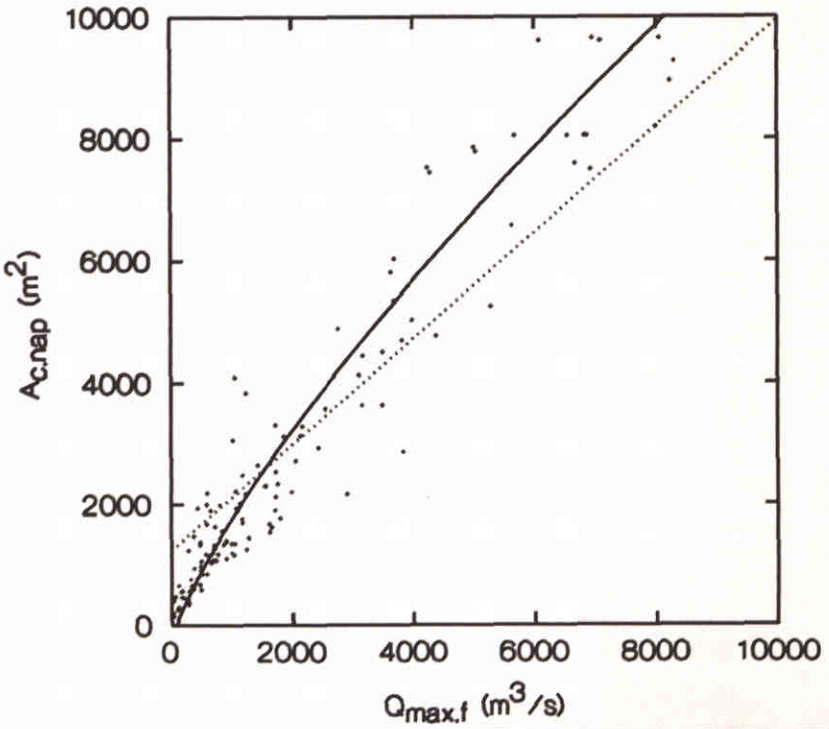

CORRELATION OF $Q_{max.f}$ WITH $A_{c.nap}$

DELFT HYDRAULICS | H 1300 | FIG. 3.15

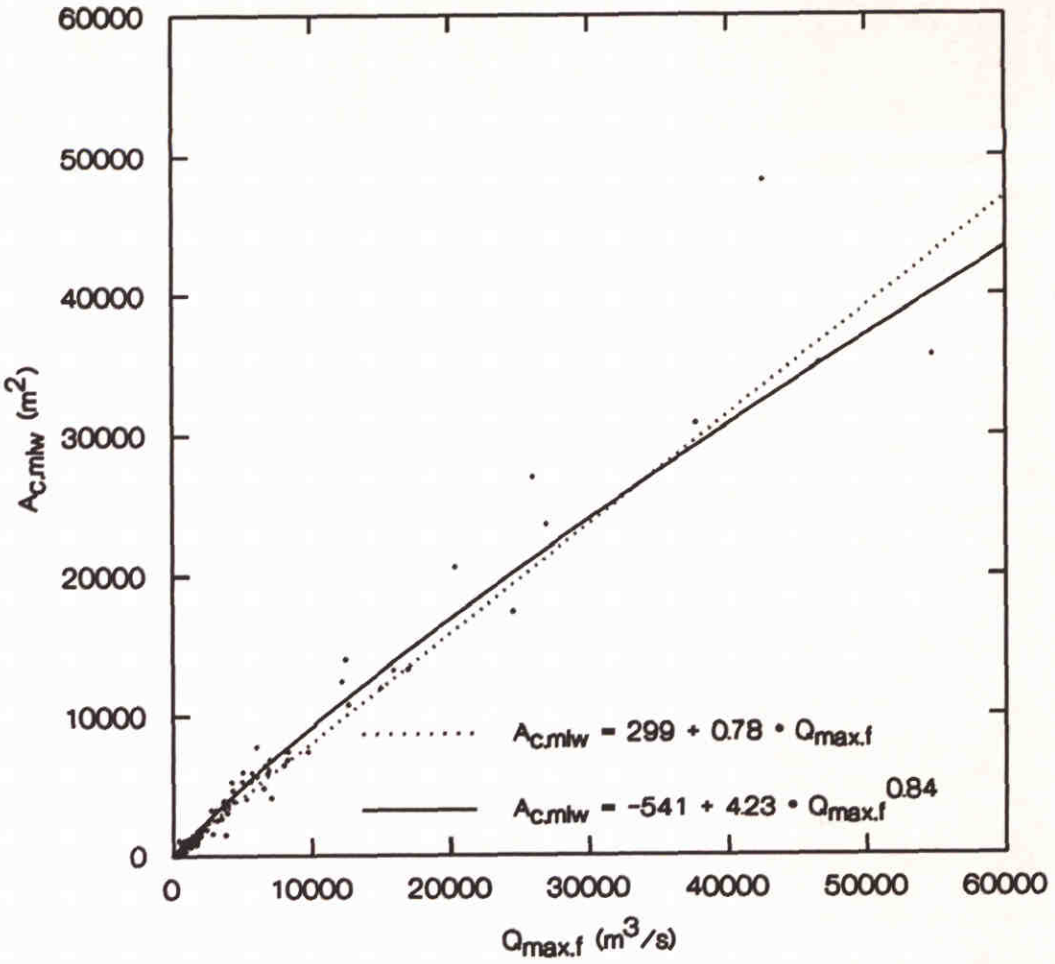

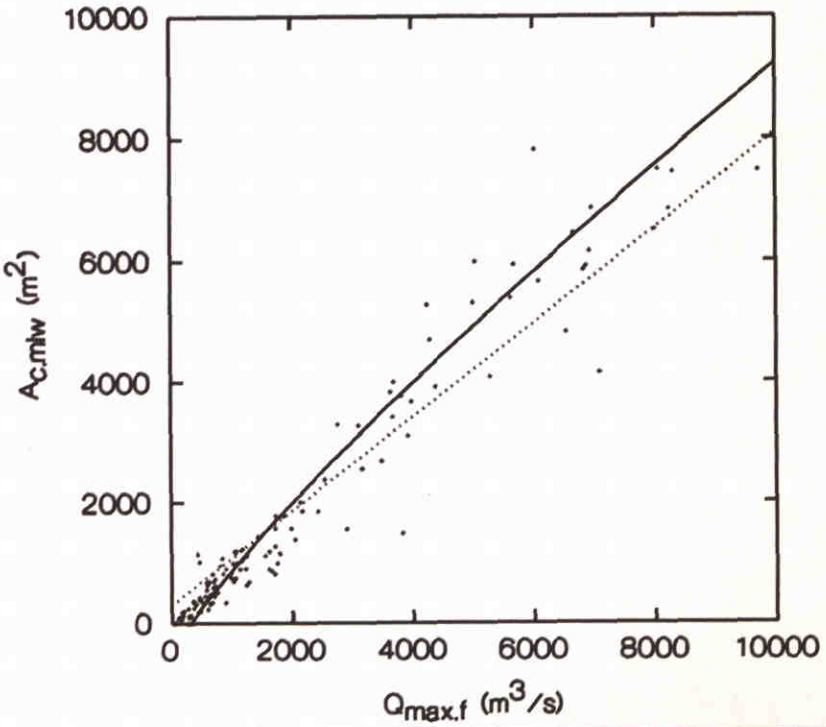

CORRELATION OF $Q_{max.f}$ WITH $A_{c.mlw}$

DELFT HYDRAULICS | H 1300 | FIG. 3.16

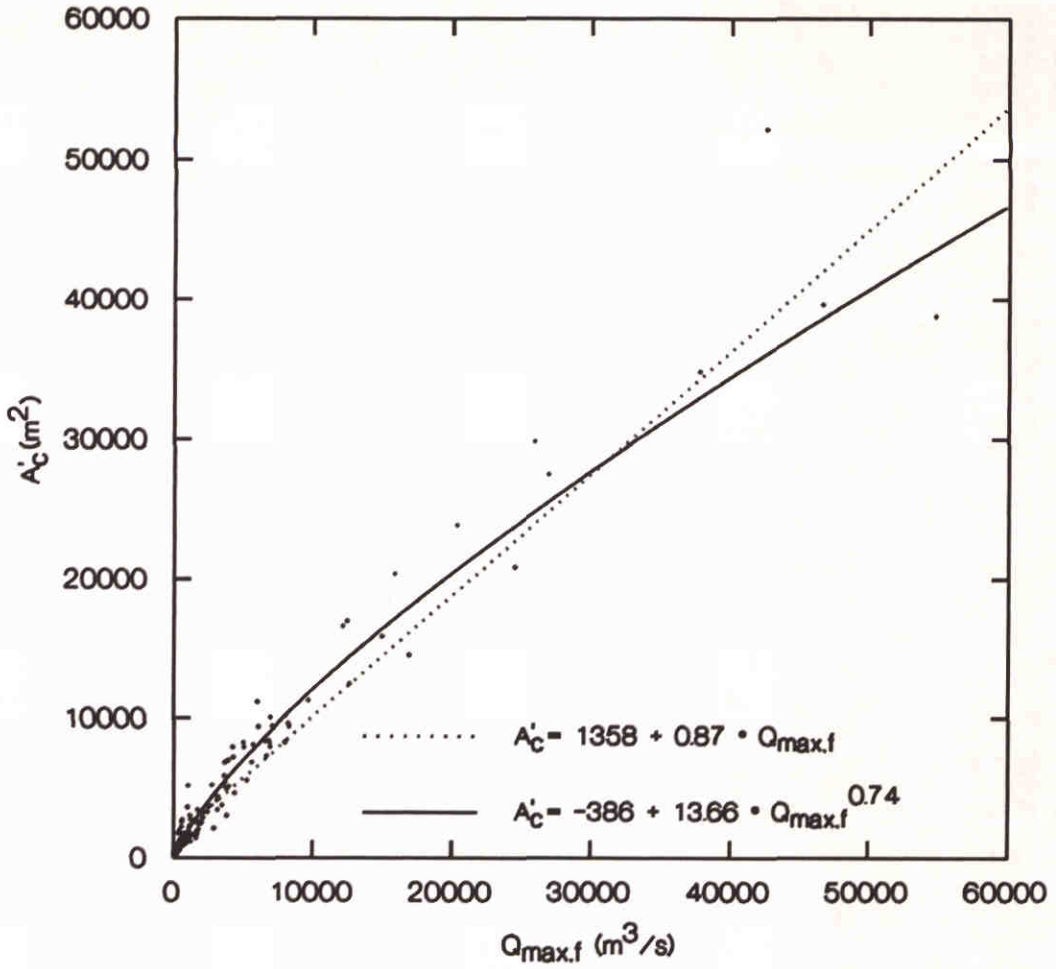

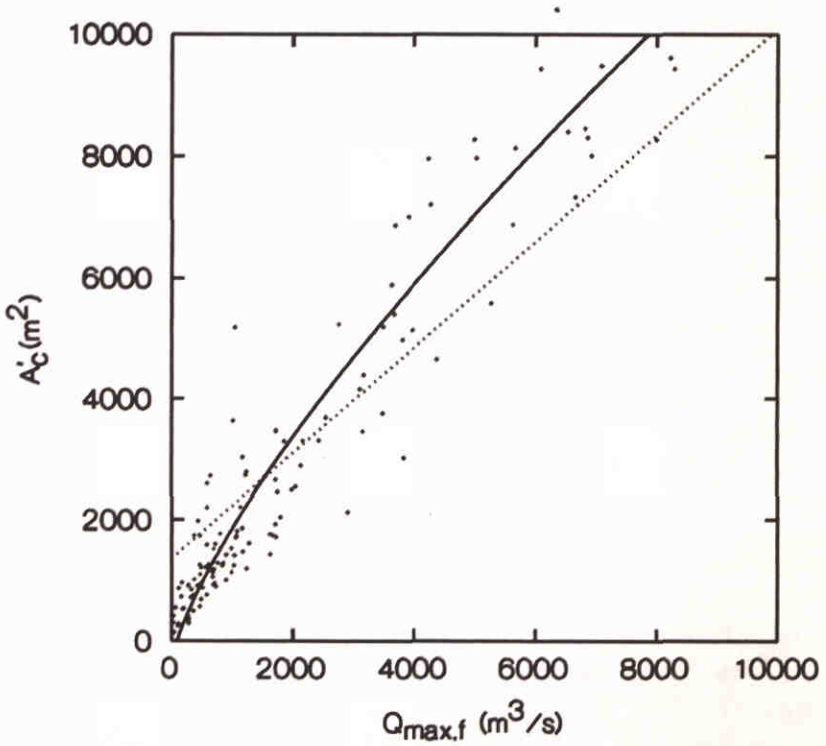

CORRELATION OF $Q_{max.f}$ WITH A'_c

DELFT HYDRAULICS | H 1300 | FIG. 3.17

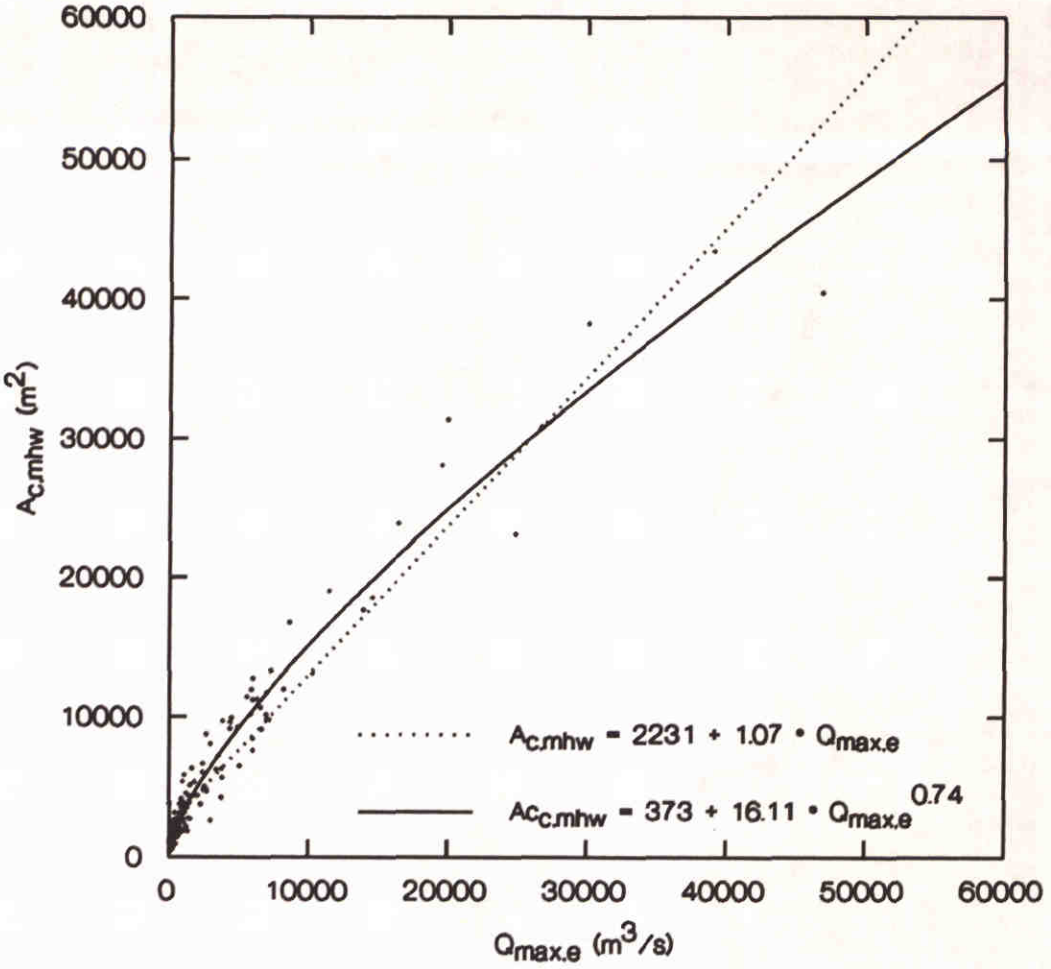

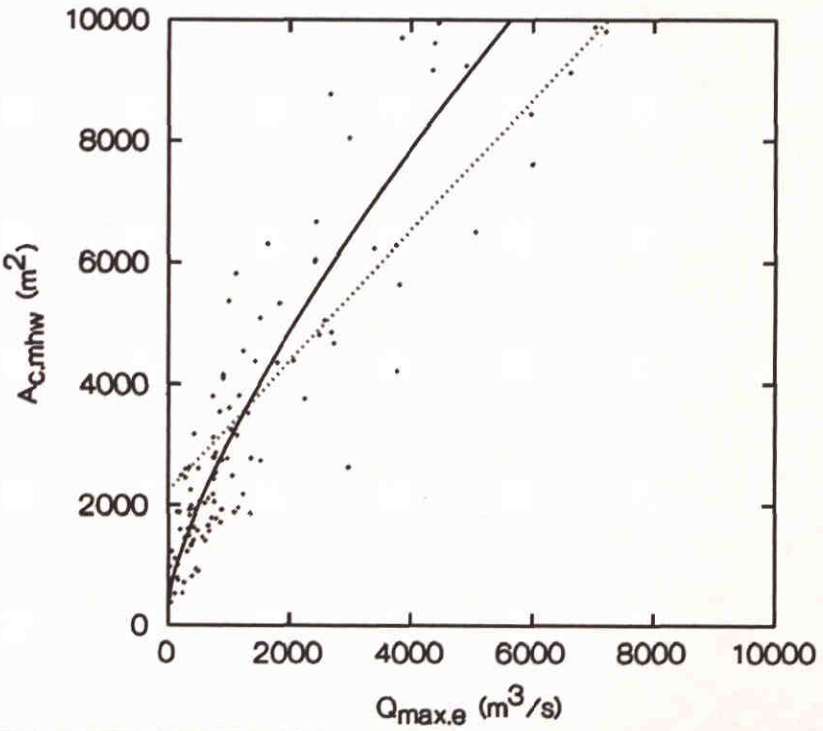

CORRELATION OF $Q_{max.e}$ WITH $A_{c.mhw}$

DELFT HYDRAULICS | H 1300 | FIG. 3.18

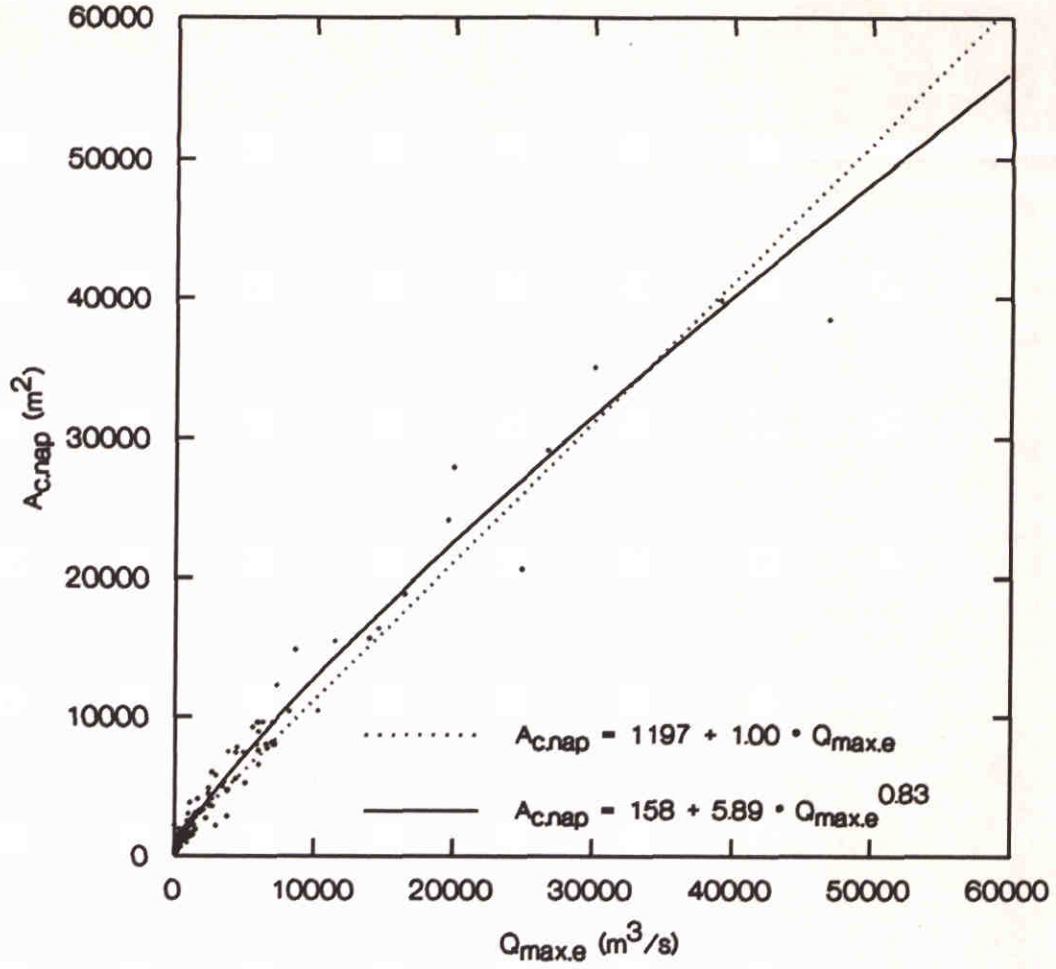

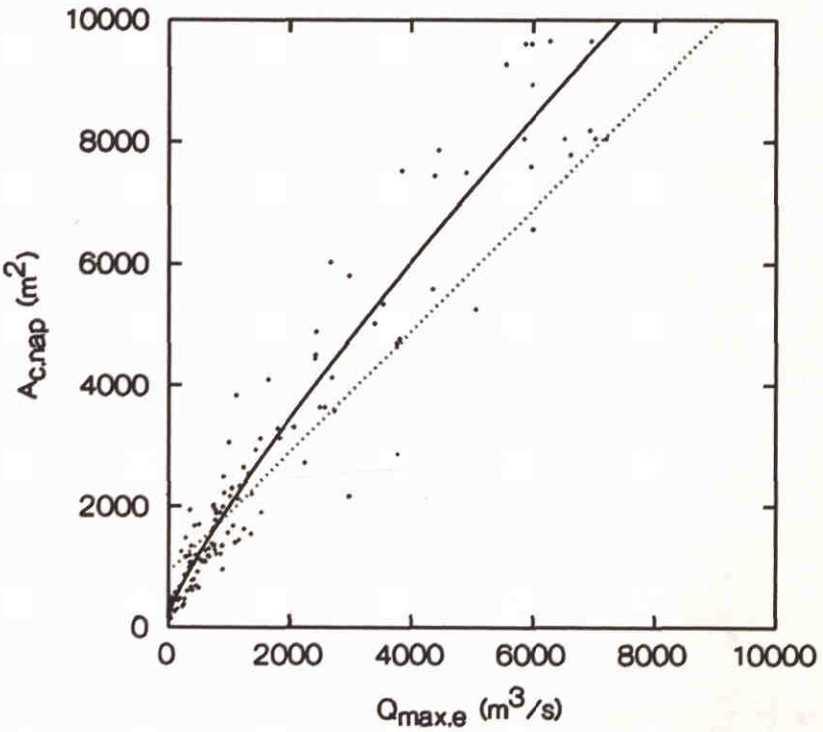

CORRELATION OF $Q_{max.e}$ WITH $A_{c.nap}$

DELFT HYDRAULICS | H 1300 | FIG. 3.19

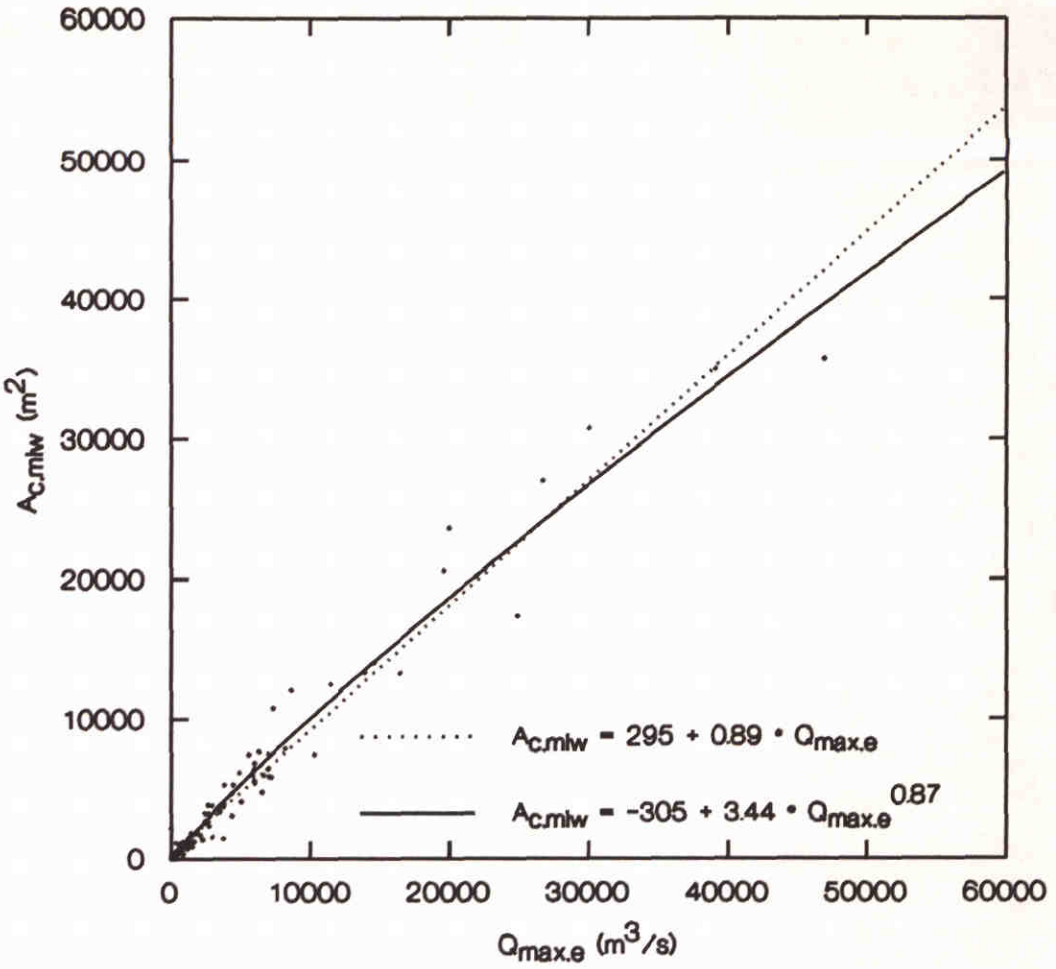

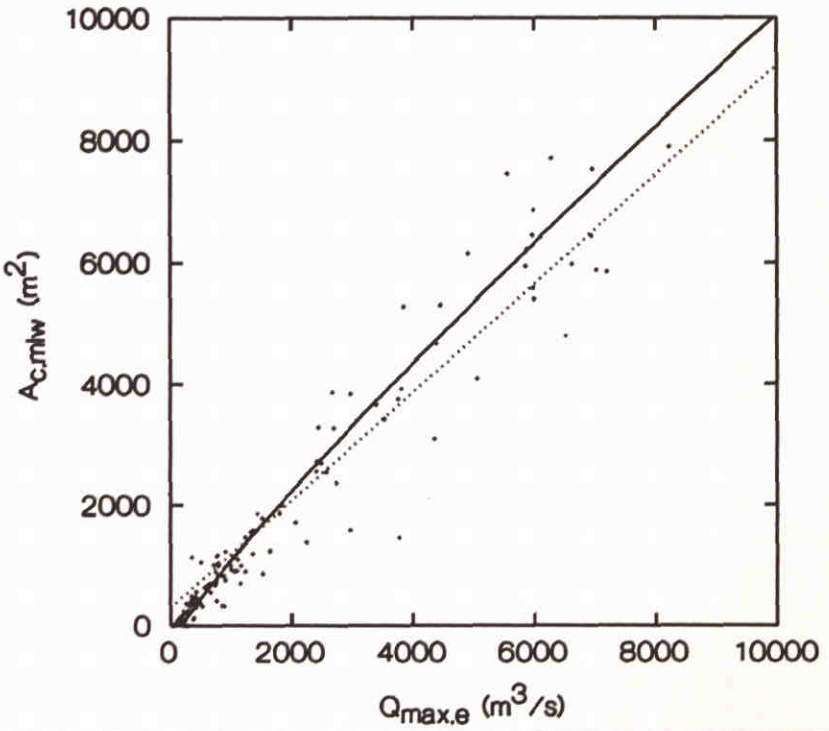

CORRELATION OF $Q_{max.e}$ WITH $A_{c.mlw}$

DELFT HYDRAULICS | H 1300 | FIG. 3.20

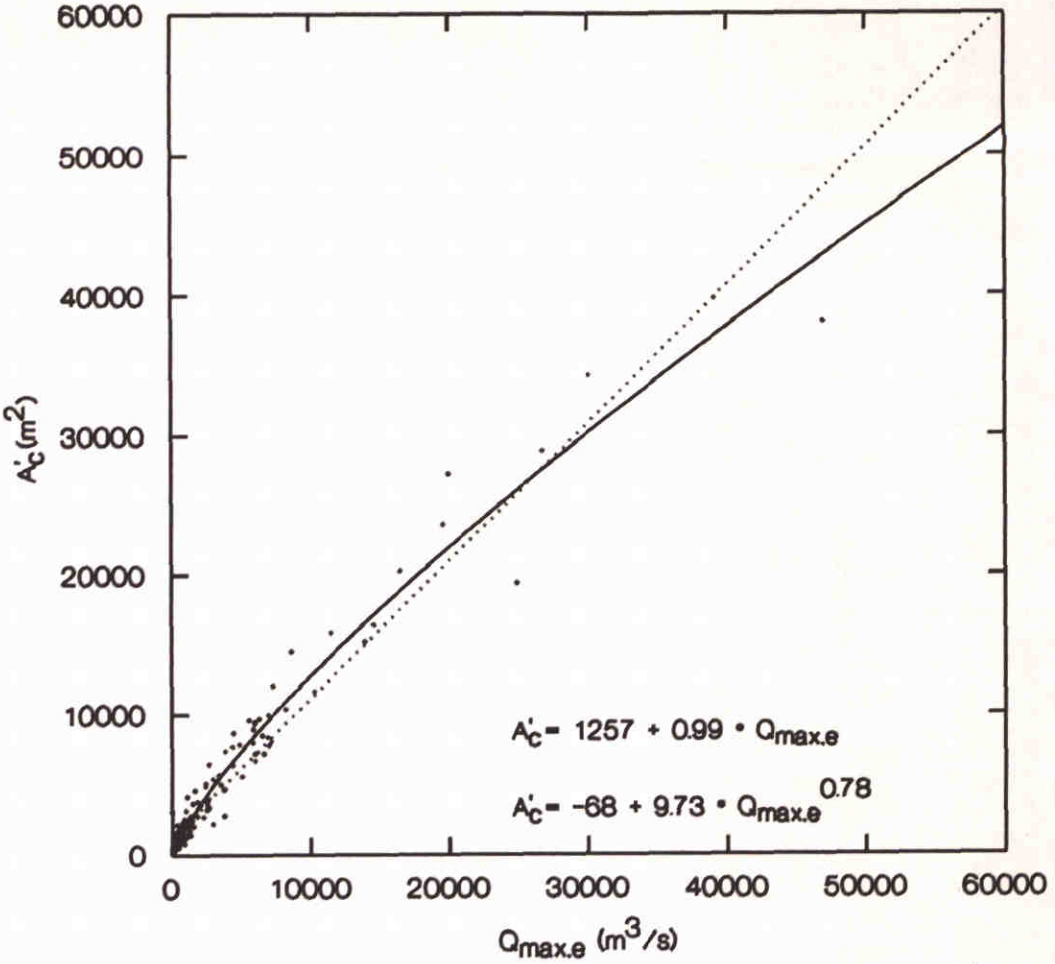

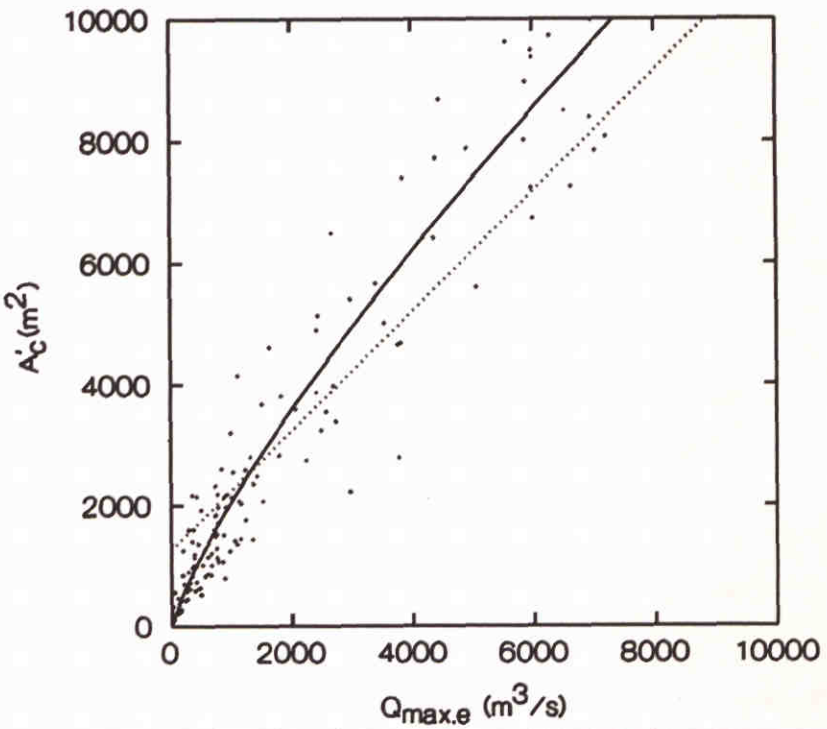

CORRELATION OF $Q_{max.e}$ WITH A'_c

DELFT HYDRAULICS | H 1300 | FIG. 3.21

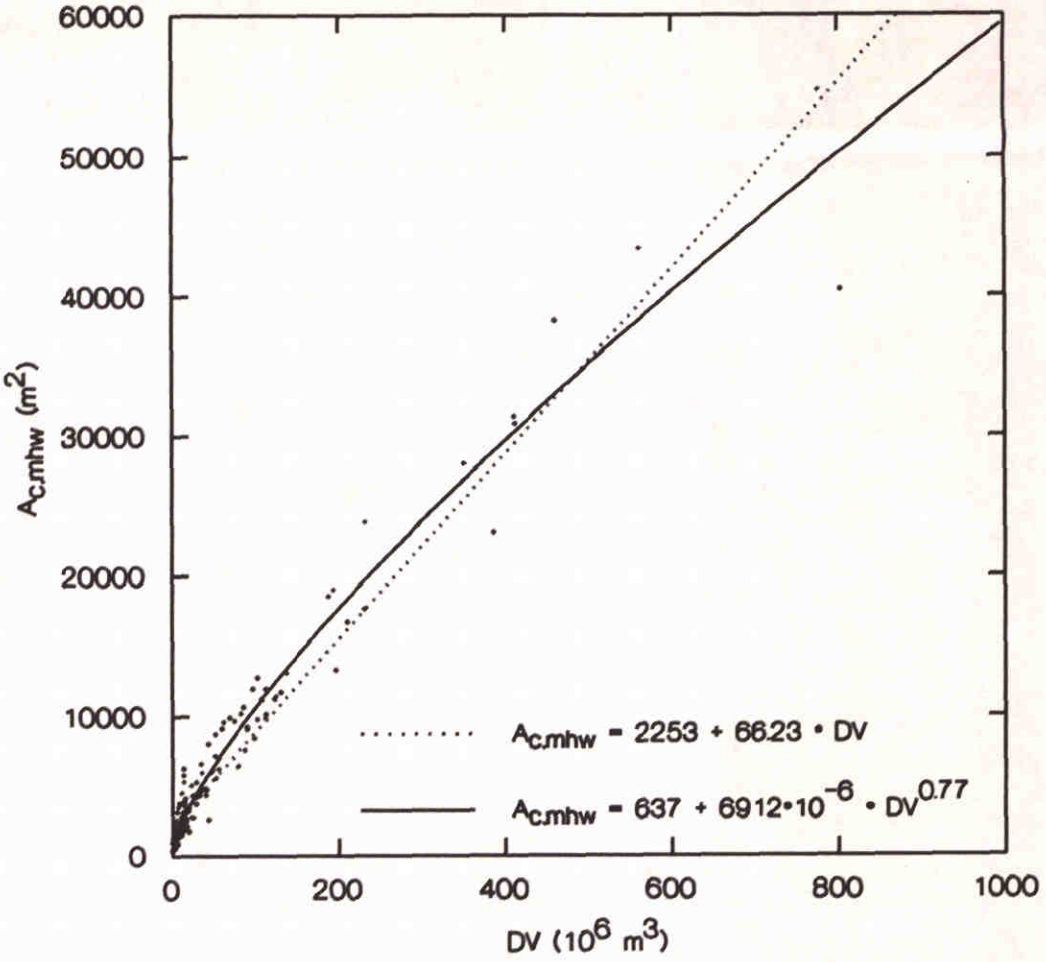

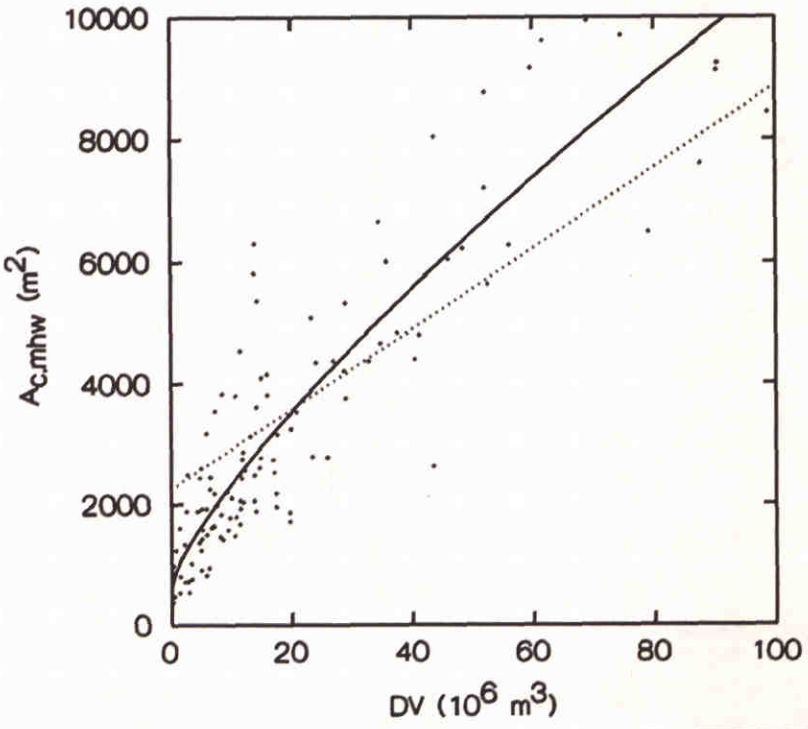

CORRELATION OF DV WITH $A_{c.mhw}$

DELFT HYDRAULICS | H 1300 | FIG. 3.22

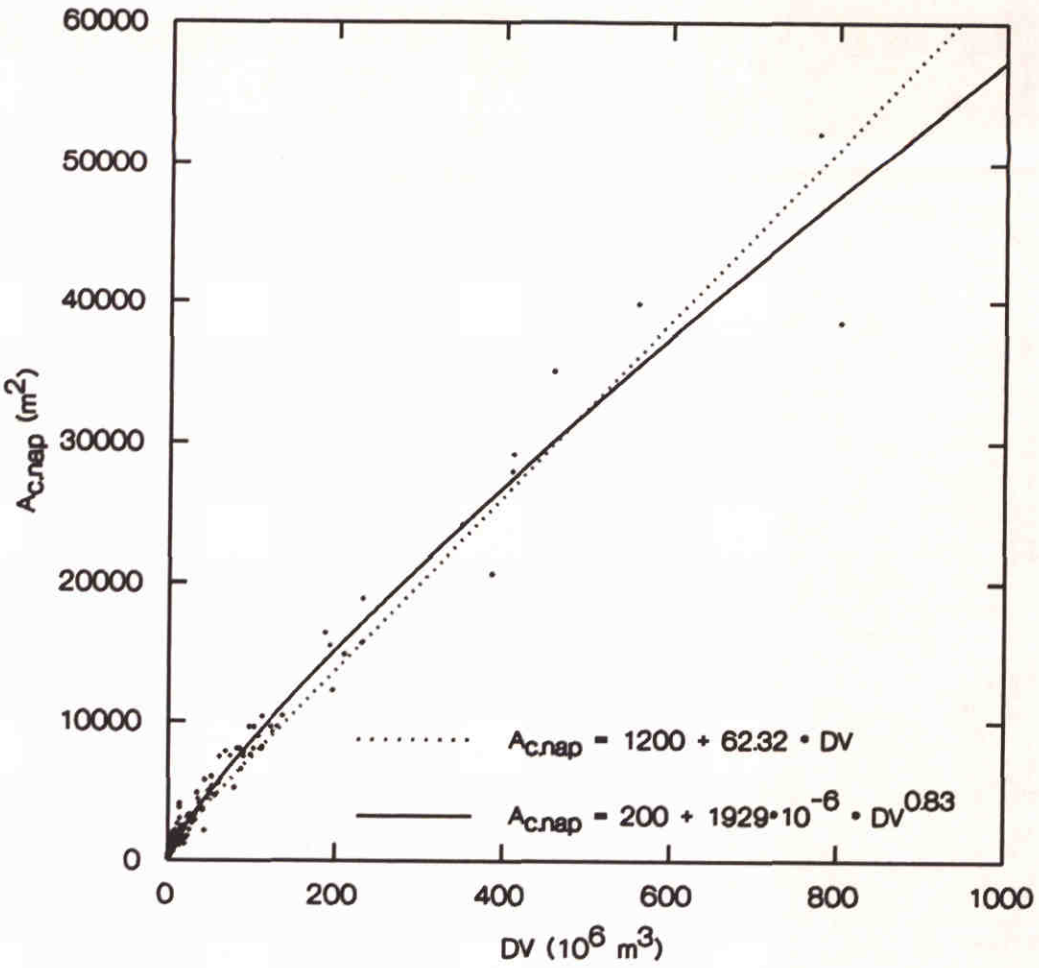

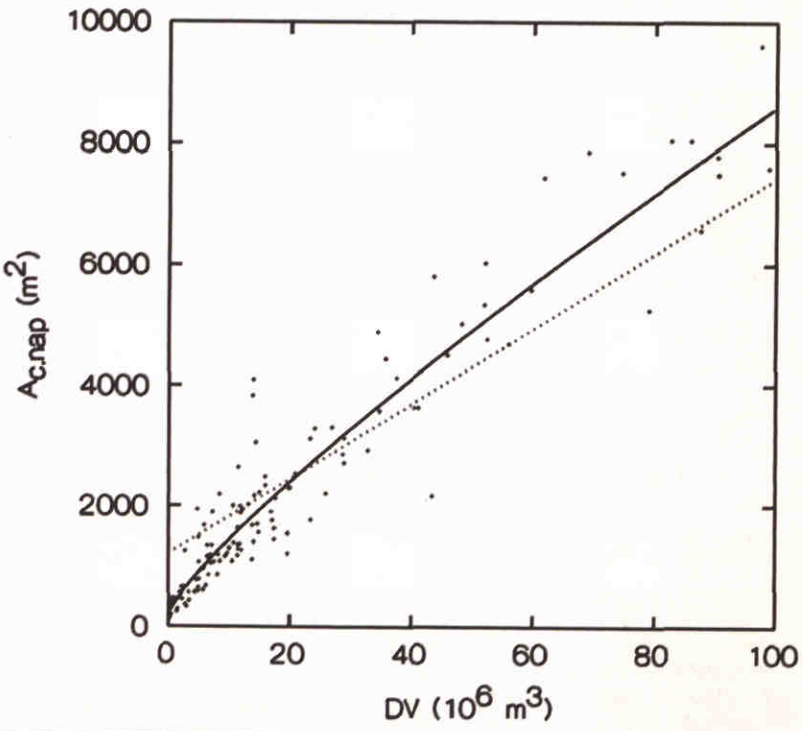

CORRELATION OF DV WITH $A_{c.nap}$

DELFT HYDRAULICS | H 1300 | FIG. 3.23

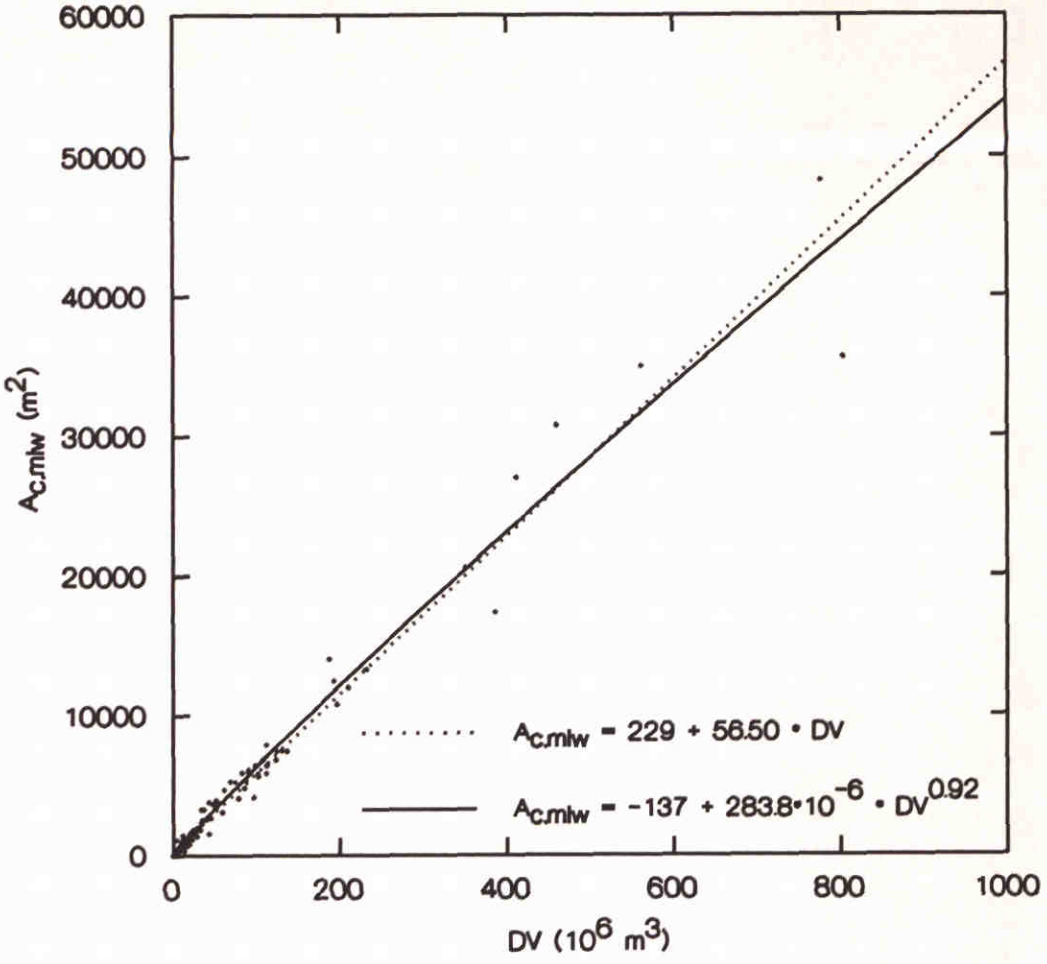

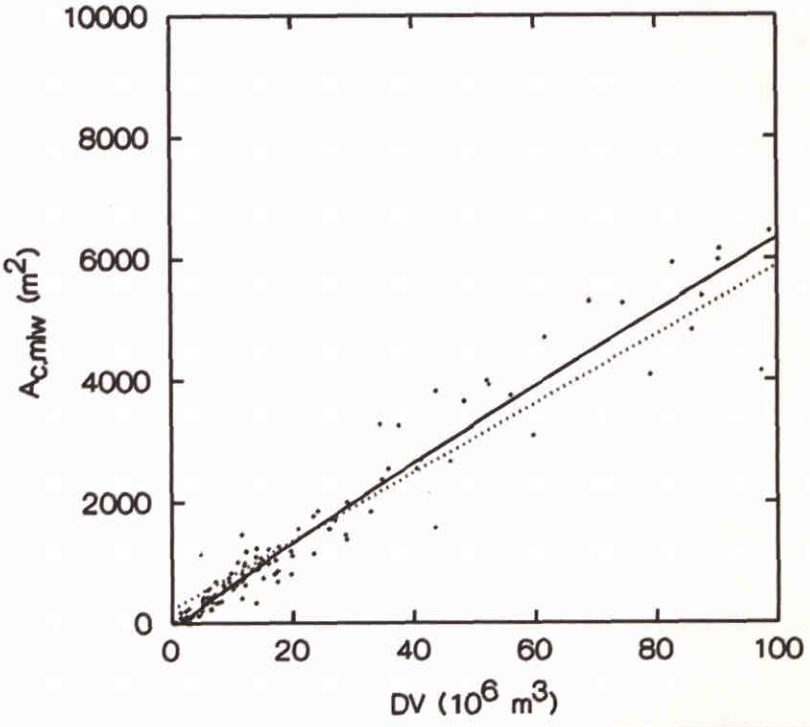

CORRELATION OF DV WITH $A_{c,mlw}$

DELFT HYDRAULICS | H 1300 | FIG. 3.24

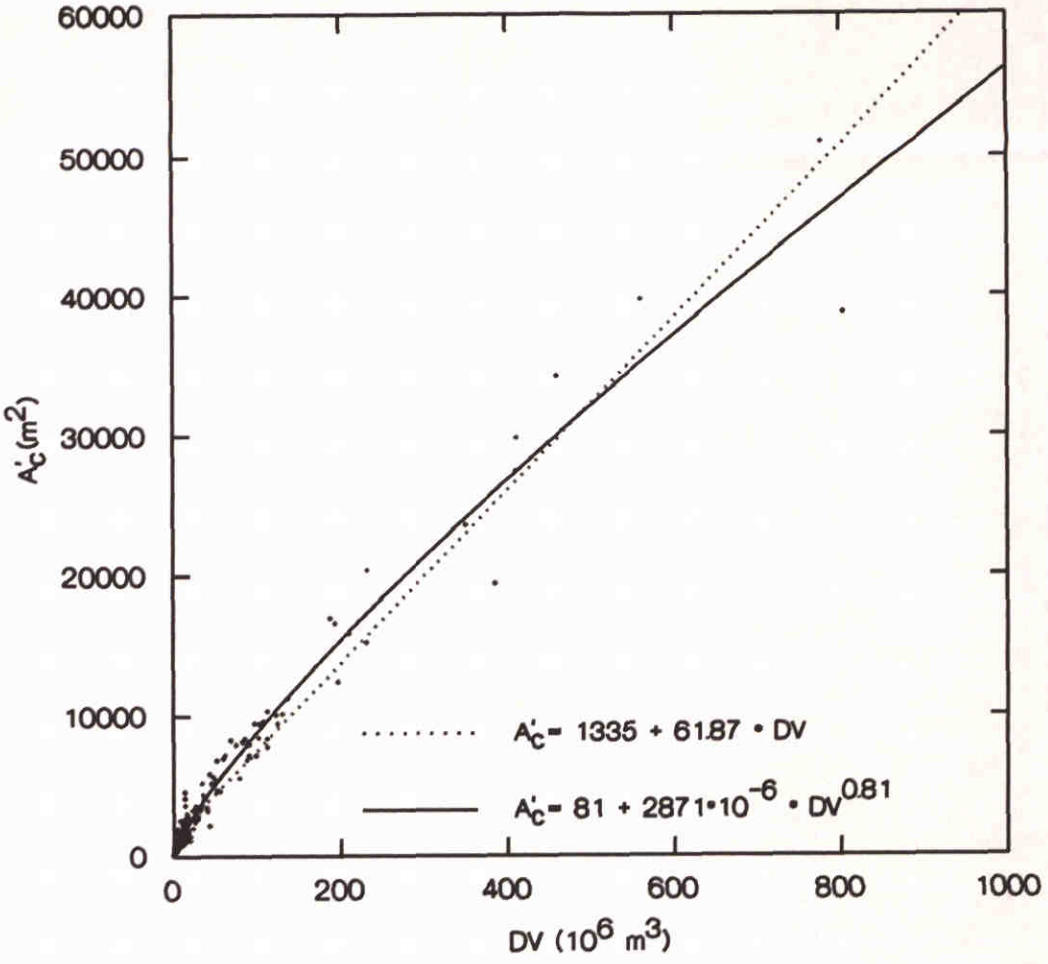

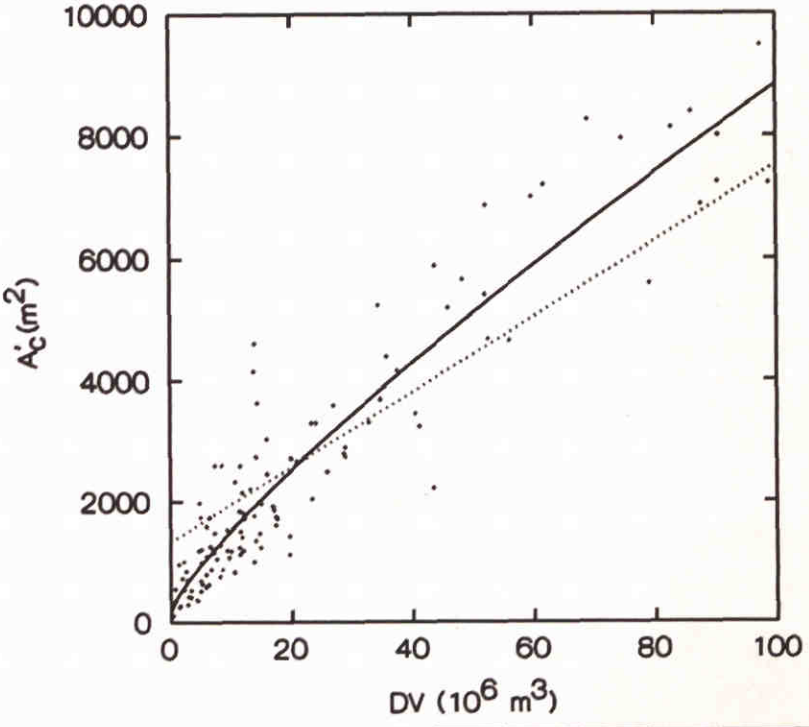

CORRELATION OF DV WITH A'_c

DELFT HYDRAULICS | H 1300 | FIG. 3.25

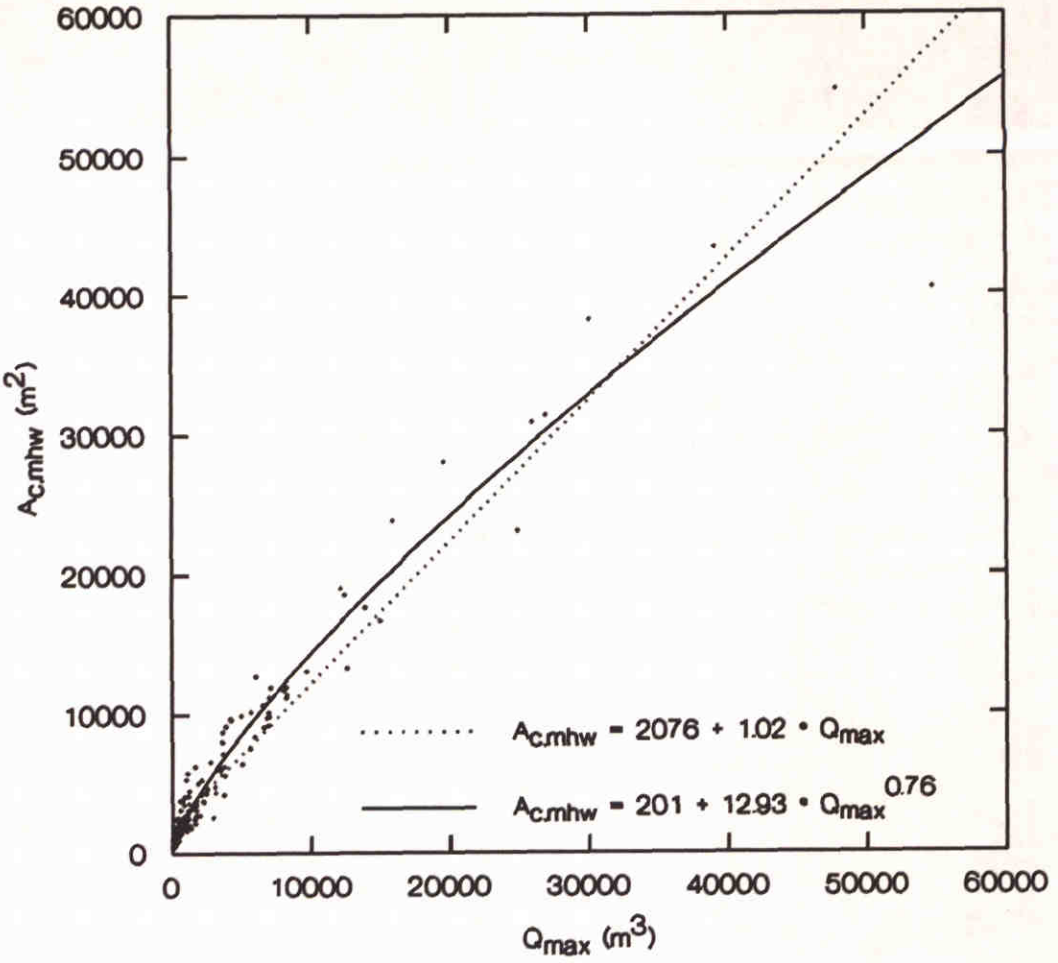

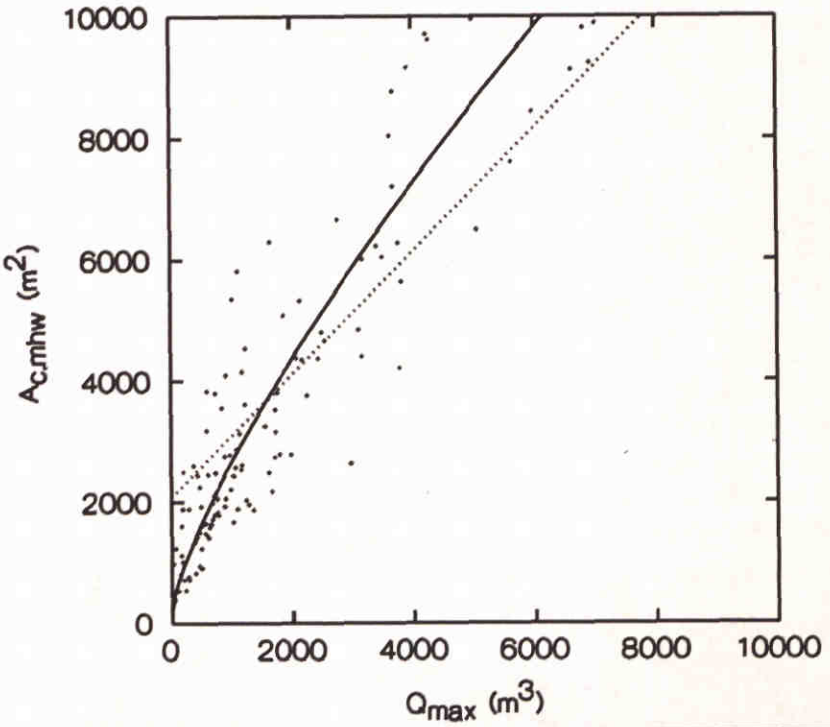

CORRELATION OF Q_{max} WITH $A_{c.mhw}$

DELFT HYDRAULICS | H 1300 | FIG. 3.26

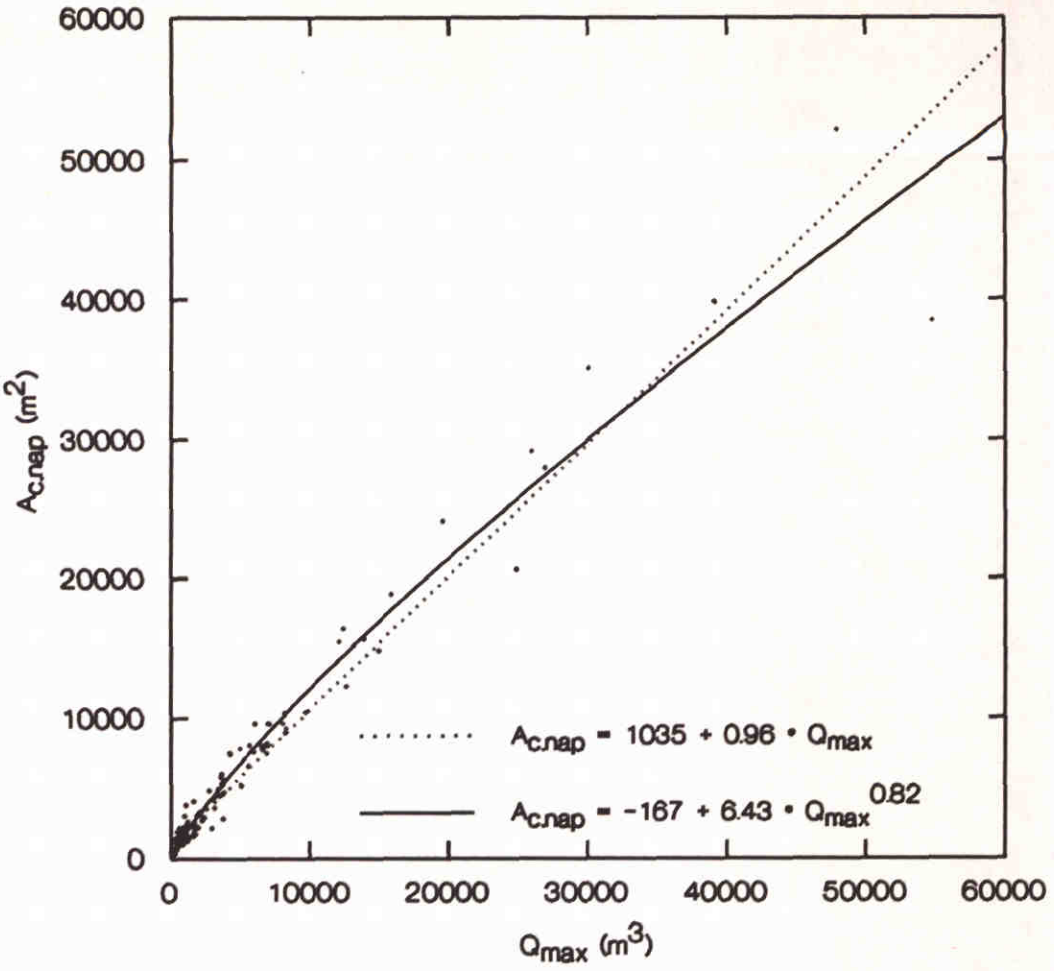

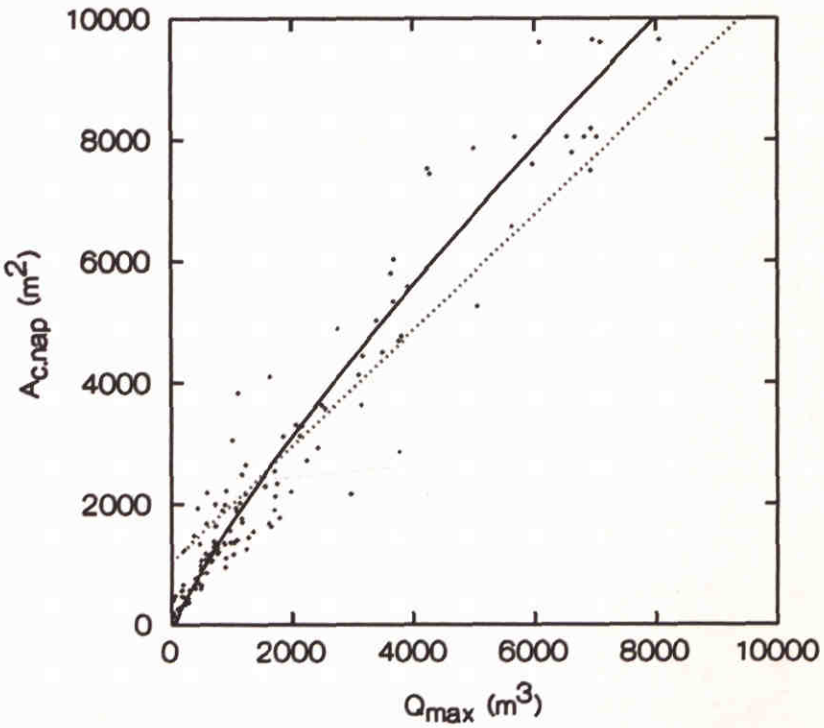

CORRELATION OF Q_{max} WITH $A_{c.nap}$

DELFT HYDRAULICS | H 1300 | FIG. 3.27

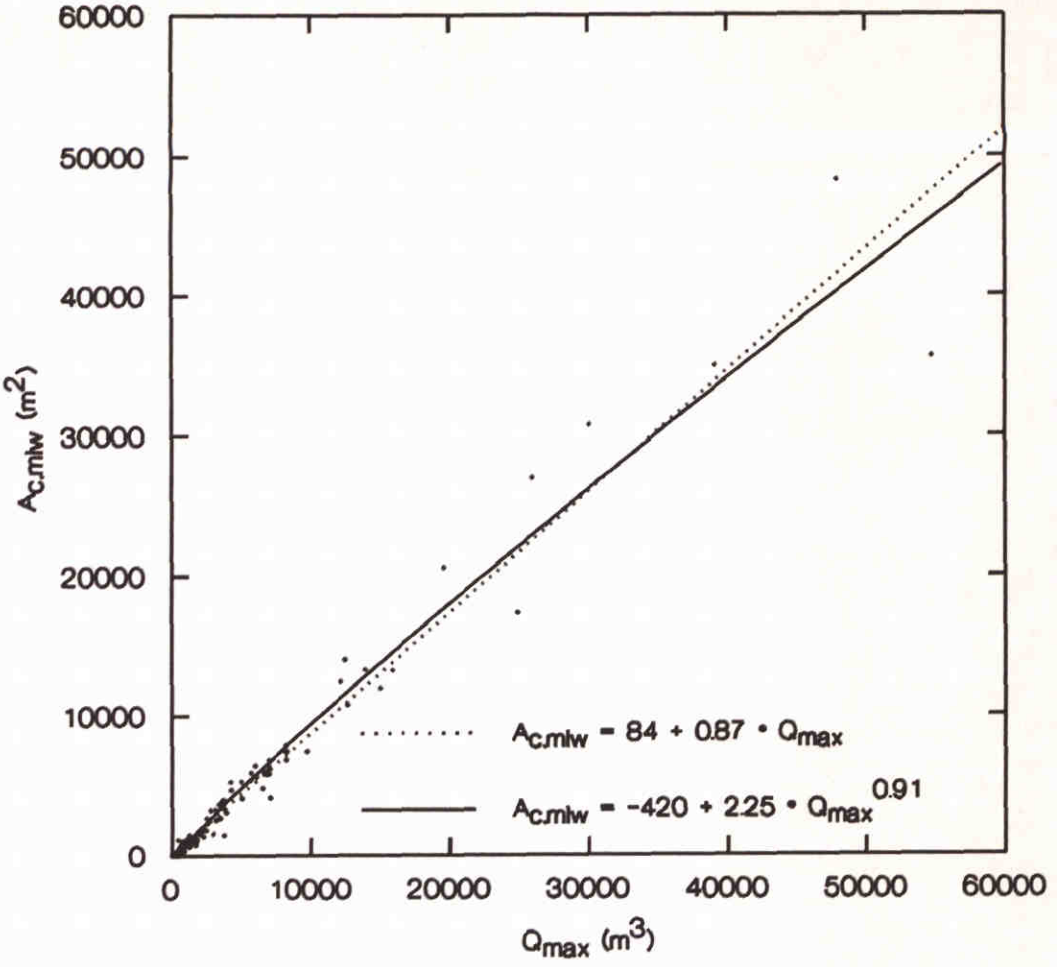

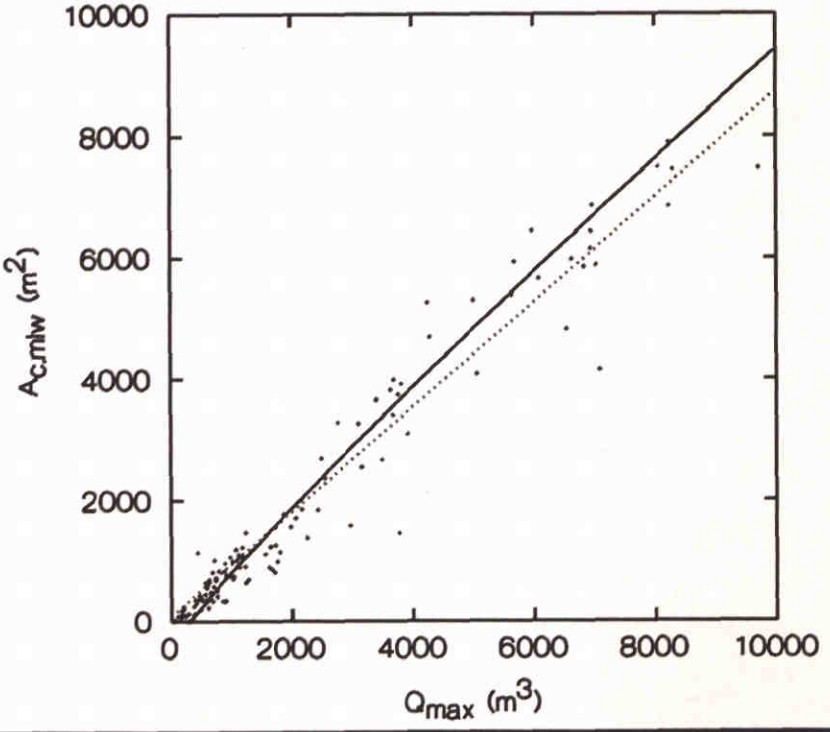

CORRELATION OF Q_{max} WITH $A_{c.mlw}$

DELFT HYDRAULICS | H 1300 | FIG. 3.28

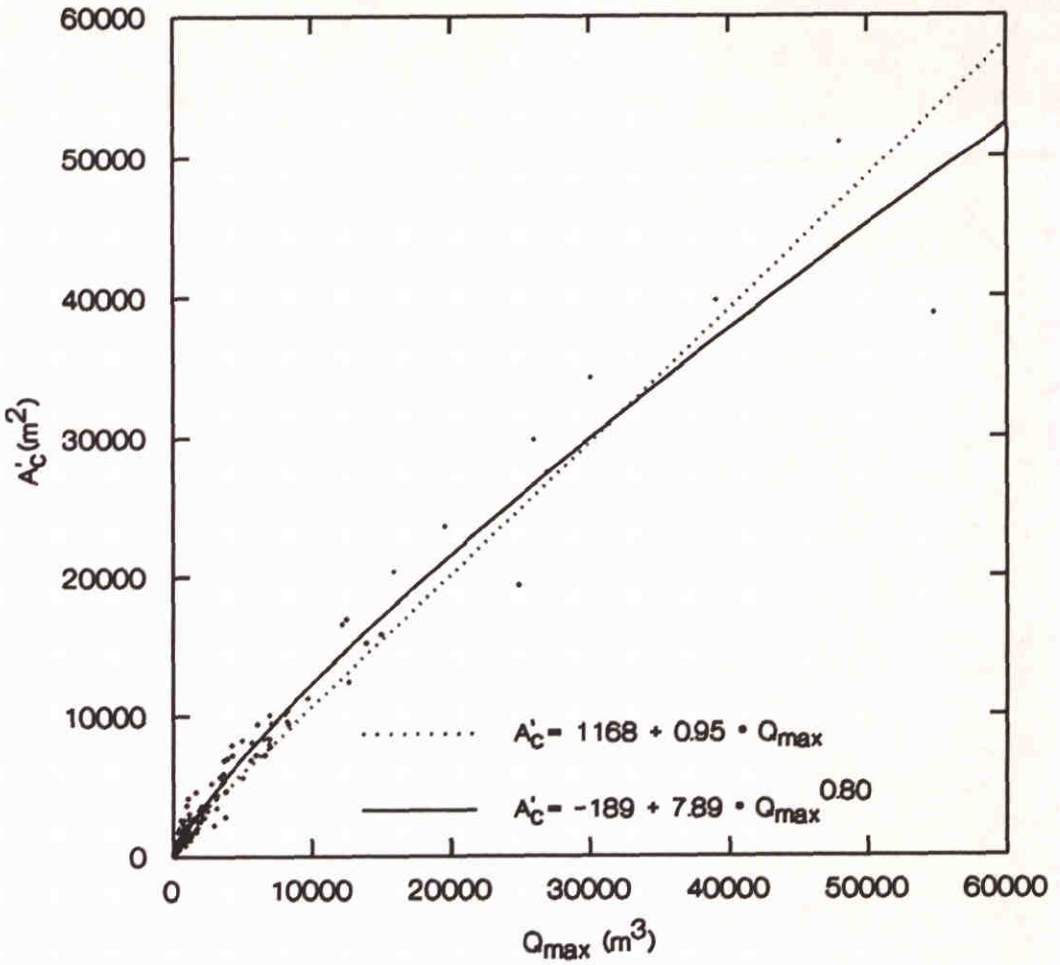

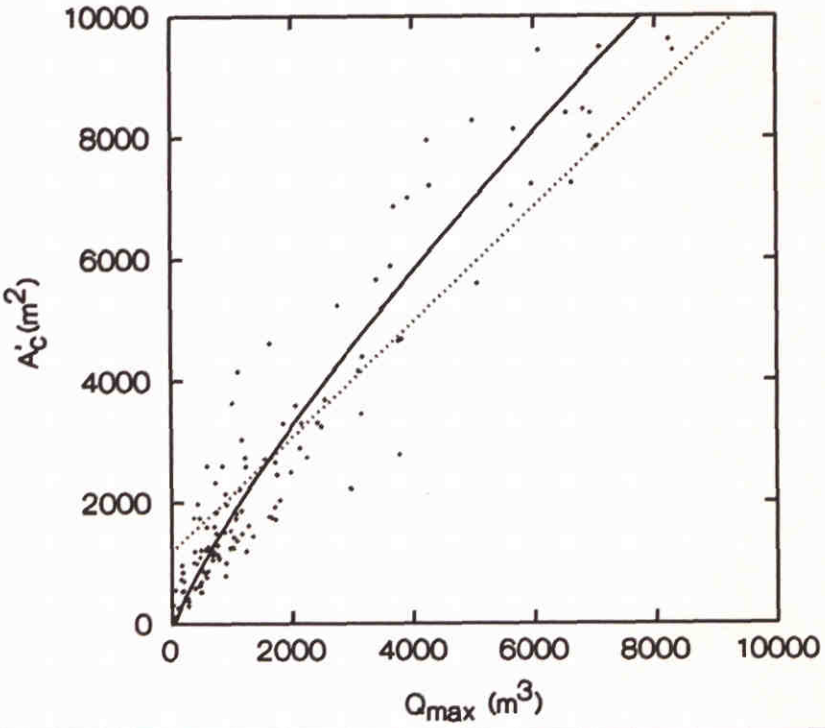

CORRELATION OF Q_{max} WITH A'_c

DELFT HYDRAULICS | H 1300 | FIG. 3.29

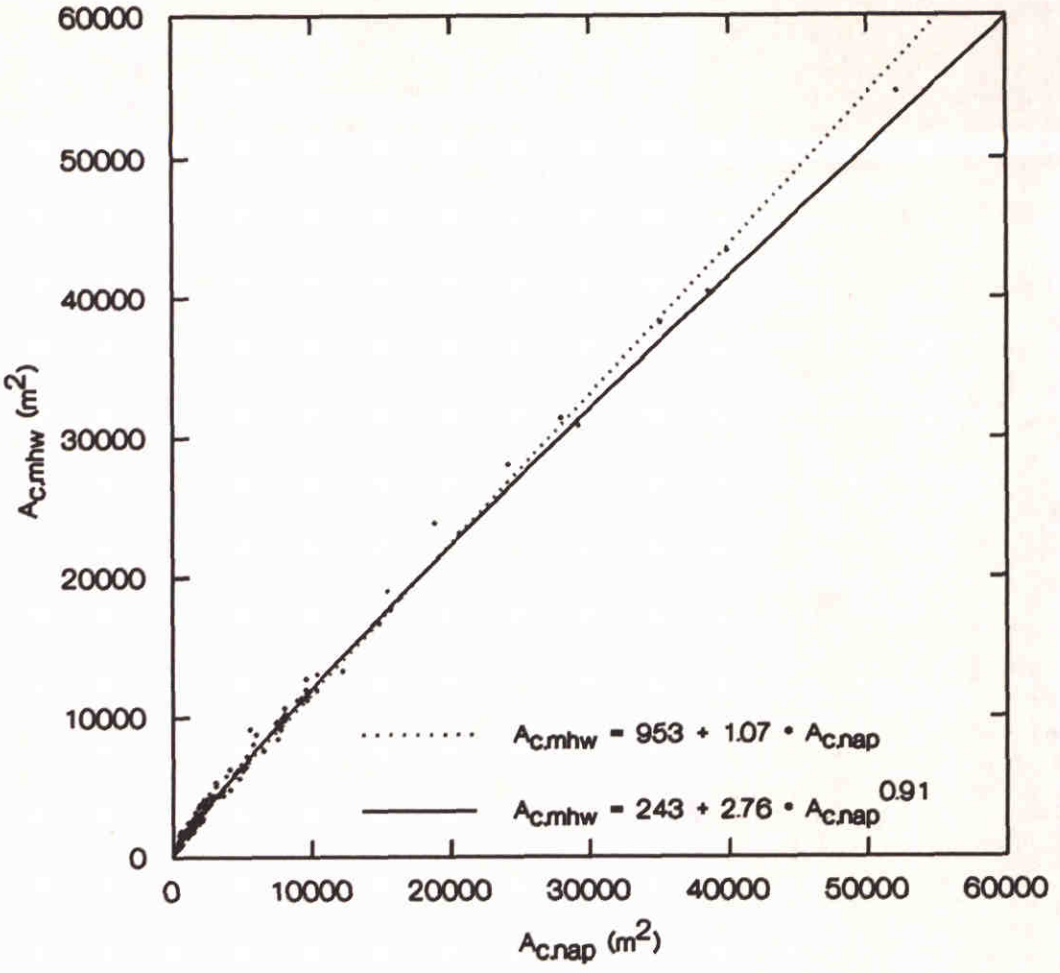

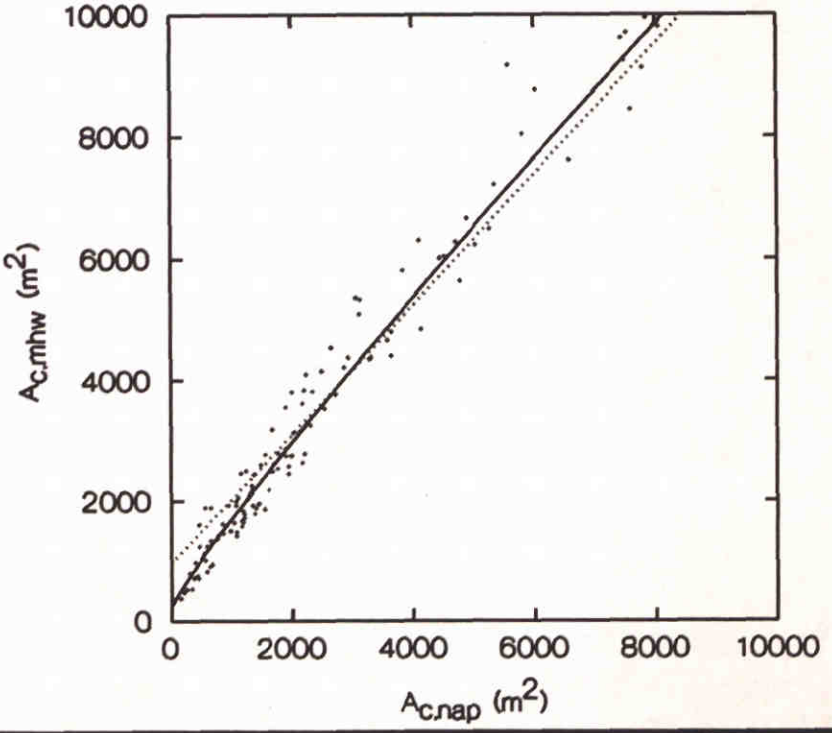

CORRELATION OF $A_{c,nap}$ WITH $A_{c,mhw}$

DELFT HYDRAULICS | H 1300 | FIG. 3.30

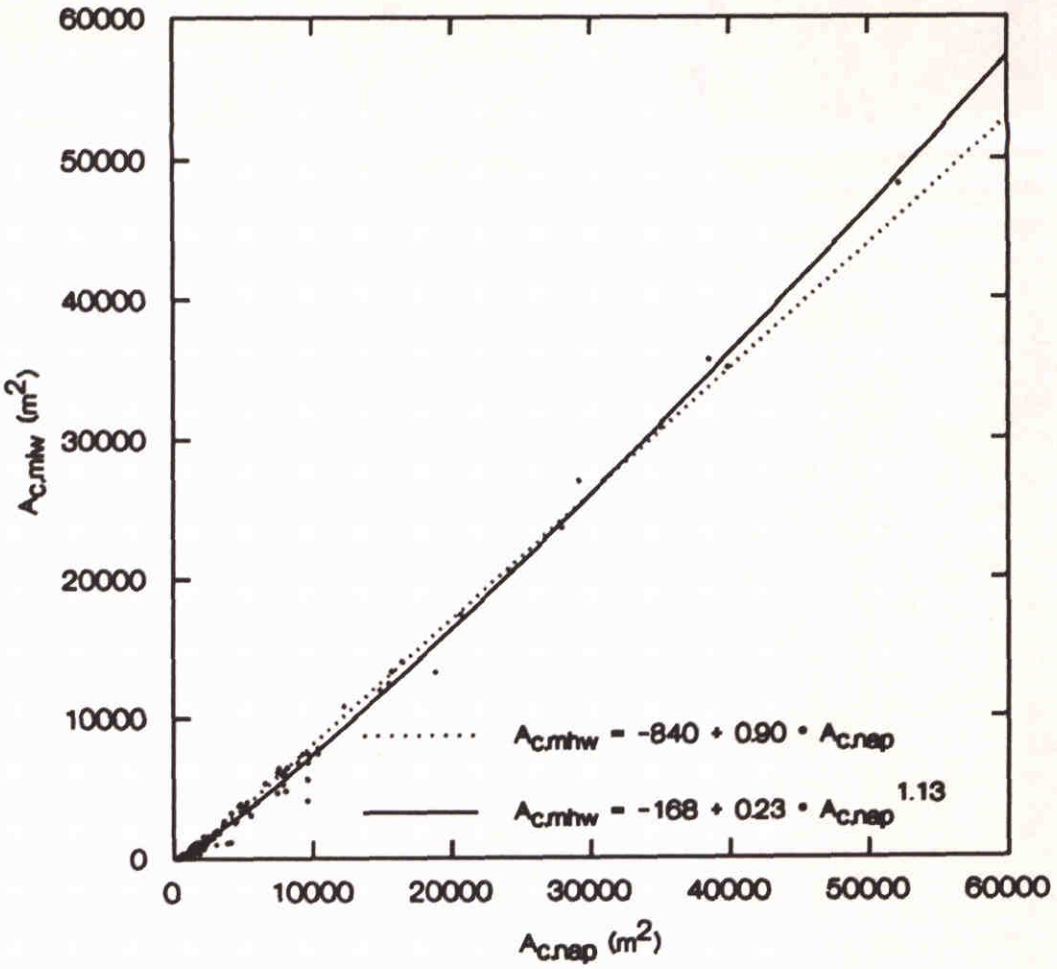

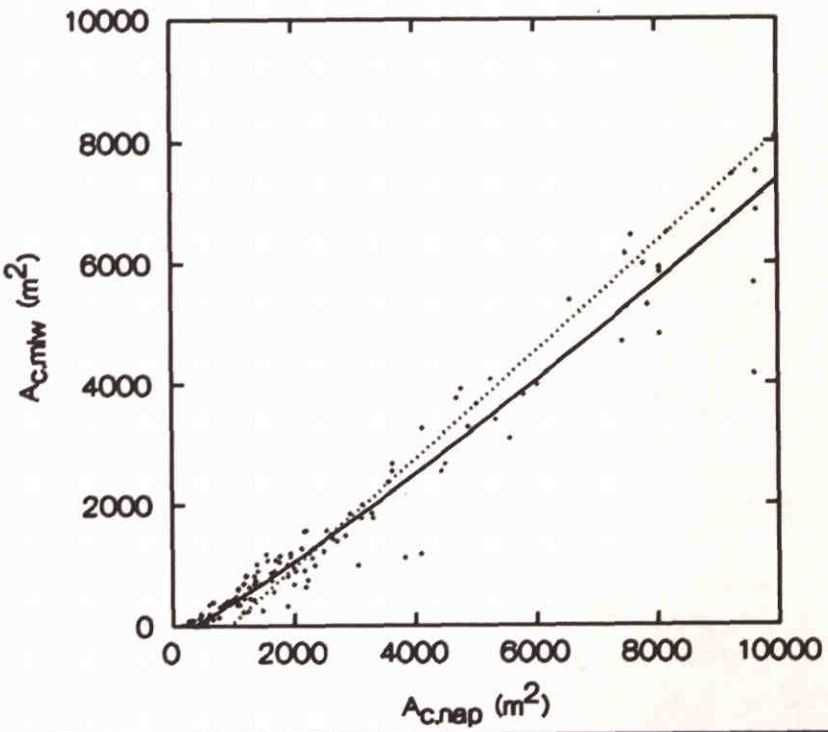

CORRELATION OF $A_{c,nap}$ WITH $A_{c,mlw}$

DELFT HYDRAULICS | H 1300 | FIG. 3.31

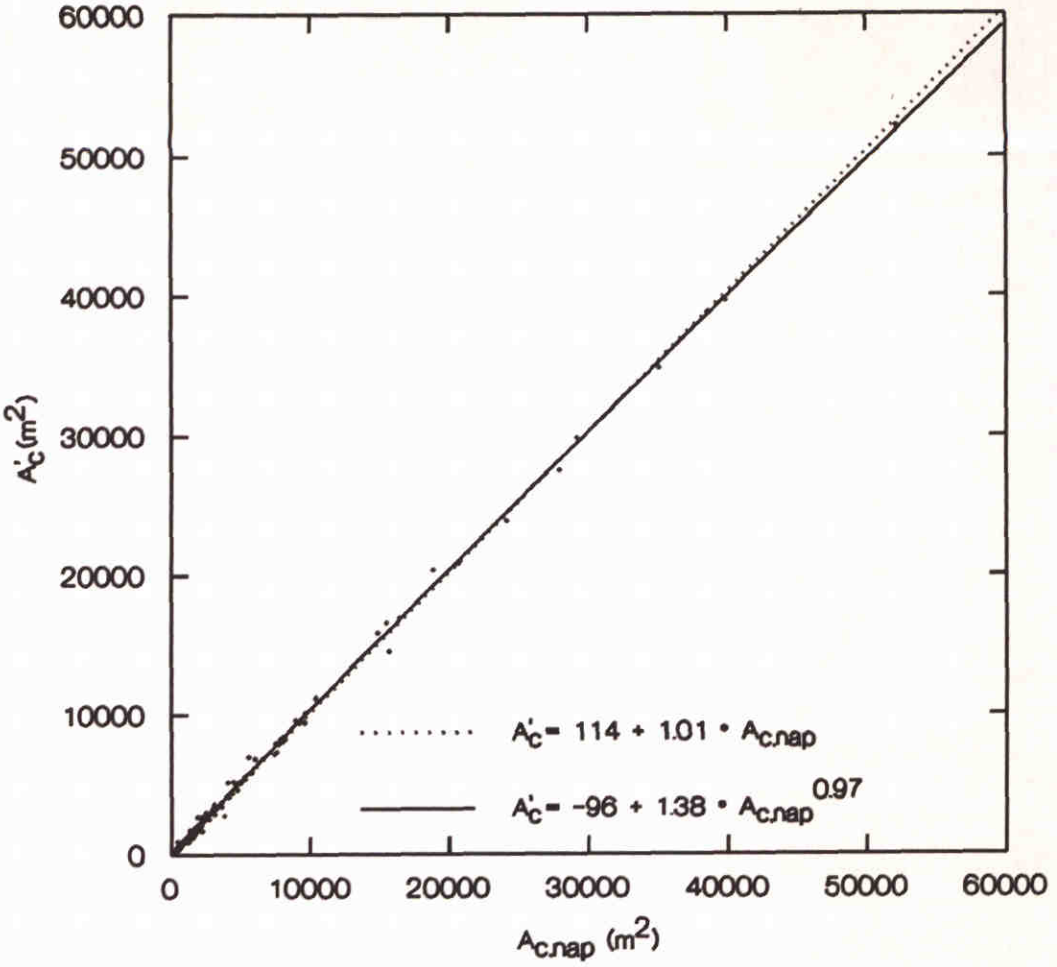

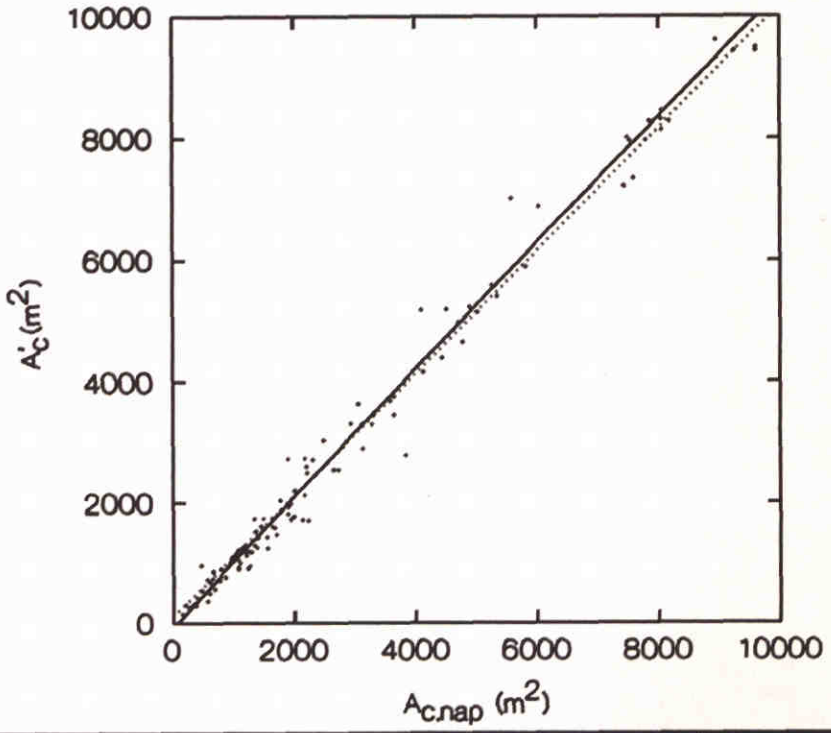

CORRELATION OF $A_{c.nap}$ WITH A'_c

DELFT HYDRAULICS | H 1300 | FIG. 3.32

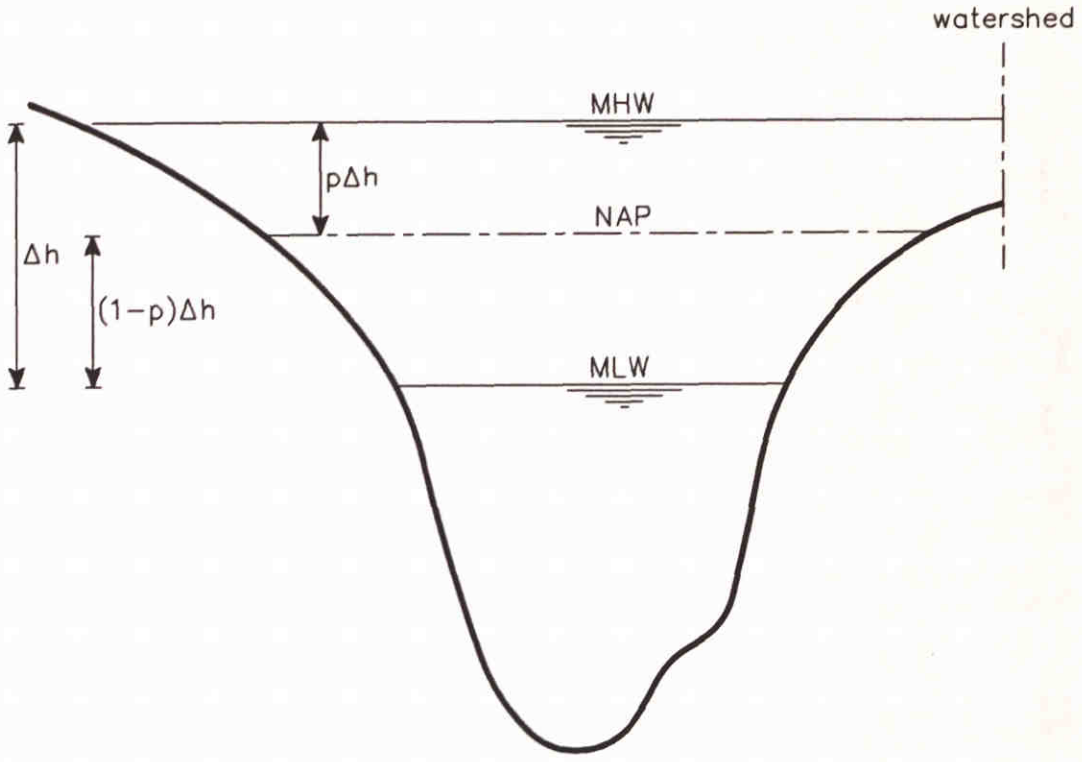

definition: $S1 = (W_{MHW} - W_{NAP})/2p\Delta h$

$S2 = (W_{NAP} - W_{MLW})/2(1-p)\Delta h$

due to the presence of watersheds especially S1 will be an approximation of reality

DEFINITION SKETCH CROSS-SECTIONAL CHANNEL PROFILES		
DELFT HYDRAULICS	H 1300	FIG. 3.33

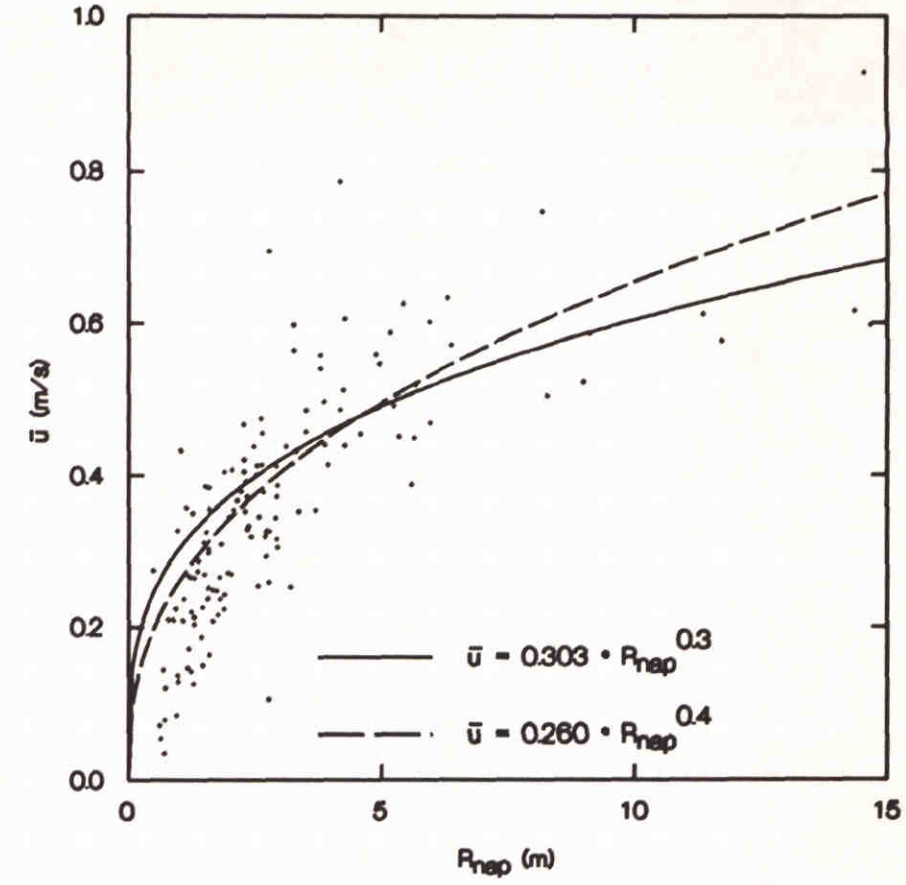

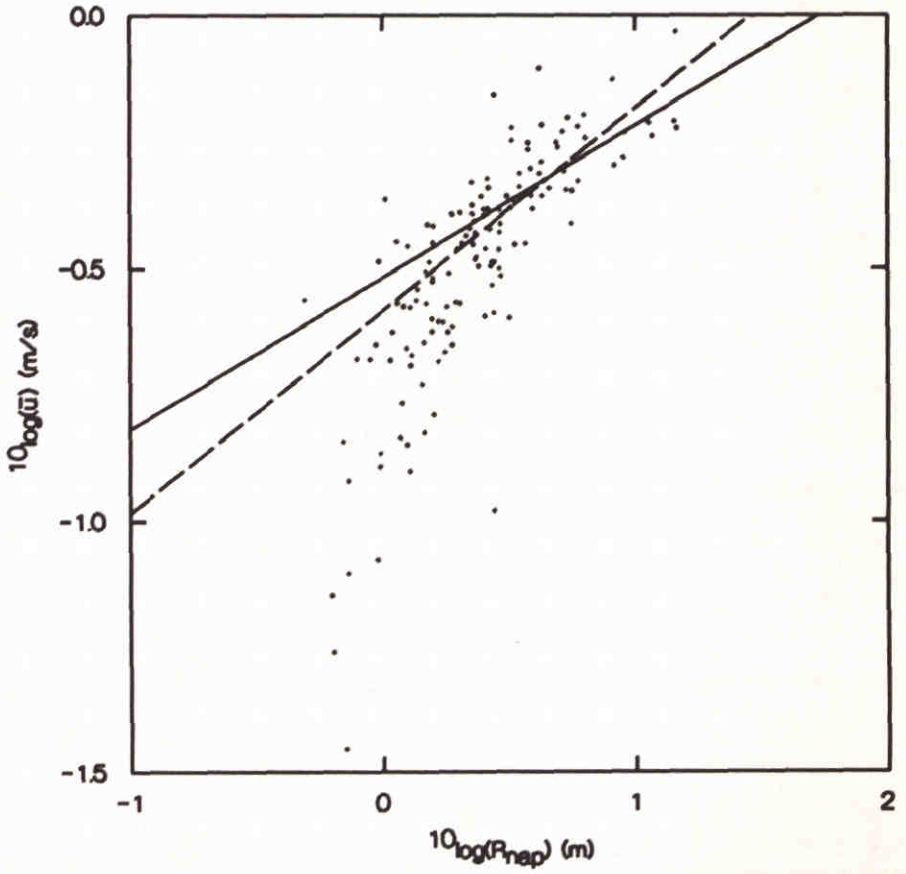

CORRELATION OF ū RELATED TO TV WITH R_{nap}

DELFT HYDRAULICS | H 1300 | FIG. 3.34

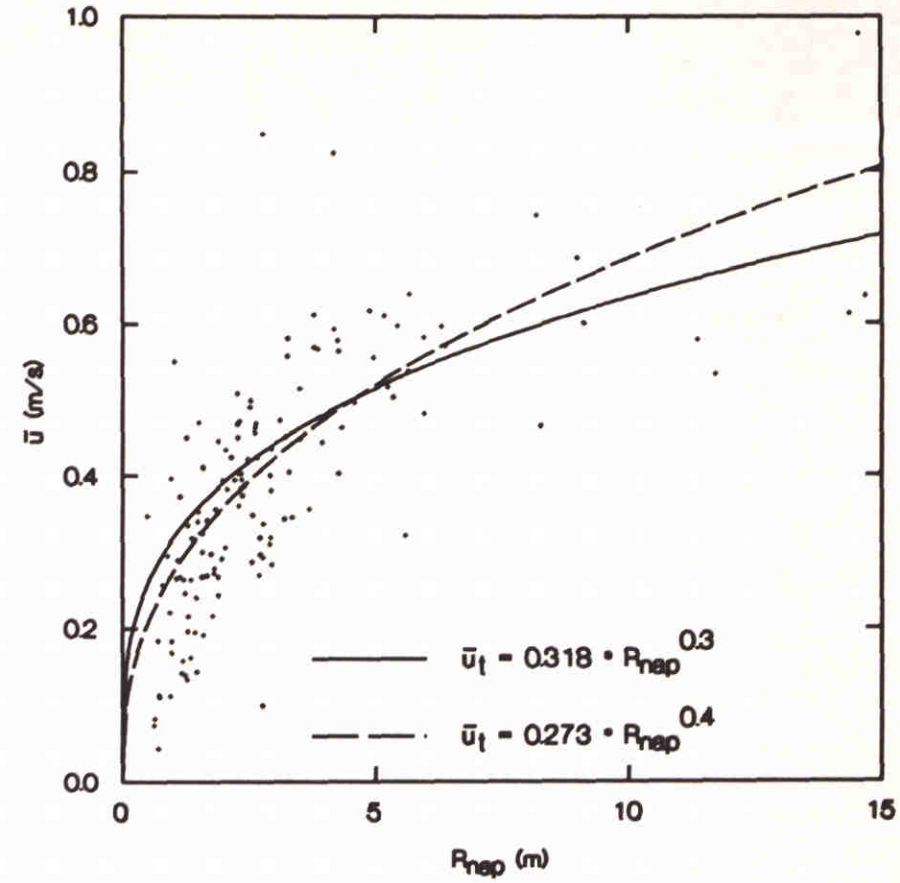

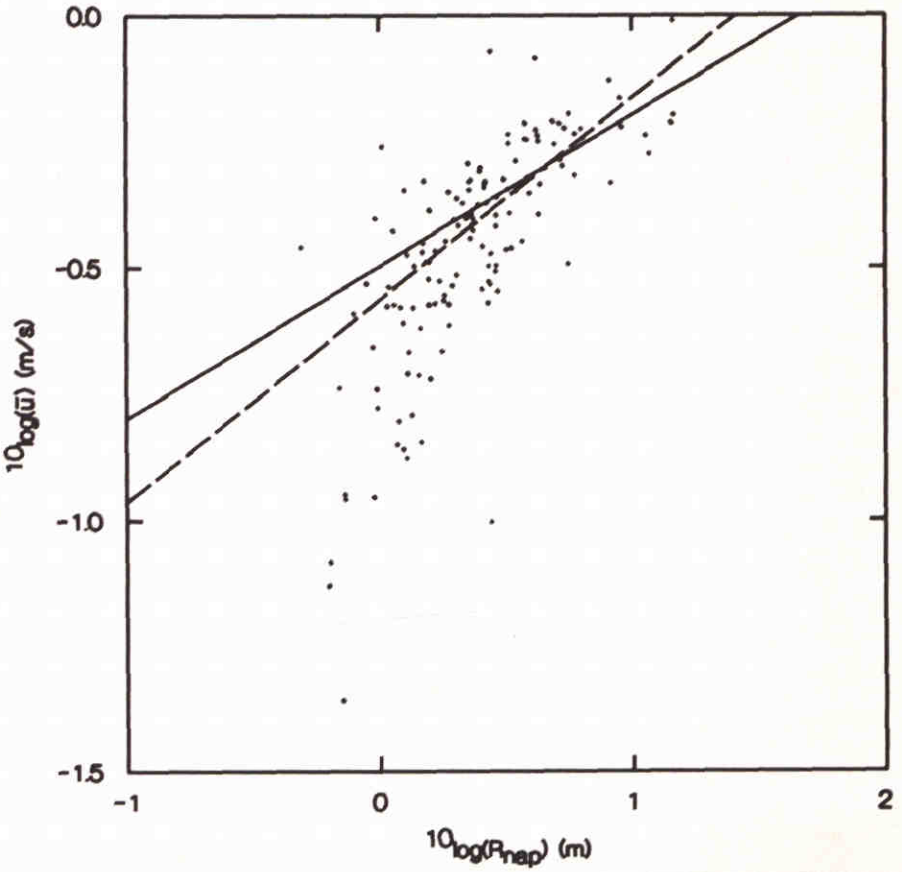

CORRELATION OF ū RELATED TO DV WITH R_{nap}

DELFT HYDRAULICS | H 1300 | FIG. 3.35

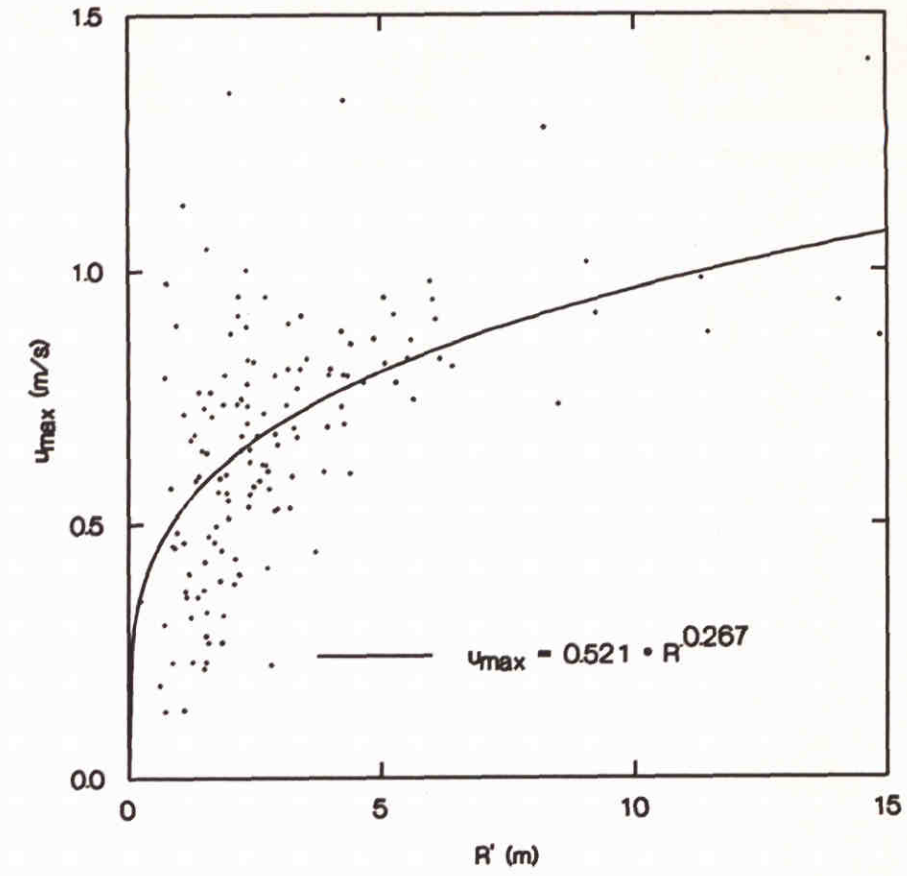

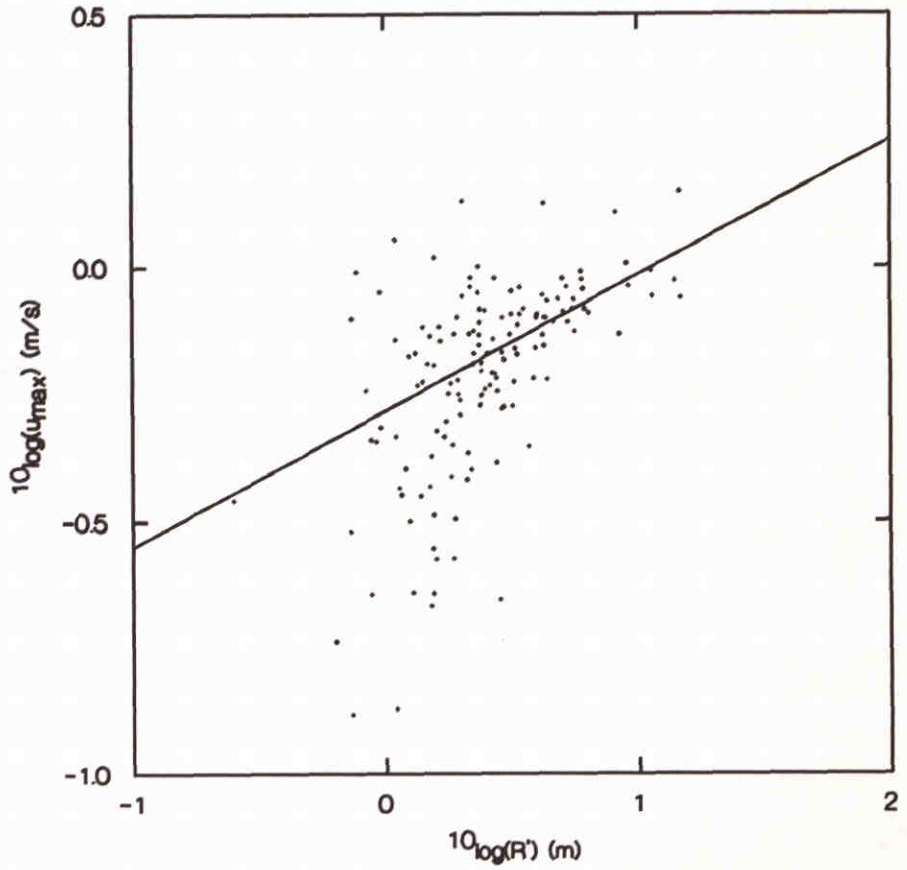

CORRELATION OF u_{max} RELATED TO Q_{max} WITH R'

DELFT HYDRAULICS | H 1300 | FIG. 3.36

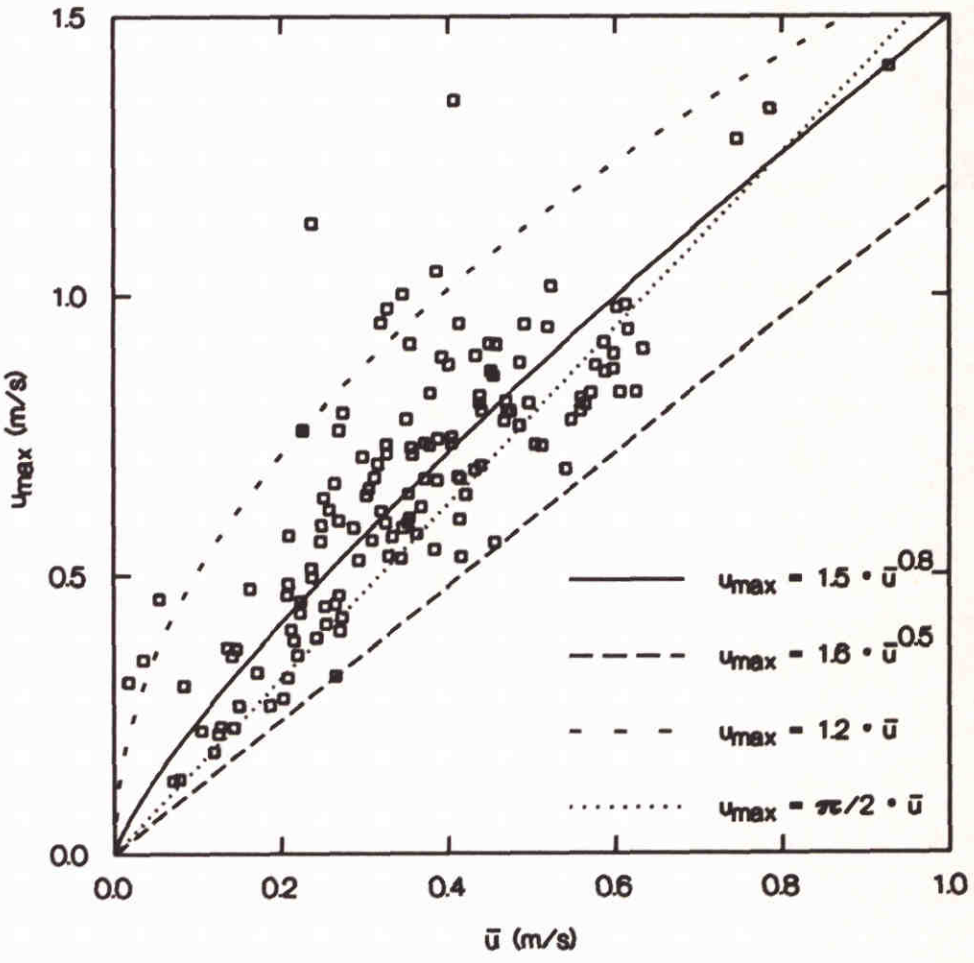

CORRELATION OF $\bar{u}$ WITH u_{max}

DELFT HYDRAULICS | H 1300 | FIG. 3.37

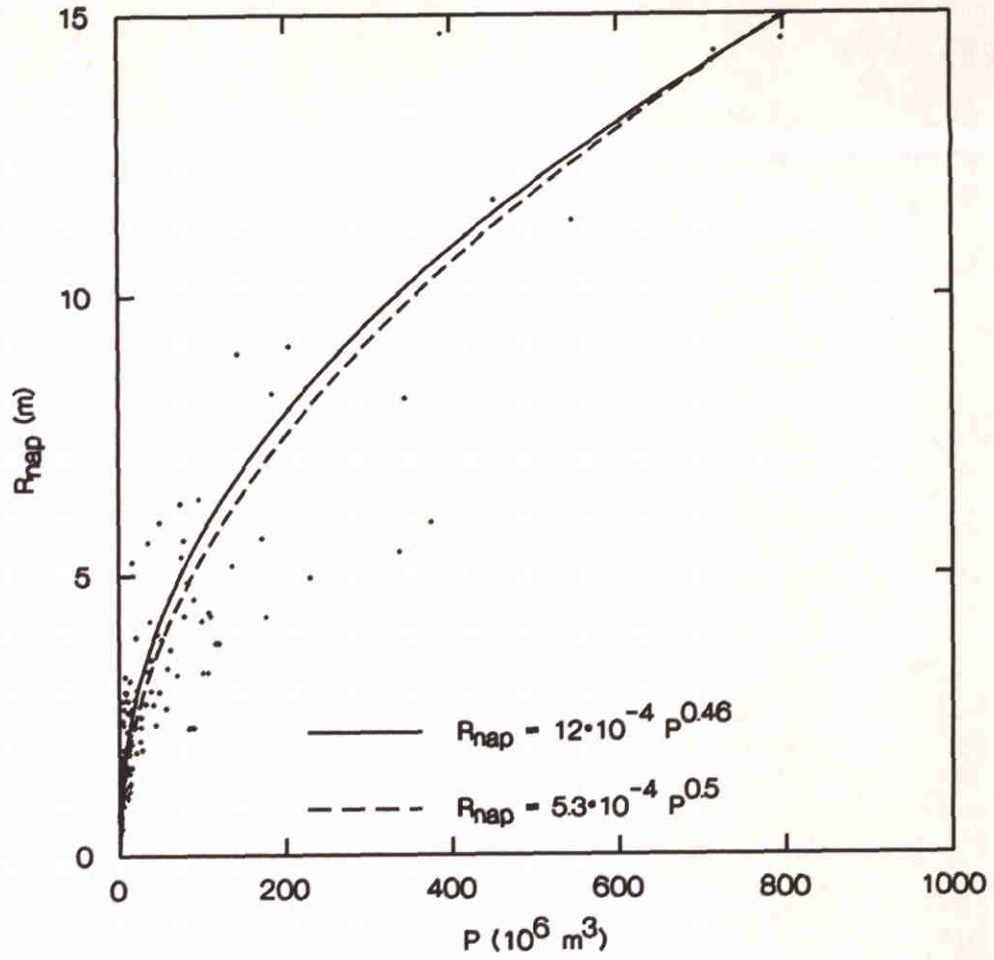

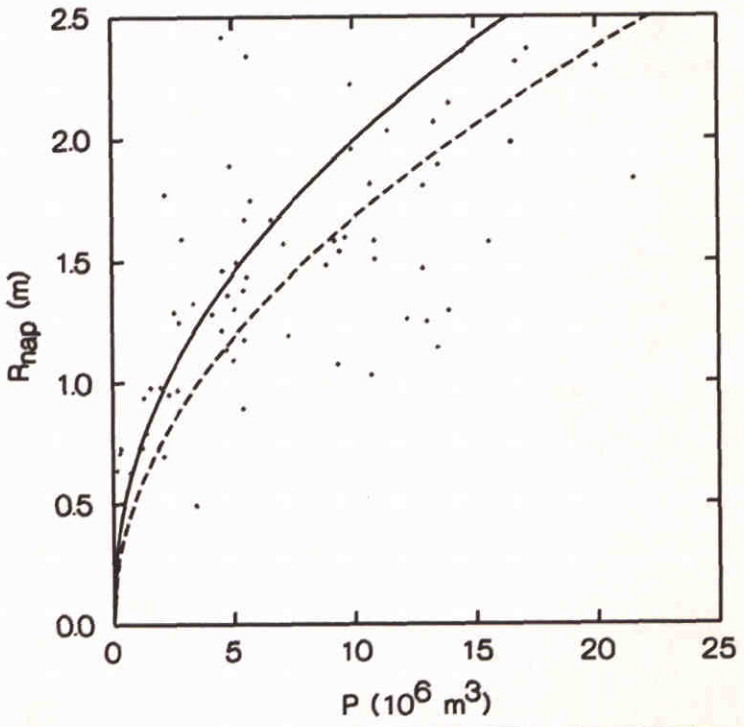

CORRELATION OF P WITH R_{nap}

DELFT HYDRAULICS | H 1300 | FIG. 3.38

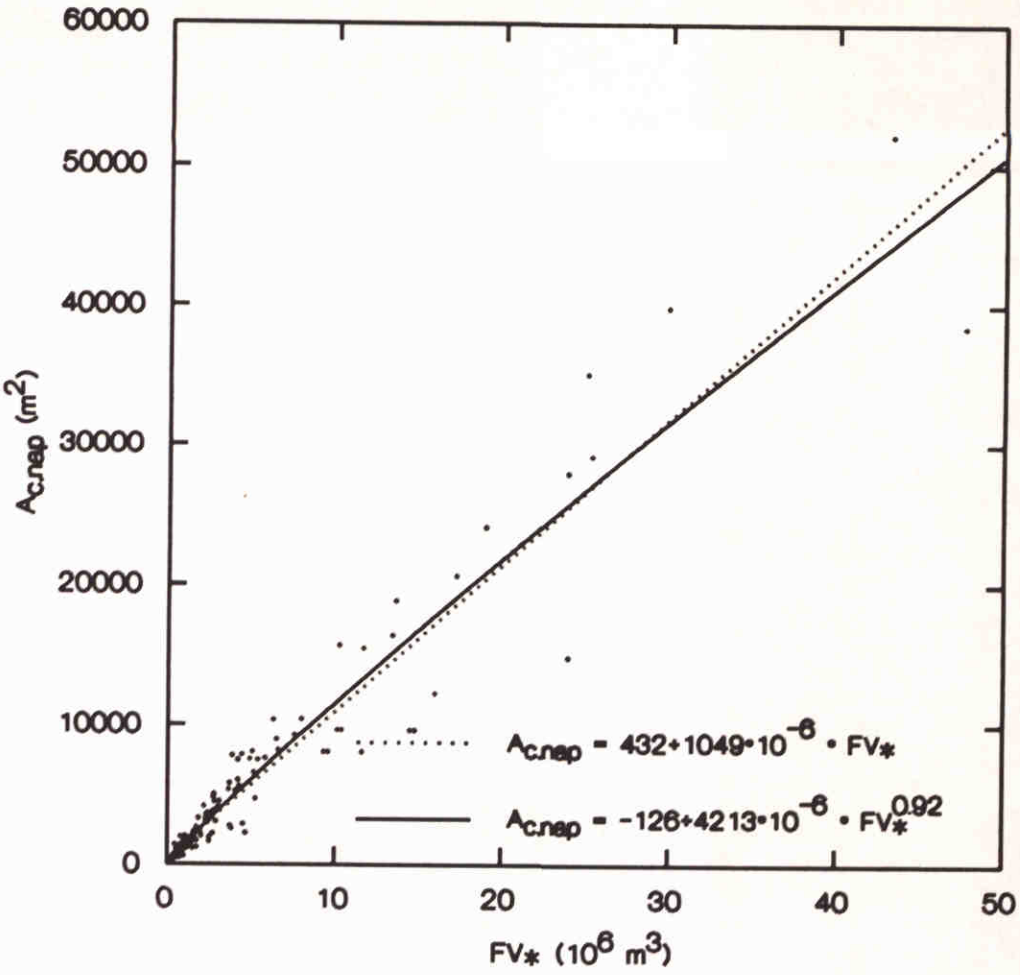

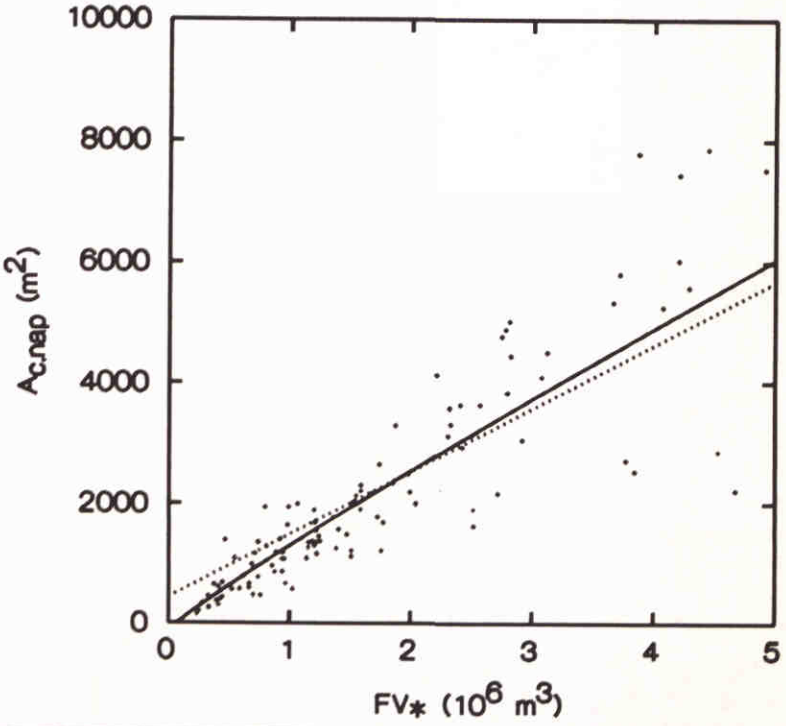

CORRELATION OF FV_* WITH $A_{c.nap}$

DELFT HYDRAULICS | H 1300 | FIG. 3.39

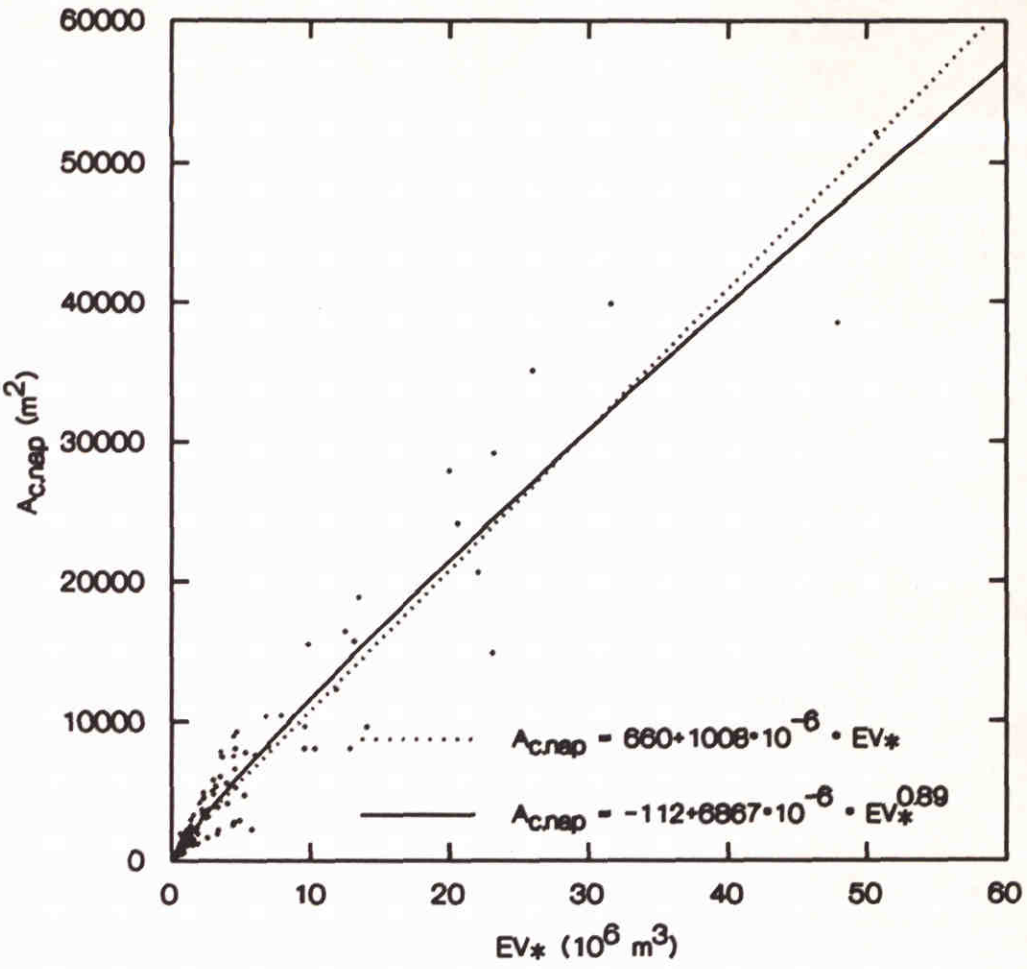

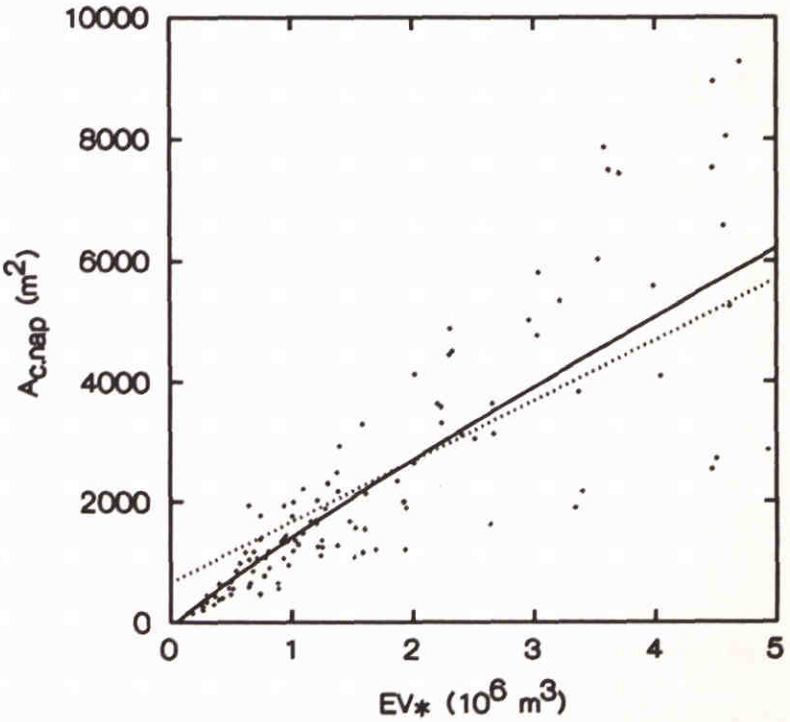

CORRELATION OF EV_* WITH $A_{c.nap}$

DELFT HYDRAULICS | H 1300 | FIG. 3.40

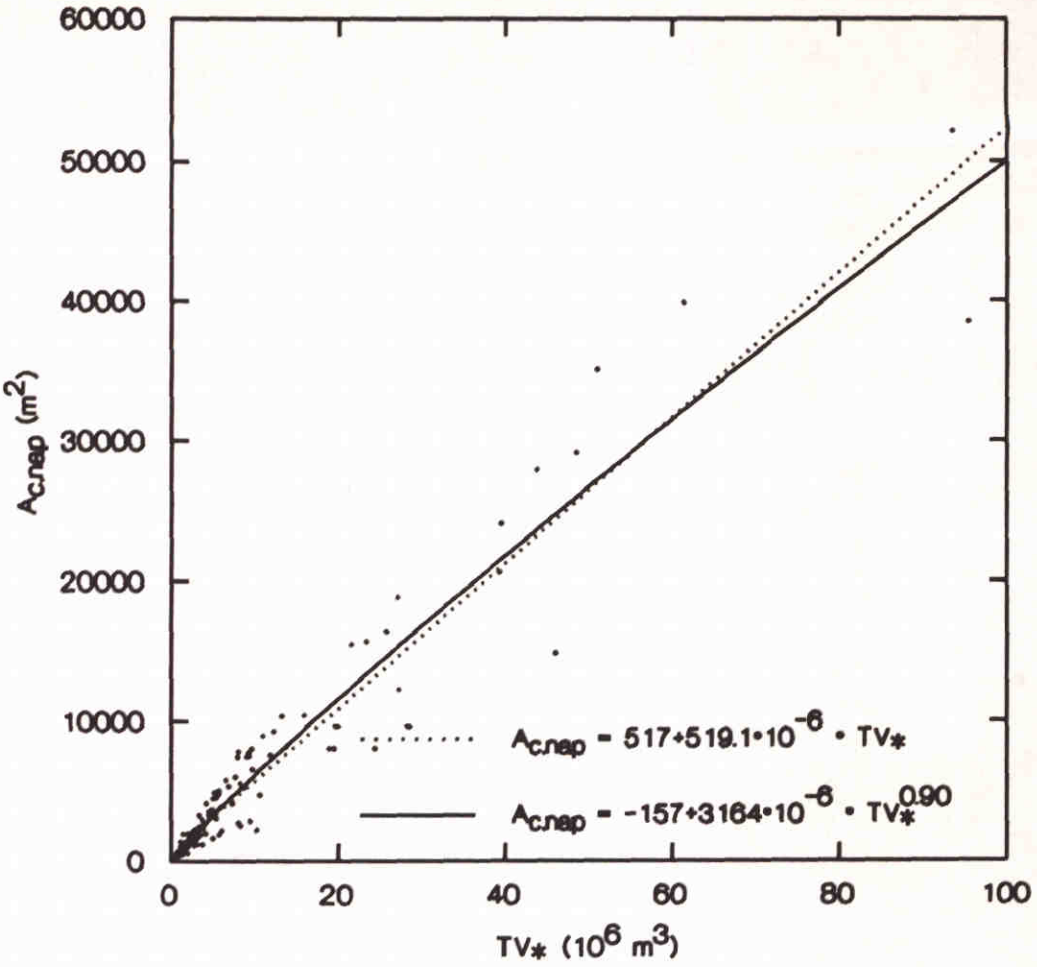

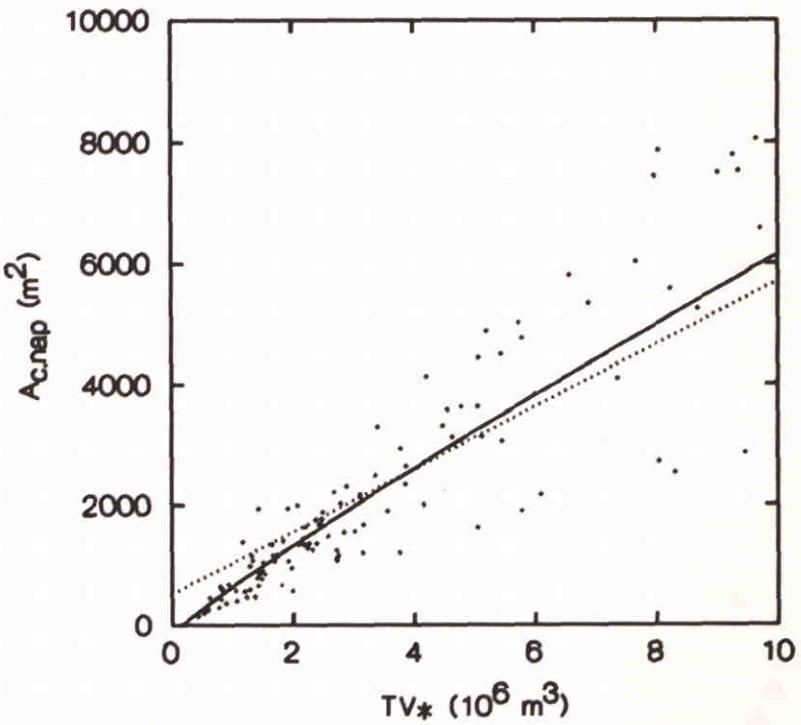

CORRELATION OF TV_* WITH $A_{c.nap}$

DELFT HYDRAULICS | H 1300 | FIG. 3.41

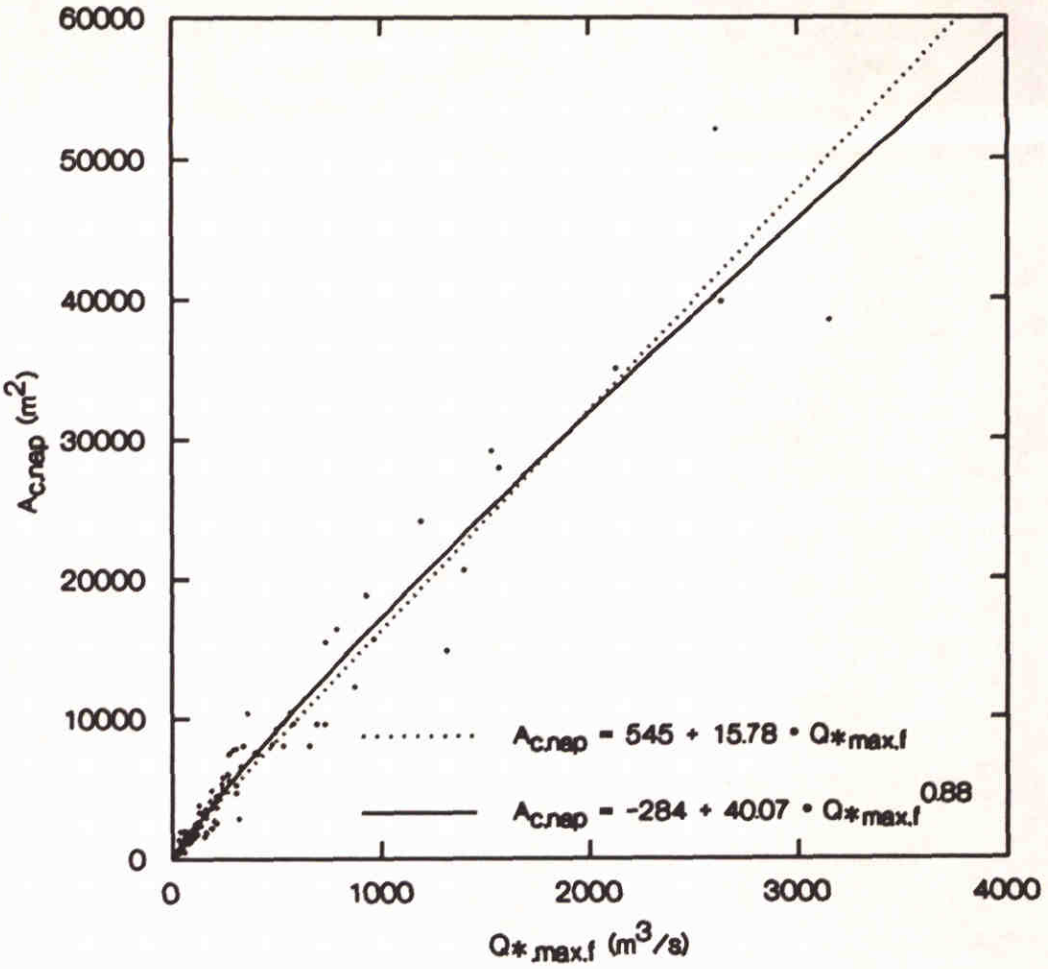

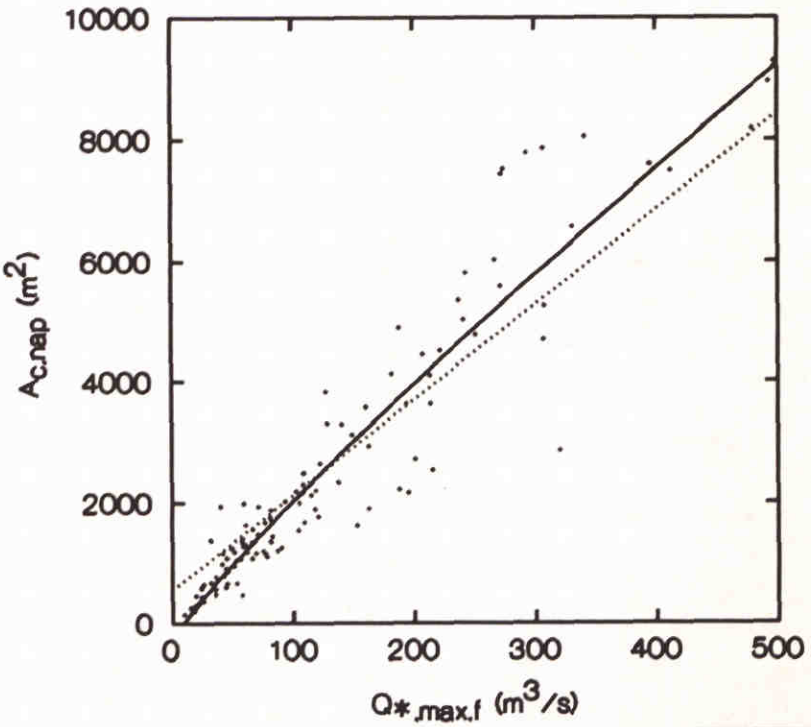

CORRELATION OF $Q*_{max,f}$ WITH $A_{c,nap}$

DELFT HYDRAULICS | H 1300 | FIG. 3.42

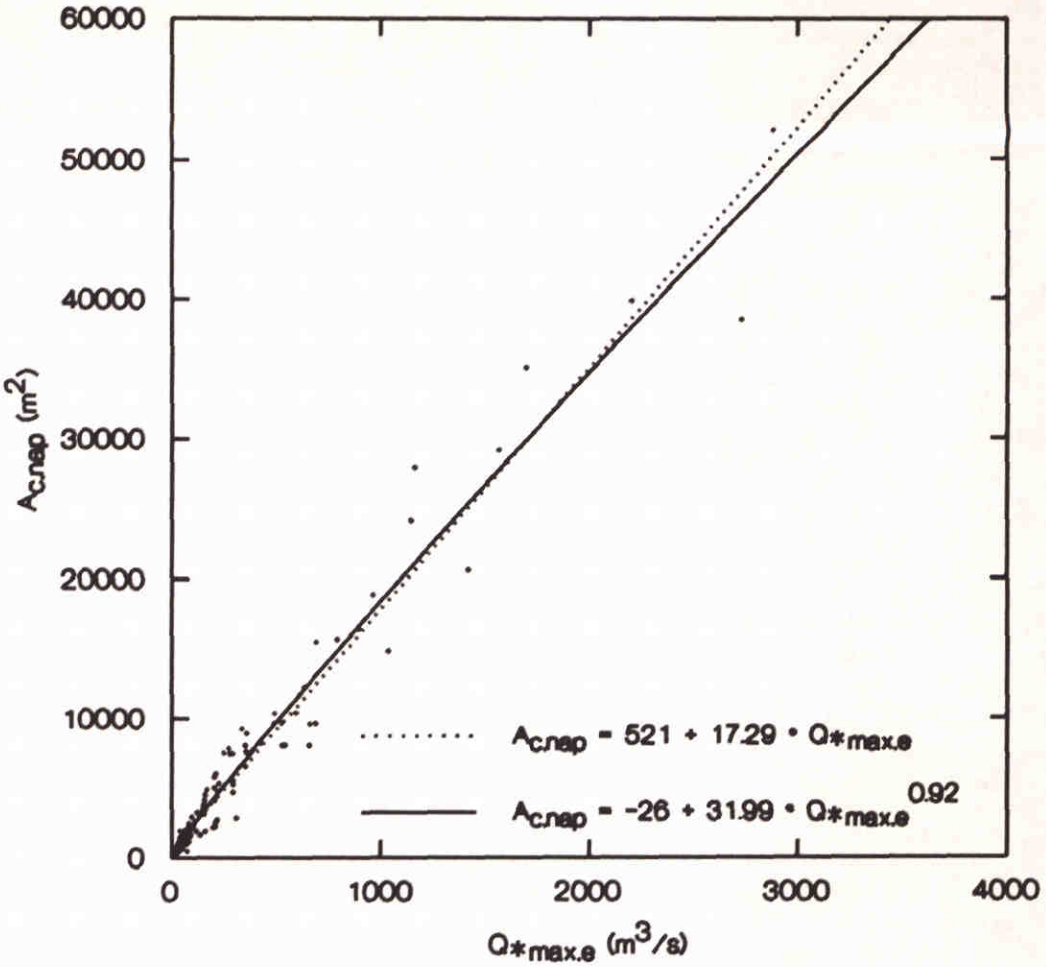

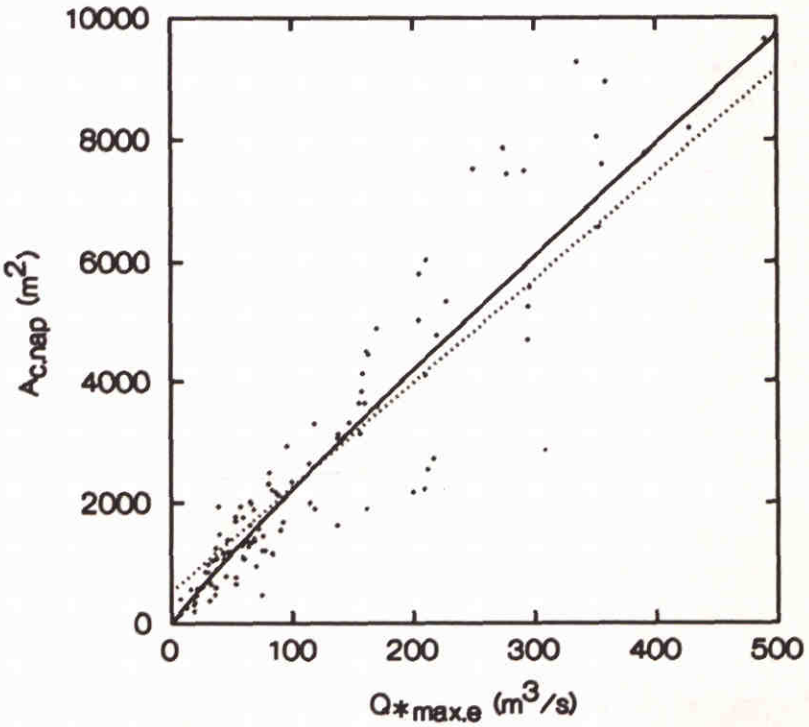

CORRELATION OF $Q*_{max.e}$ WITH $A_{c.nap}$

DELFT HYDRAULICS | H 1300 | FIG. 3.43

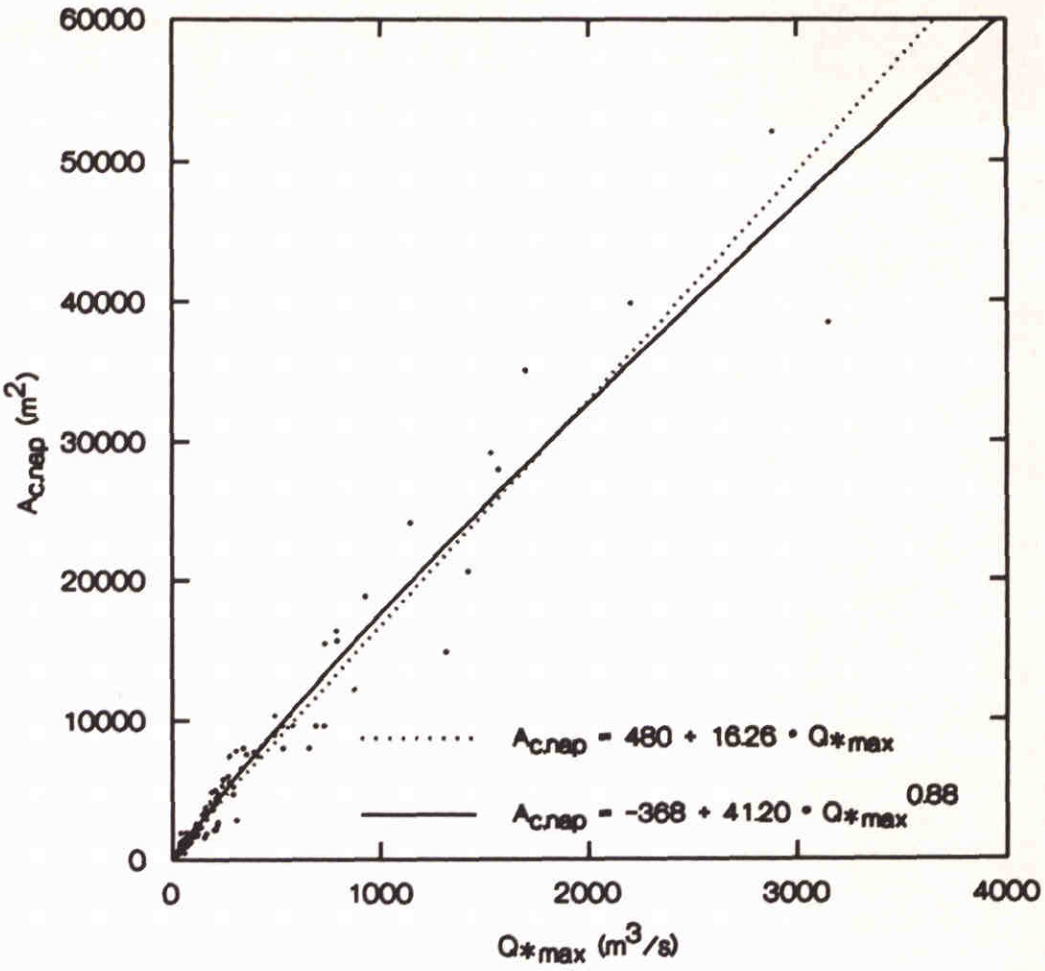

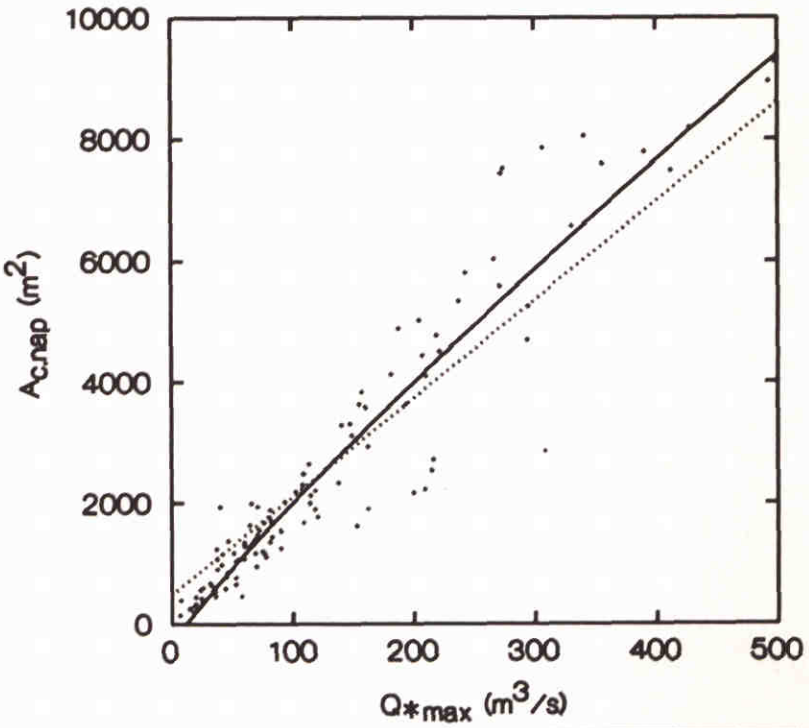

CORRELATION OF $Q*_{max}$ WITH $A_{c.nap}$

DELFT HYDRAULICS | H 1300 | FIG. 3.44

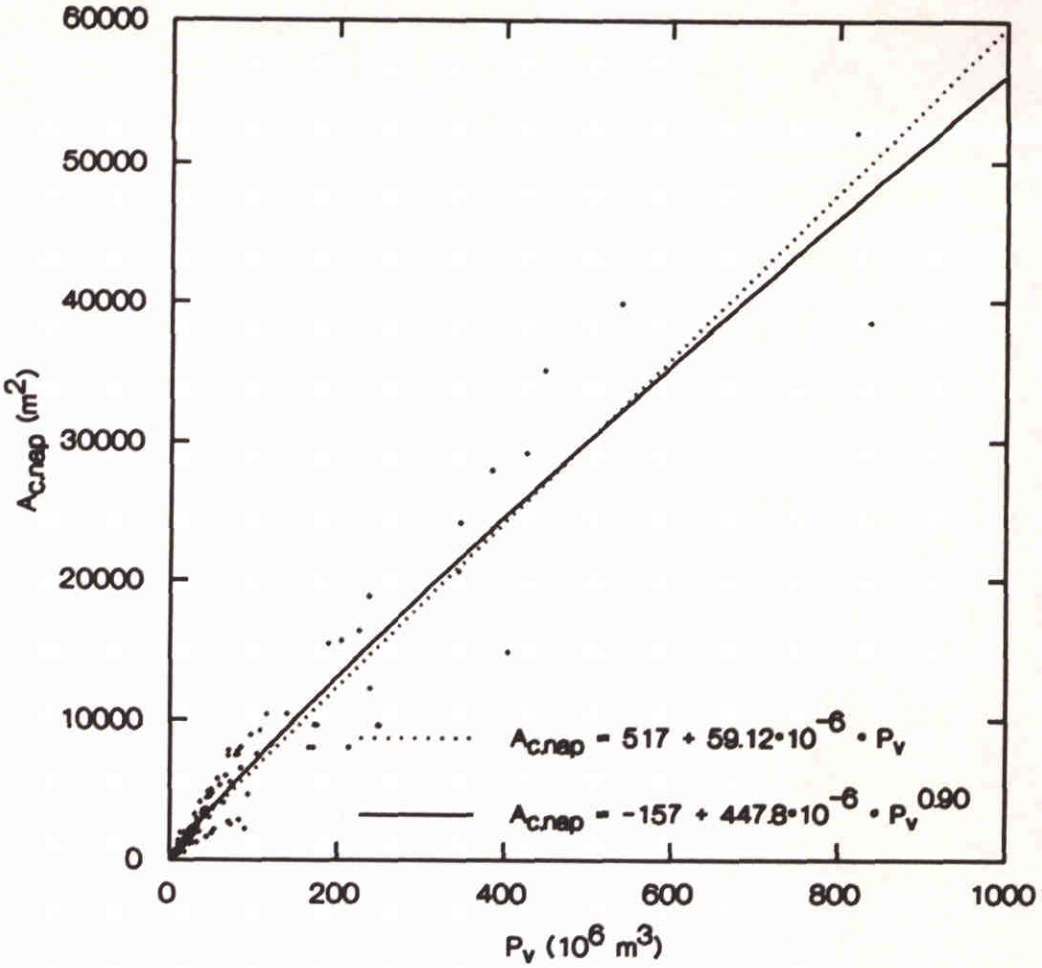

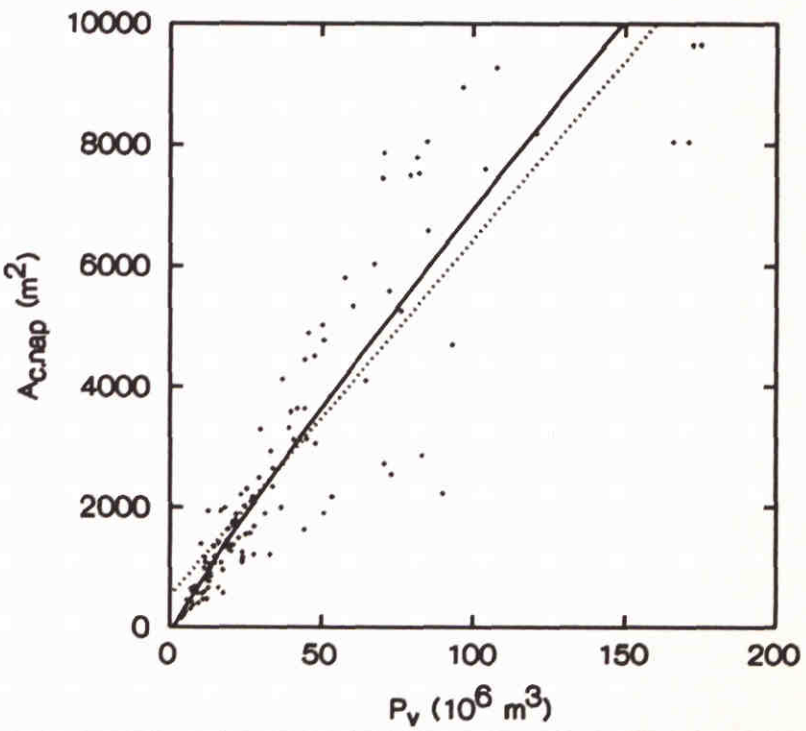

CORRELATION OF P_v WITH $A_{c.nap}$

DELFT HYDRAULICS | H 1300 | FIG. 3.45

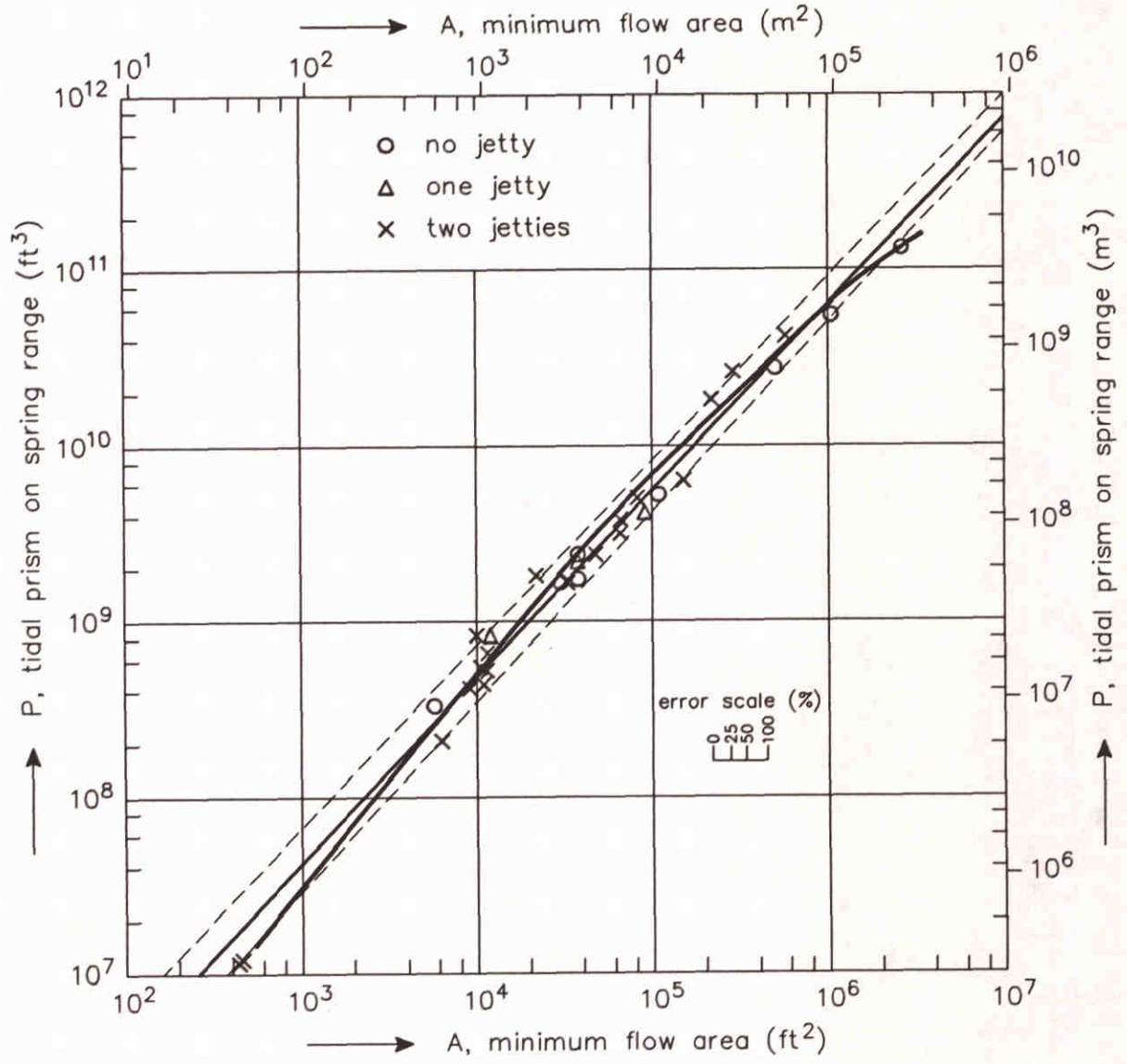

TIDAL INLET DATA PRESENTED BY O'BRIEN (1969)

DELFT HYDRAULICS | H 1300 | FIG. 3.46

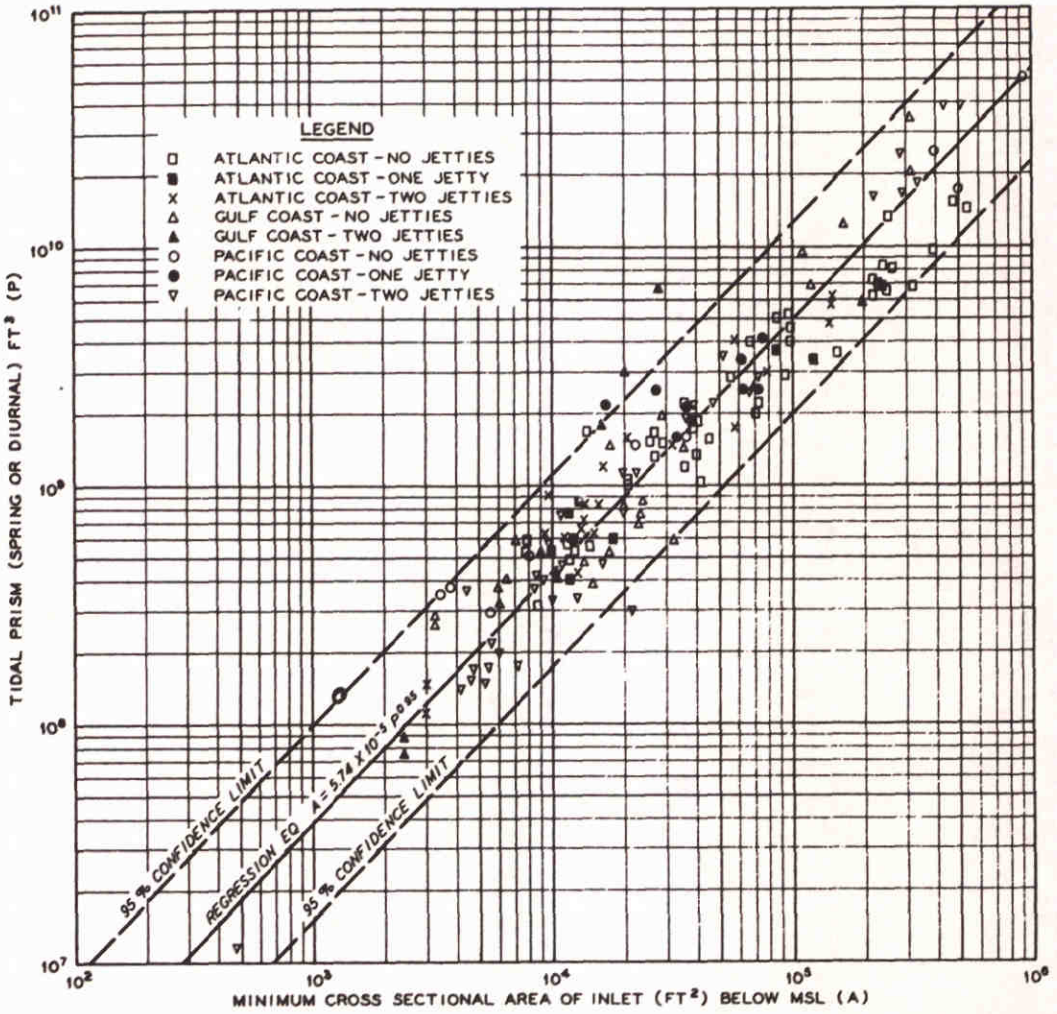

NOTE REGRESSION CURVE WITH 95 PERCENT CONFIDENCE LIMITS

TIDAL PRISM VS CROSS-SECTIONAL AREA

ALL INLETS ON ATLANTIC, GULF, AND PACIFIC COASTS

PLATE 1

TIDAL INLET RELATIONS OF JARRET (1976) ALL DATA		
DELFT HYDRAULICS	H 1300	FIG. 3.47

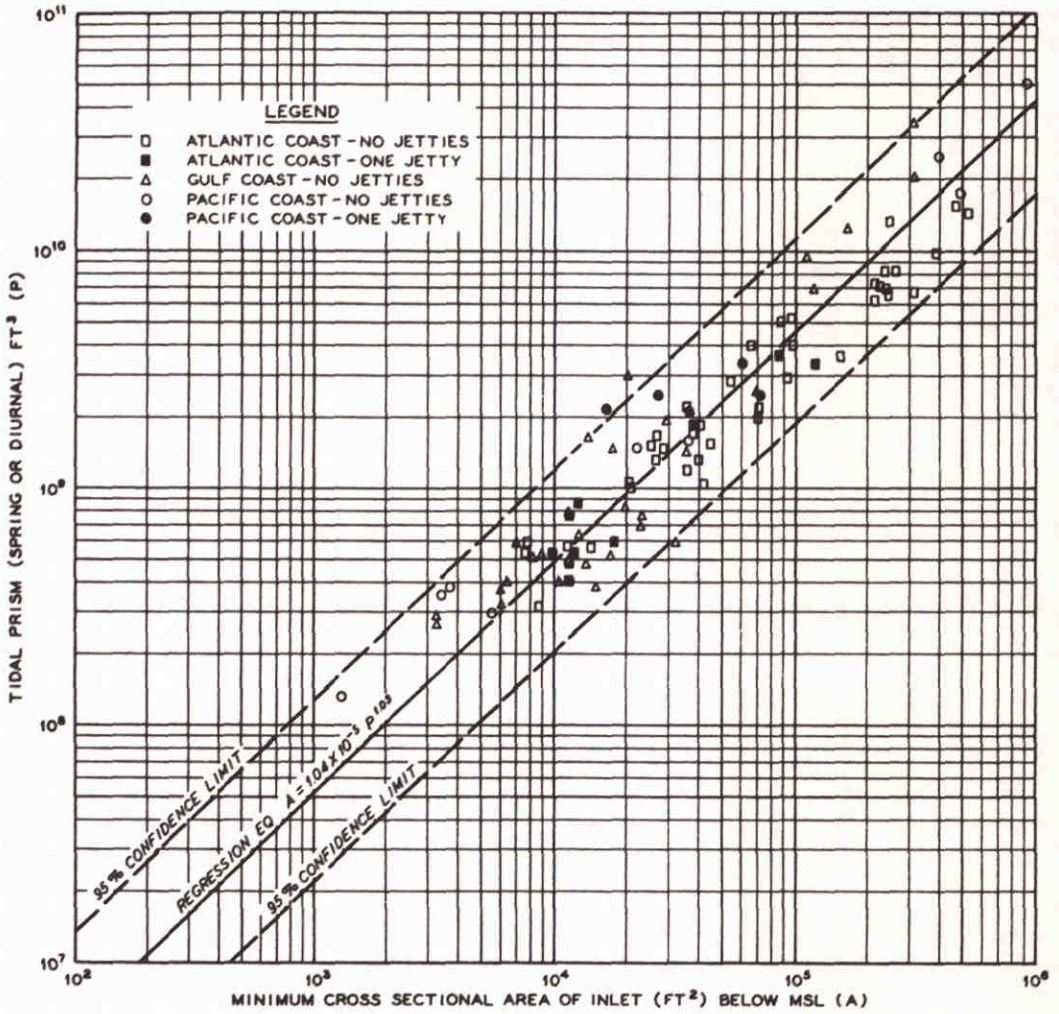

NOTE: REGRESSION CURVE WITH 95 PERCENT CONFIDENCE LIMITS.

TIDAL PRISM VS CROSS-SECTIONAL AREA

INLETS ON ATLANTIC, GULF, AND PACIFIC COASTS WITH ONE OR NO JETTIES

PLATE 5

TIDAL INLET RELATIONS OF JARRET (1976) ALL DATA WITH ONE OR NO JETTY		
DELFT HYDRAULICS	H 1300	FIG. 3.48

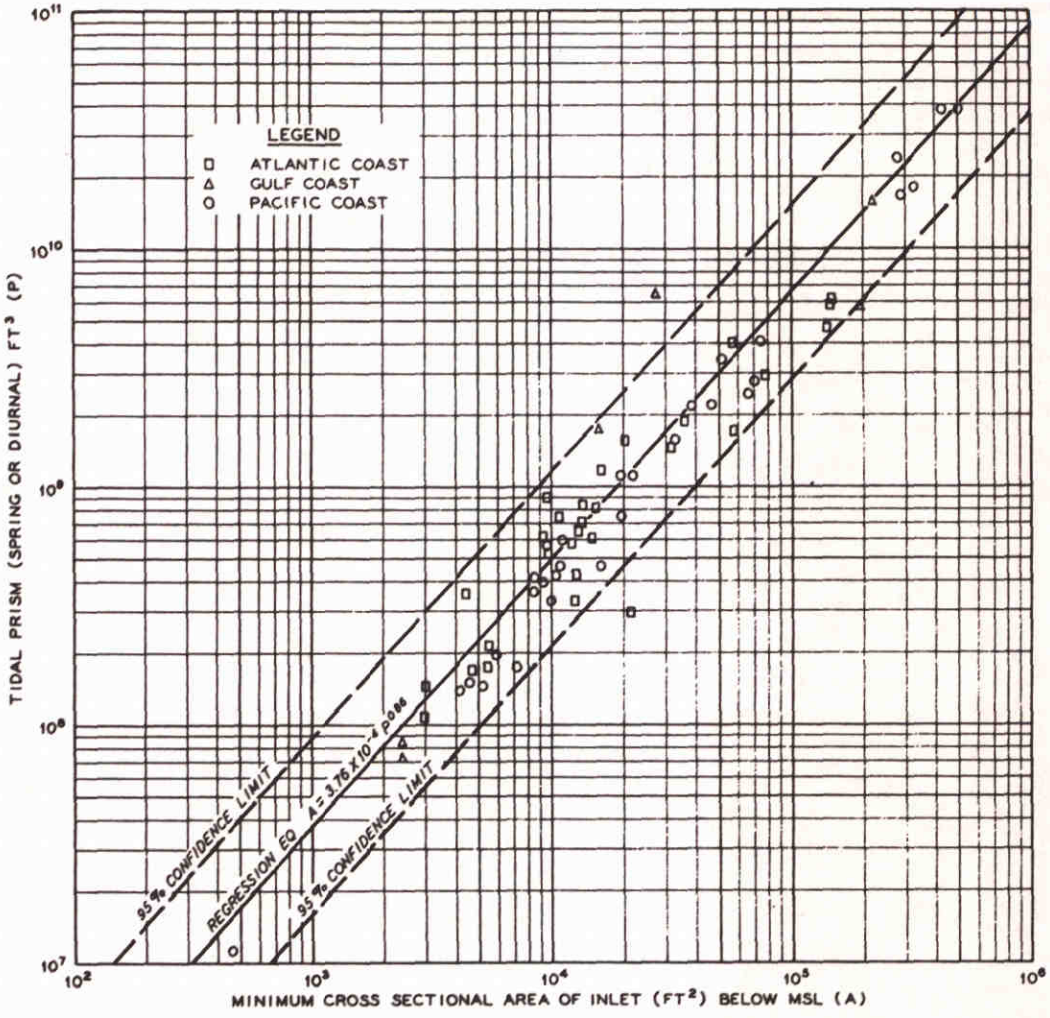

NOTE REGRESSION CURVE WITH 95 PERCENT CONFIDENCE LIMITS

TIDAL PRISM VS CROSS-SECTIONAL AREA

INLETS ON ATLANTIC, GULF, AND PACIFIC COASTS WITH TWO JETTIES

PLATE 9

TIDAL INLET RELATIONS OF JARRET (1976) ALL DATA WITH TWO JETTIES		
DELFT HYDRAULICS	H 1300	FIG. 3.49

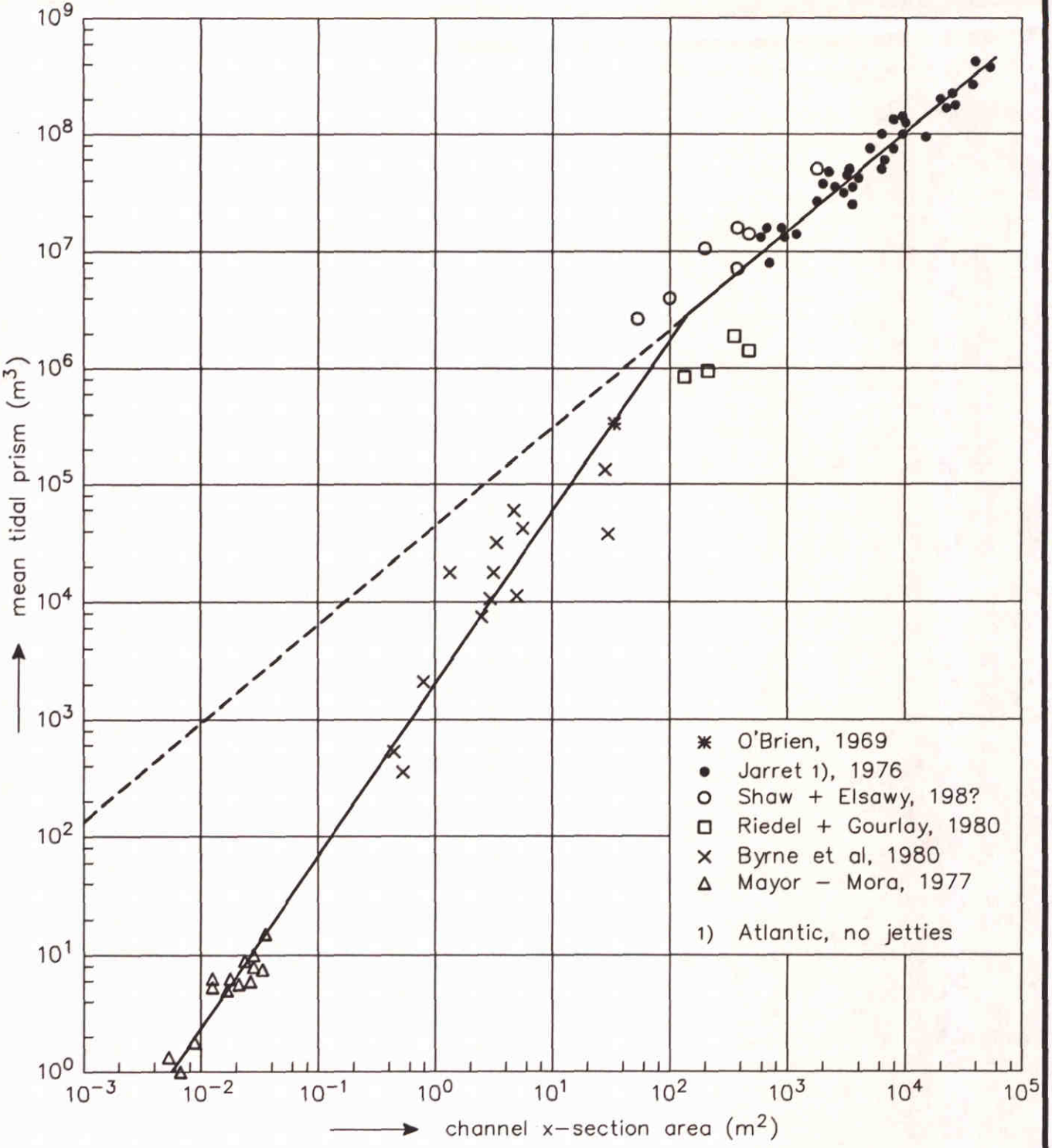

TIDAL INLET DATA OF LARGE AND SMALL INLETS

DELFT HYDRAULICS | H 1300 | FIG. 3.50

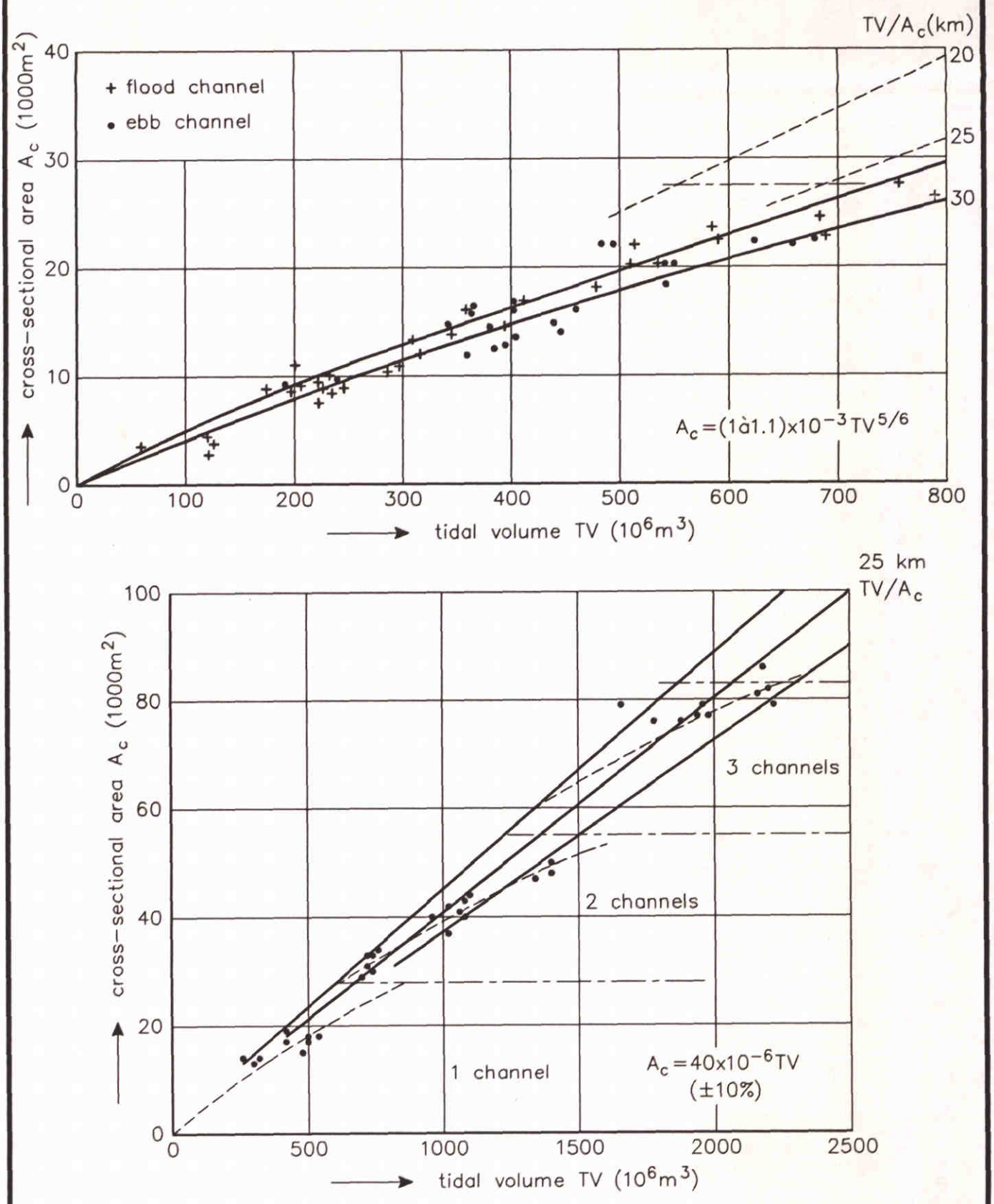

RELATION ON CHANNEL PROFILES OF THE WESTERN SCHELDT ESTUARY (ALLERSMA, 1991)

DELFT HYDRAULICS | H 1300 | FIG. 3.51

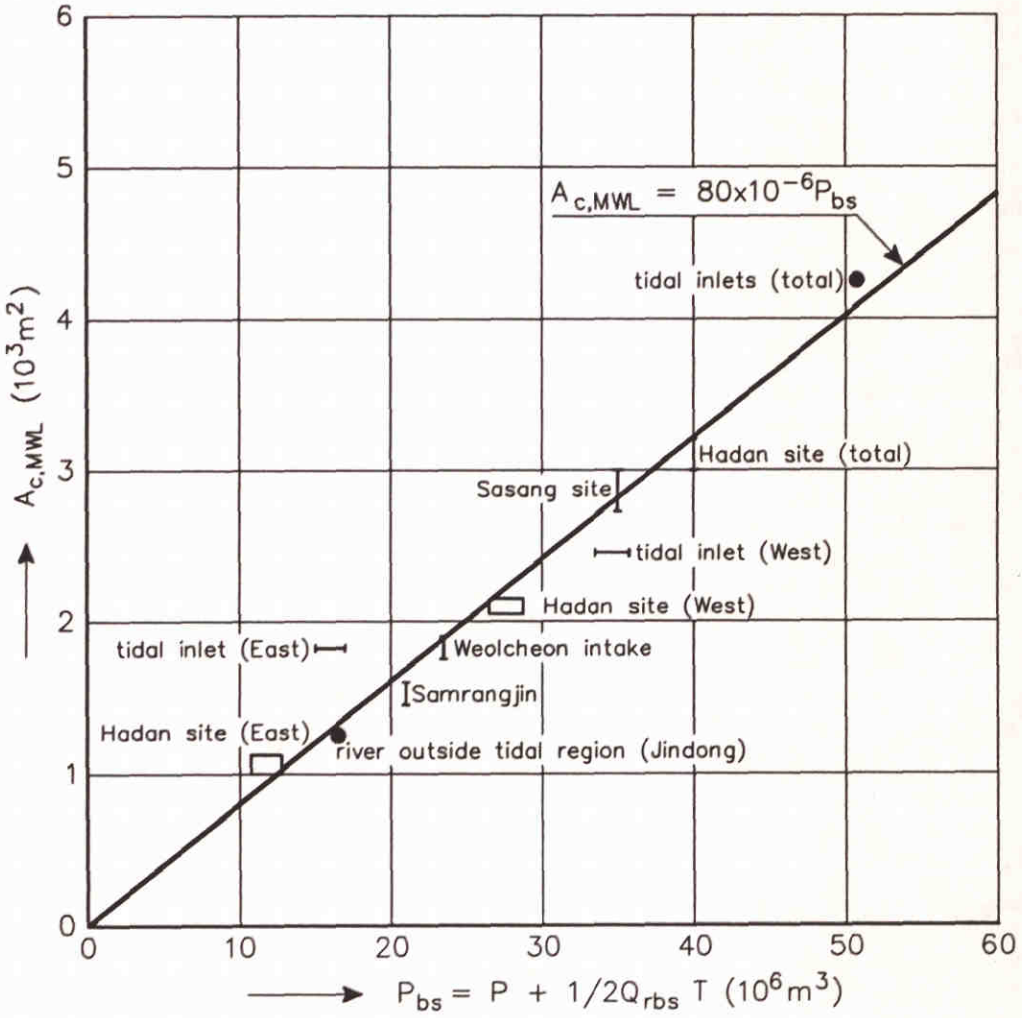

RELATION ON CHANNEL PROFILES OF THE NAKDONG ESTUARY INCLUDING THE EFFECT OF RIVER DISCHARGE (EYSINK, 1983)

DELFT HYDRAULICS | H 1300 | FIG. 3.52

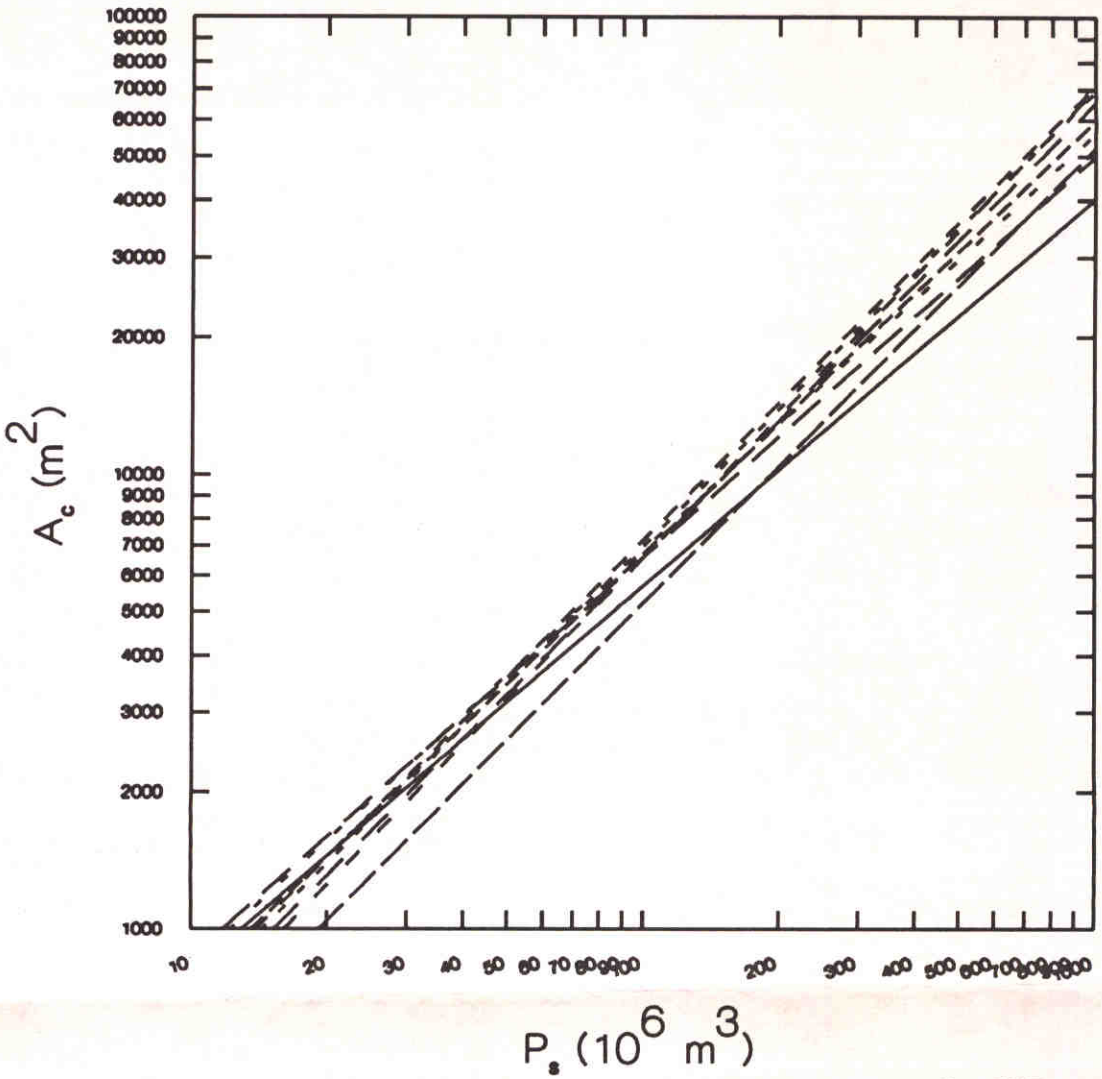

———	O'Brien (1931)	$A_c = 902 \cdot 10^{-6} P_s^{0.85}$
— — —	O'Brien (1969)	$A_c = 66 \cdot 10^{-6} P_s$
— — —	Johnson (1972)	$A_c = 600 \cdot 10^{-6} P_s^{0.88}$
— — — —	Johnson (1972)	$A_c = 52 \cdot 10^{-6} P_s$
— — — —	Jarret (1976)	$A_c = 38 \cdot 10^{-6} P_s$
— — — — -	Haring (1967)	$A_c = 72 \cdot 10^{-6} P_s$
— — — — —	Hume and Herdendorf (1990)	$A_c = 159 \cdot 10^{-6} P_s^{0.953}$
- - - - -	Dieckmann et al. (1988)	$A_c = 327 \cdot 10^{-6} P_s^{0.915}$
- - - - -	Eysink (1983.1991b).Allersma (1991)	$A_c = 70 \cdot 10^{-6} P_s$

COMPARISON OF VARIOUS RELATIONSHIPS FOR TIDAL INLETS AND CHANNELS FROM LITERATURE

DELFT HYDRAULICS | H 1300 | FIG. 3.53

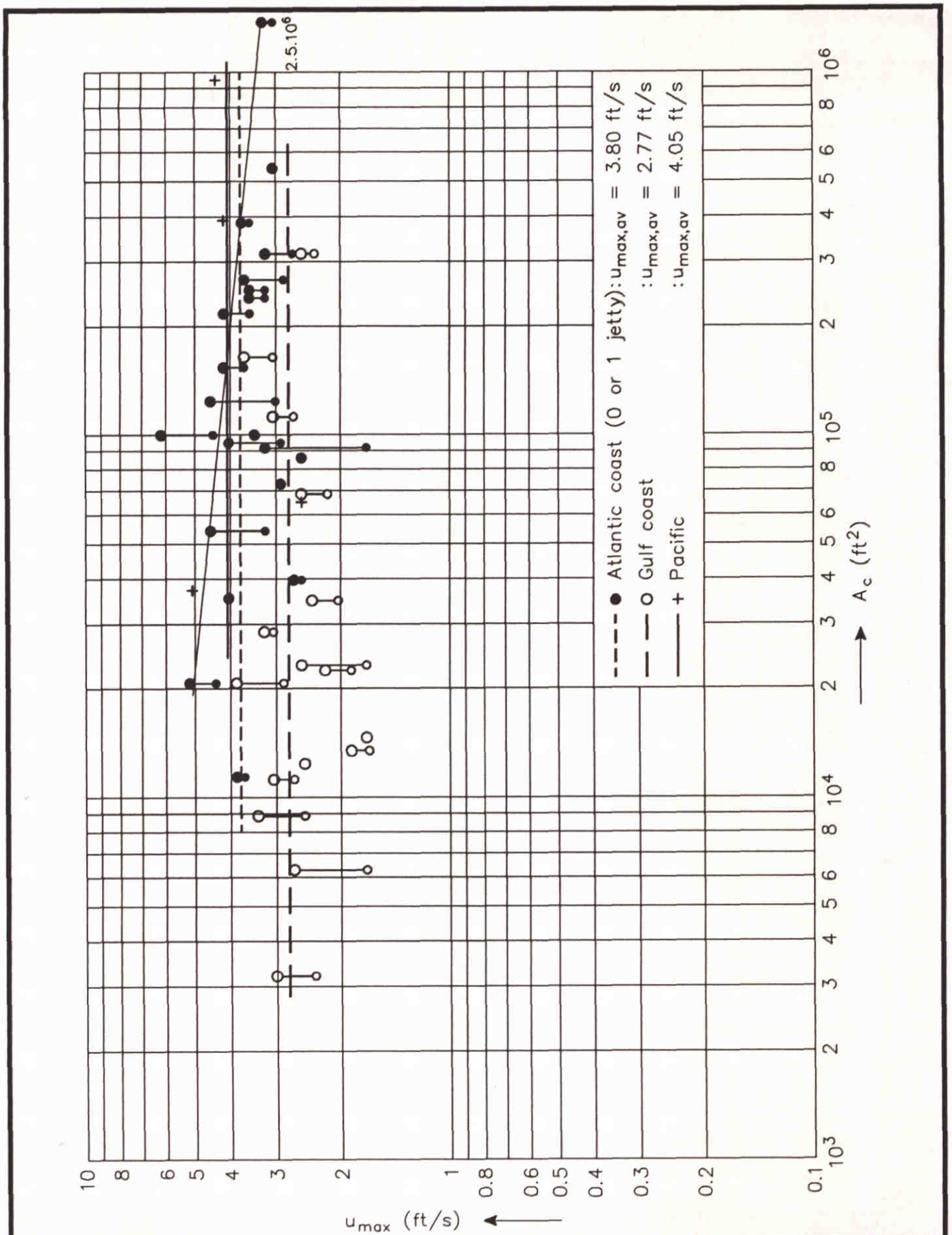

MAXIMUM FLOW VELOCITIES VERSUS TIDAL INLET PROFILES ACCORDING TO DATA OF JARRET (1976)

DELFT HYDRAULICS | H 1300 | FIG. 3.54

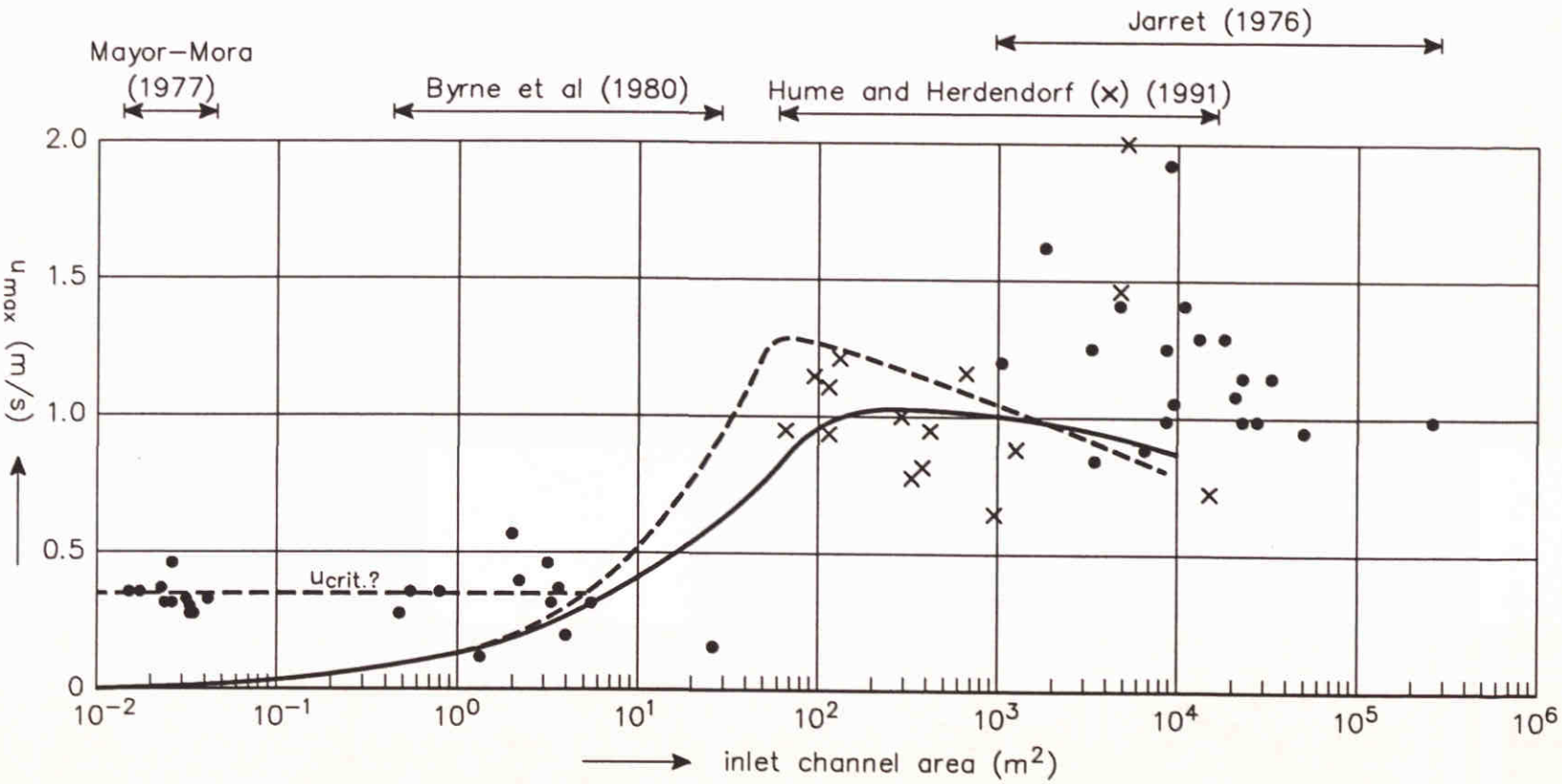

springtide conditions

OBSERVED MAXIMUM FLOW VELOCITIES VERSUS THROAT CROSS-SECTIONAL AREA; DATA FROM DIFFERENT AUTHORS

DELFT HYDRAULICS

H 1300

FIG. 3.55

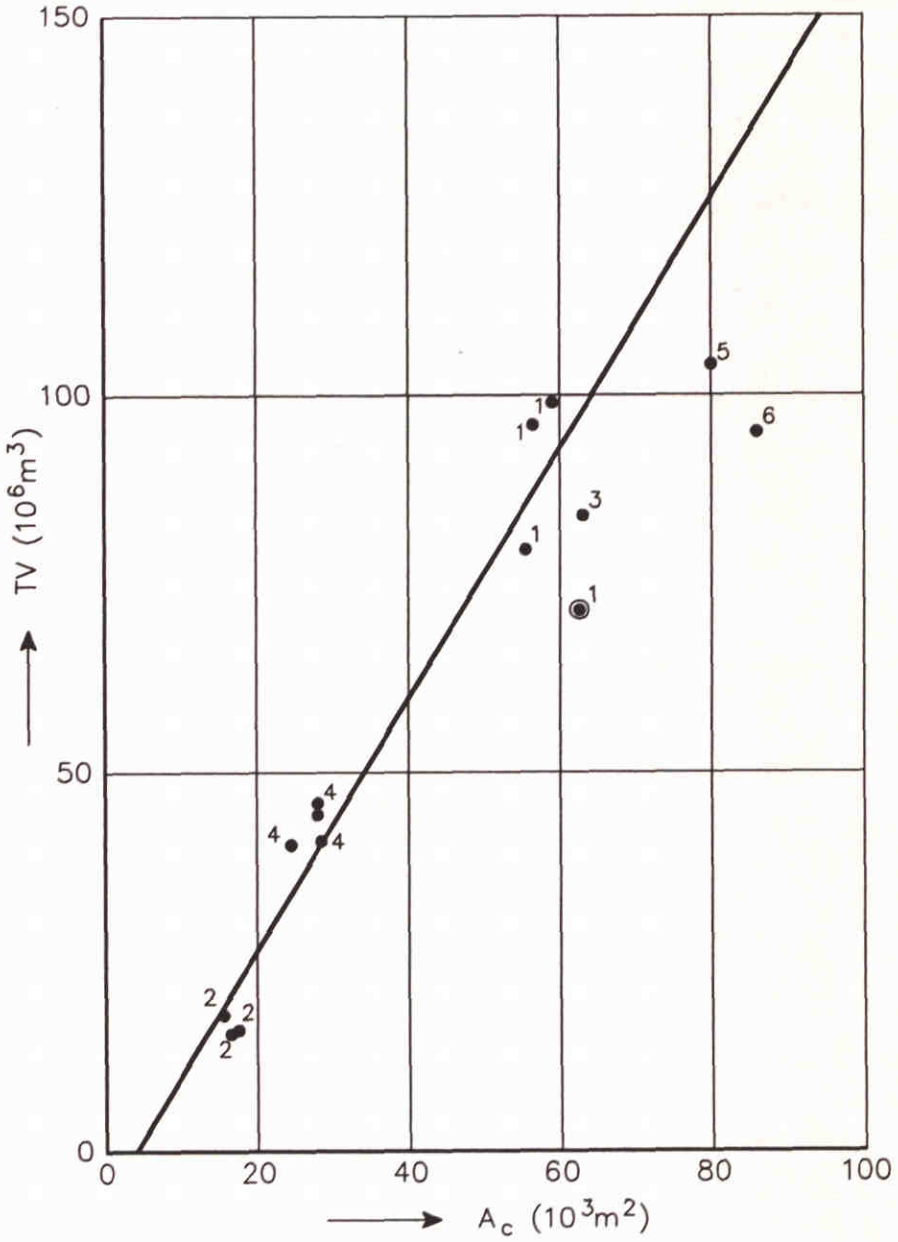

1 to 4 : inlet cross-sections of Marsdiep to Borndiep

5 and 6 : cross-sections in outer deltas of Marsdiep and Vlie resp.

◉1 : inlet of Marsdiep before closure of Zuiderzee

CORRELATION OF A_c WITH TV BY GERRITSEN AND JONG, 1985		
DELFT HYDRAULICS	H 1300	FIG. 3.56

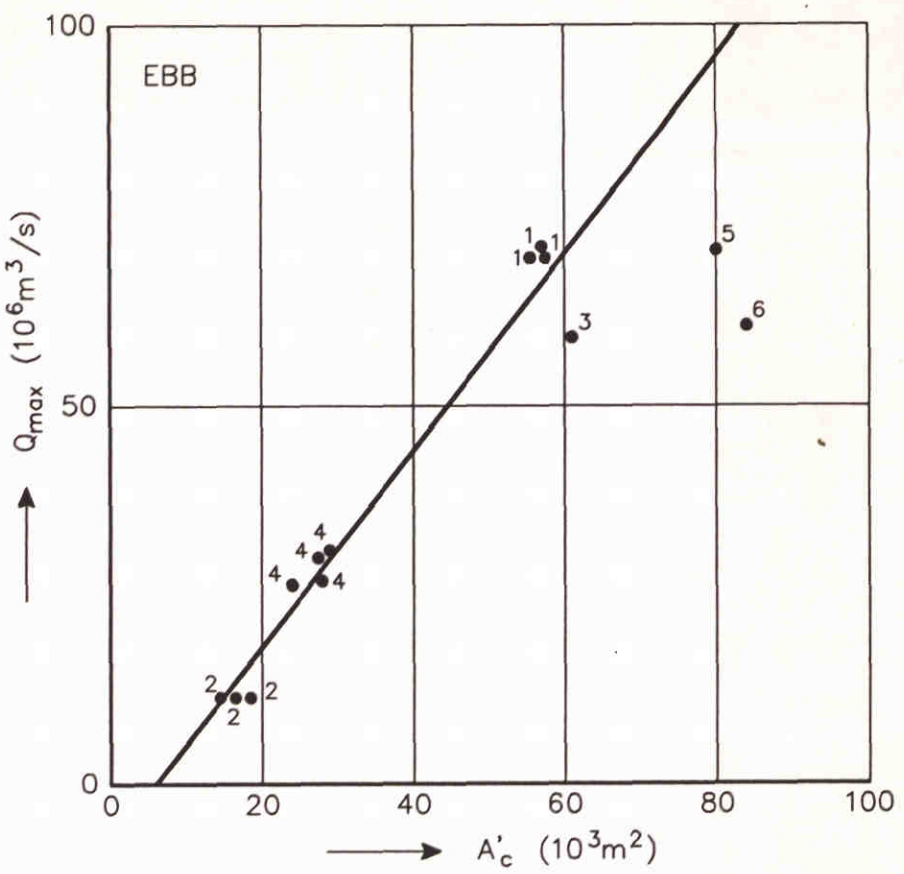

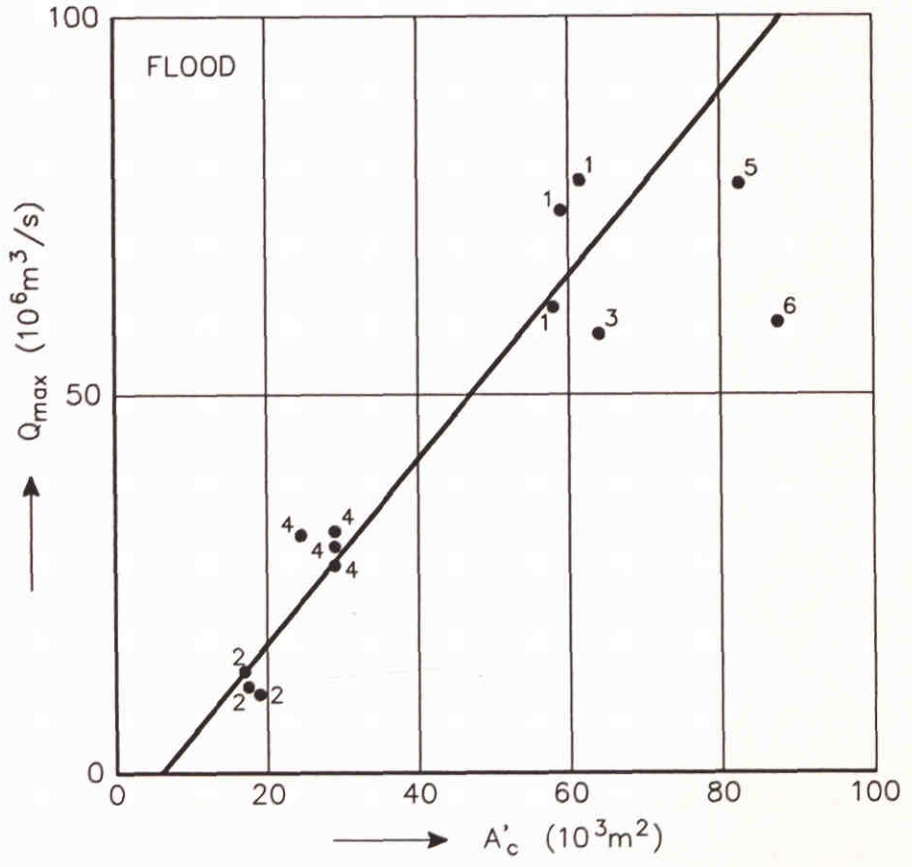

CORRELATION A'_c WITH Q_{max} BY GERRITSEN AND JONG, 1985

DELFT HYDRAULICS | H 1300 | FIG. 3.57

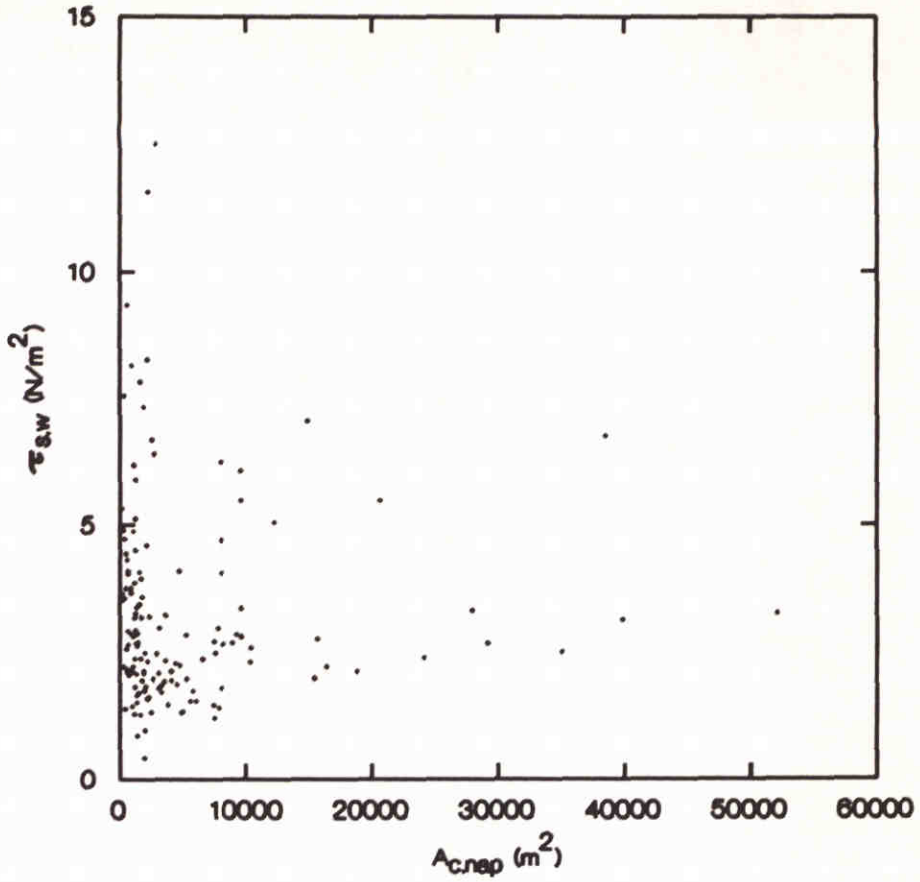

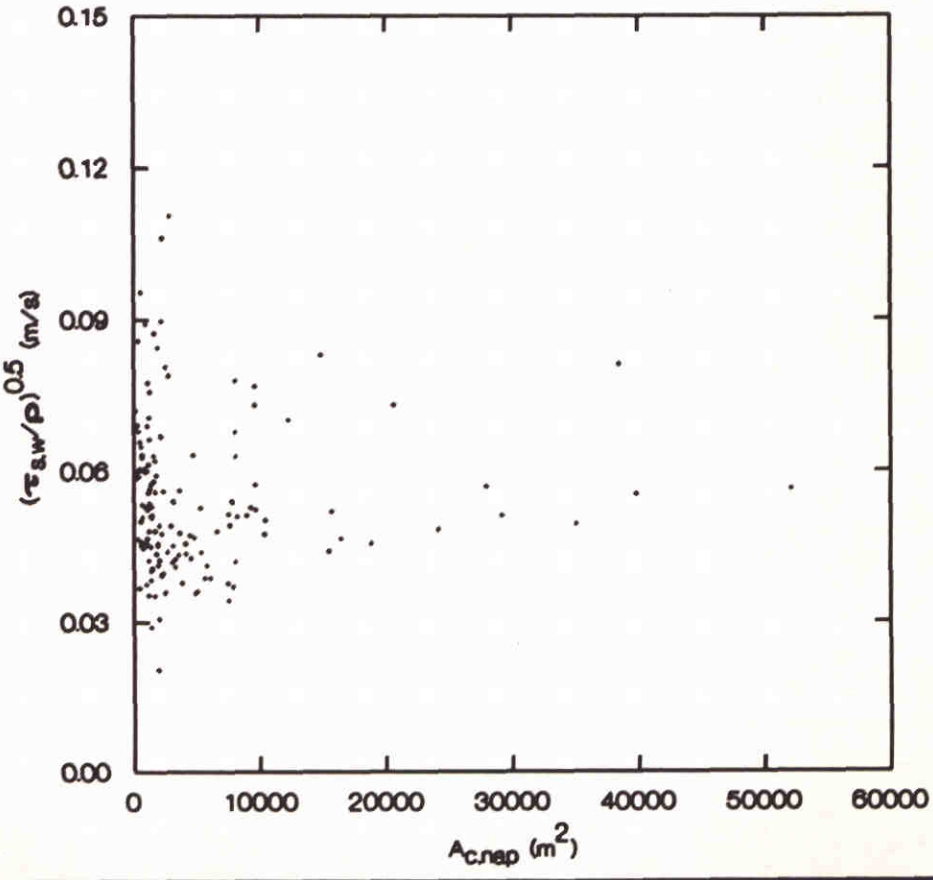

STABILITY SHEAR STRESS VALUES
FOR MEAN TIDAL CONDITIONS
WITH WAVE EFFECT

DELFT HYDRAULICS | H 1300 | FIG. 3.58

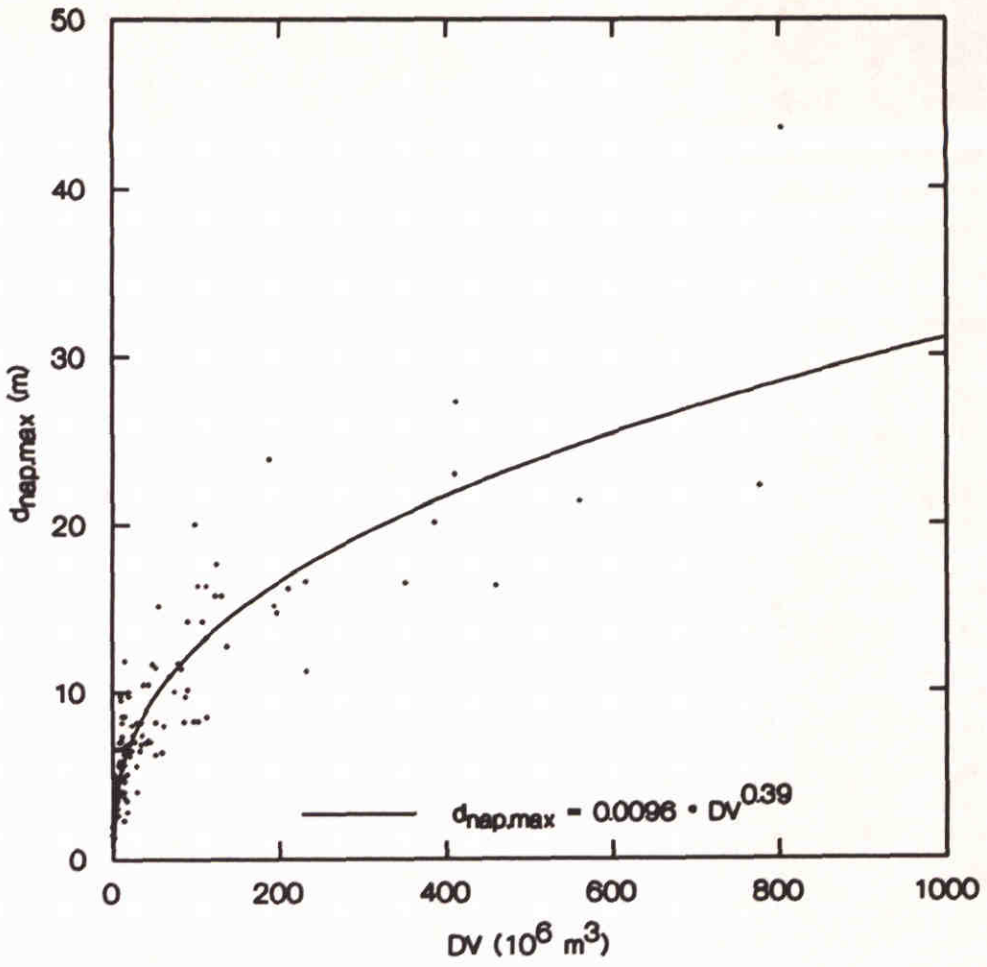

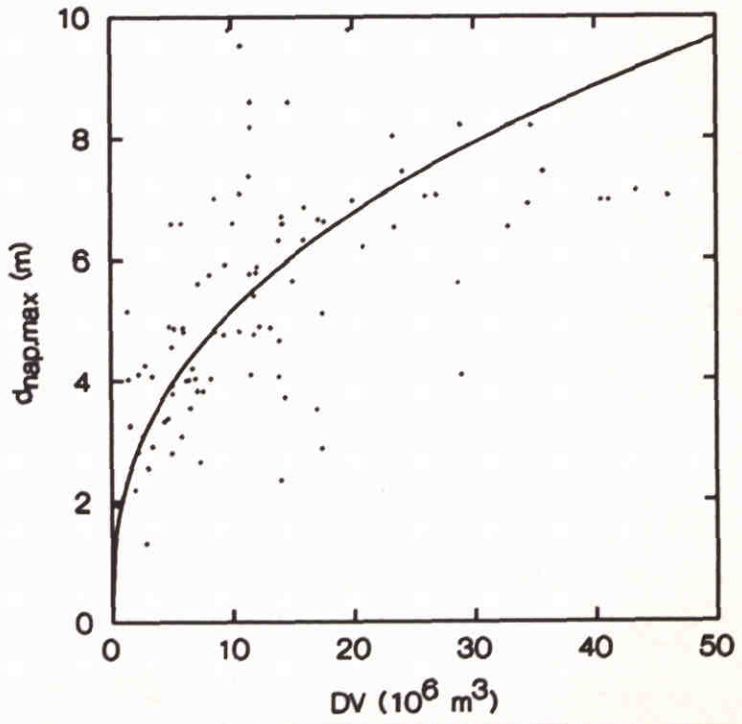

CORRELATION OF $d_{nap,max}$ WITH DV

DELFT HYDRAULICS | H 1300 | FIG. 4.1

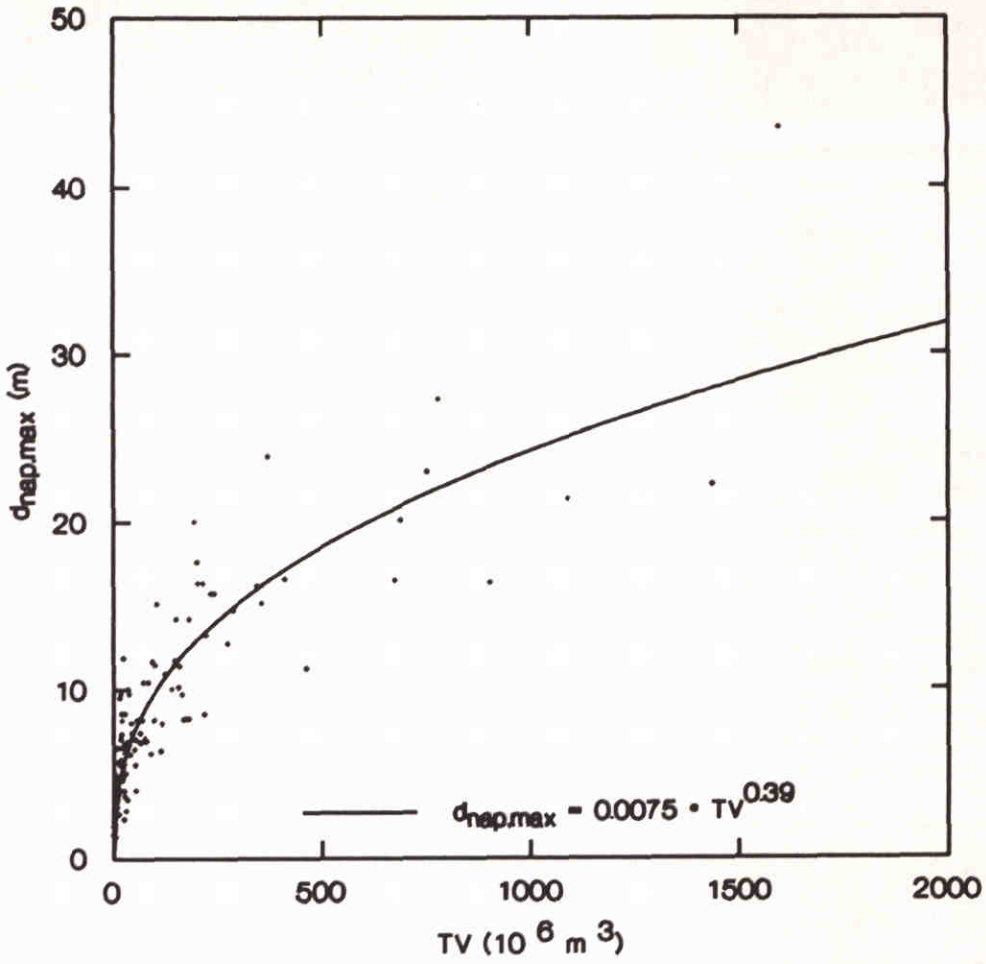

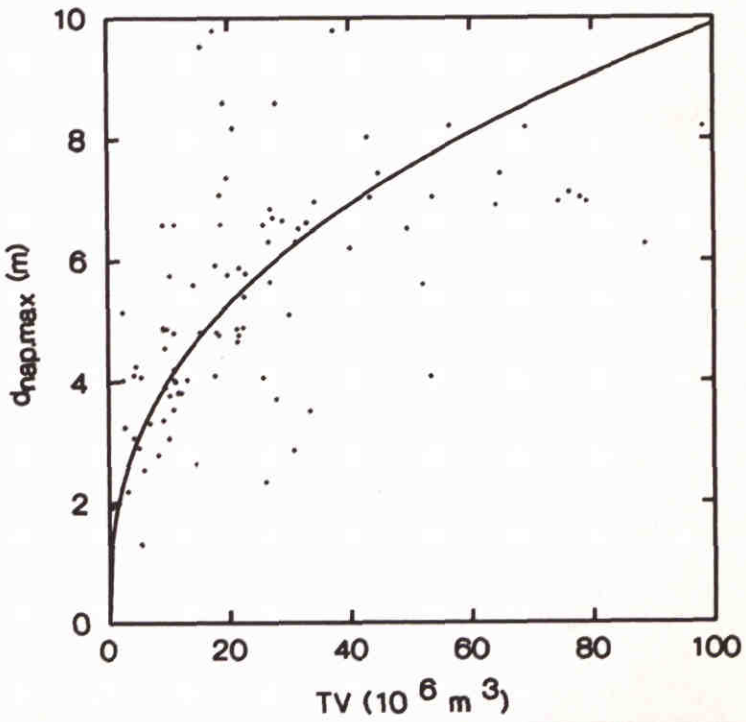

CORRELATION OF $d_{nap.max}$ WITH TV

DELFT HYDRAULICS | H 1300 | FIG. 4.2

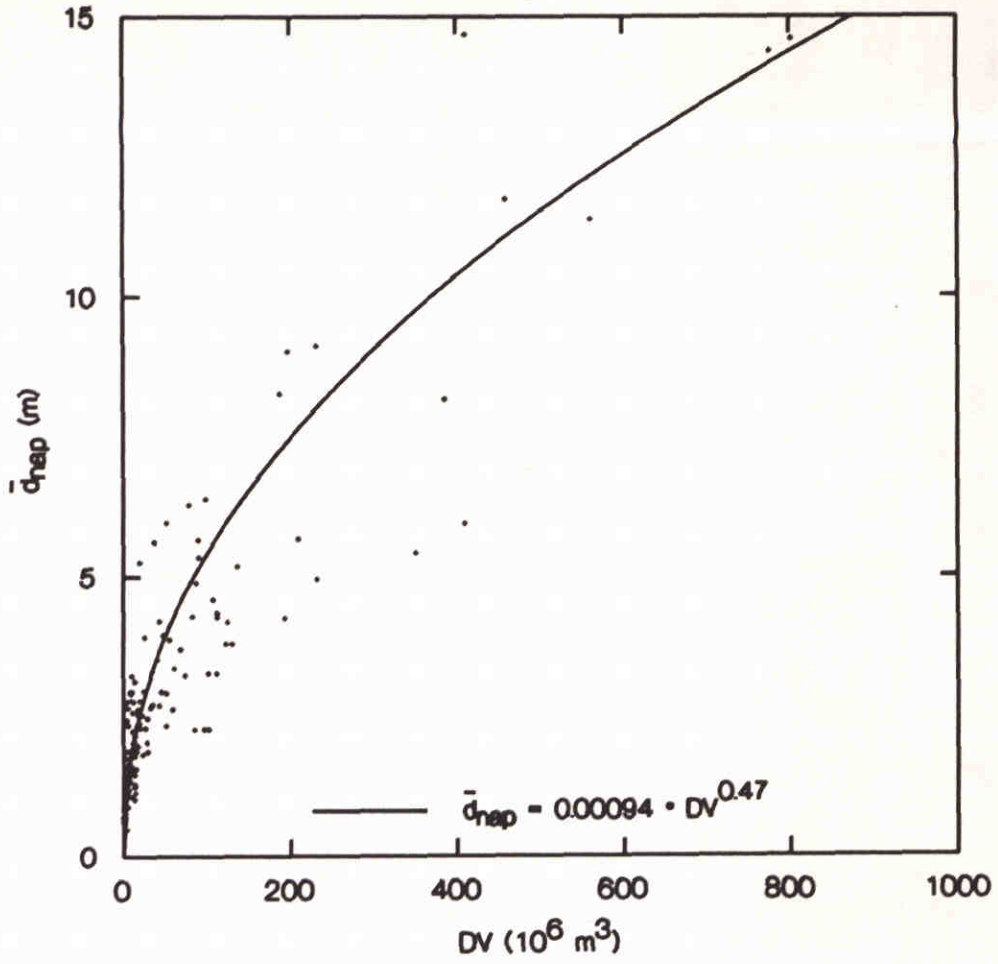

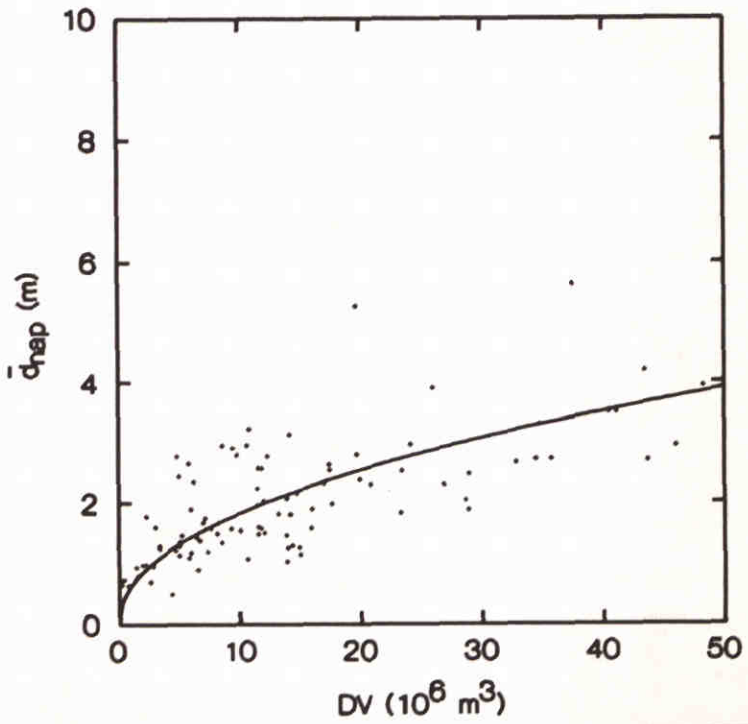

CORRELATION OF $\bar{d}_{nap}$ WITH DV

DELFT HYDRAULICS | H 1300 | FIG. 4.3

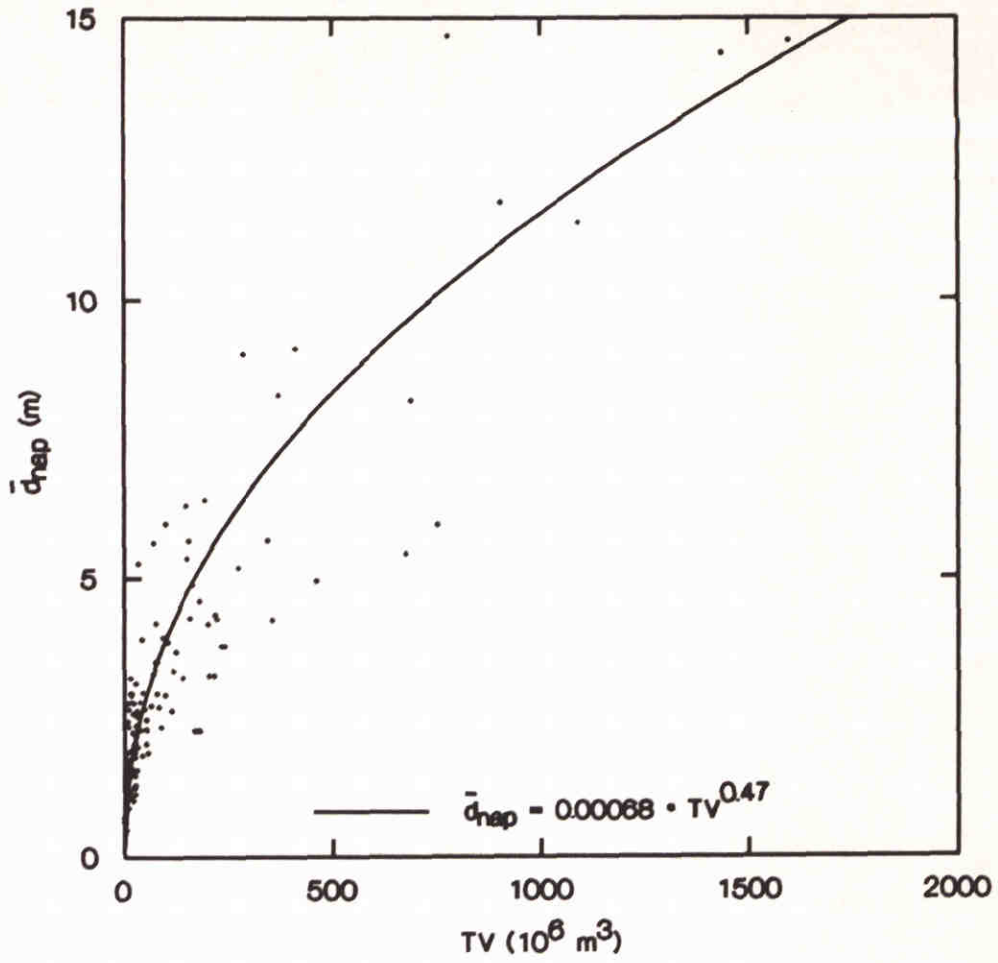

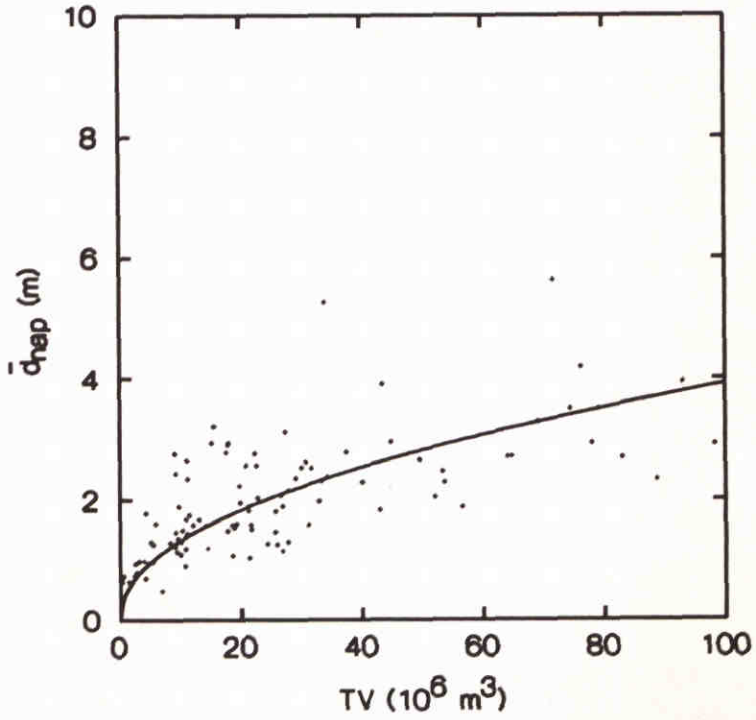

CORRELATION OF $\bar{d}_{nap}$ WITH TV

DELFT HYDRAULICS | H 1300 | FIG. 4.4

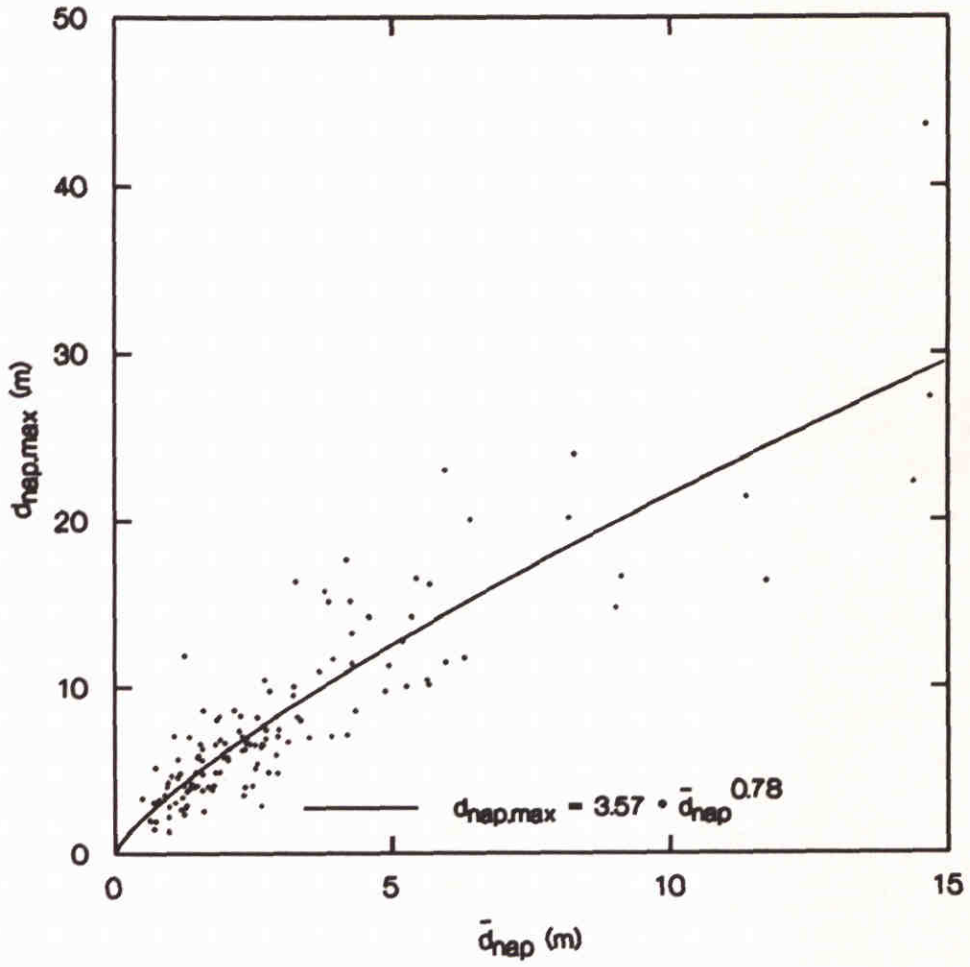

CORRELATION OF $\bar{d}_{nap}$ WITH $d_{nap,max}$

DELFT HYDRAULICS | H 1300 | FIG. 4.5

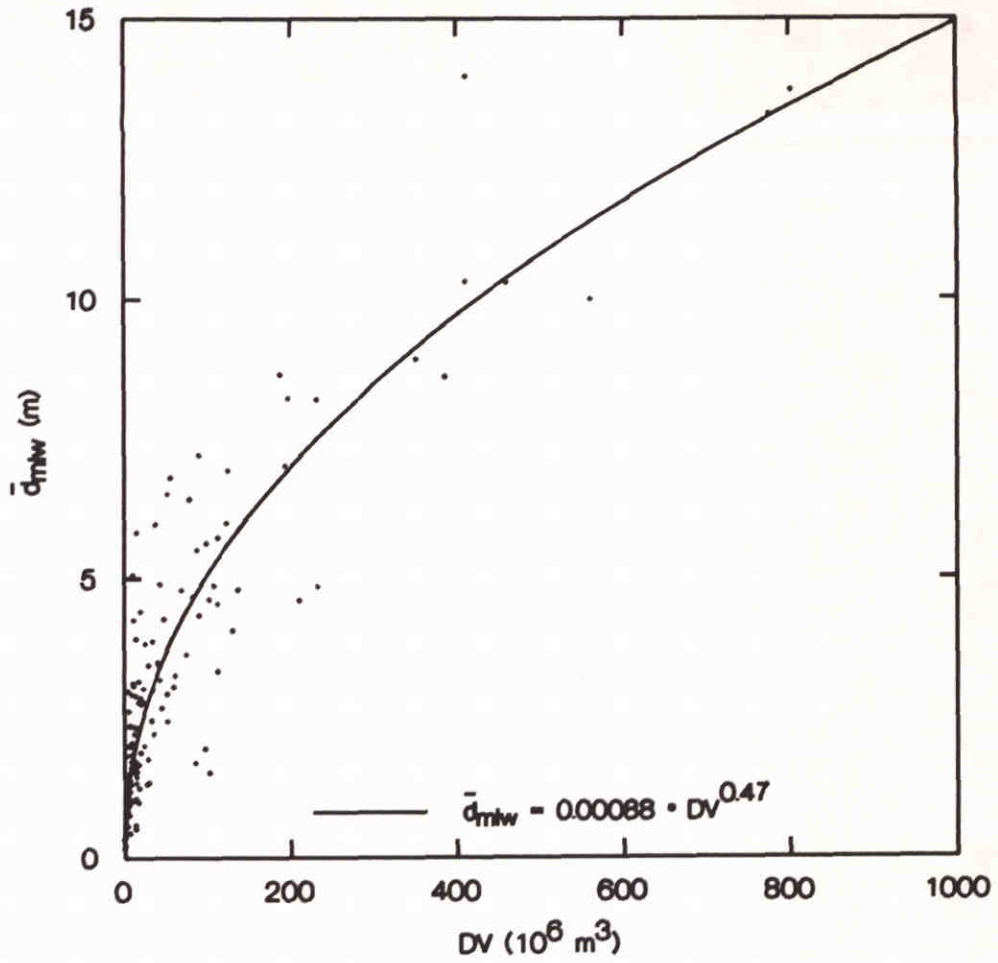

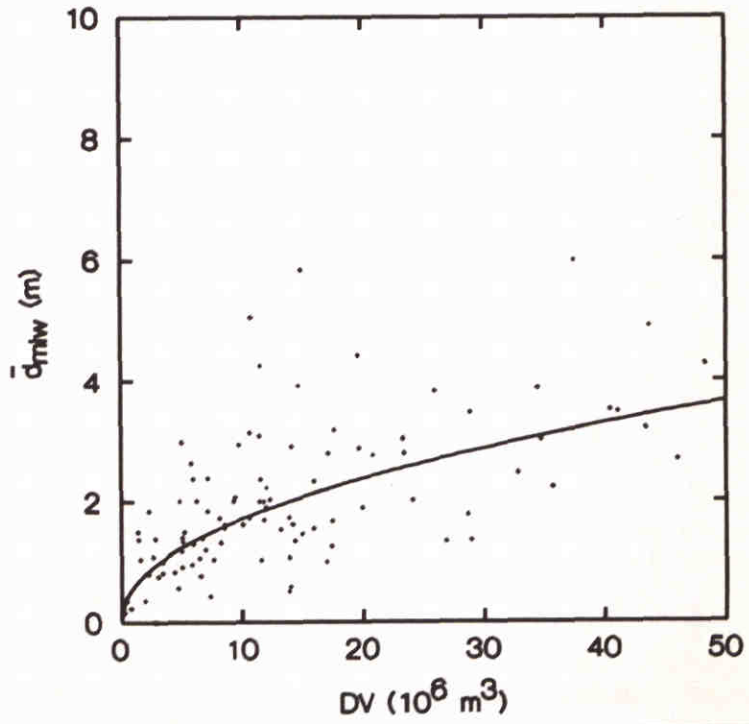

CORRELATION OF $\bar{d}_{mlw}$ WITH DV

DELFT HYDRAULICS | H 1300 | FIG. 4.6

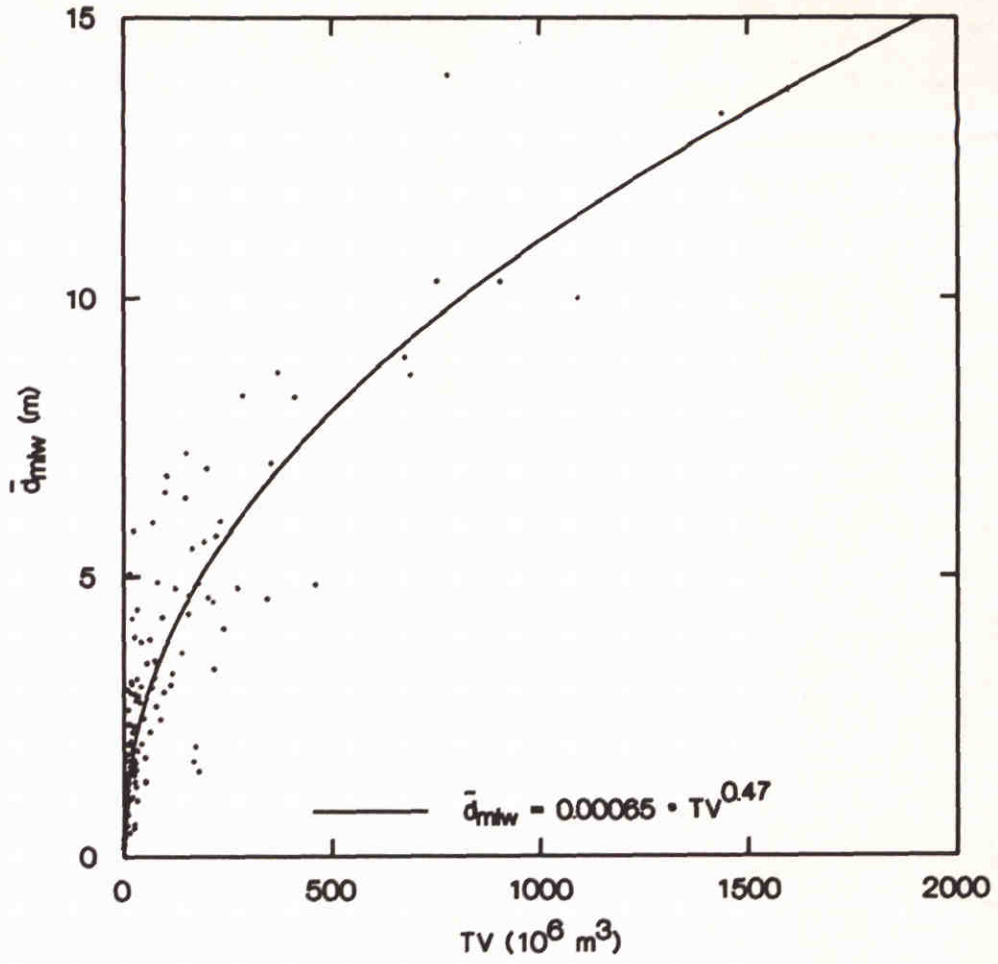

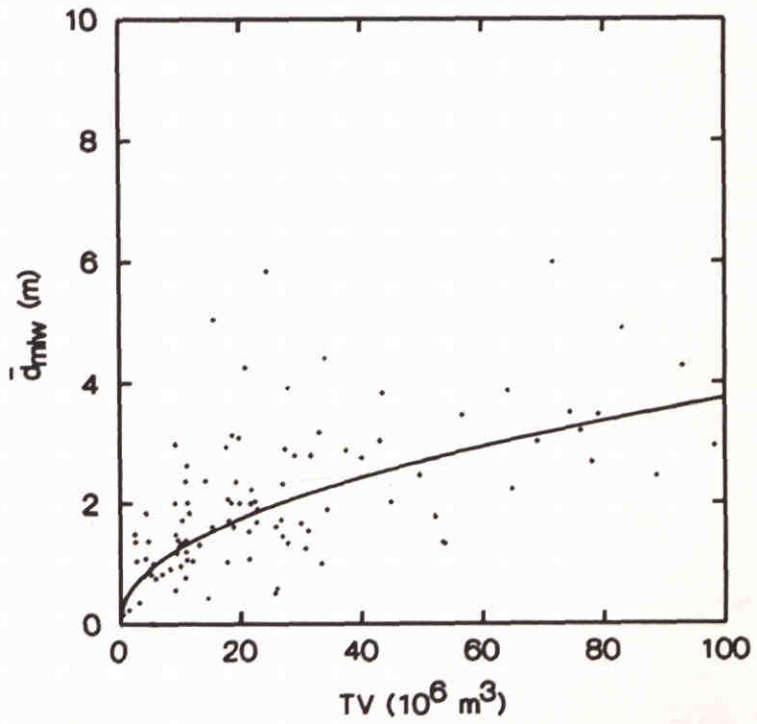

CORRELATION OF $\bar{d}_{mlw}$ WITH TV

DELFT HYDRAULICS | H 1300 | FIG. 4.7

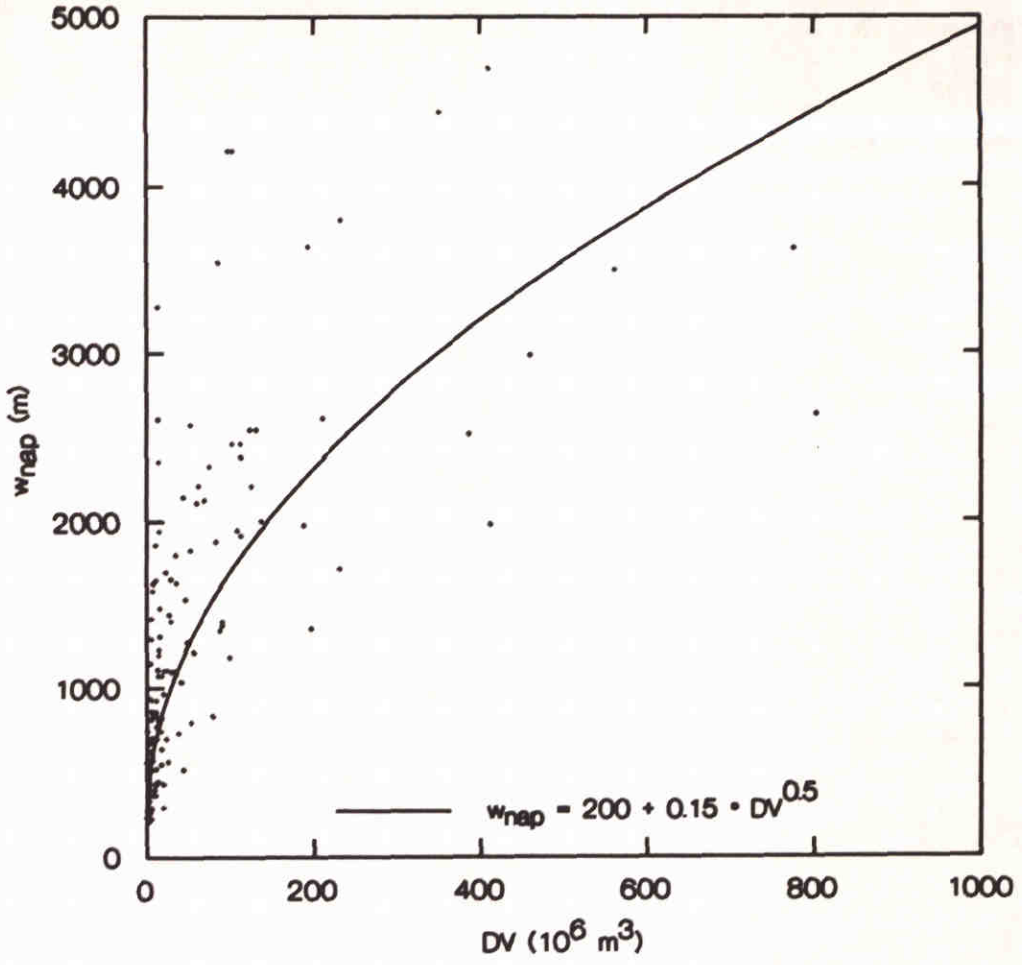

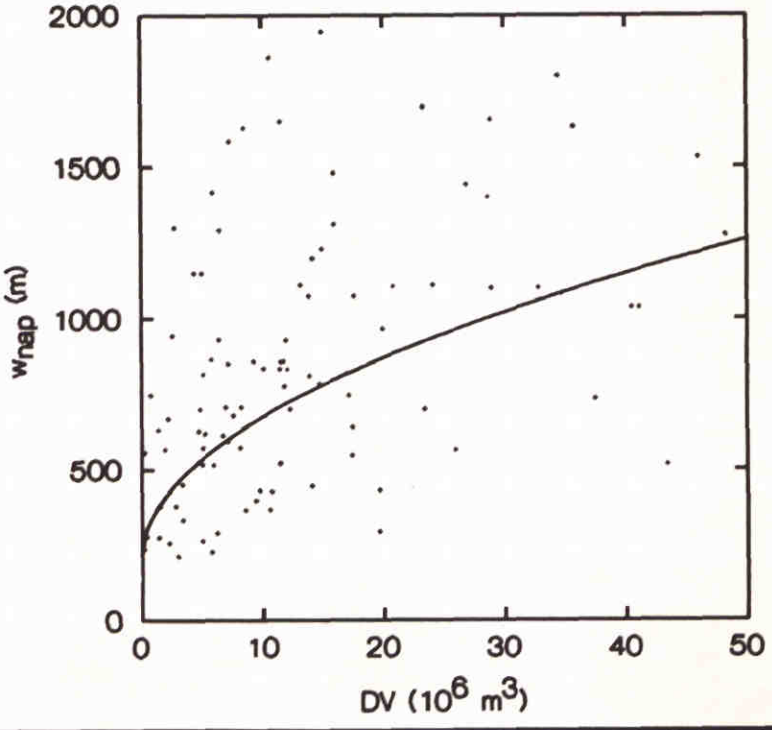

CORRELATION OF w_{nap} WITH DV

DELFT HYDRAULICS | H 1300 | FIG. 4.8

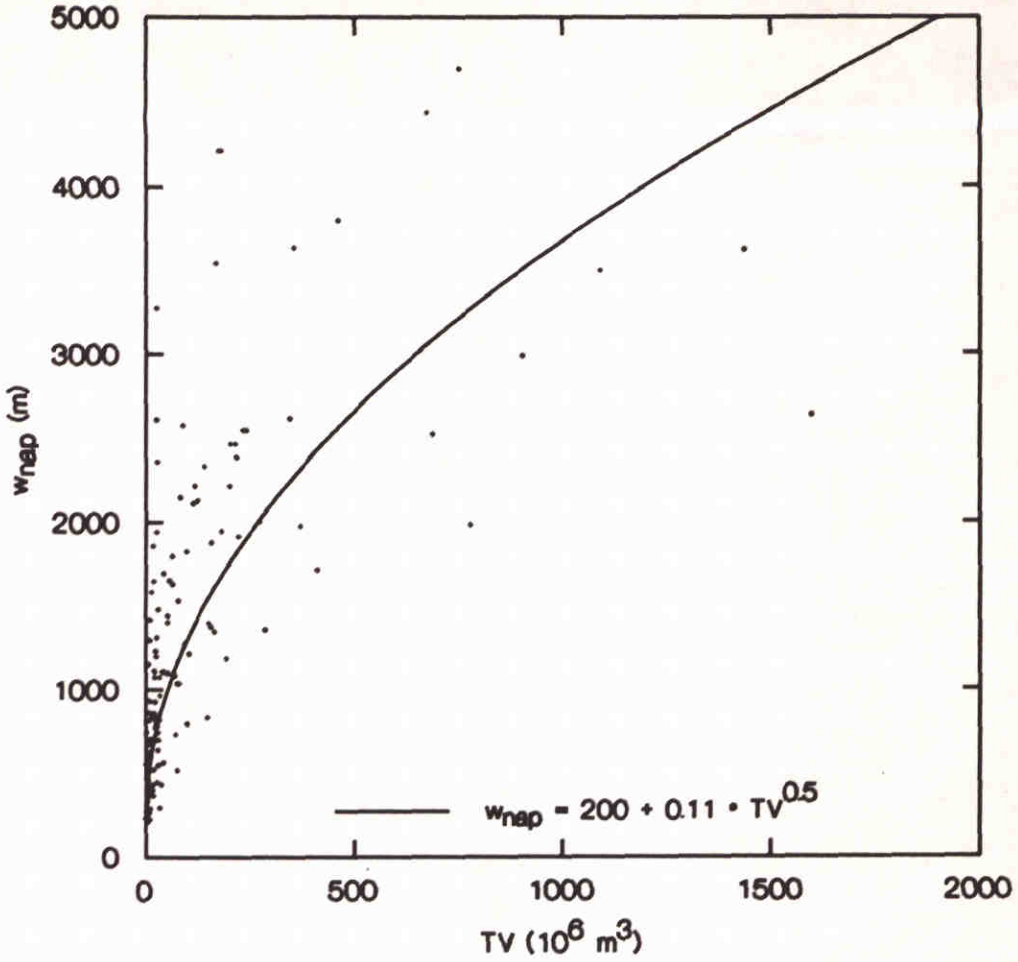

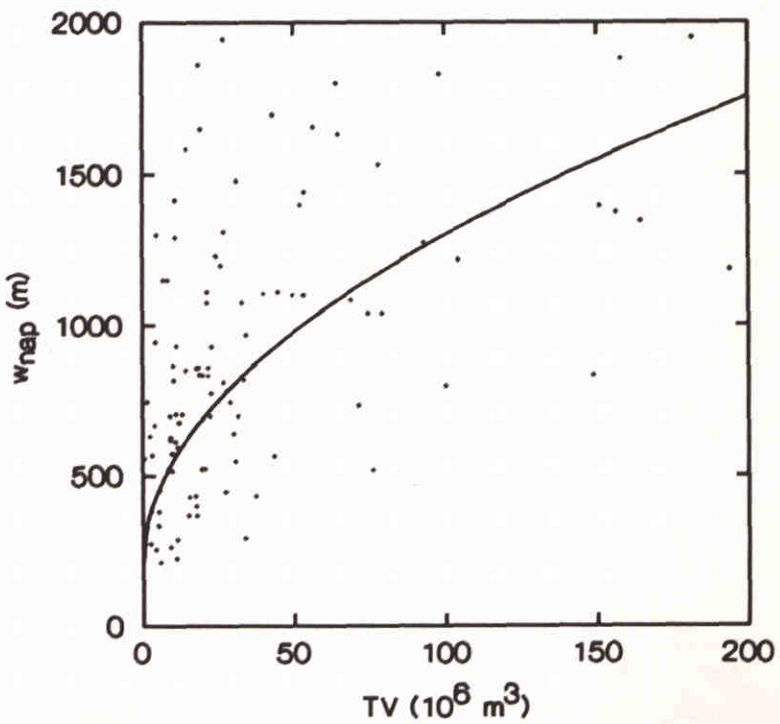

CORRELATION OF w_{nap} WITH TV

DELFT HYDRAULICS | H 1300 | FIG. 4.9

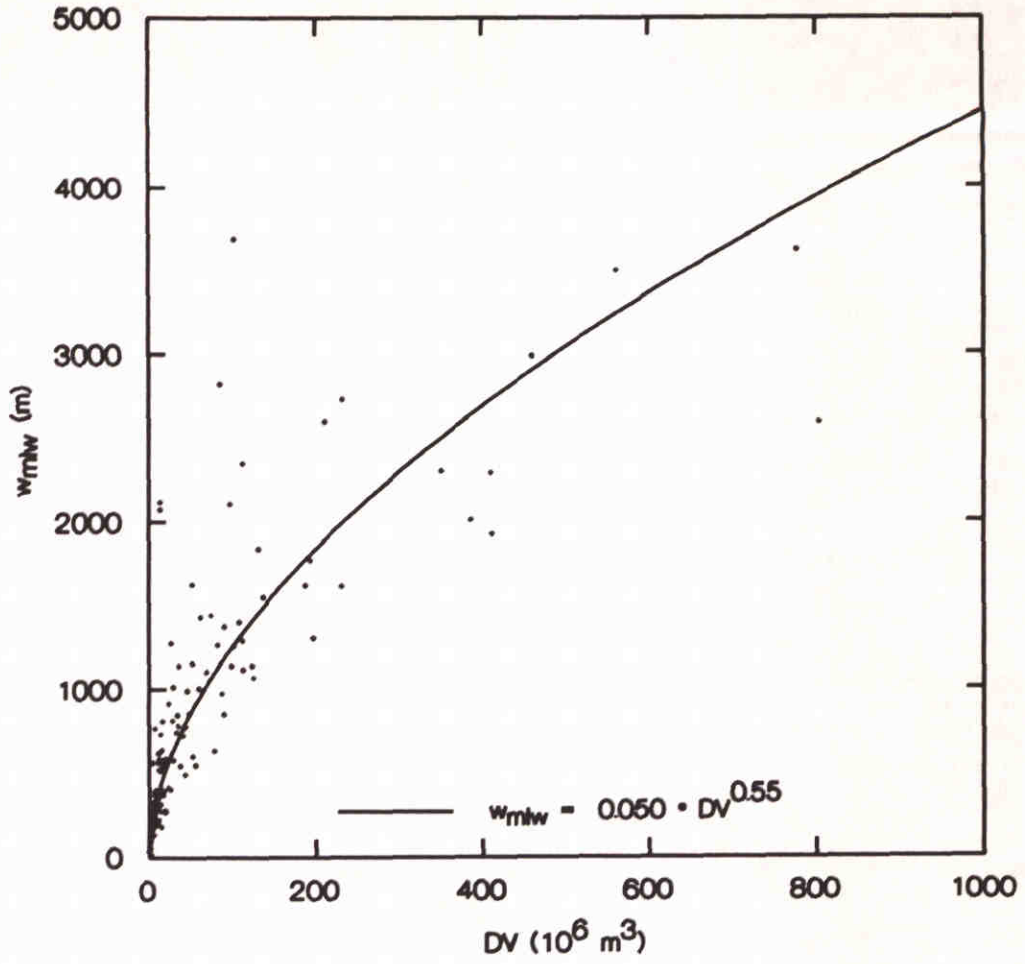

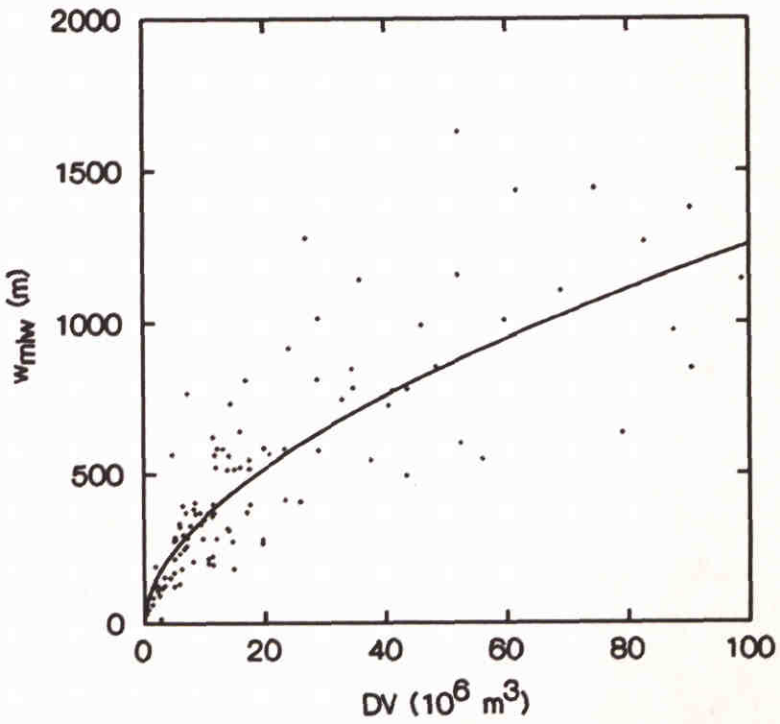

CORRELATION OF w_{mlw} WITH DV

DELFT HYDRAULICS | H 1300 | FIG. 4.10

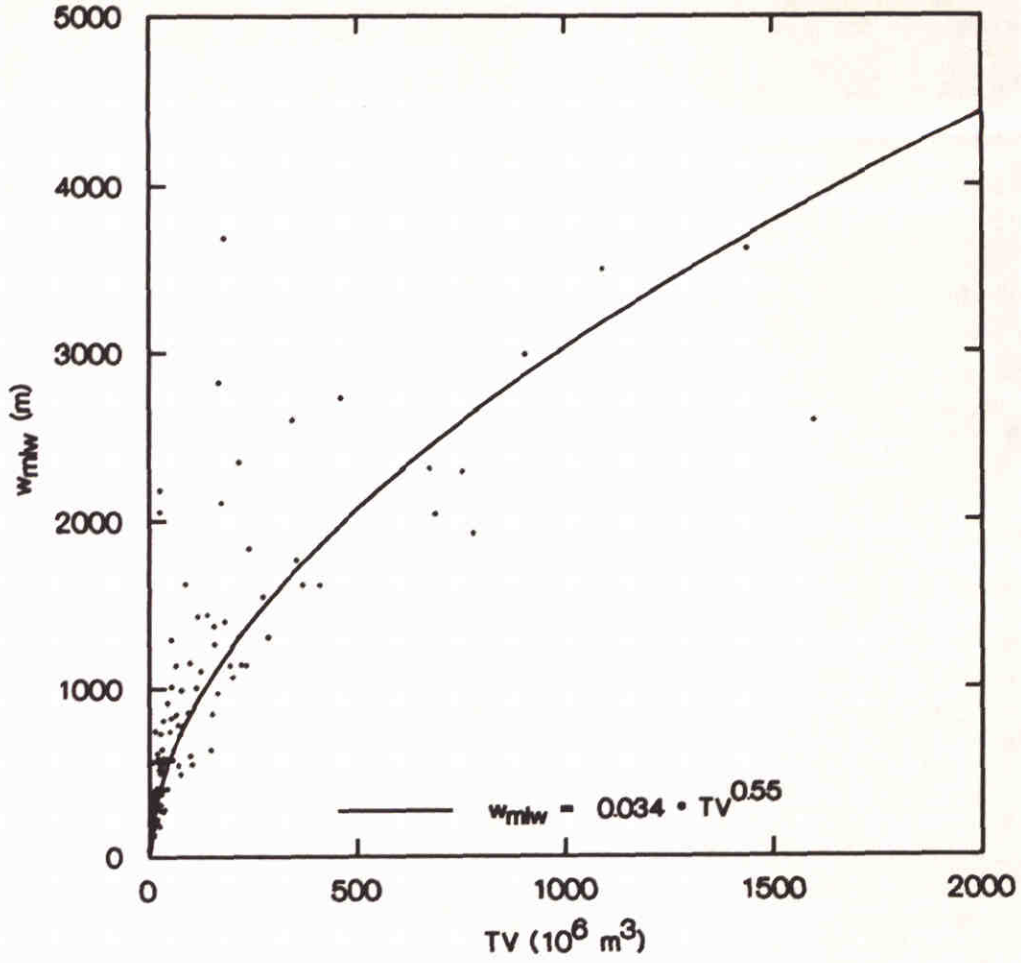

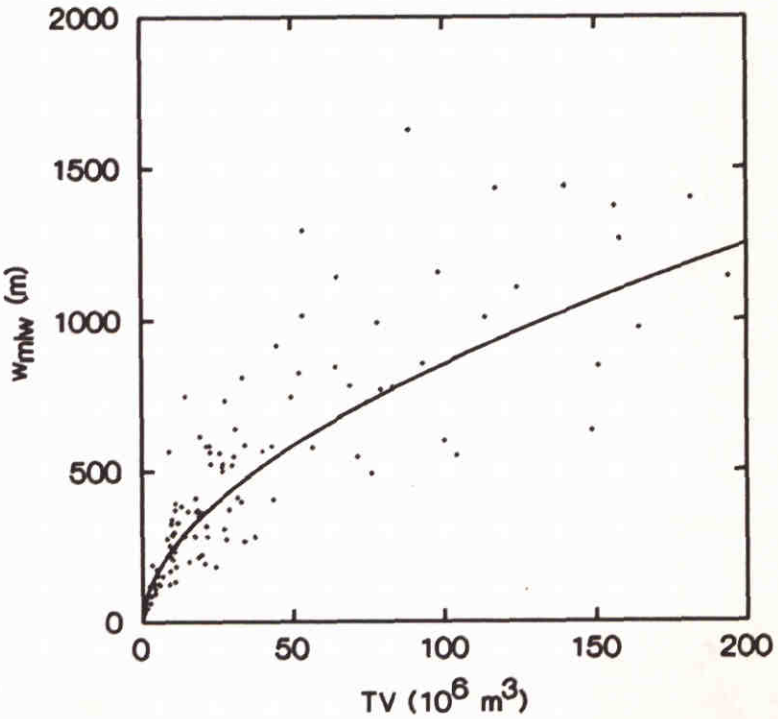

CORRELATION OF w_{mlw} WITH TV

DELFT HYDRAULICS | H 1300 | FIG. 4.11

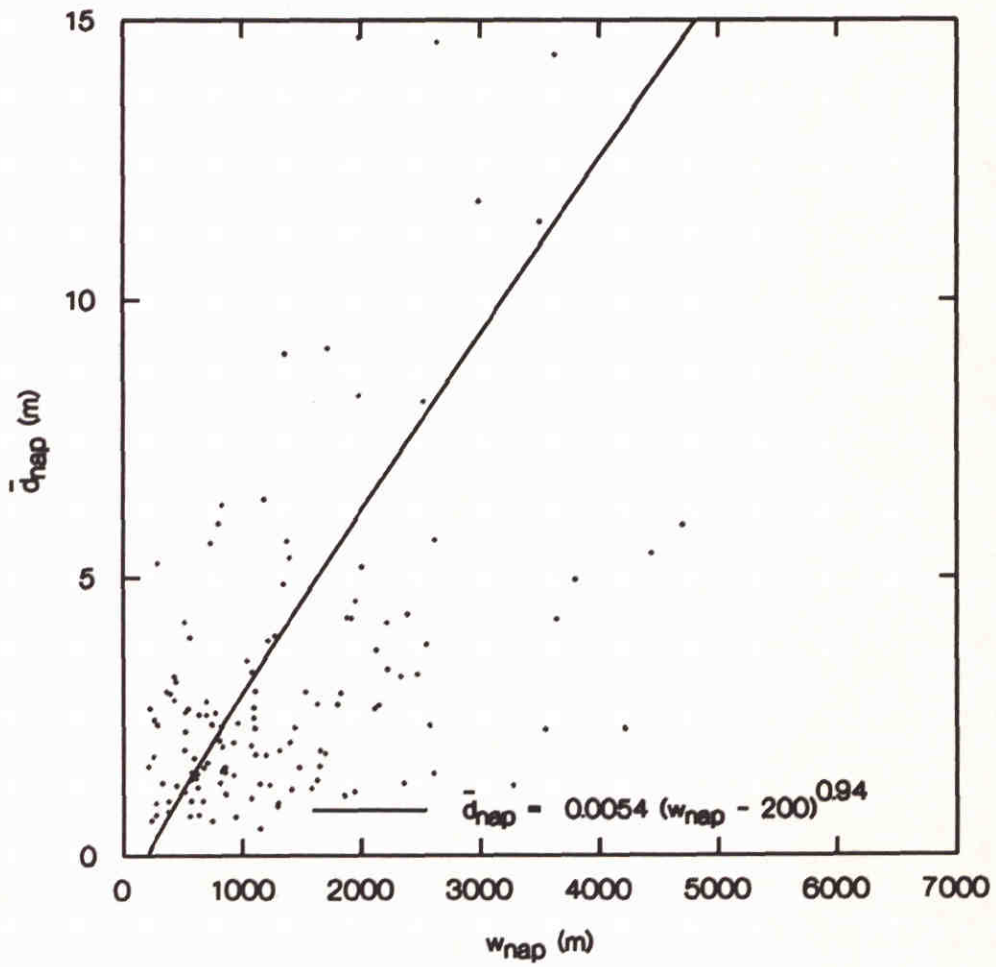

CORRELATION OF w_{nap} WITH $\bar{d}_{nap}$

DELFT HYDRAULICS | H 1300 | FIG. 4.12

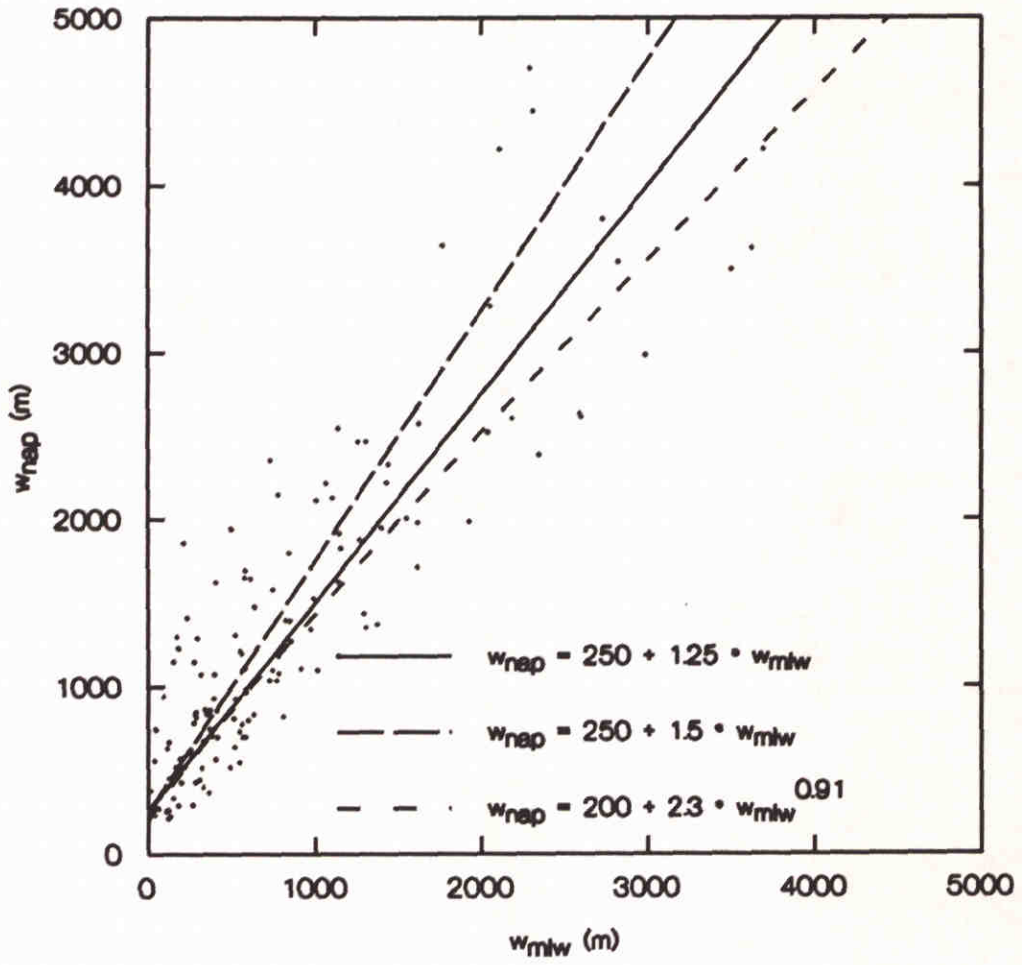

CORRELATION OF w_{nap} WITH w_{mlw}

DELFT HYDRAULICS | H 1300 | FIG. 4.13

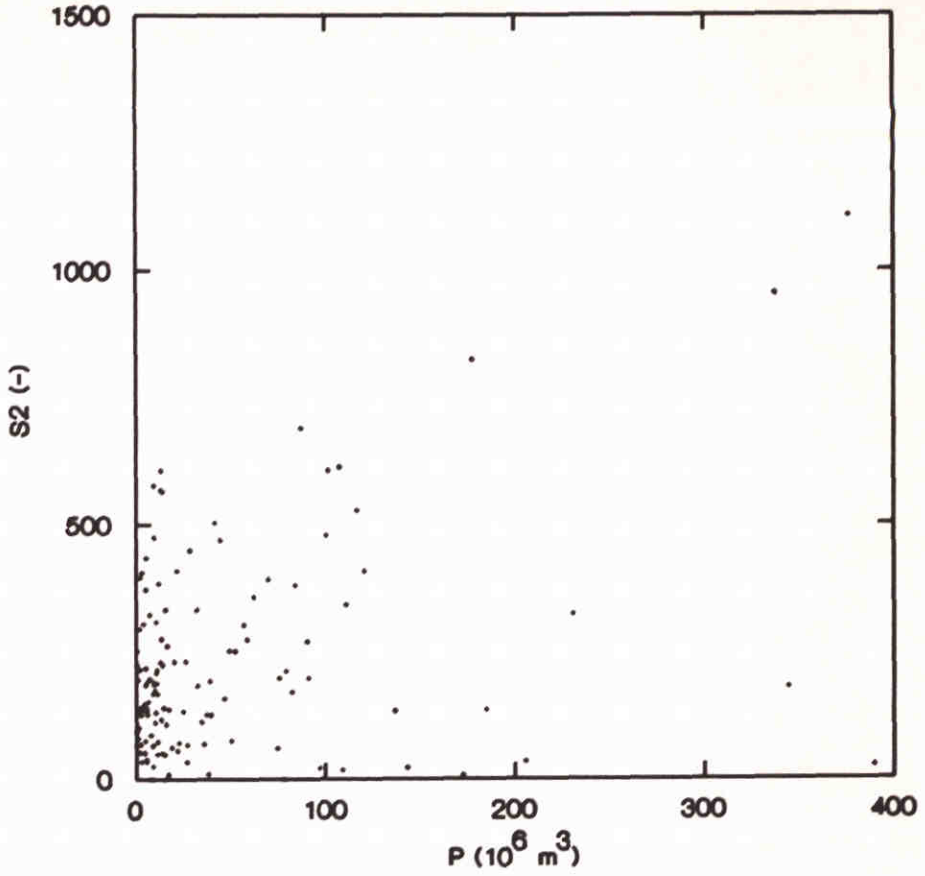

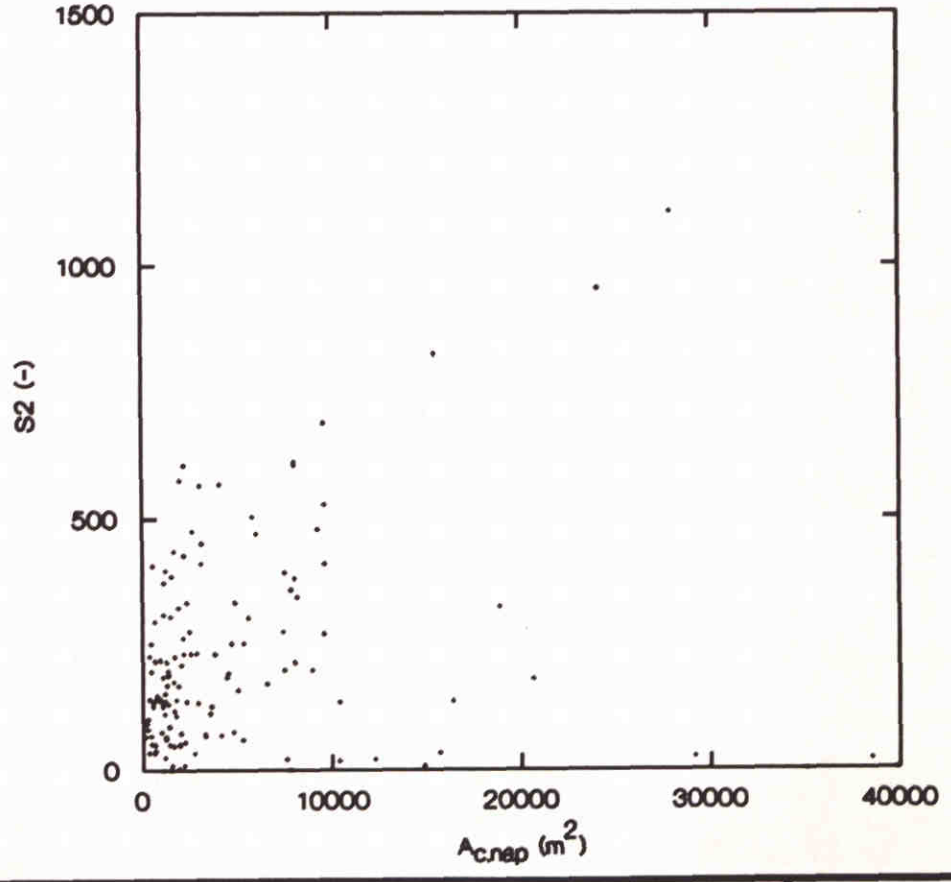

CORRELATION OF P AND $A_{c,nap}$ WITH S2

DELFT HYDRAULICS | H 1300 | FIG. 4.14

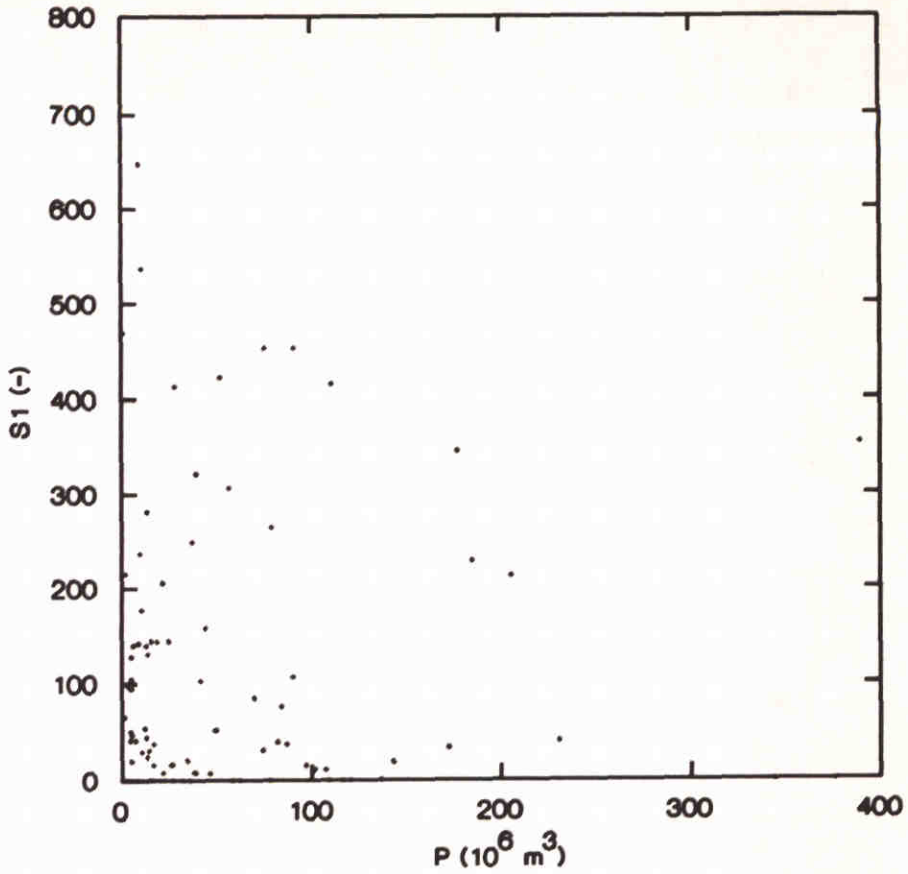

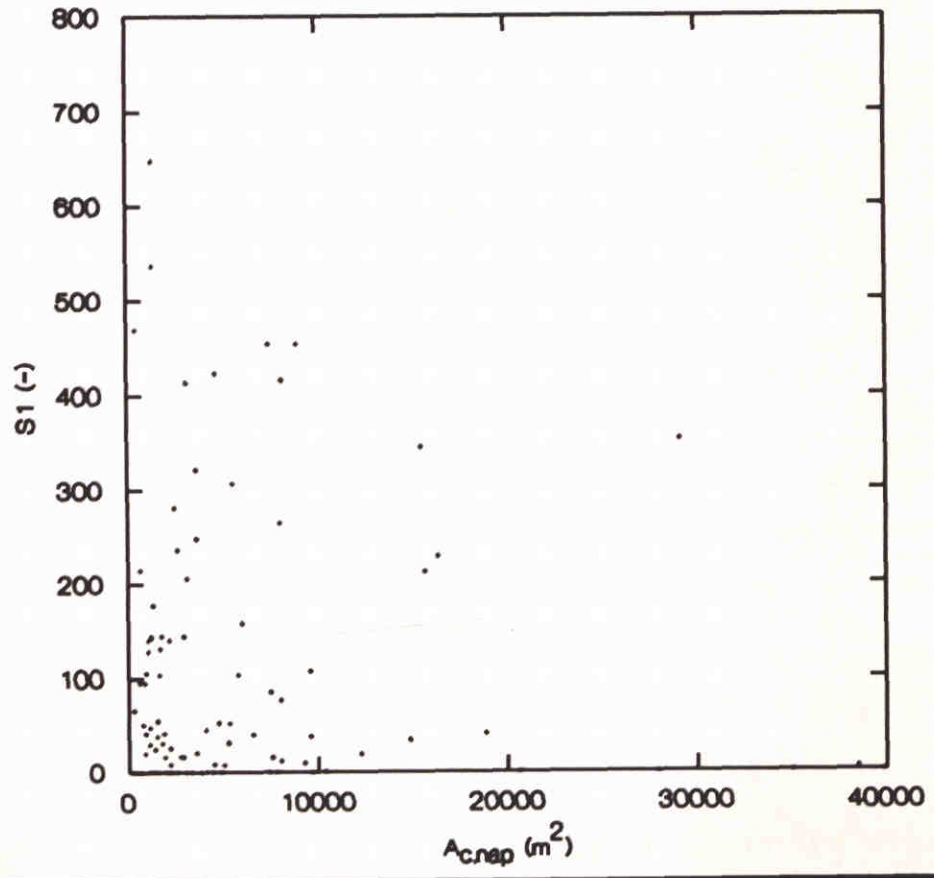

CORRELATION OF P AND $A_{c.nap}$ WITH S1

DELFT HYDRAULICS

H 1300

FIG. 4.15

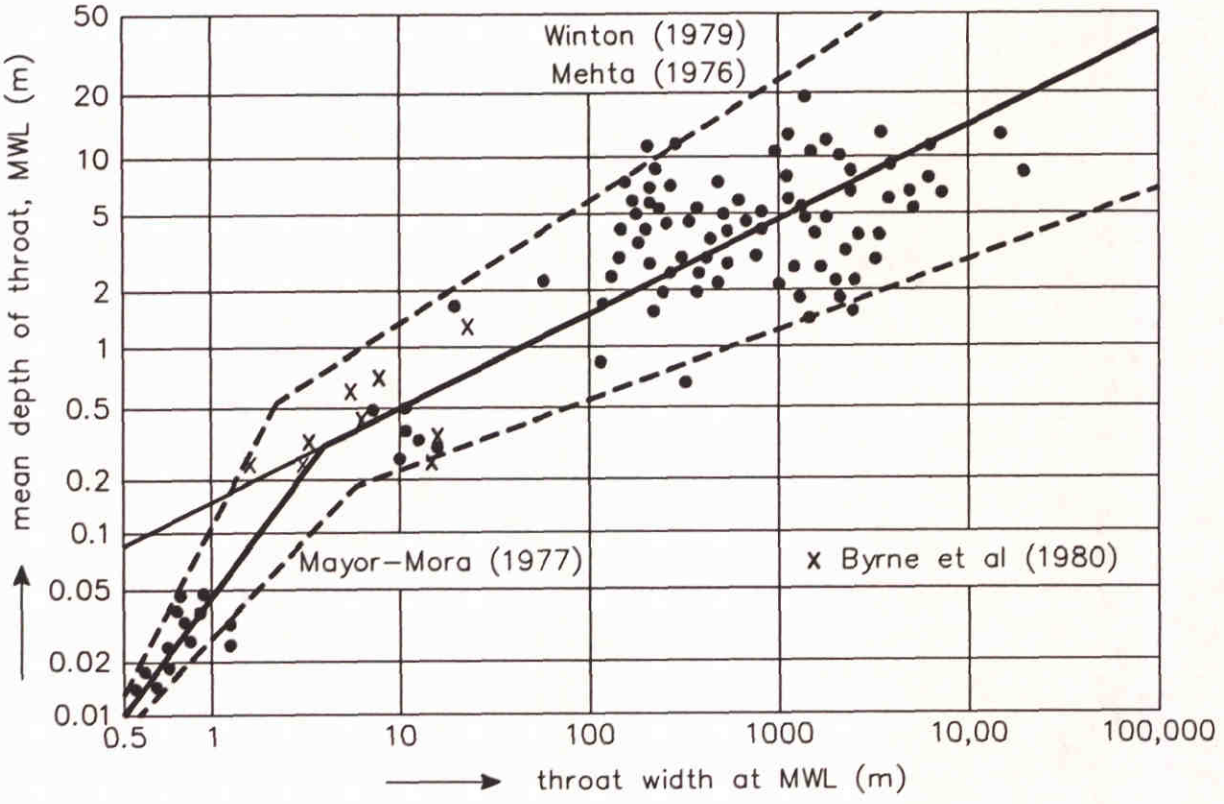

WIDTH–DEPTH RELATIONSHIP FOR SOME NORTH–AMERICAN INLETS WITHOUT JETTIES (BYRNE ET AL, 1980)

DELFT HYDRAULICS | H 1300 | FIG. 4.16

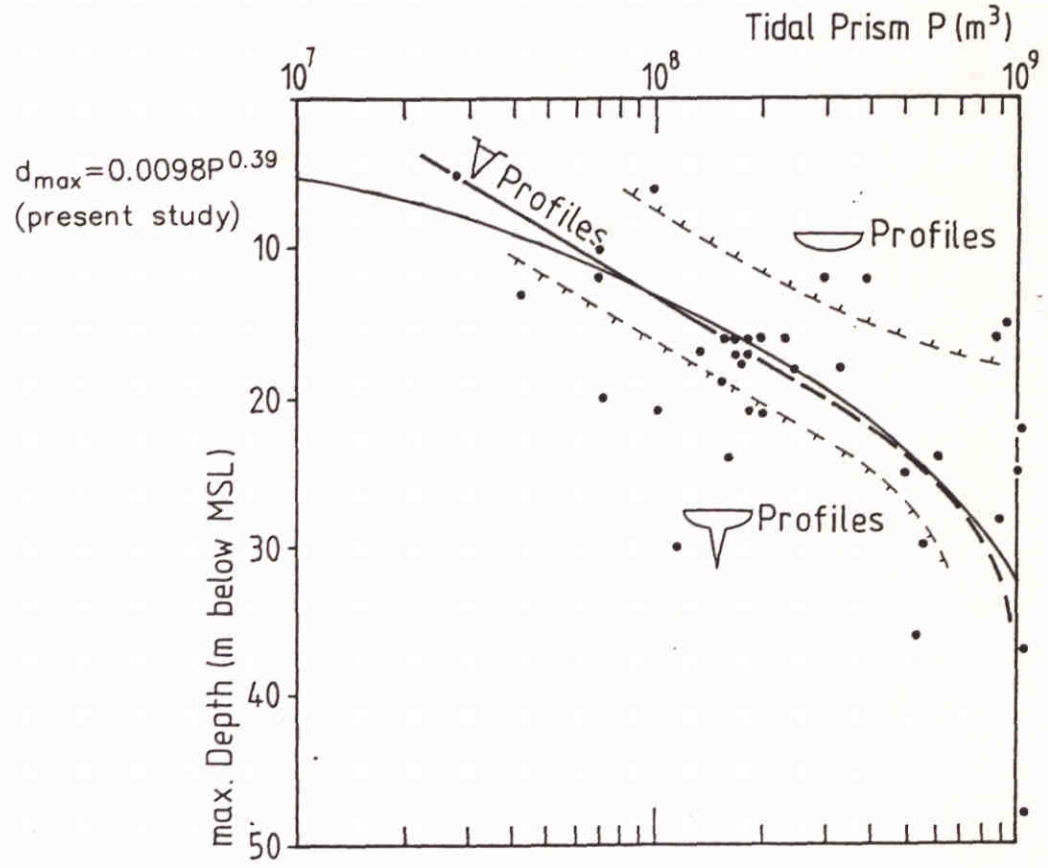

RELATIONSHIP BETWEEN TIDAL PRISM AND MAXIMUM DEPTH OF INLETS IN THE GERMAN BIGHT (DIECKMANN ET AL, 1988)

DELFT HYDRAULICS | H 1300 | FIG. 4.17

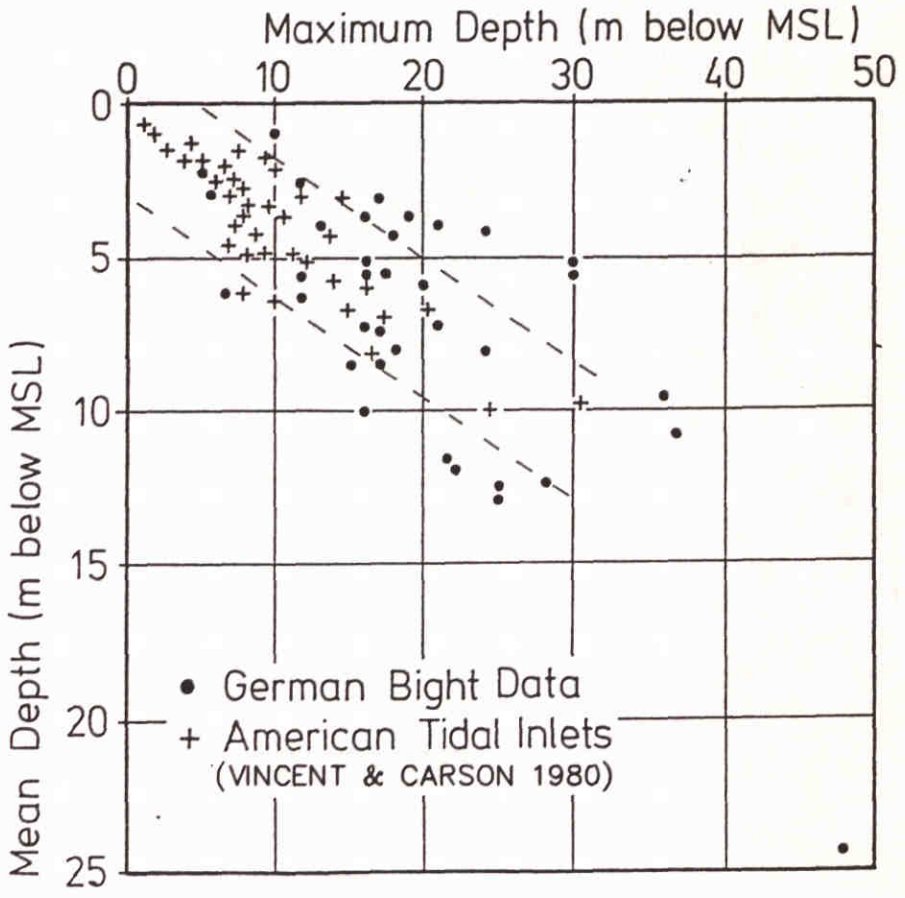

RELATIONSHIP BETWEEN MEAN AND MAXIMUM DEPTH IN AN INLET CROSS-SECTION (DIECKMANN ET AL, 1988)

DELFT HYDRAULICS | H 1300 | FIG. 4.18

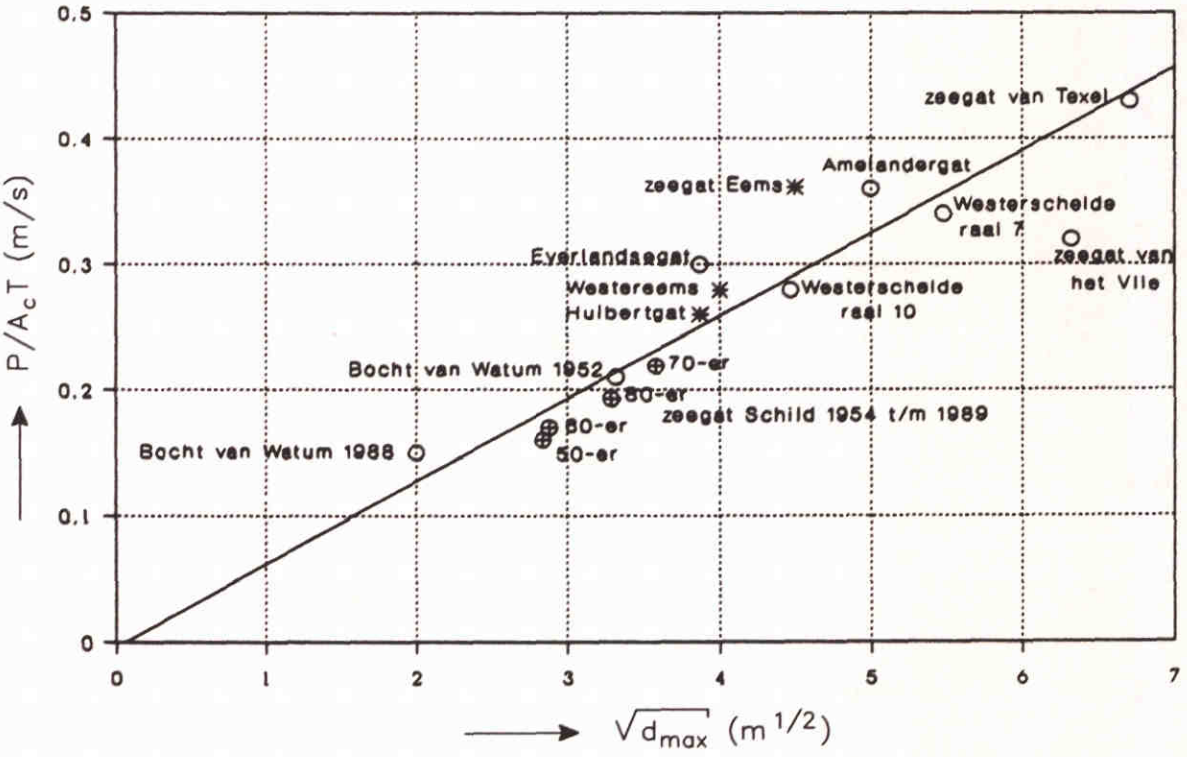

from: Duits–Nederlandse Eems–Dollardcommissie, 1989

TIDAL VELOCITY VERSUS SQUARE ROOT OF MAXIMUM DEPTH OF VARIOUS TIDAL INLETS AND CHANNELS		
DELFT HYDRAULICS	H 1300	FIG. 4.19

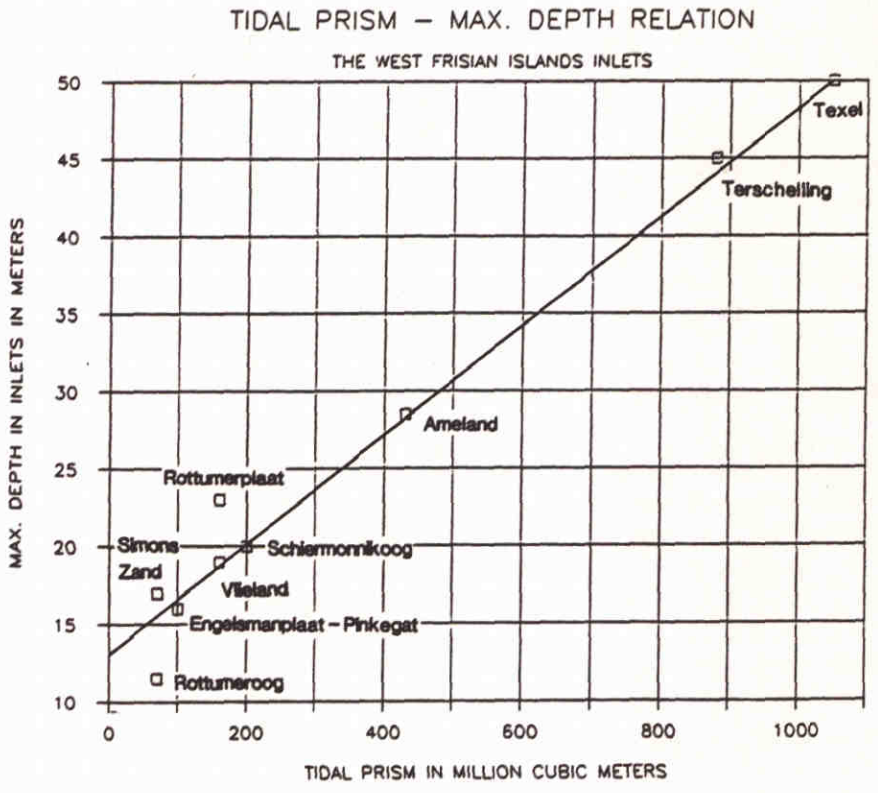

MAXIMUM DEPTHS OF DUTCH WADDEN SEA INLETS VERSUS MEAN TIDAL PRISM (SHA, 1990)

DELFT HYDRAULICS | H 1300 | FIG. 4.20

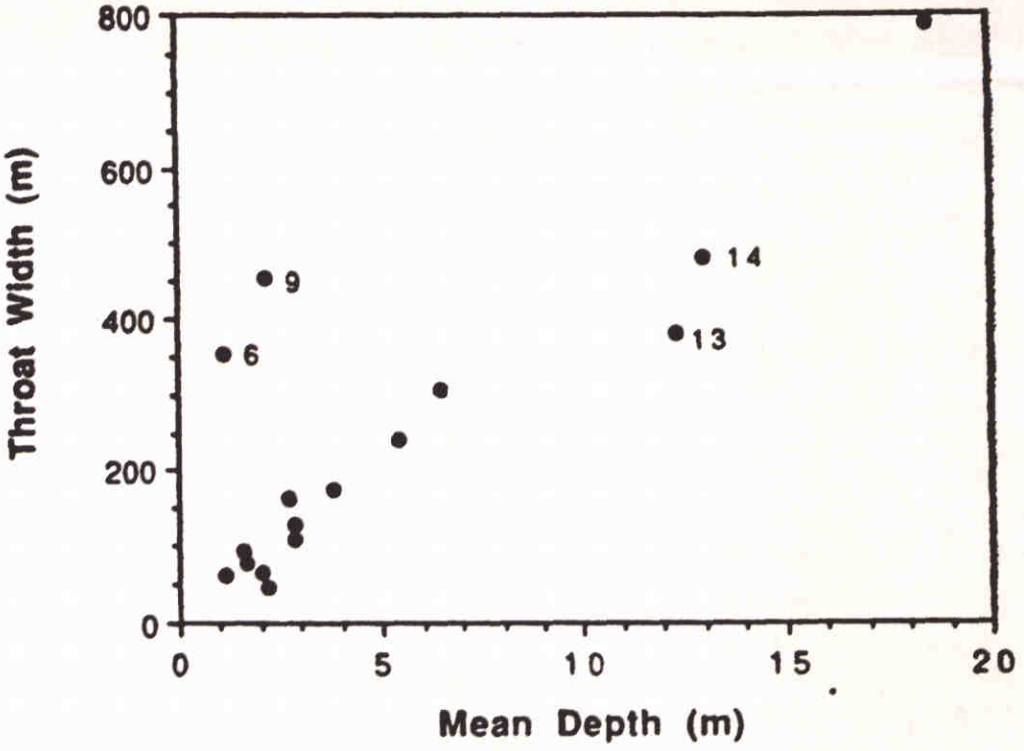

A. Relationship between mean depth and throat width

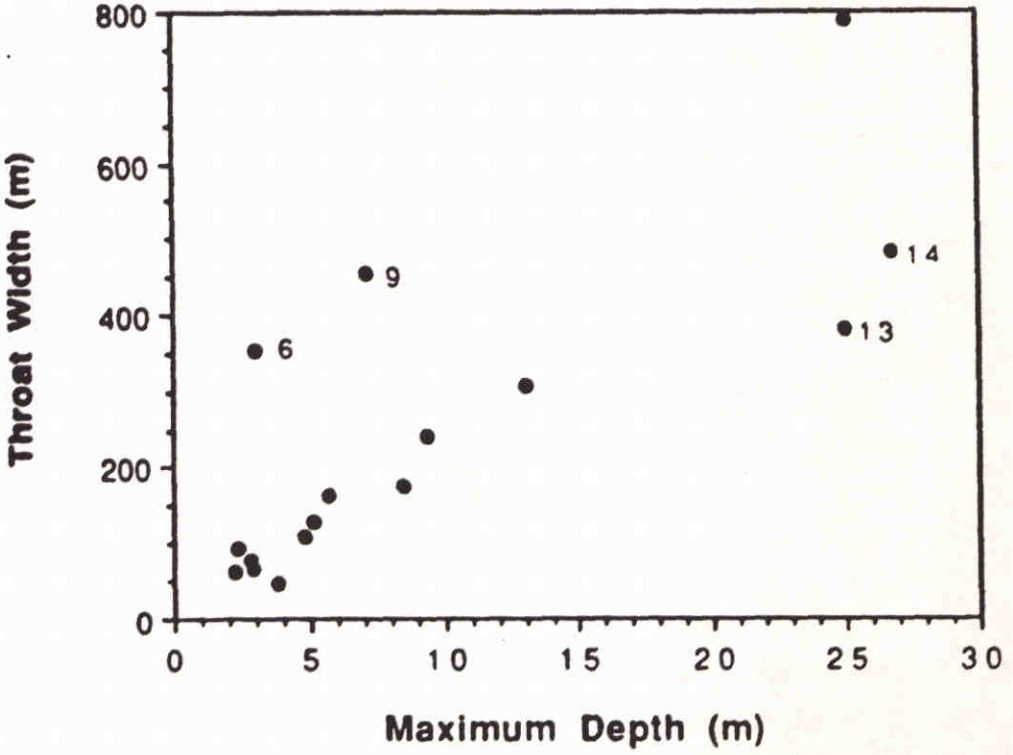

B. Relationship between maximum depth and throat width

MEAN AND MAXIMUM DEPTHS OF SOME NEW ZEALAND INLETS VERSUS INLET WIDTH (HUME AND HERDENDORF, 1990)		
DELFT HYDRAULICS	H 1300	FIG. 4.21

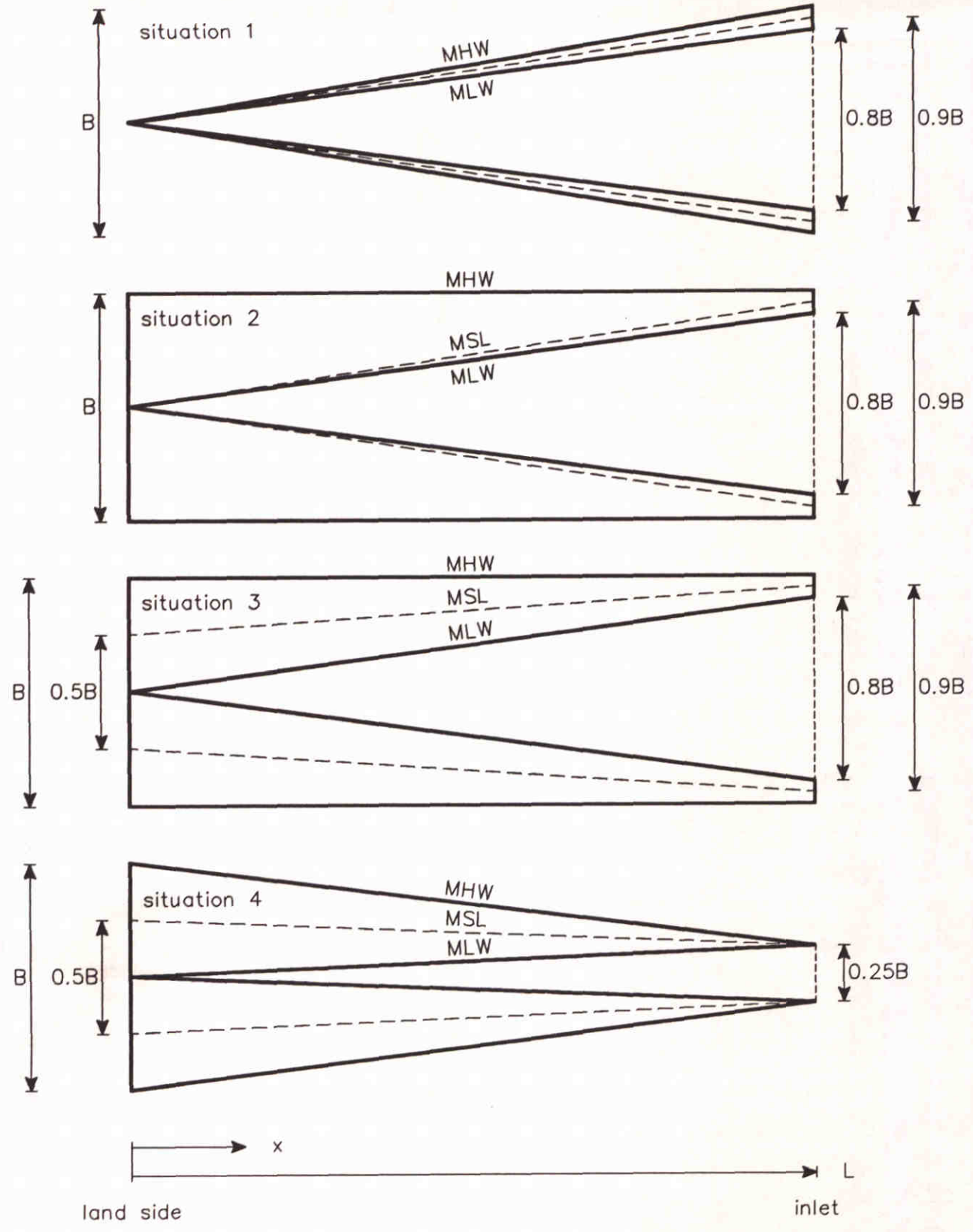

DEFINITION OF THEORETICAL BASIN (PLAN VIEW)

DELFT HYDRAULICS | H 1300 | FIG. 5.1

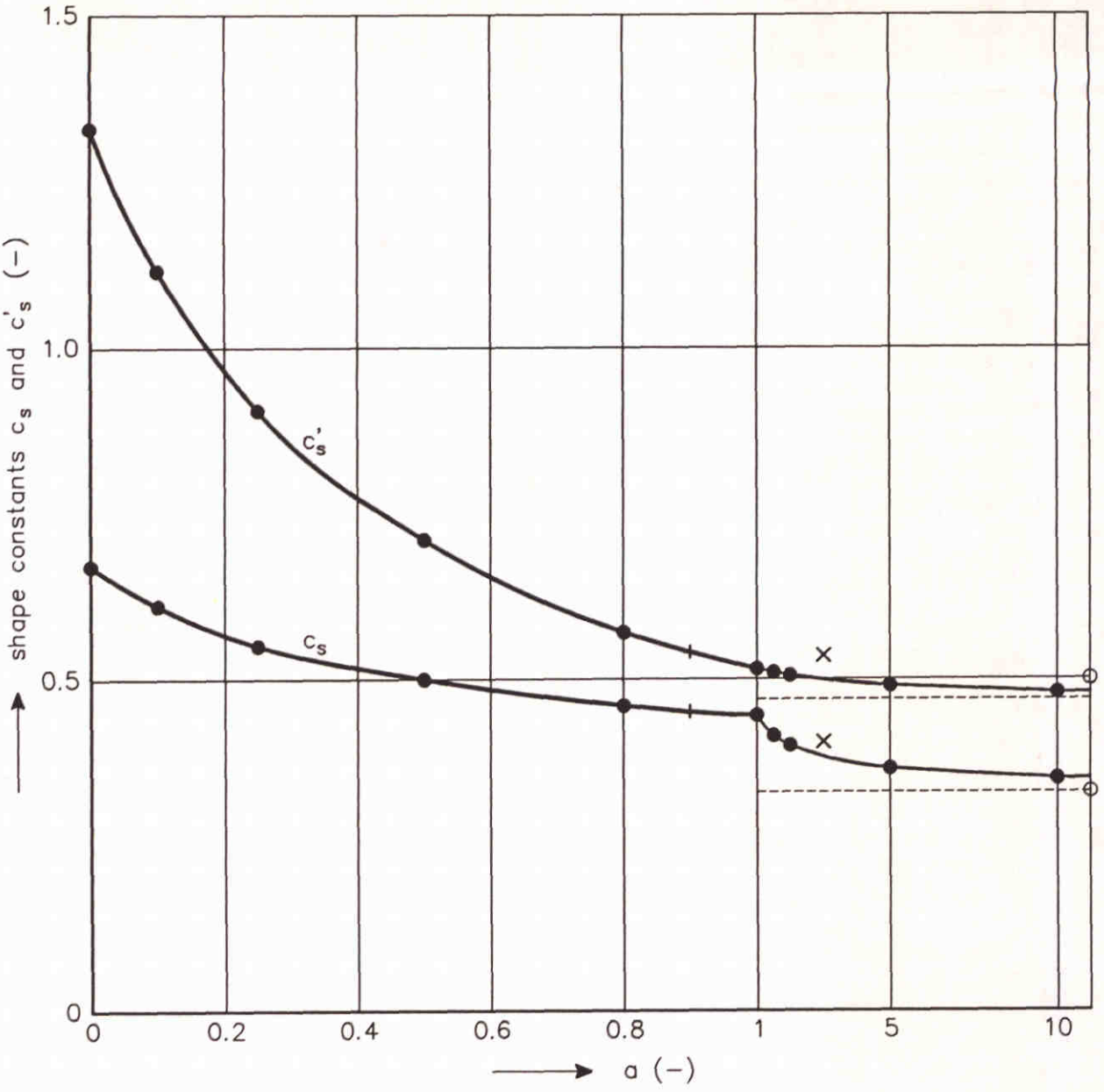

- o situation 1
- × situation 2
- \+ situation 3
- ● situation 4 with width of entrance aB
  (for a > 1 the definition of B in the formula becomes
  aB = largest width of the basin)

$$V_{MSL} = c_s c_A V_r L = c'_s c_A \left(\frac{L/B}{\Delta h}\right)^{1/2} V_r^{3/2}$$

SHAPE PARAMETERS c_s AND c'_s FOR DIFFERENT SITUATIONS (TOTAL SYSTEM: x=L)		
DELFT HYDRAULICS	H 1300	FIG. 5.2

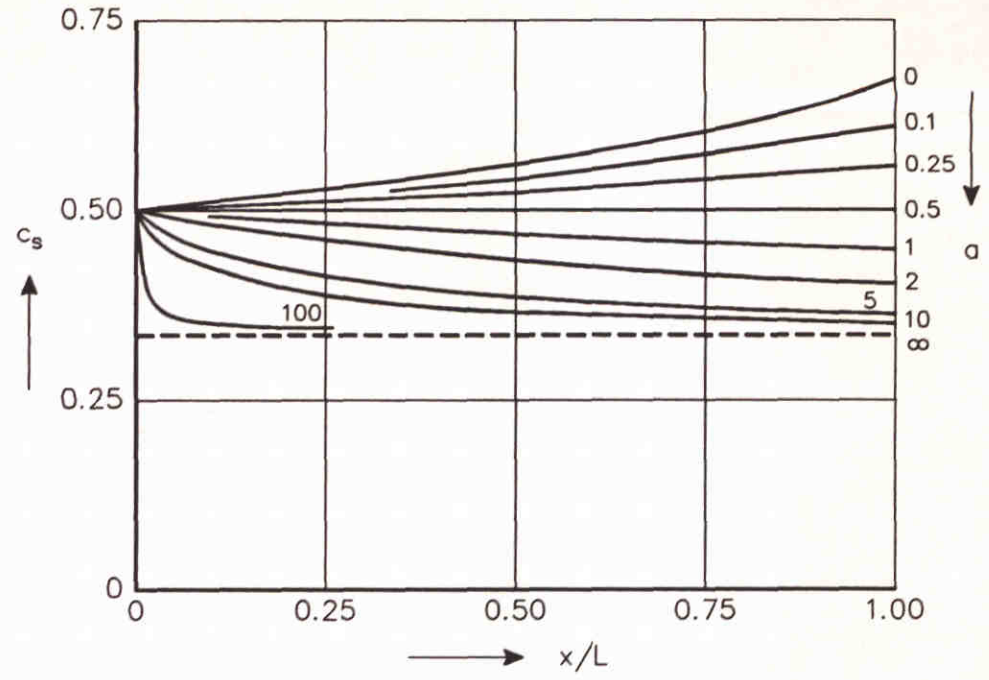

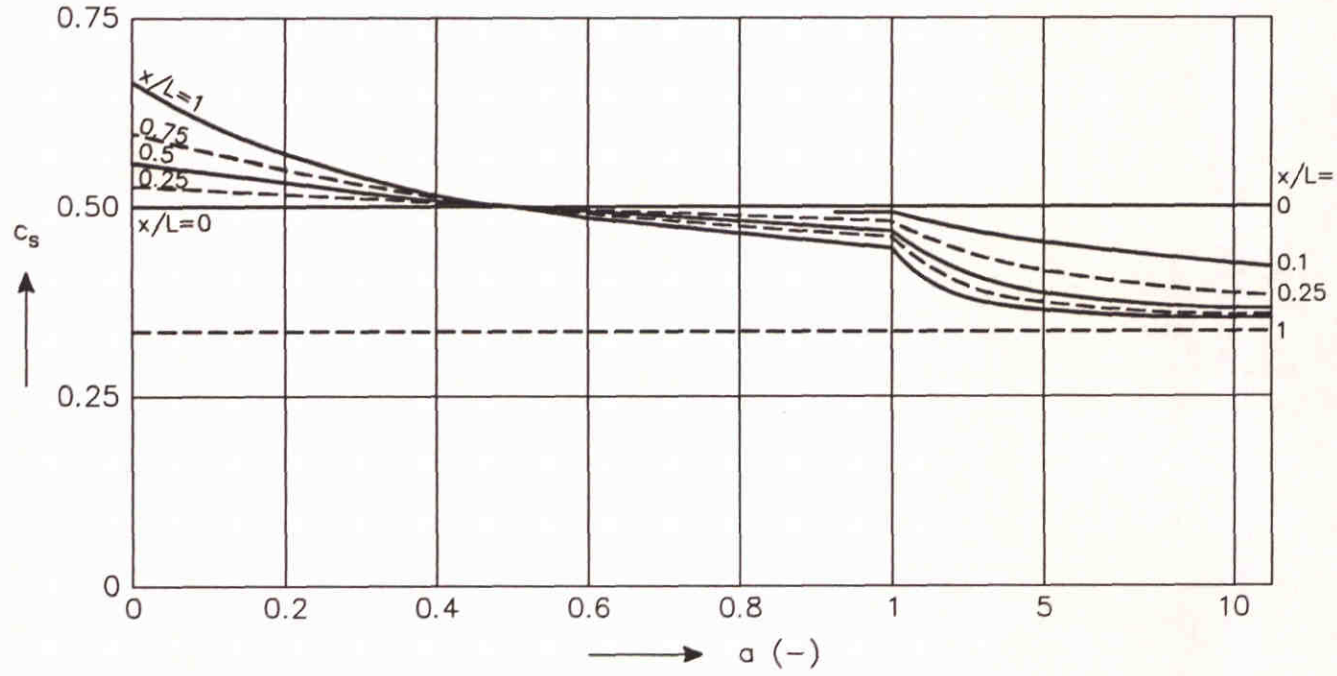

$$V_{MSL} = c_s c_A V_r L$$

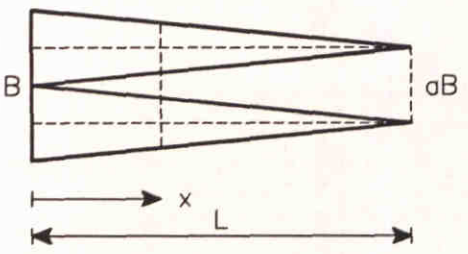

SHAPE PARAMETER c_s FOR SITUATION 4
WITH ENTRANCE WIDTH aB

DELFT HYDRAULICS | H 1300 | FIG. 5.3

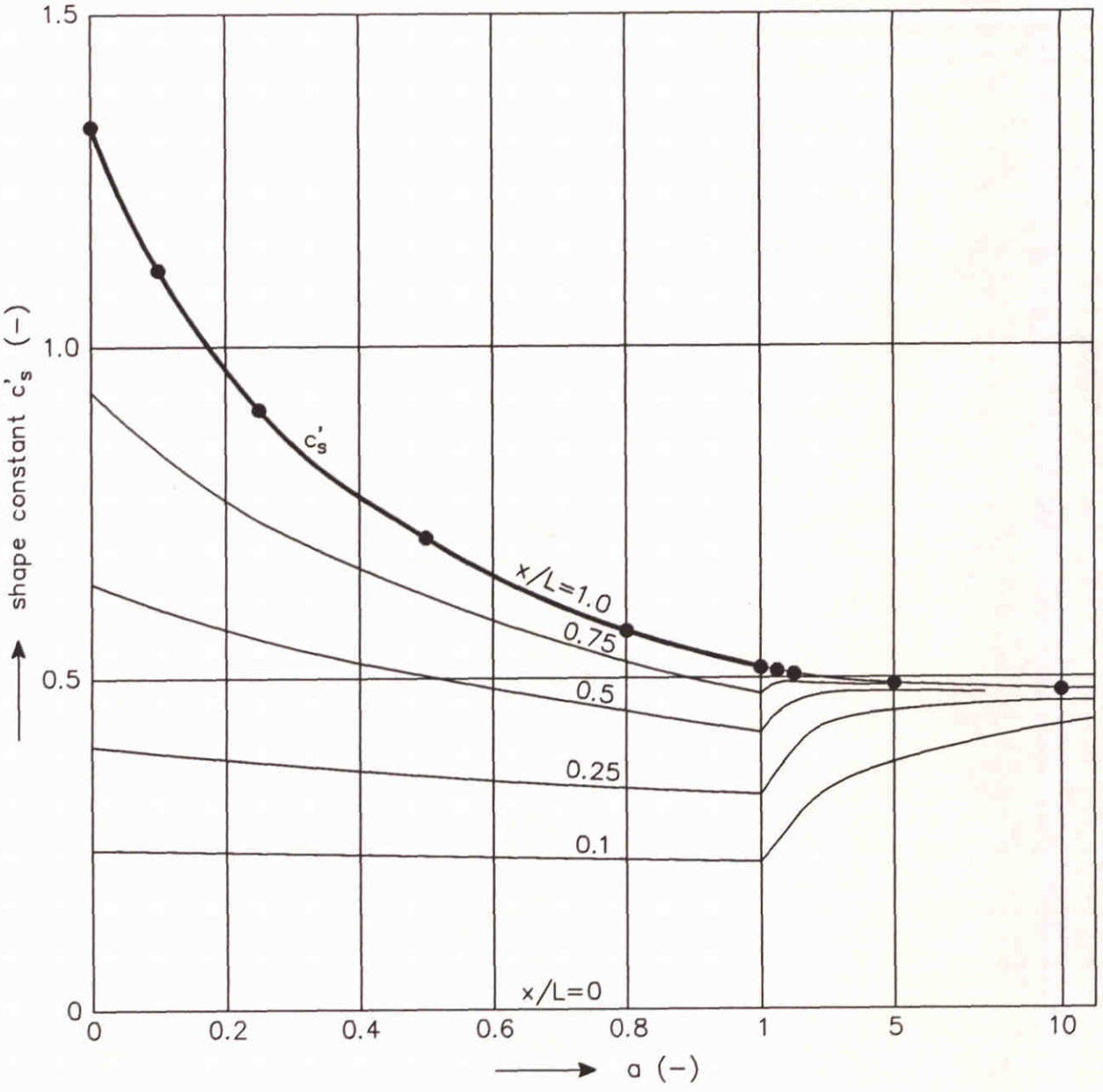

- situation 4 with width of entrance aB
  (for a > 1 the definition of B in the formula becomes
  aB = largest width of the basin)

$$V_{MSL} = c_s c_A V_r L = c'_s c_A \left(\frac{L/B}{\Delta h}\right)^{1/2} V_r^{3/2}$$

SHAPE PARAMETER c'_s FOR SITUATION 4 WITH ENTRANCE WIDTH aB		
DELFT HYDRAULICS	H 1300	FIG. 5.4

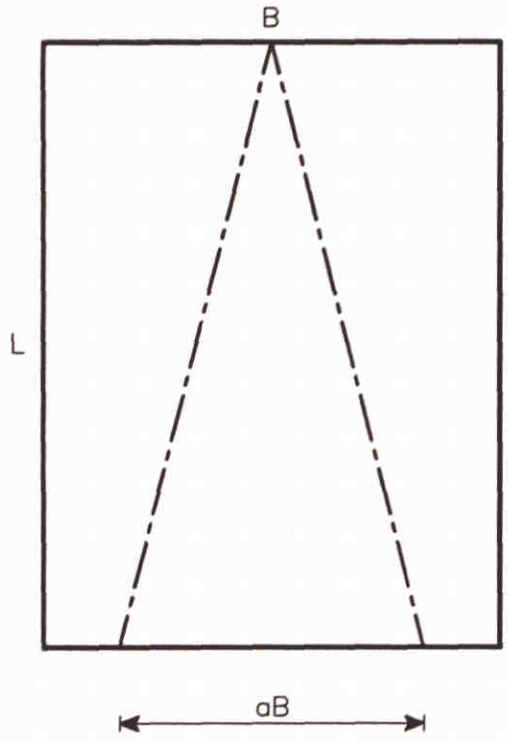

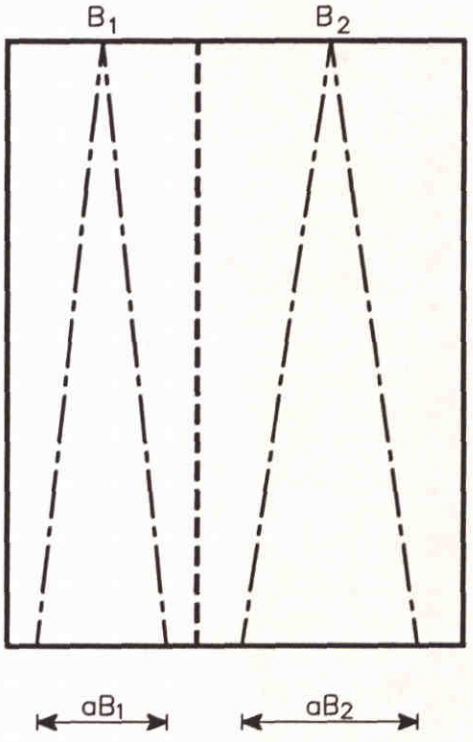

BASIN 1

$$V_{MSL} = c_A . c'_s \left(\frac{L/B}{\Delta h}\right)^{1/2} P^{1.5}$$

BASIN 2

$$B = B_1 + B_2$$

$$c_A . c'_s = c_1 \qquad B_1 = xB$$

$$V_{MSL,1} = c_1 \left\{\frac{L/(xB)}{\Delta h}\right\}^{1/2} (xP)^{1.5}$$

$$V_{MSL,2} = c_1 \left[\frac{L/\{(1-x)B\}}{\Delta h}\right]^{1/2} (1-x)^{1.5} P^{1.5}$$

$$V_{MSL,1} + V_{MSL,2} = c_1 \left(\frac{L/B}{\Delta h}\right)^{1/2} P^{1.5} (x+1-x) = V_{MSL}$$

VALIDITY OF RELATION (5.5) FOR COMPOSITE BASINS		
DELFT HYDRAULICS	H 1300	FIG. 5.5

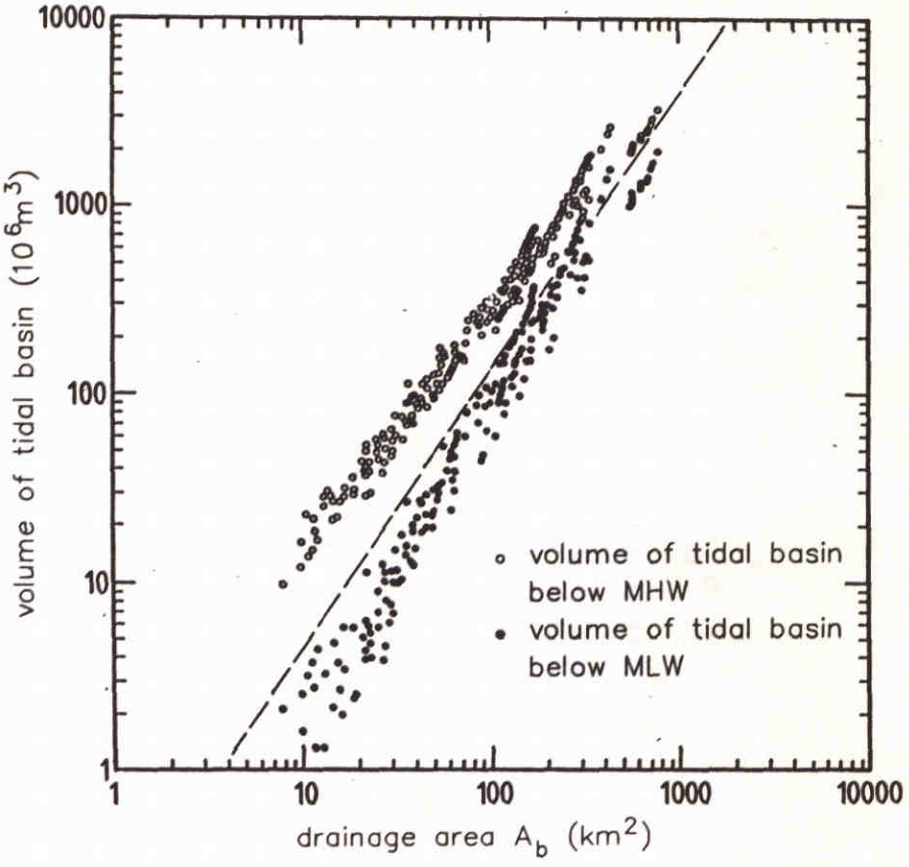

RELATIONSHIPS BETWEEN THE VOLUMETRIC CAPACITY BELOW MLW AND MHW AND THE DRAINAGE AREA OF TIDAL BASINS IN THE GERMAN BIGHT (DIECKMANN, 1985; DIECKMANN AND PARTENSCKY, 1986)		
DELFT HYDRAULICS	H 1300	FIG. 5.6

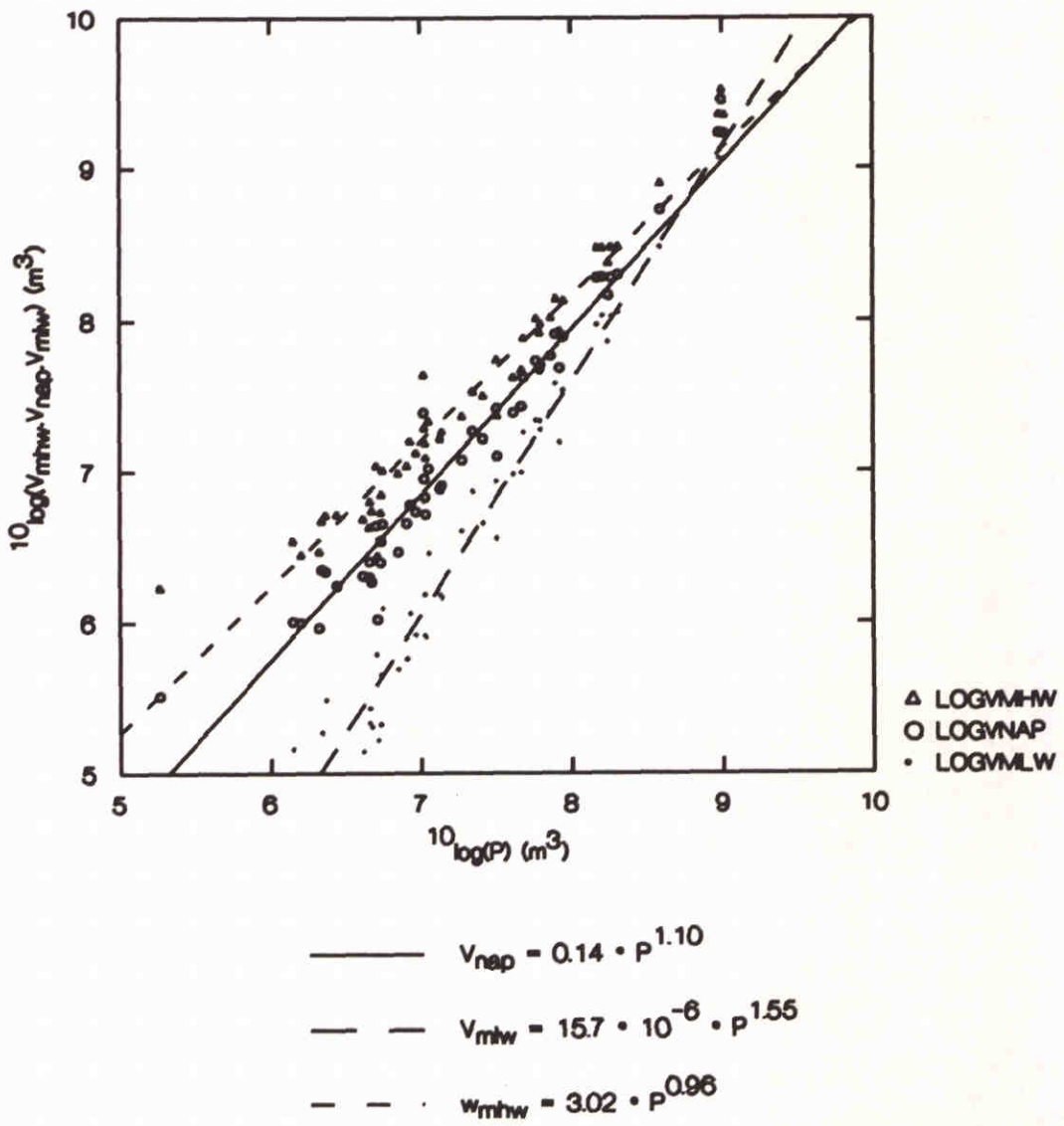

CORRELATION OF P WITH V_{mhw}.V_{nap} and V_{mlw}		
DELFT HYDRAULICS	H 1300	FIG. 5.7

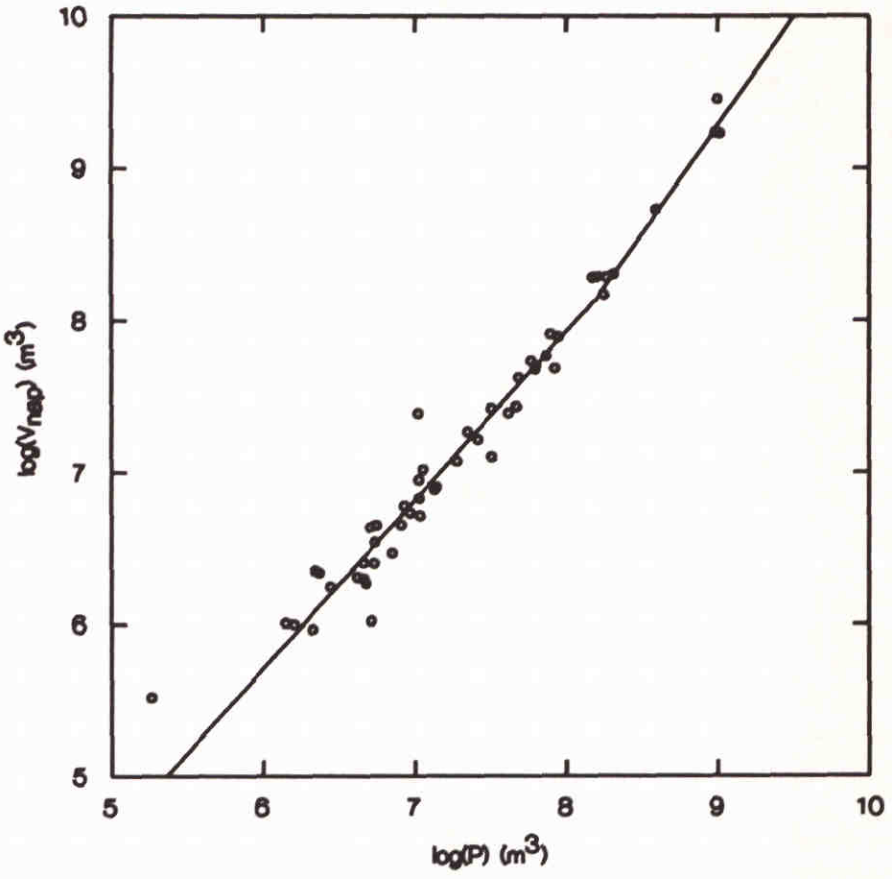

$10^6 < P < 160 \cdot 10^6$ $\quad V_{nap} = 0.11 \cdot P^{1.11}$

$160 \cdot 10^6 < P < 1000 \cdot 10^6$ $\quad V_{nap} = 259 \cdot 10^{-6} \cdot P^{1.43}$

CORRELATION OF P WITH V_{nap}		
DELFT HYDRAULICS	H 1300	FIG. 5.8

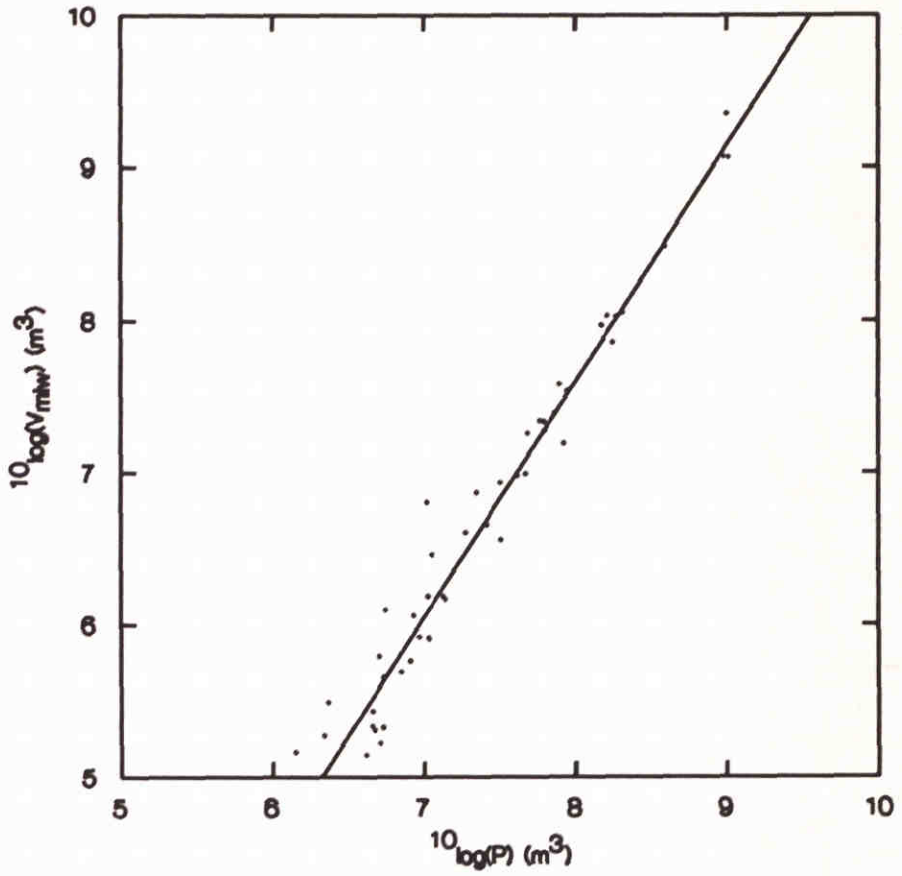

$V_{mlw} = 16 \cdot 10^{-6} \cdot P^{1.55}$

CORRELATION OF P WITH V_{mlw}		
DELFT HYDRAULICS	H 1300	FIG. 5.9

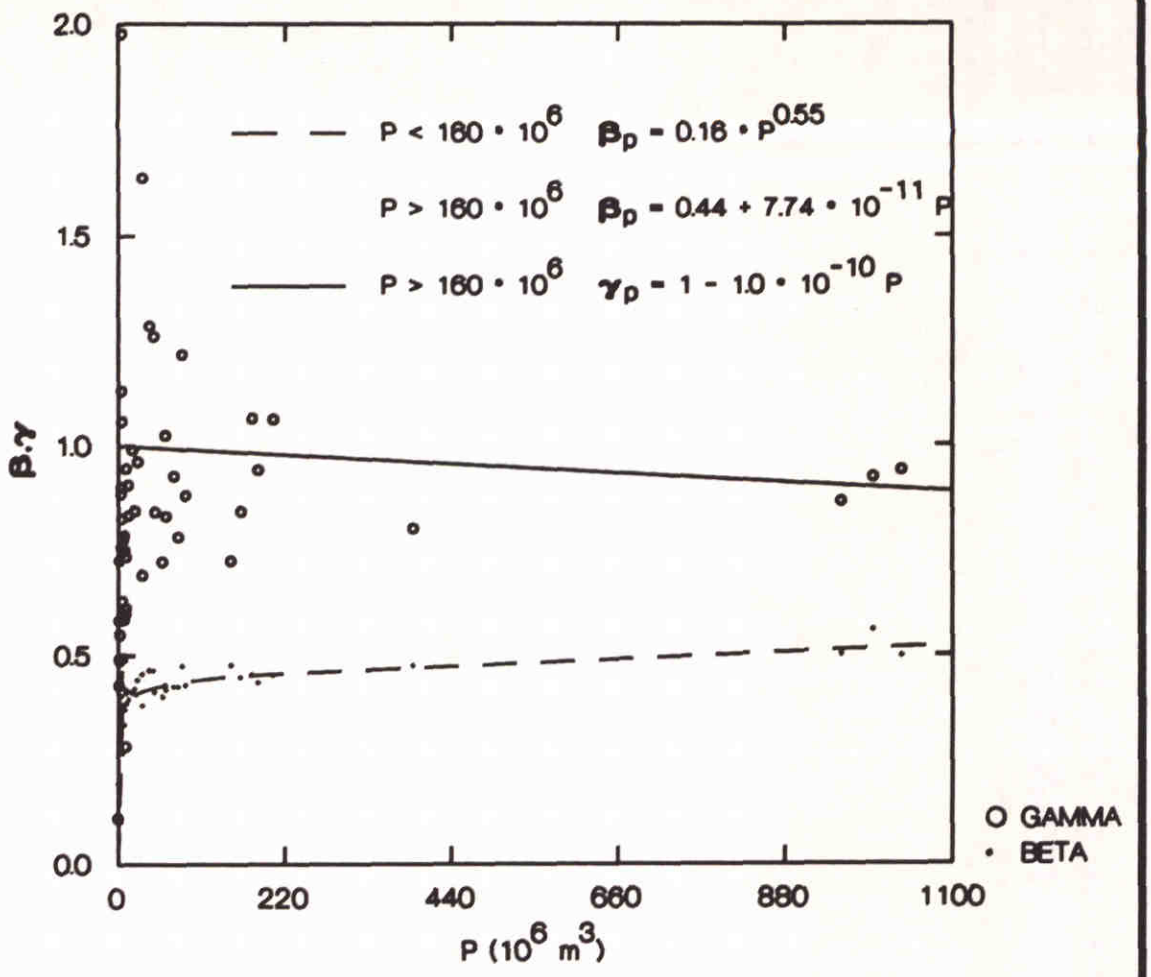

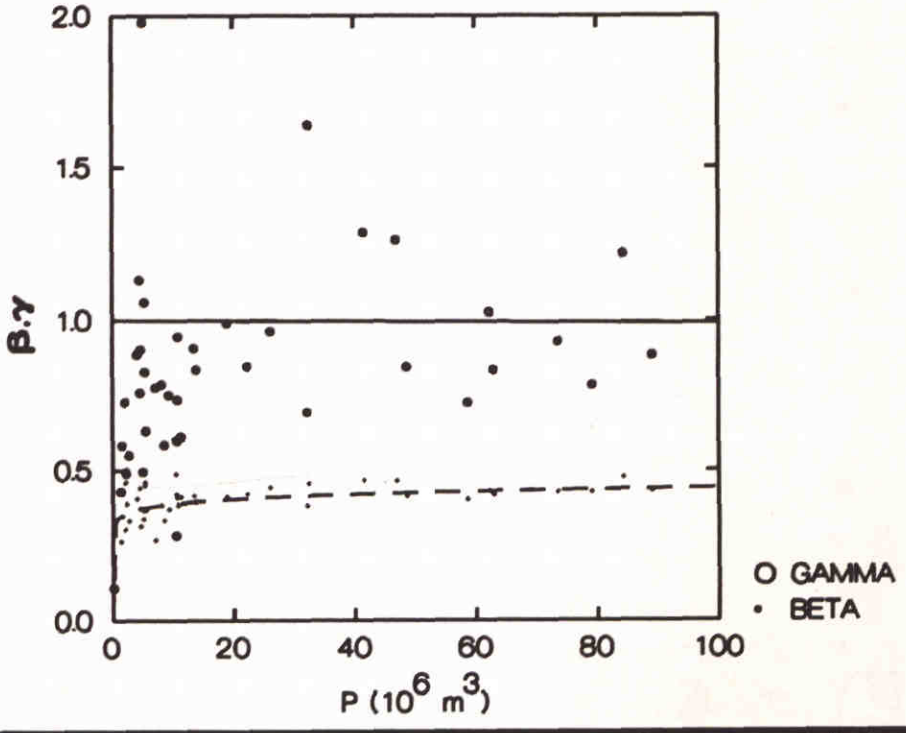

CORRELATION OF P WITH β_p AND γ_p

DELFT HYDRAULICS | H 1300 | FIG. 5.10

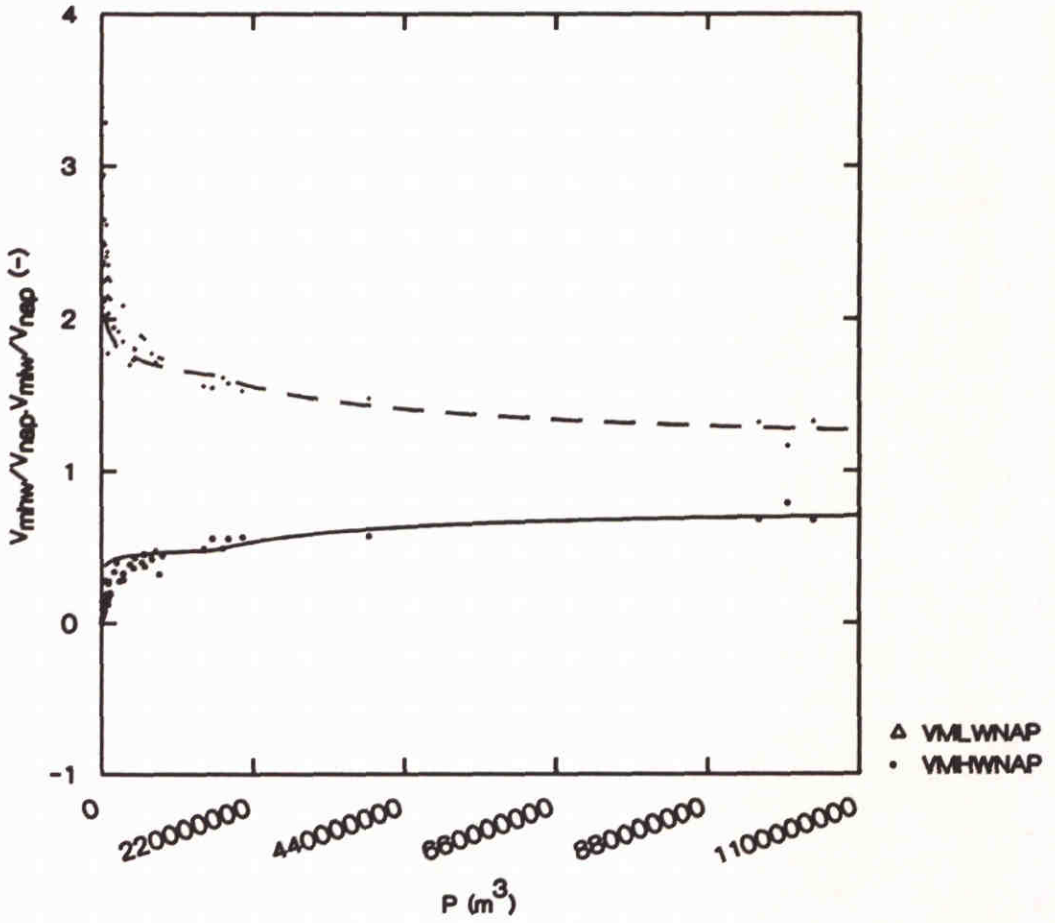

——— V_{mlw}/V_{nap}

— — V_{mhw}/V_{nap}

CORRELATION OF P WITH V_{mhw}/V_{nap} AND V_{mlw}/V_{nap}		
DELFT HYDRAULICS	H 1300	FIG. 5.11

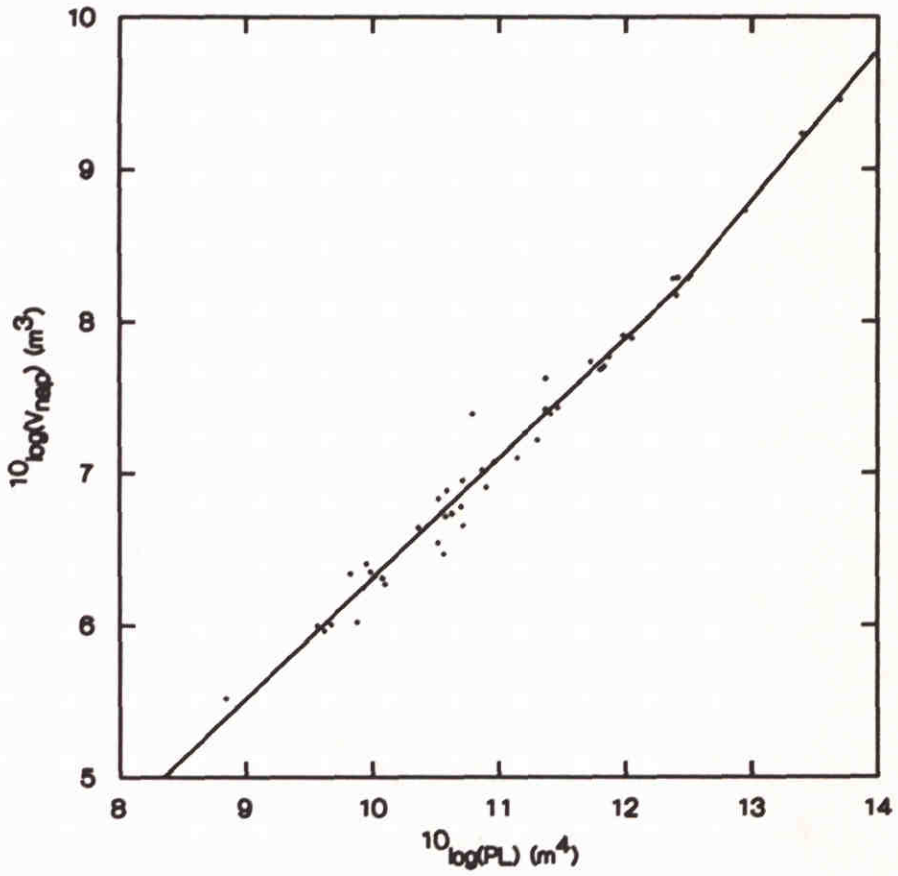

$V_{nap} = 2.55 \cdot 10^{-2} \cdot (PL)^{0.79}$ $PL < 2.5 \cdot 10^{12}$

$V_{nap} = 84.16 \cdot 10^{-6} \cdot (PL)^{0.99}$ $2.5 \cdot 10^{12} < PL < 50 \cdot 10^{12}$

CORRELATION OF V_{nap} WITH PL

DELFT HYDRAULICS | H 1300 | FIG. 5.12

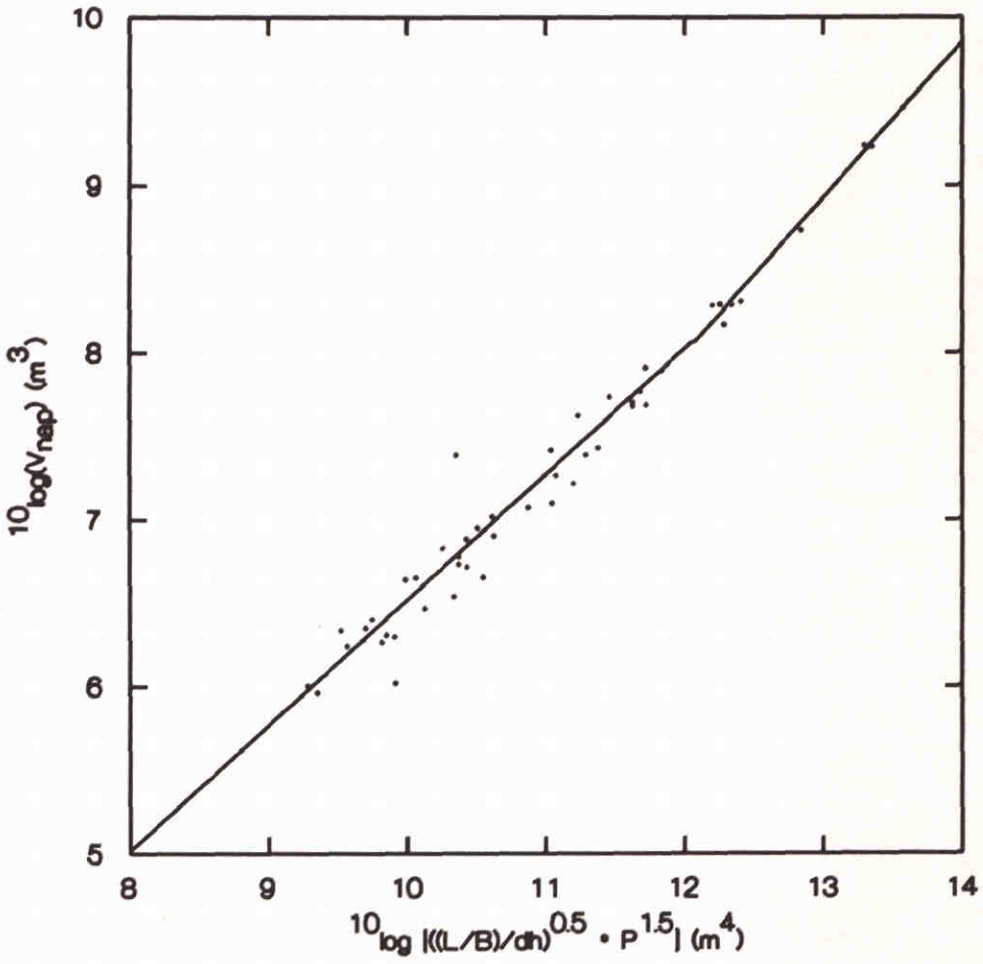

$V_{nap} = 0.10 \cdot [\,.\,.\,]^{0.75} \qquad [\,.\,.\,] < 1.15 \cdot 10^{12}$

$V_{nap} = 679 \cdot 10^{-6} \cdot [\,.\,.\,]^{0.93} \qquad 1.15 \cdot 10^{12}\ [\,.\,.\,] < 40 \cdot 10^{12}$

CORRELATION OF V_{nap} WITH $\|((L/B)/\Delta\bar{h})^{0.5} \cdot P^{1.5}\|$		
DELFT HYDRAULICS	H 1300	FIG. 5.13

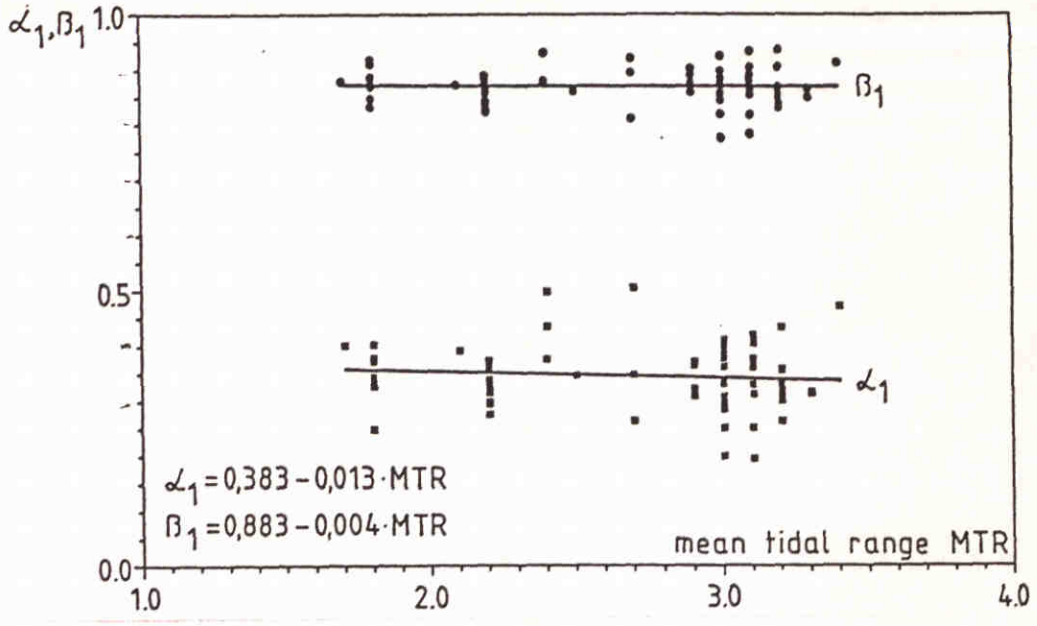

A. Regression coefficients α_1 and β_1

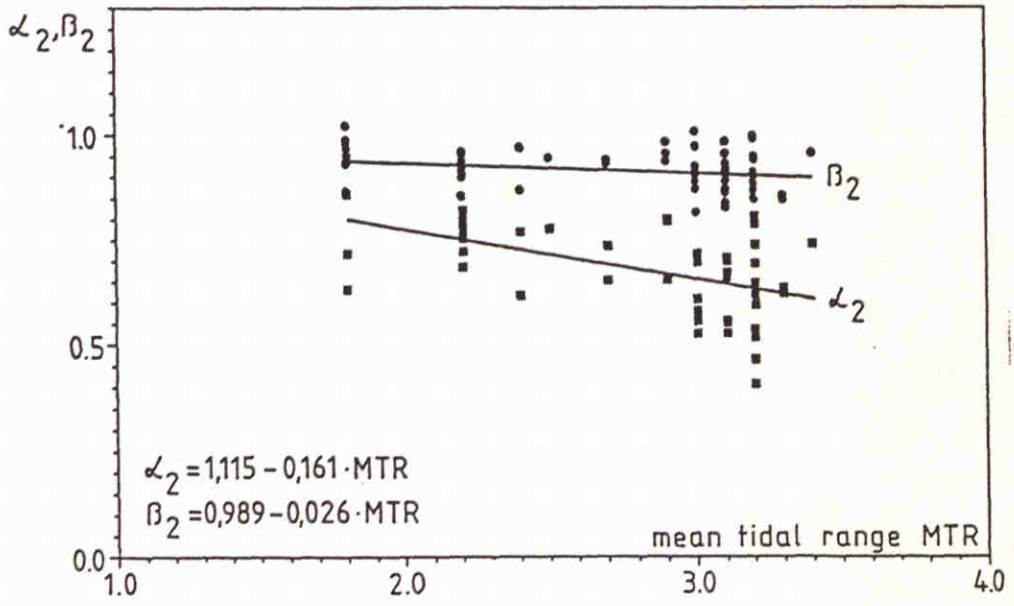

B. Regression coefficients α_2 and β_2

REGRESSION COEFFICIENTS α_1, β_1, α_2 AND β_2 OF DIECKMANN AND PARTENSCKY (1986)		
DELFT HYDRAULICS	H 1300	FIG. 5.14

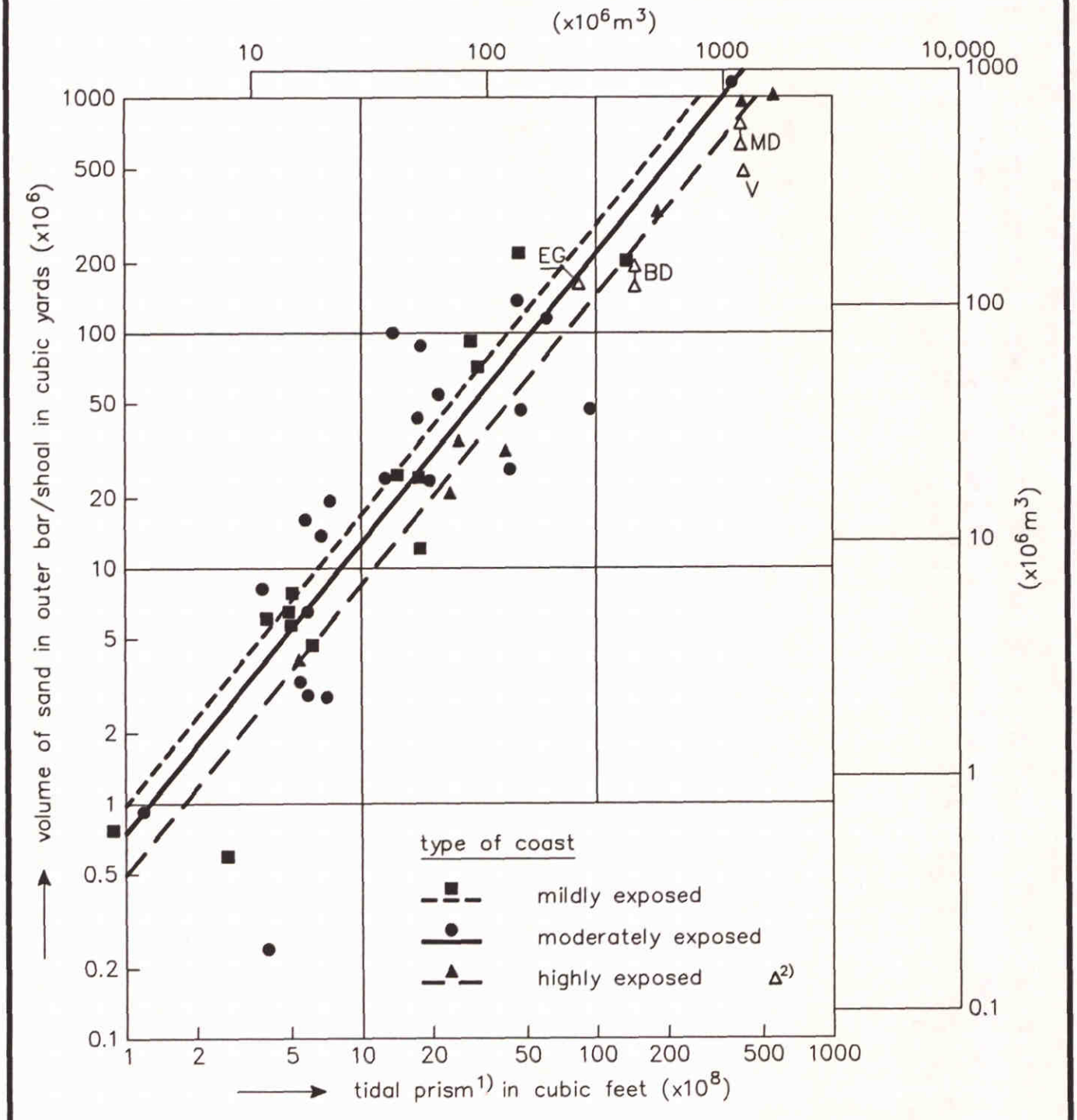

$V_{od} = c_{od} P^{1.23}$

1) springtide ior diurnal range
2) dutch Wadden Sea inlets

SAND VOLUME OUTER DELTAS IN USA IN RELATION TO THE MEAN TIDAL VOLUME OF THE INLET ACCORDING TO WALTON AND ADAMS [59]

DELFT HYDRAULICS | H 1300 | FIG. 6.1

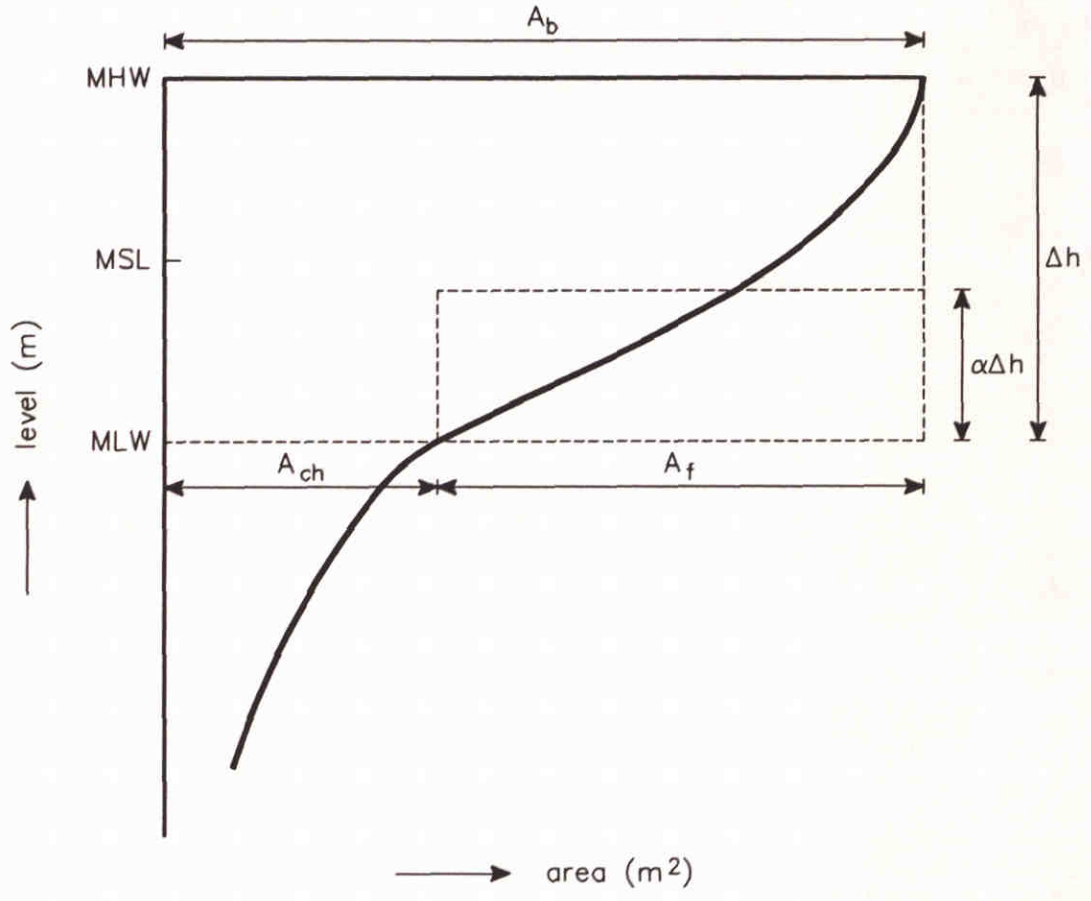

$$P \approx A_b \Delta h - A_f \alpha \Delta h = (1 - \alpha A_f / A_b)\, A_b \Delta h$$

$\alpha\Delta h$: average height of tidal flats above MLW

REDUCTION OF TIDAL PRISM OF A BASIN DUE TO TIDAL FLATS		
DELFT HYDRAULICS	H 1300	FIG. 7.1

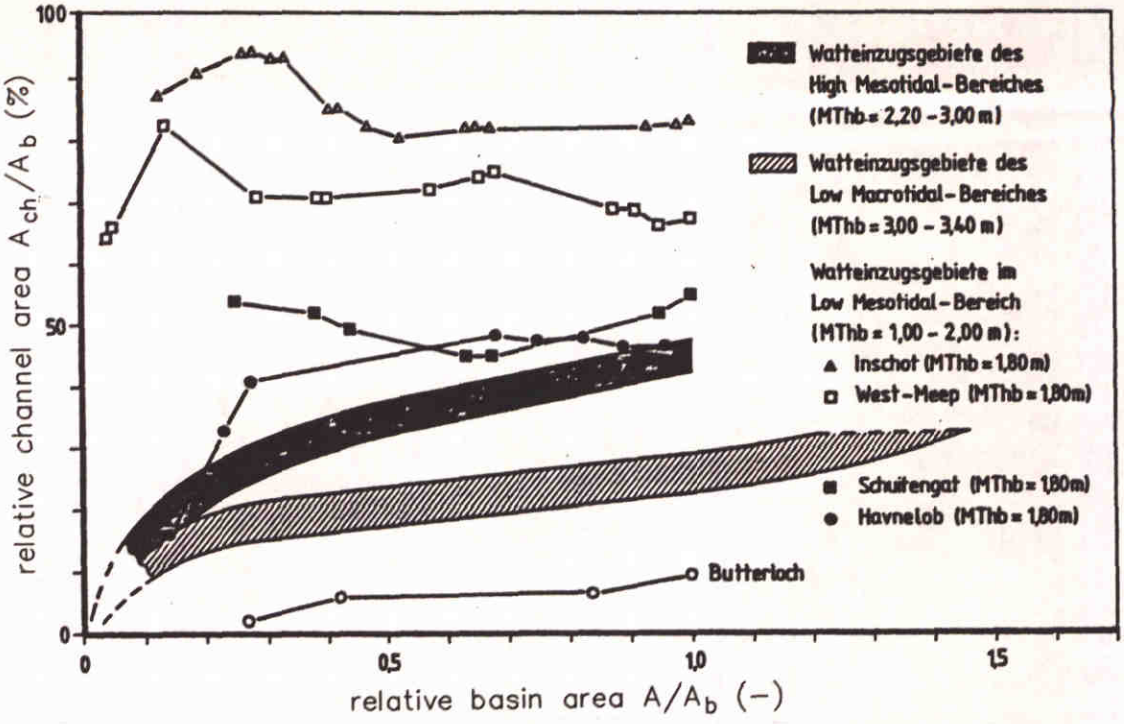

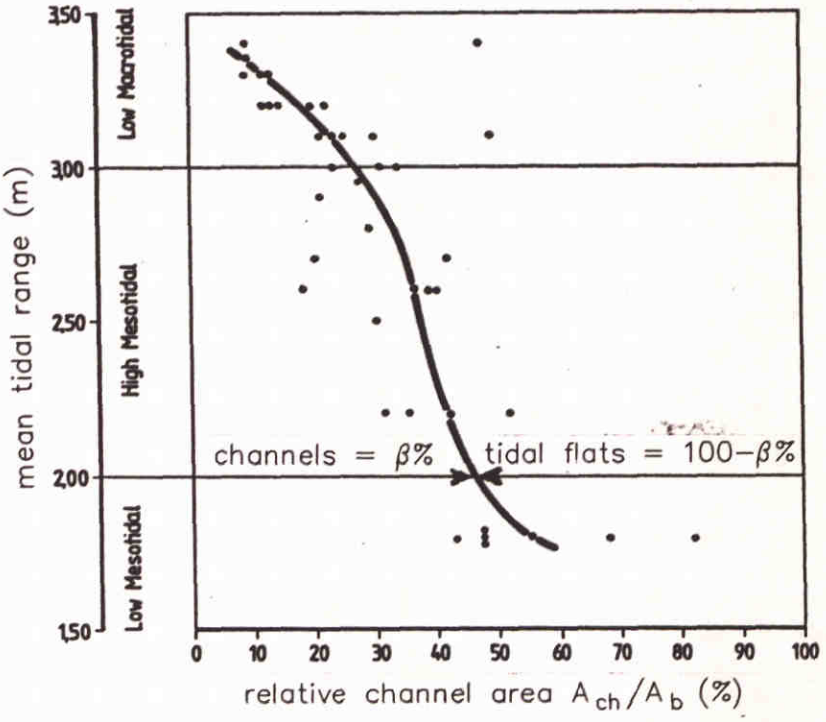

RELATION BETWEEN MEAN TIDAL RANGE AND RELATIVE CHANNEL AND TIDAL FLAT AREAS (DIECKMANN, 1985)		
DELFT HYDRAULICS	H 1300	FIG. 7.2

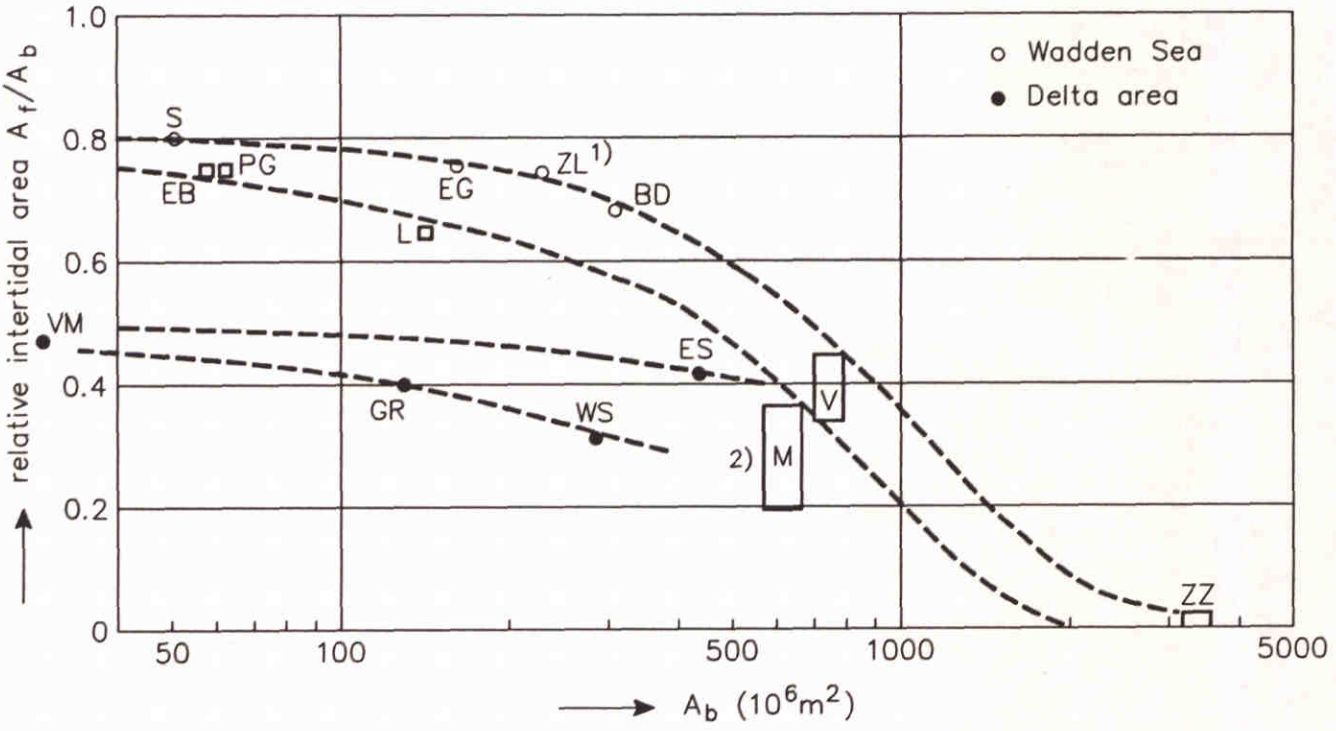

1) before closure of the Lauwerszee

2) after closure of the Zuiderzee (IJsselmeer); no equilibrium yet ?

WADDEN SEA

M = Marsdiep/Zeegat van Texel
EG = Eijerlandse Gat
V = Vlie
BD = Borndiep
PG = Pinkegat
ZL = Zoutkamperlaag
EB = Eilanderbalg
L = Lauwers
S = Schild

DELTA AREA

WS = Western Scheldt
VM = Veerse Meer
ES = Eastern Scheldt
GR = Grevelingen

RELATIVE AREA OF THE INTERTIDAL ZONES IN THE DUTCH WADDEN SEA AND DELTA AREA

DELFT HYDRAULICS | H 1300 | FIG. 7.3

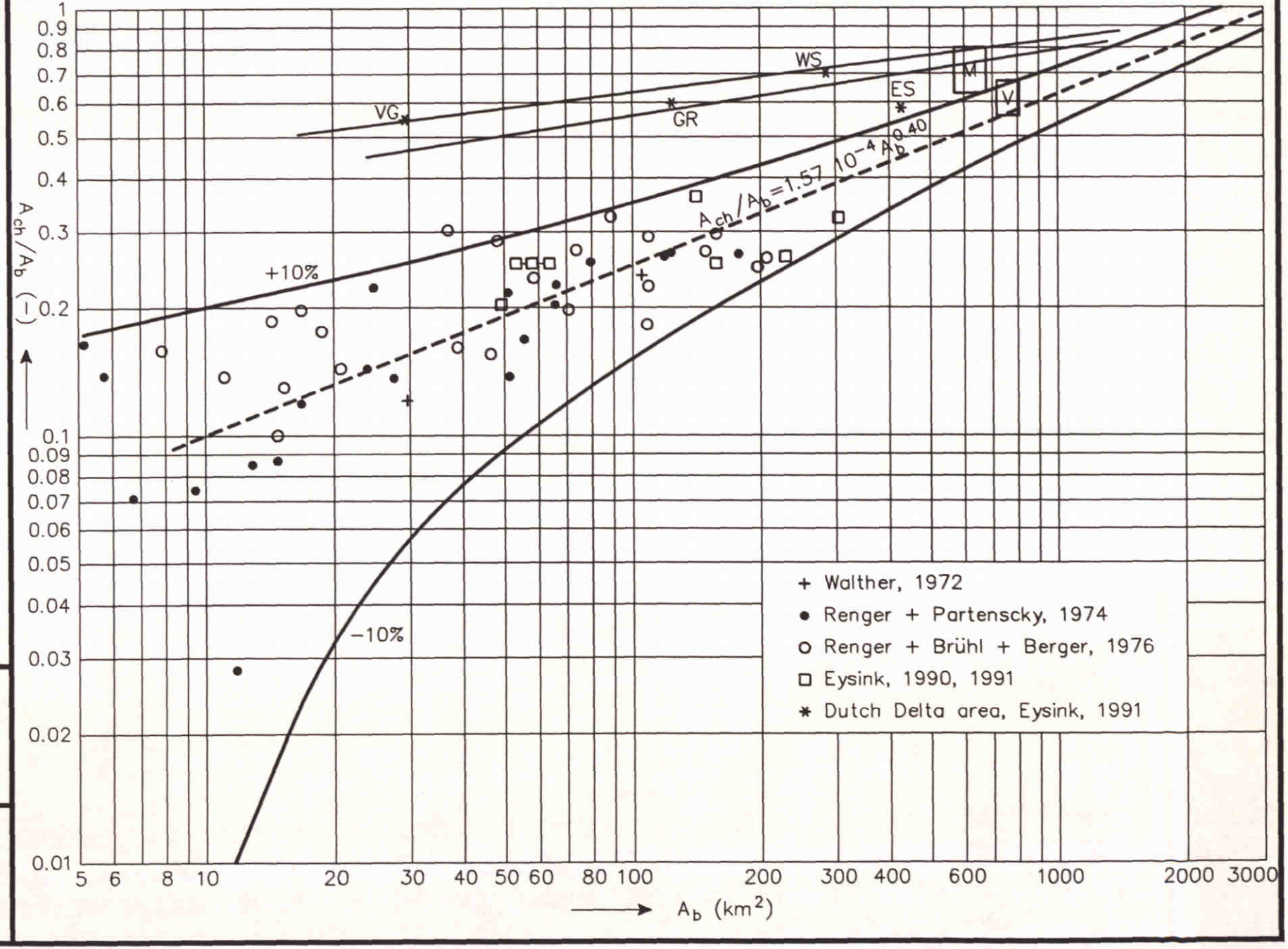

RELATIVE CHANNEL AREA IN THE DUTCH AND GERMAN WADDEN SEA. DATA FROM LITERATURE

DELFT HYDRAULICS

H 1300

FIG. 7.4

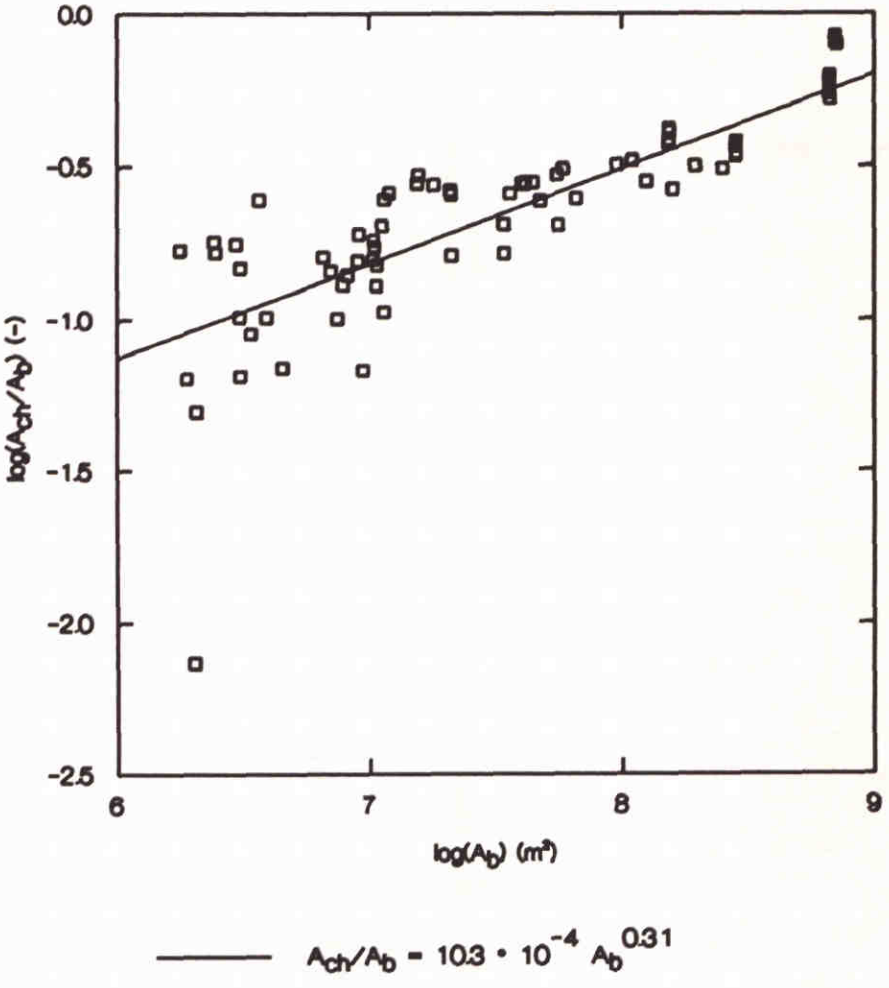

CORRELATION OF RELATIVE CHANNEL AREA A_{ch}/A_b WITH SIZE OF THE BASIN A_b

DELFT HYDRAULICS | H 1300 | FIG. 7.5

AMPLIFICATION OF TIDAL RANGE ALONG THE MAIN CHANNEL OF A BASIN

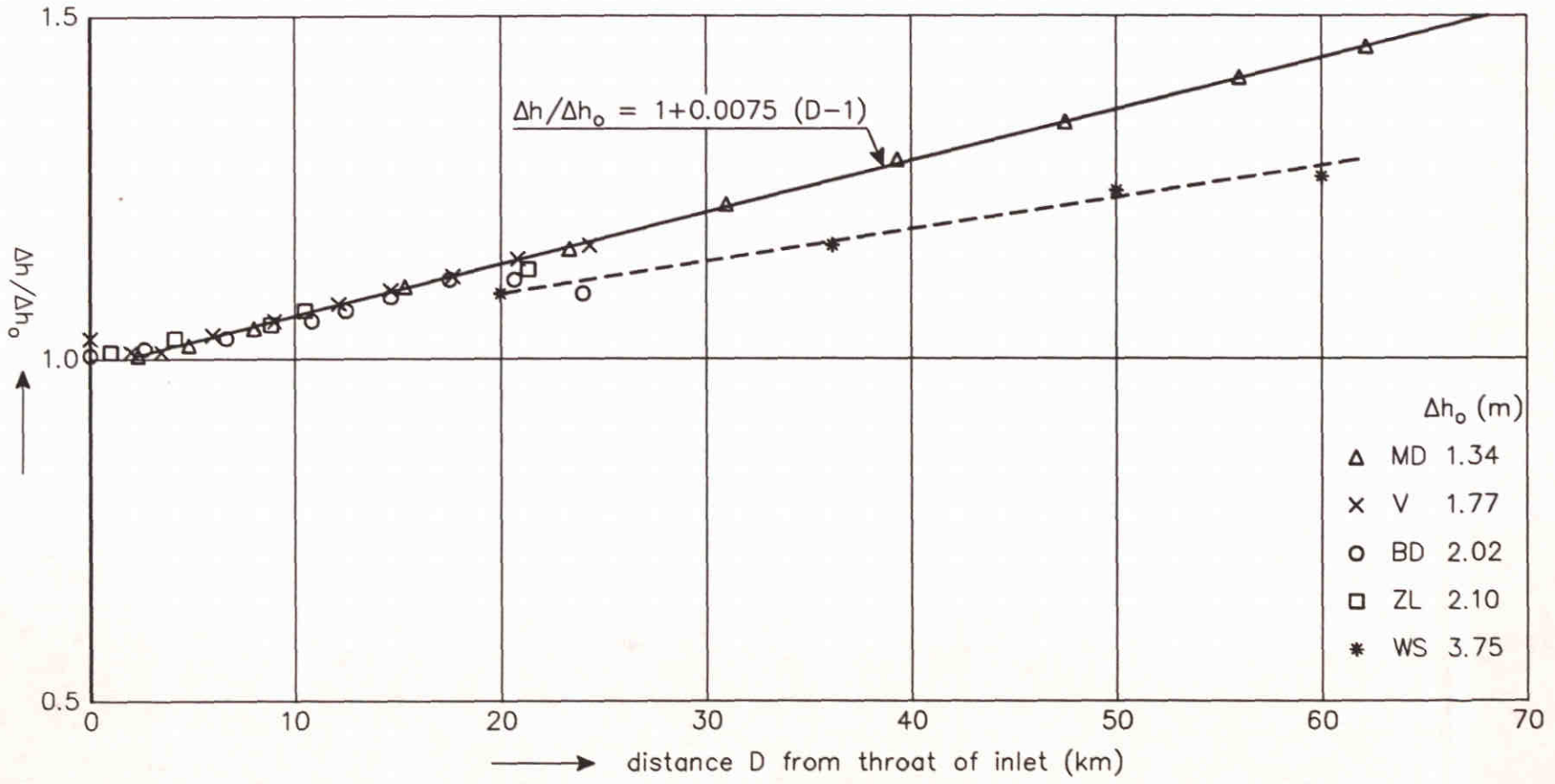

DELFT HYDRAULICS

H 1300

FIG. 7.6

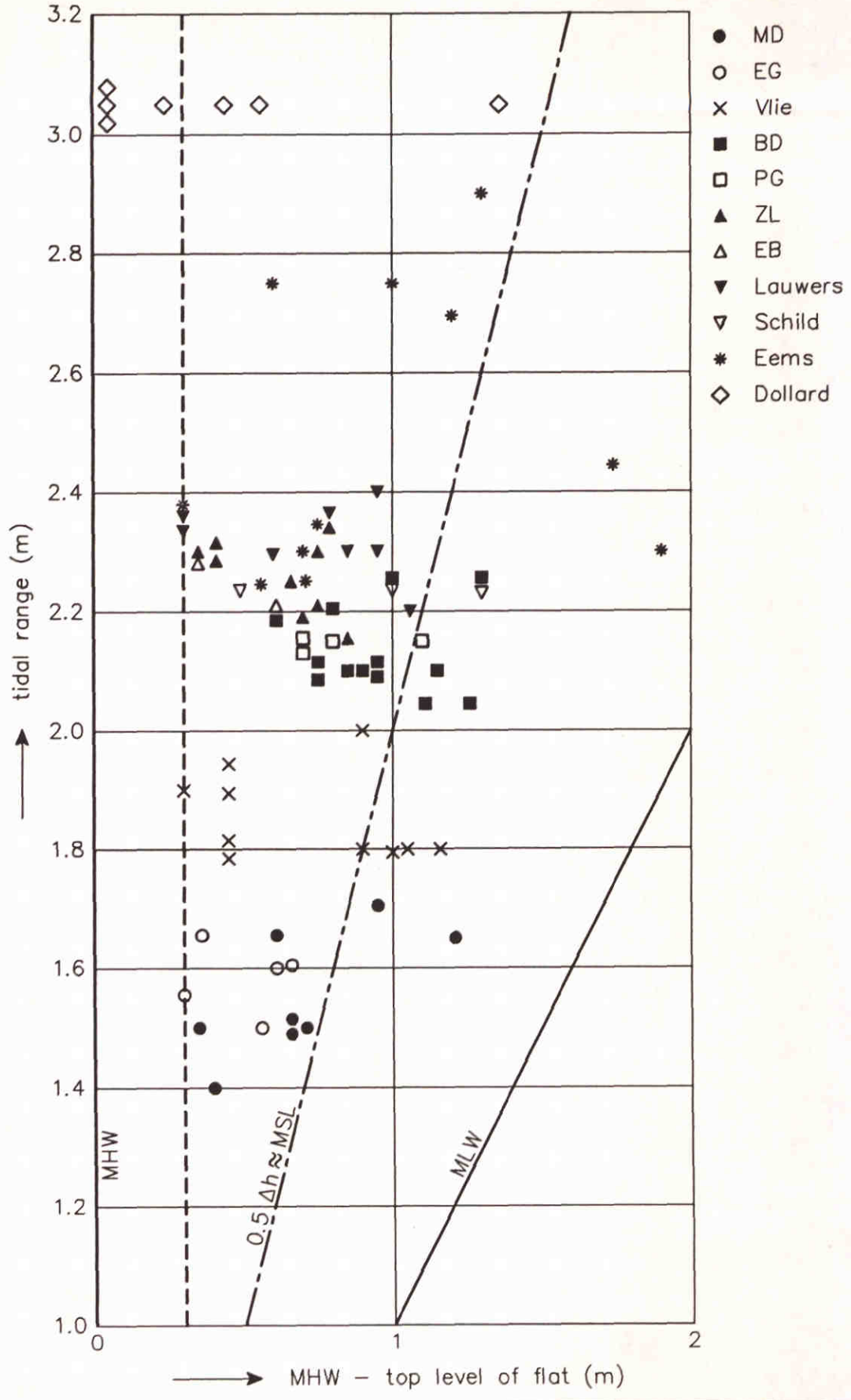

CORRELATION OF TOP LEVELS OF TIDAL FLATS IN THE DUTCH WADDEN SEA WITH MHW AND MEAN TIDAL RANGE

DELFT HYDRAULICS | H 1300 | FIG. 7.7

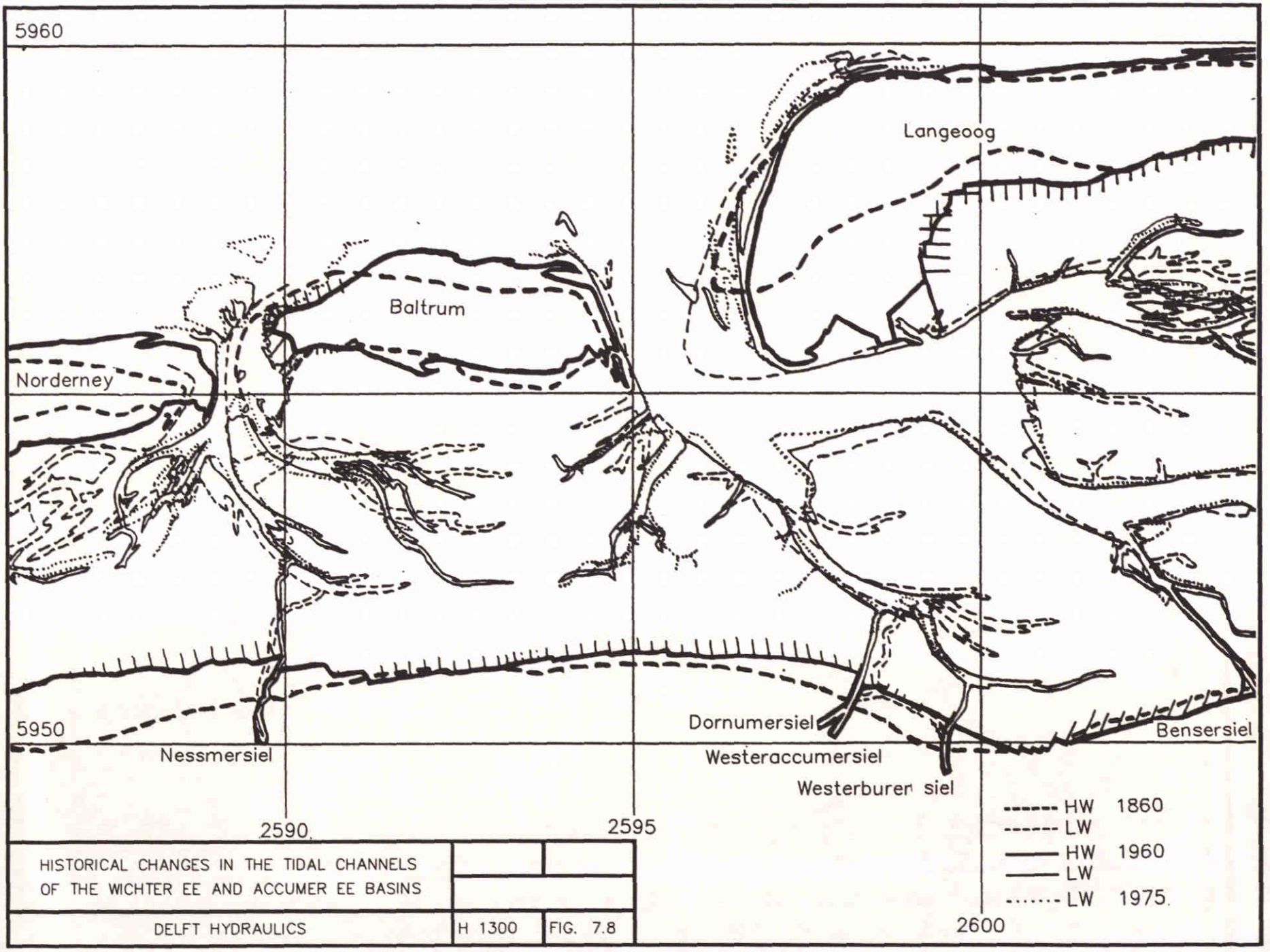

HISTORICAL CHANGES IN THE TIDAL CHANNELS OF THE WICHTER EE AND ACCUMER EE BASINS		
DELFT HYDRAULICS	H 1300	FIG. 7.8

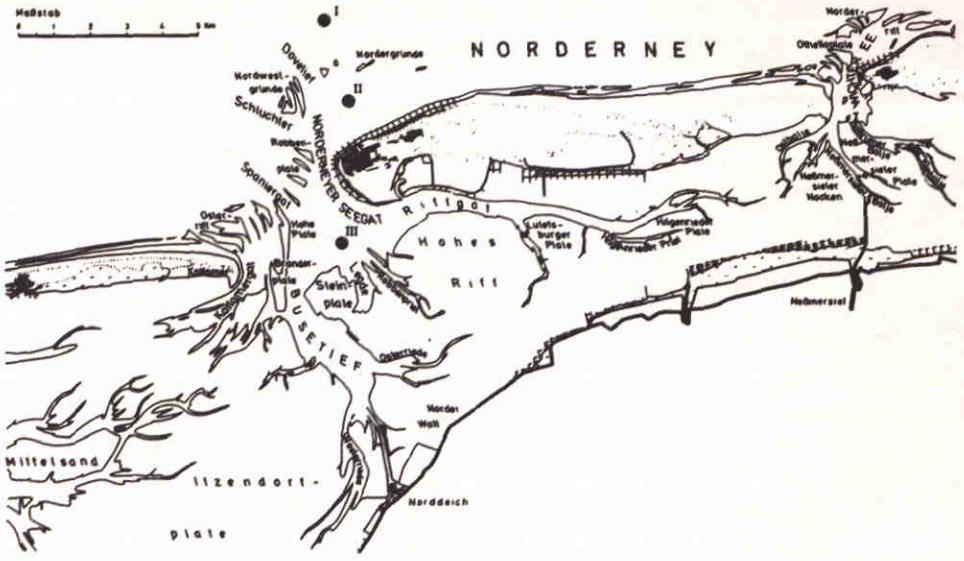

wave gauge locations at Norderney

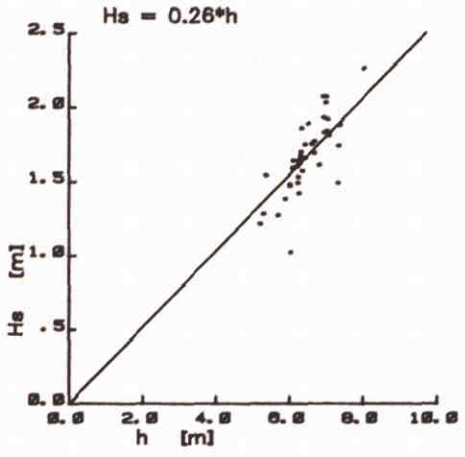

station II

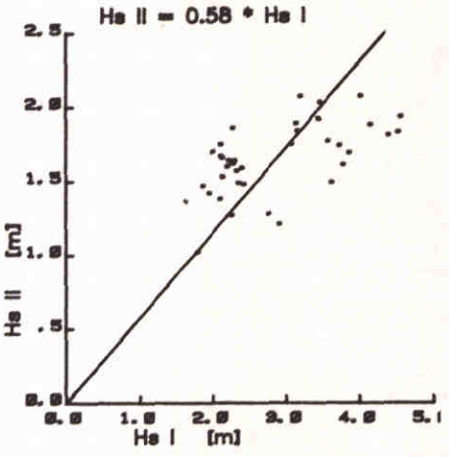

station II versus I

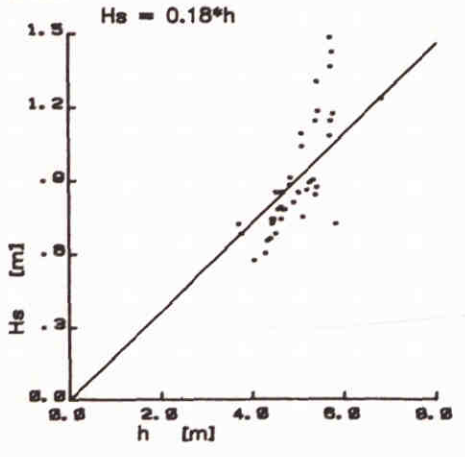

station III

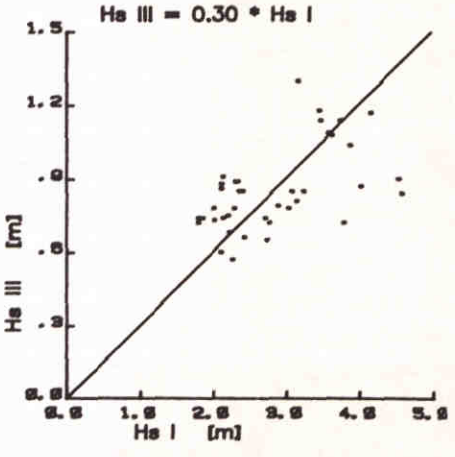

station III versus I

WAVE HEIGHT RELATED TO LOCAL WATER DEPTH AND LOCATION (NIEMEYER, 1986)		
DELFT HYDRAULICS	H 1300	FIG. 7.9

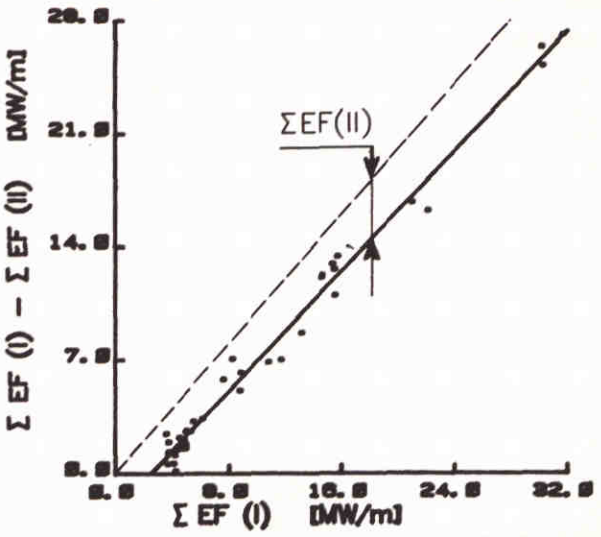

loss of wave energy between stations I and II

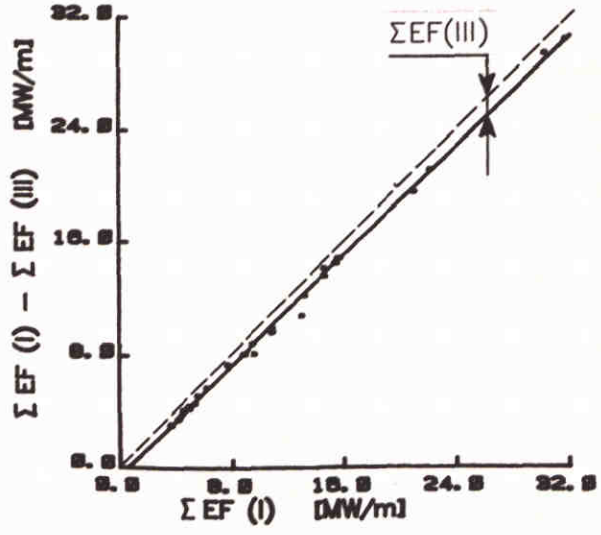

loss of wave energy between stations I and III

for location of stations see Fig. 7.9

REDUCTION OF WAVE ENERGY JUST OUTSIDE AND INSIDE THE INLET OF NORDERNEY (NIEMEYER, 1986)		
DELFT HYDRAULICS	H 1300	FIG. 7.10

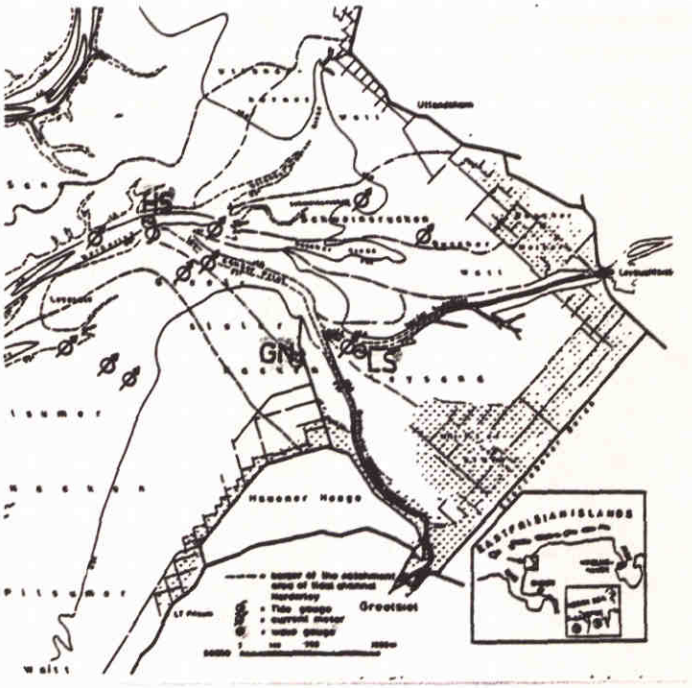

situation Ley Bay

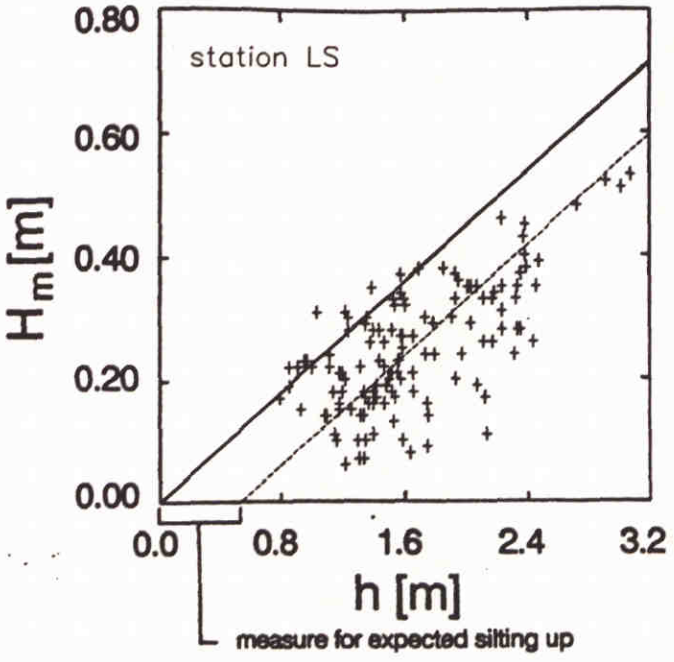

stable flat relation

present relation

from: Niemeyer, 1991

ESTIMATION OF FUTURE SEDIMENTATION BASED ON COMPARISON OF LOCAL WAVE DATA WITH A WAVE HEIGHT–DEPTH RELATION FOR STABLE FLATS		
DELFT HYDRAULICS	H 1300	FIG. 7.11

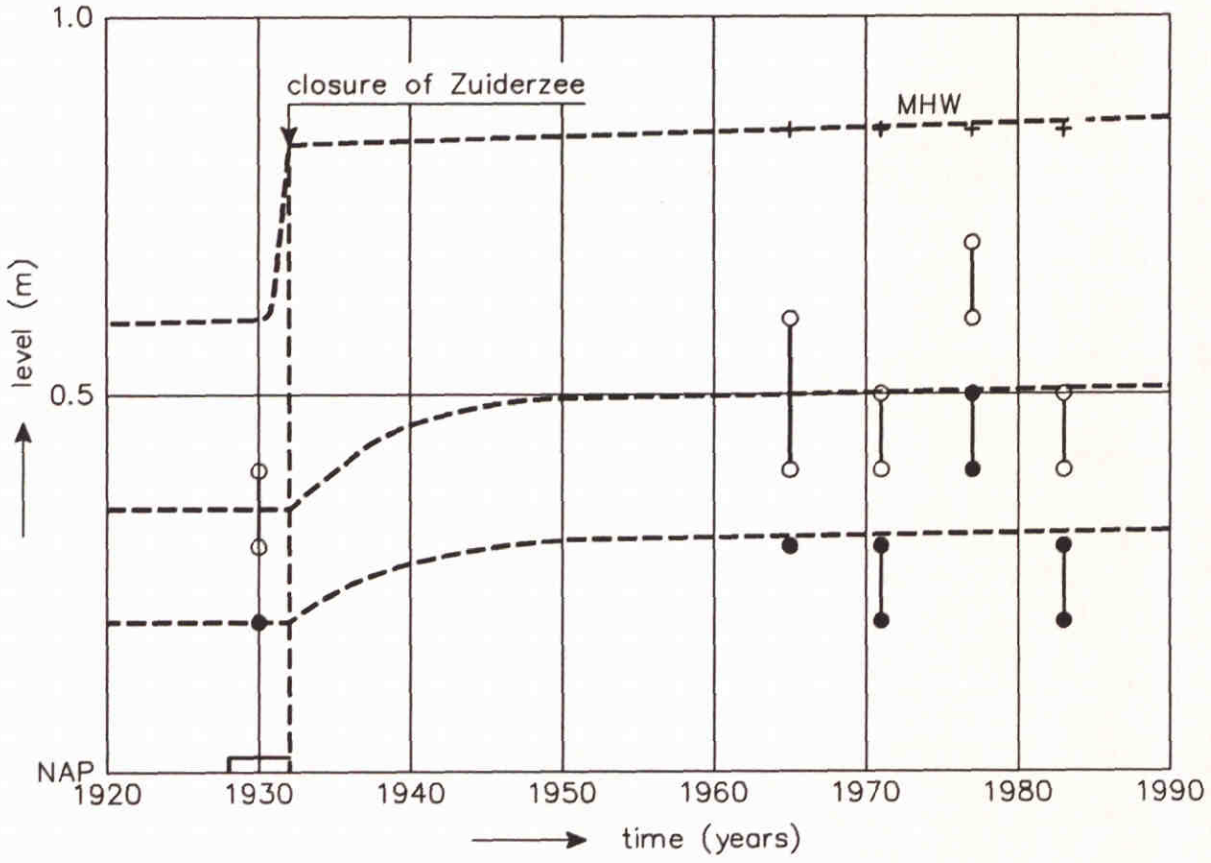

● West of Griend

○ East of Griend

HISTORIES OF TOP LEVELS OF THE GRIENDERWAARD AND OF LOCAL MHW		
DELFT HYDRAULICS	H 1300	FIG. 7.12

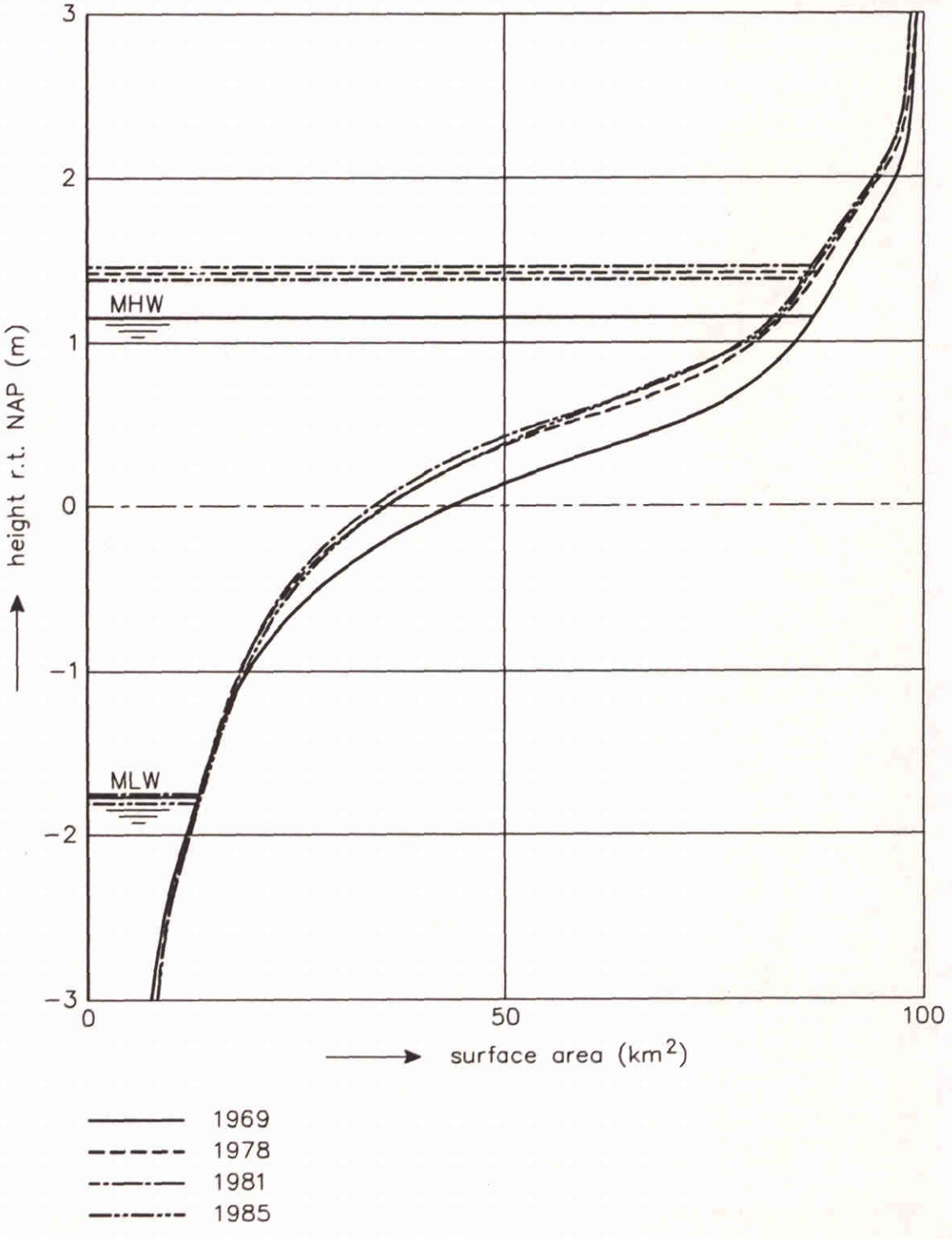

from: Duits–Nederlandse Eemscommissie, 1989

CHANGES IN THE HYPSOMETRIC CURVE OF THE DOLLARD COMPARED WITH CHANGES IN TIDE LEVELS		
DELFT HYDRAULICS	H 1300	FIG. 7.13

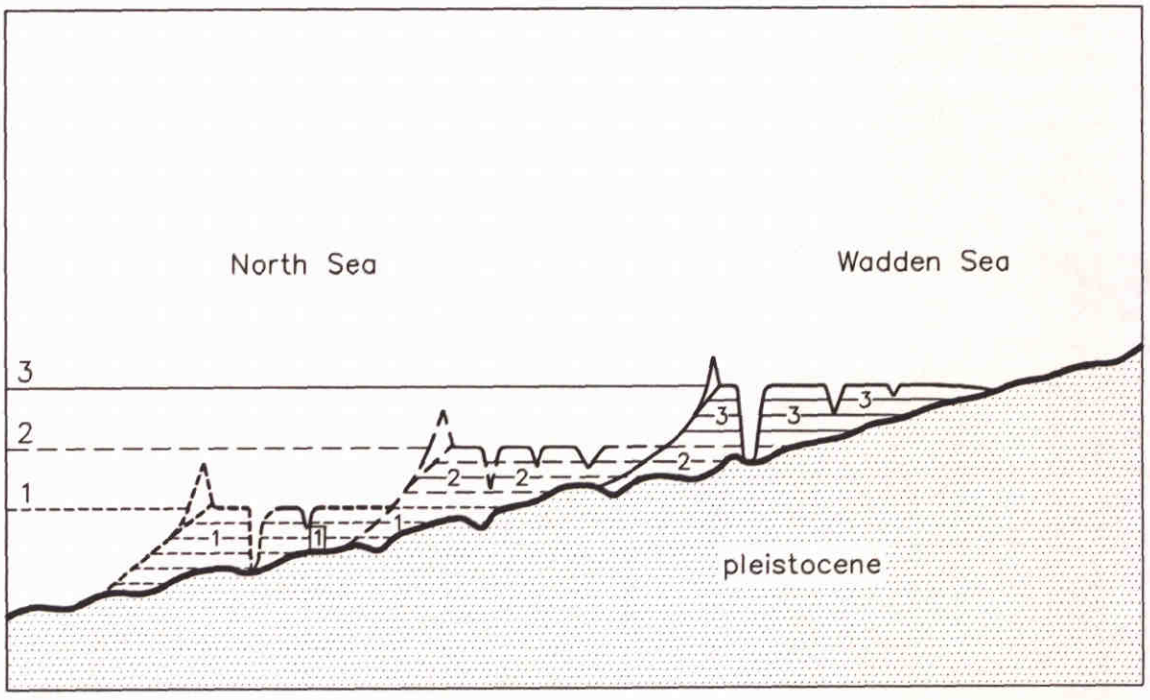

From: Straaten, 1975

HYPOTHESIS OF LANDWARD MIGRATION OF THE WADDEN SEA SYSTEM WITH SEA LEVEL RISE		
DELFT HYDRAULICS	H 1300	FIG. 7.14

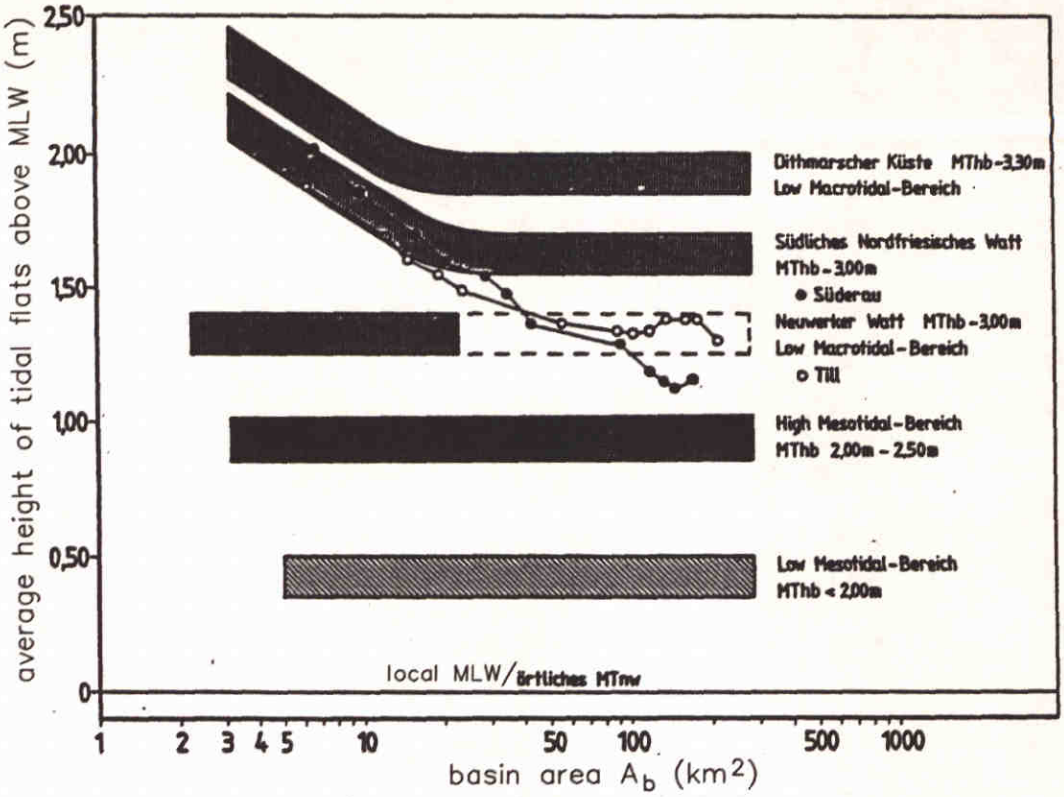

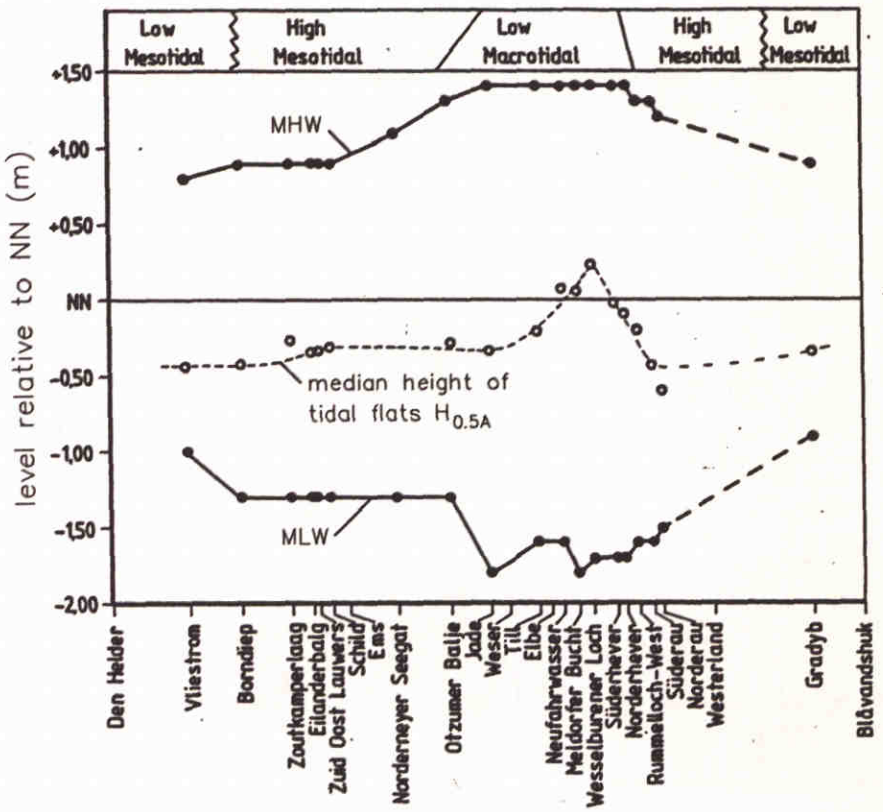

CORRELATIONS OF THE MEDIAN TIDAL FLAT HEIGHT WITH TIDAL DATA AND BASIN AREA (DIECKMANN, 1985)

DELFT HYDRAULICS | H 1300 | FIG. 7.15

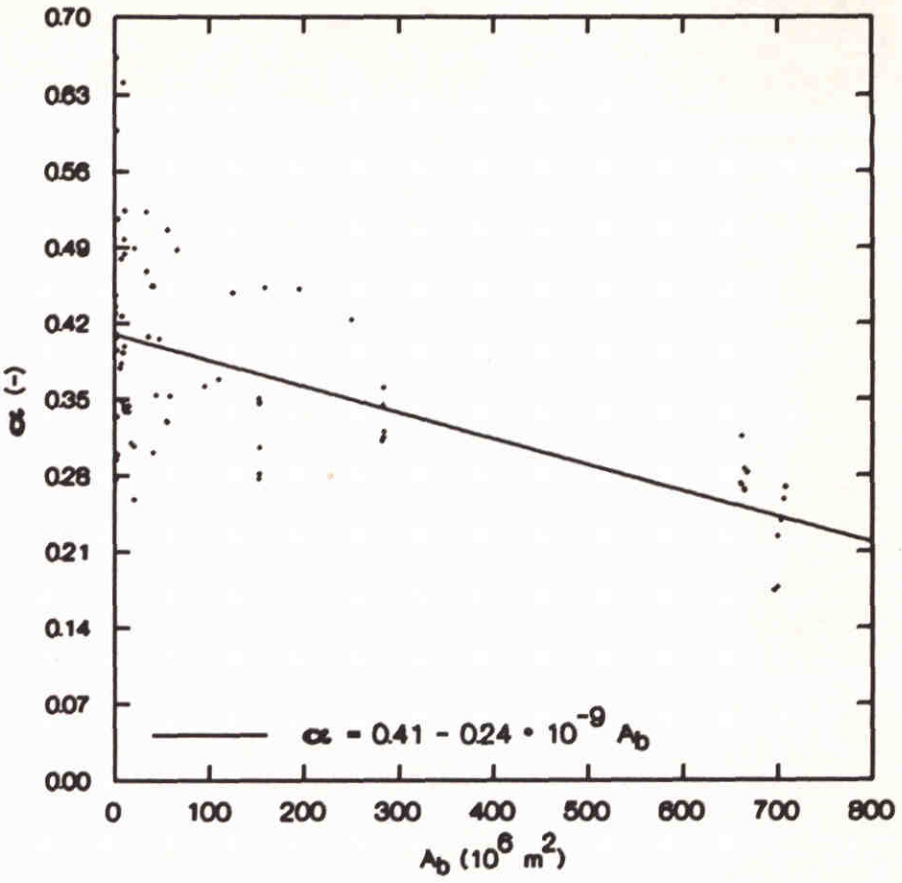

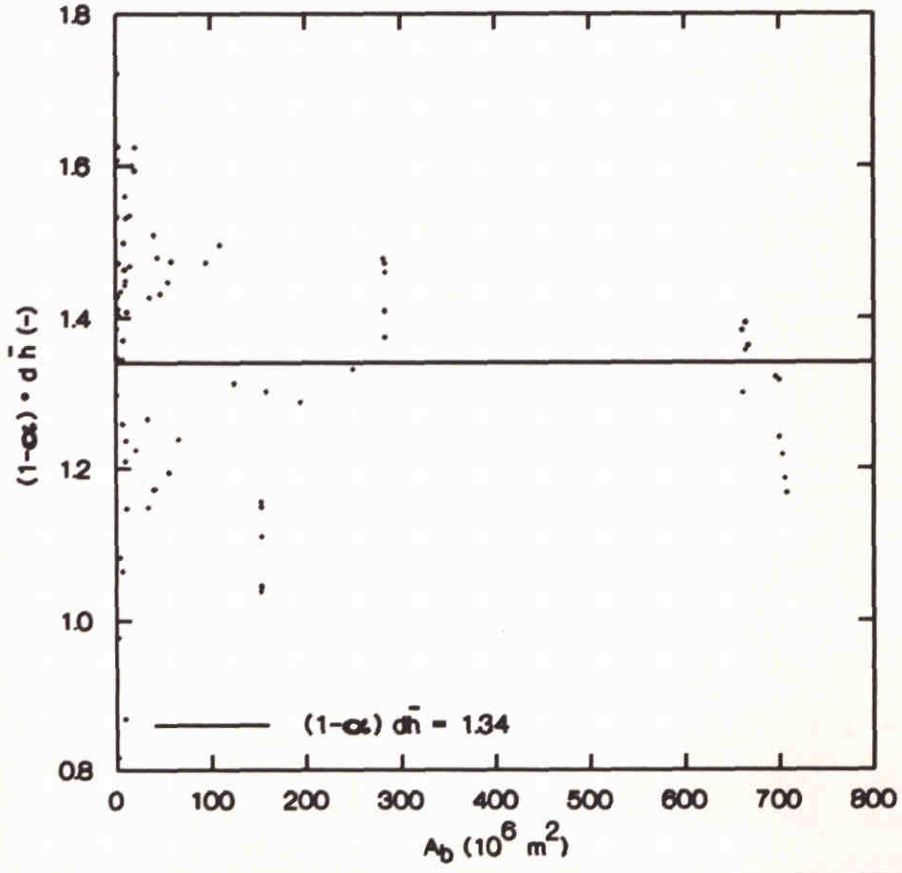

CORRELATION OF AVERAGE LEVEL OF TIDAL FLATS WITH SIZE OF BASIN AND MHW AND MLW

DELFT HYDRAULICS | H 1300 | FIG. 7.16

main office
Rotterdamseweg 185
p.o. box 177
2600 MH Delft
The Netherlands
telephone (31) 15 - 56 93 53
telefax (31) 15 - 61 96 74
telex 38176 hydel-nl

location ' De Voorst'
Voorsterweg 28, Marknesse
p.o. box 152
8300 AD Emmeloord
The Netherlands
telephone (31) 5274 - 29 22
telefax (31) 5274 - 35 73
telex 42290 hylvo-nl